

Adrenomedullin in Dental Tissues

by

David Musson

A thesis submitted to the Faculty of Medicine and Dentistry of
the University of Birmingham for the degree of
Doctor of Philosophy



School of Dentistry
The University of Birmingham
June 2010

UNIVERSITY OF
BIRMINGHAM

University of Birmingham Research Archive

e-theses repository

This unpublished thesis/dissertation is copyright of the author and/or third parties. The intellectual property rights of the author or third parties in respect of this work are as defined by The Copyright Designs and Patents Act 1988 or as modified by any successor legislation.

Any use made of information contained in this thesis/dissertation must be in accordance with that legislation and must be properly acknowledged. Further distribution or reproduction in any format is prohibited without the permission of the copyright holder.

Abstract

Tooth development is complex and dependent on epithelial-mesenchymal interactions involving key molecular signalling pathways. Preliminary data indicate that the pleiotropic growth factor adrenomedullin (ADM) is expressed during tooth development. Furthermore, in osteoblasts, cells which share structural and functional similarities to odontoblasts, ADM increases proliferation *in vitro* and can promote mineralised bone volume and strength *in vivo*.

Immunohistochemical analysis of ADM demonstrated expression during key stages in tooth development in particular in cells responsible for signalling odontoblast differentiation and subsequently in secretory odontoblasts. Similarities with the temporo-spatial expression profile of TGF- β 1 were also observed. *In vitro* analysis using the developmentally derived dental cell lines, MDPC-23 and OD-21, demonstrated ADM stimulated a biphasic response in dental cell numbers with peak stimulation at 10^{-11} M and that it stimulated mineral deposition at levels comparable to that of the known mineralising agent dexamethasone. Analysis of tooth tissue volume and key mandibular measurements in Swiss mice systemically treated with ADM using techniques including micro-Computer Tomography did not identify significant differences in craniofacial mineralised tissue structures compared to sham treated controls.

The data presented here along with the known pleiotropic properties of ADM indicate it may be an important regulator of tooth development particularly in the processes of cell proliferation, differentiation and mineralisation. However, in adult animals systemic ADM supplementation appears to have limited affect on mandibular bone and dentine synthesis.

Acknowledgements

First and foremost I would like to thank my supervisors, Paul and Tony. Your support, knowledge and unerring faith knows no bounds and I appreciate every chance you have given me. Also Alistair, who along with Paul, was there from the start and gave me this fantastic opportunity, thank you. To all the technicians on floor 7, Gay, Sue and Kevin, I could not have done this without your help and advice, so thank you so much. I also owe a lot to my fellow post-grads, Lee and Minal who helped me through the shock of my first year, and to Rich, Lisa and Jen for keeping spirits high and making the office a pleasure to be in.

I would also like to thank Professor Jill Cornish and everyone in her lab in New Zealand, who not only allowed me to visit their lab but made me feel so welcome that I immediately felt at home. This was an amazing opportunity and would not have been possible without funding from the universitas 21 scheme (<http://www.u21.bham.ac.uk>), which also allowed me to ship the ADM treated mice back from New Zealand and provided me with months worth of experiments. These experiments would not have been possible without Liam Glover and his colleagues in the Chemical Engineering department at the University of Birmingham who kindly let me use their μ CT scanner.

Outside of university I would like to thank all my friends for helping me through. Especially my friends from Torquay and everyone in 1-4-9, you are all like brothers to me and given me much needed support throughout the highs and lows.

Last but not least I would like to thank my family. Your support and love means everything to me. A special thanks to my parents, without you I would not be where I am today, obviously. I love you all.

Table of Contents

Section	Page No.
<u>1.0</u> <u>Introduction</u>	1
1.1 Project Aims	1
1.2 Teeth in Oral Function during Health and Disease	2
1.3 Tooth Structure	3
1.4 Craniofacial Development	8
1.4.1 Development of the Mandible	8
1.4.2 Development of the Tooth	10
1.4.2.1 Initiation of Tooth Development	10
1.4.2.2 Bud, Cap and Bell Stages during tooth development	13
1.4.2.3 Odontogenesis	16
1.4.2.4 Molecular Regulation of Odontoblast Differentiation	18
1.5 Dental Tissue Disease – Caries	19
1.6 Molecular and Cellular Components of Dental Tissue Regeneration	20
1.7 Adrenomedullin (ADM) and its Potential Role in Dental Tissues	23
1.7.1 ADM and ADM receptors	25
1.7.2 ADM in Development	26
1.8 Transforming Growth Factor-Beta 1 (TGF- β 1)	29
1.9 Role of Glucocorticoids in Mineralisation	31
1.10 <i>In vivo</i> , <i>ex vivo</i> and <i>in vitro</i> approaches used for studying mineralised tissue biology	33
1.10.1 <i>In vivo</i> experimental models	33
1.10.2 <i>Ex vivo</i> experimental models	41
1.10.3 <i>In vitro</i> experimental models	42

1.10.4	<i>In vitro</i> mineralisation analyses	47
<u>2.0</u>	<u>Materials and Methods</u>	50
2.1	Histology	50
2.1.1	Tissue specimens	50
2.1.2	Fixing and Demineralisation	50
2.1.3	Test for Decalcification End-point	50
2.1.4	Tissue Processing and Embedding	51
2.1.5	Tissue Sectioning	51
2.1.6	Tissue Staining	52
2.1.7	Immunohistochemistry	52
2.1.8	Image Analysis	54
2.2	Cell Culture	55
2.2.1	Cell lines	55
2.2.2	Cell culture procedures for analysis of ADM, dexamethasone and dentine matrix protein extracts exposure	56
2.3	Analysis of cell culture mineralisation	57
2.3.1	Cell Culture	57
2.3.2	Von Kossa staining	58
2.3.3	Digital analysis of von Kossa stained cultures	58
2.4	Gene Expression Analysis	59
2.4.1	Exposure of cell cultures to ADM for gene expression analysis	59
2.4.2	RNA Isolation and Extraction	59
2.4.3	Reverse Transcription	60
2.4.4	Purification of cDNA	61

2.4.5	Quantification of RNA and cDNA	61
2.4.6	Polymerase Chain Reaction (PCR)	62
2.4.7	Agarose gel electrophoresis	64
2.4.8	Image analysis	65
2.5	Systemic Administration of ADM	66
2.6	Micro-Computed Tomography (MicroCT) analysis of dental and craniofacial structures from experimental animals from sham and ADM exposed mice	66
2.6.1	MicroCT scanning and specimen reconstruction	66
2.6.2	Volumetric Measurements	69
2.8	Digital analysis of heads from ADM treated mice	70
2.8	Statistical Analyses	70
<u>3.0</u>	<u>Results Chapter 1</u>	71
3.1	Expression of ADM and TGF- β 1 in the developing tooth: An immunohistochemical study	71
3.2	Histological study of tooth development in rats	73
3.3	Immunohistochemical analyses of ADM and TGF- β 1 in the developing tooth organ of male Wistar rats	85
<u>4.0</u>	<u>Results Chapter 2</u>	105
4.1	Effect of ADM, Dexamethasone and DMPs on dental cell behaviour	105
4.2	Effect of ADM cellular exposure on ADM receptor and PCNA gene expression	108

4.2.1	Analysis of CRLR, RAMP-2 and PCNA transcript levels in MDPC-23, OD-21 and 3T3 cells	108
4.3	Effect of ADM on MDPC-23, OD-21 and 3T3 cell number	112
4.4	Analysis of the ADM ₂₂₋₅₂ antagonist on MDPC-23, OD-21 and 3T3 cell number	116
4.5	Antagonistic effect of ADM ₂₂₋₅₂ on ADM's ability to increase cell number	119
4.5.1	Antagonistic effect of ADM ₂₂₋₅₂ on the proliferative effect of ADM in MDPC-23, OD-21 and 3T3 cells	119
4.6	Effect of DMP exposure on MDPC-23, OD-21 and 3T3 cell numbers	124
4.6.1	Cell number characterisation following exposure of MDPC-23, OD-21 and 3T3 cells to DMPs and comparable concentrations of ADM	125
4.7	Effect of Dexamethasone exposure on MDPC-23, OD-21 and 3T3 cell numbers	130
4.8	Effect of Dexamethasone exposure on ADM expression in MDPC-23 and OD-21 cells	134
<u>5.0</u>	<u>Results Chapter 3</u>	138
5.1	Effect of ADM on extracellular matrix secretion by dental cells <i>in vitro</i>	138
5.2	Effect of ADM exposure on the MDPC-23 cell ECM secretion	139
5.3	Effect of ADM exposure on OD-21 cell ECM secretion	164
5.4	ECM secretion analysis of 3T3 fibroblast cultures exposed to ADM	190

<u>6.0</u>	<u>Results Chapter 4</u>	197
6.1	Systemic administration of ADM to adult male Swiss mice	197
6.2	Effect of systemic ADM administration on murine molar and lower incisor tooth hard tissue volume	201
6.2.1	Effect of systemic ADM administration on murine molar hard tissue volume	201
6.2.2	Effect of systemic administration of ADM on murine lower incisor hard tissue volume	203
6.2.3	Effect of systemic administration of ADM on total dentition hard tissue volume in mice	203
6.3	Effect of systemic administration of ADM on murine mandible hard tissue volume	203
6.4	Effect of systemic administration of ADM on key murine mandibular measurements	205
6.4.1	Effect of systemic administration of ADM on mandibular corpus measurements	205
6.4.2	Effect of systemic administration of ADM on mandibular ramus and alveolar process measurements	205
6.4.3	Effect of systemic administration of ADM on mandibular ramus and condylar measurements	210
<u>7.0</u>	<u>Discussion</u>	214
<u>8.0</u>	<u>References</u>	233
<u>9.0</u>	<u>Published Paper</u>	262

List of Figures

Table	Page No.
Figure 1.1 – Diagram of a mammalian tooth	7
Figure 1.2 – Bud stage of tooth development	13
Figure 1.3 – Cap stage of tooth development	15
Figure 1.4 – Bell stage of tooth development	16
Figure 1.5 – Histological image of developing molar during hard tissue secretion	18
Figure 1.6 – Diagram of tooth’s regenerative response to dental trauma	22
Figure 1.7 – Example images of mouse mandible taken using μ CT technology	40
Figure 1.8 – Alizarin red staining of periodontal ligament cells	48
Figure 1.9 – Von Kossa staining of adipocyte stem cells	49
Figure 2.1 – Picture of Skyscan 1172 (Skyscan, Belgium)	67
Figure 2.2 – Diagrammatic representation of the μ CT scanning process	68
Figure 2.3 – Picture of author using CTrecon software (Skyscan, Belgium)	69
Figure 3.1 – H&E staining of developing rat incisor and molar at E16	75 & 76
Figure 3.2 – H&E staining of developing rat incisor and molar at E18	78 – 80
Figure 3.3 – H&E staining of developing rat incisor and molar at E20	82 – 84
Figure 3.4 – Immunohistochemical staining for the presence of ADM in adult male Wistar rat heart with relevant controls	87 – 89
Figure 3.5 - Immunohistochemical staining for the presence of ADM in developing rat incisors at E16 with relevant controls	91 – 94
Figure 3.6 - Immunohistochemical staining for the presence of ADM in developing rat incisors at E18 with relevant controls	96 – 99
Figure 3.7 - Immunohistochemical staining for the presence of ADM and TGF- β 1 in developing rat incisors at E20 with relevant controls	101 – 104
Figure 4.1 - Gene expression profile of GAPDH, PCNA, CRLR and RAMP-2 in MDPC-23, OD-21 and 3T3 cells following exposure to a range of concentrations of ADM	110 & 111

- Figure 4.2** - Effect of a range of concentrations of ADM on MDPC-23, OD-21 and 3T3 cell number following 48-hour exposure **114 & 115**
- Figure 4.3** - Effect of a range of concentrations of ADM₂₂₋₅₂ on MDPC-23, OD-21 and 3T3 cell number following 48-hour exposure **117 & 118**
- Figure 4.4** - Antagonistic effect of ADM₂₂₋₅₂ on the ability of ADM to increase MDPC-23, OD-21 and 3T3 cell number **122 & 123**
- Figure 4.5** - Effect of a range of concentrations of E-DMPs and ADM on MDPC-23, OD-21 and 3T3 cell number following 48-hour exposure **128 & 129**
- Figure 4.6** - Effect of a range of concentrations of DEX on MDPC-23, OD-21 and 3T3 cell number following 48-hour exposure **132 & 133**
- Figure 4.7** - Gene expression profile of ADM and RAMP-2 in MDPC-23 and OD-21 cells following exposure to a range of concentrations of DEX **136 & 137**
-
- Figure 5.1** – Detectable ECM secretion determined by von Kossa staining of MDPC-23 cells following 3 days exposure to a range of concentrations of ADM and either 50mg/ml Ascorbic Acid (A.A) and 10mM β-glycerophosphate (β-G), or 50mg/ml A.A, 10mM β-G and 10⁻⁸M DEX **140 – 142**
- Figure 5.2** – Detectable ECM secretion determined by von Kossa staining of MDPC-23 cells following 7 days exposure to a range of concentrations of ADM and either 50mg/ml Ascorbic Acid (A.A) and 10mM β-glycerophosphate (β-G), or 50mg/ml A.A, 10mM β-G and 10⁻⁸M DEX **144 – 146**
- Figure 5.3** – Detectable ECM secretion determined by von Kossa staining of MDPC-23 cells following 11 days exposure to a range of concentrations of ADM and either 50mg/ml Ascorbic Acid (A.A) and 10mM β-glycerophosphate (β-G), or 50mg/ml A.A, 10mM β-G and 10⁻⁸M DEX **148 – 150**

- Figure 5.4** – Detectable ECM secretion determined by von Kossa staining of MDPC-23 cells following 14 days exposure to a range of concentrations of ADM and either 50mg/ml Ascorbic Acid (A.A) and 10mM β -glycerophosphate (β -G), or 50mg/ml A.A, 10mM β -G and 10^{-8} M DEX **152 – 154**
- Figure 5.5** – Detectable ECM secretion determined by von Kossa staining of MDPC-23 cells following 21 days exposure to a range of concentrations of ADM and either 50mg/ml Ascorbic Acid (A.A) and 10mM β -glycerophosphate (β -G), or 50mg/ml A.A, 10mM β -G and 10^{-8} M DEX **156 – 158**
- Figure 5.6** – Graphical representation of detectable ECM secretion determined by von Kossa staining vs. Time for MDPC-23 cells following exposure to a range of concentrations of ADM and either 50mg/ml Ascorbic Acid (A.A) and 10mM β -glycerophosphate (β -G), or 50mg/ml A.A, 10mM β -G and 10^{-8} M DEX **161 - 163**
- Figure 5.7** – Detectable ECM secretion determined by von Kossa staining of OD-21 cells following 3 days exposure to a range of concentrations of ADM and either 50mg/ml Ascorbic Acid (A.A) and 10mM β -glycerophosphate (β -G), or 50mg/ml A.A, 10mM β -G and 10^{-8} M DEX **165 – 167**
- Figure 5.8** – Detectable ECM secretion determined by von Kossa staining of OD-21 cells following 7 days exposure to a range of concentrations of ADM and either 50mg/ml Ascorbic Acid (A.A) and 10mM β -glycerophosphate (β -G), or 50mg/ml A.A, 10mM β -G and 10^{-8} M DEX **169 – 171**
- Figure 5.9** – Detectable ECM secretion determined by von Kossa staining of OD-21 cells following 11 days exposure to a range of concentrations of ADM and either 50mg/ml Ascorbic Acid (A.A) and 10mM β -glycerophosphate (β -G), or 50mg/ml A.A, 10mM β -G and 10^{-8} M DEX **173 – 175**

- Figure 5.10** – Detectable ECM secretion determined by von Kossa staining of OD-21 cells following 14 days exposure to a range of concentrations of ADM and either 50mg/ml Ascorbic Acid (A.A) and 10mM β -glycerophosphate (β -G), or 50mg/ml A.A, 10mM β -G and 10^{-8} M DEX **177 – 179**
- Figure 5.11** – Detectable ECM secretion determined by von Kossa staining of OD-21 cells following 21 days exposure to a range of concentrations of ADM and either 50mg/ml Ascorbic Acid (A.A) and 10mM β -glycerophosphate (β -G), or 50mg/ml A.A, 10mM β -G and 10^{-8} M DEX **182 – 184**
- Figure 5.12** – Graphical representation of detectable ECM secretion determined by von Kossa staining vs. Time for OD-21 cells following exposure to a range of concentrations of ADM and either 50mg/ml Ascorbic Acid (A.A) and 10mM β -glycerophosphate (β -G), or 50mg/ml A.A, 10mM β -G and 10^{-8} M DEX **187 – 189**
- Figure 5.13** – Representative images demonstrating detectable ECM secretion of 3T3 cells determined by von Kossa staining following 3, 7, 11, 14 and 21 days exposure to a range of concentrations of ADM and either 50mg/ml Ascorbic Acid (A.A) and 10mM β -glycerophosphate (β -G), or 50mg/ml A.A, 10mM β -G and 10^{-8} M DEX **191 – 193**
- Figure 5.14** – Graphical representation of detectable ECM secretion determined by von Kossa staining vs. Time for 3T3 cells following exposure to a range of concentrations of ADM and either 50mg/ml Ascorbic Acid (A.A) and 10mM β -glycerophosphate (β -G), or 50mg/ml A.A, 10mM β -G and 10^{-8} M DEX **194 – 196**
- Figure 6.1** – Example images of a Swiss mouse mandible obtained using a Skyscan 1172 μ CT (Skyscan, Belgium) **199**
- Figure 6.2** – Sample pages of CTan software (Skyscan, Belgium) demonstrating the isolation of mice molars, incisors and mandibles for subsequent volumetric analysis **200**

Figure 6.3 – Swiss mouse 1 st , 2 nd and 3 rd molar hard tissue volume following systemic administration of either ADM or saline solution	202
Figure 6.4 - Swiss mouse lower incisor, complete dentition and mandible hard tissue volume following systemic administration of either ADM or saline solution	204
Figure 6.5 – Key mandibular measurements, as proposed by Atchley <i>et al</i> , (1984) in Swiss mice following systemic administration of either ADM or saline solution	207 - 209
Figure 6.6 – Key mandibular measurements, as proposed by Atchley <i>et al</i> , (1984) in Swiss mice following systemic administration of either ADM or saline solution	204 - 206

List of Tables

Table	Page No.
Table 2.1 – Antibody specifications used in histochemical study	54
Table 2.2 – Primers and PCR conditions used for gene expression analysis	63
Table 4.1 – Concentrations of ADM sequestered from E-DMPs and those examined in Section 4.2	125

List of Abbreviations

2D – 2-dimensional

3D – 3-dimensional

A.A – Ascorbic acid

ADM – Adrenomedullin

B-G – Beta glycerophosphate

BMP – Bone morphogenic protein

BSA – Bovine serum albumin

BSP – Bone sialoprotein

Ca – Calcium

cAMP – Adenylate cyclase

CGRP – Calcitonin gene-related peptide

Coll-1 α – Collagen-1 alpha

CPM – Counts per minute

CRLR – Calcitonin receptor-like receptor

DAB – 3,3'-diaminobenzidine

Dex – Dexamethasone

DMEM – Dulbecco's Modified Eagle Media

DMP – Dentin matrix protein

DNA – Deoxyribulose nucleic acid

DPP – Dentin phosphoprotein

DSP – Dentin sialoprotein

ECM – Extracellular matrix

EtB – Ethidium bromide

FCS – Foetal calf serum

FGF – Fibroblast growth factor

FITR – Fourier transform infrared spectroscopy

GAPDH – Glyceraldehydes-3-phosphate-dehydrogenase

GPCR – G-Protein-coupled receptor

H&E – Haematoylin and eosin

H₂O₂ – Hydrogen peroxide

IBM – Isobutylmethylxanthine

IDE – Inner dental epithelium

IGF – Insulin growth factor
IL-1 β – Interleukin-1 beta
IMS – Industrial methylated spirit
 μ CT – Micro-computed tomography
NaCu – Copper sulphate
ODE – Outer dental epithelium
OE – Oral epithelium
PBS – Phosphate buffered saline
PCNA – Proliferating cell nuclear antigen
PCR – Polymerase chain reaction
PDGF – Platelet-derived growth factor
PDL – Periodontal ligament
PTH – Parathyroid hormone
RAMP – Receptor activity modifying protein
RNA – Ribulose nucleic acid
RPM - Revolutions per minute
RT – Reverse transcription
s.e.m – Standard error of the mean
Shh – Sonic hedgehog
SR – Stellate reticulum
TAE – Tris acetate EDTA
TGF- β – Transforming growth factor – beta
TGF- β R – Transforming growth factor – beta receptor
VOI – Volume of interest

1. Introduction

1.1 Project Aims

The development of a tooth is complex and dependent on epithelial-mesenchymal interactions and involves key cellular and molecular signalling processes and pathways. It is important to gain a clearer understanding of the factors involved in tooth development as this can not only aid our understanding of the developmental process but can help to increase our knowledge of developmental defects and also help in the understanding of how growth factors could be used in the repair of teeth, as the reparative processes of odontoblast induction and dentine secretion are thought to closely mimic those of tooth development (Smith and Lesot, 2001).

Recently, preliminary data has indicated the presence of the pleiotropic growth factor adrenomedullin (ADM) in the developing tooth bud (Monuenga *et al*, 1997), however, only limited expression characterization at early stages of development were performed. Notably, ADM has demonstrated similar temporo-spatial patterns of expression during embryogenesis as TGF- β 1, a growth factor known to play a key role in tooth development. Furthermore, in osteoblasts, cells which share many structural and functional similarities to odontoblasts, data demonstrates that ADM increases proliferation *in vitro* (Cornish *et al*, 1997; Cornish *et al*, 2002) and can promote mineralised bone volume and strength *in vivo* (Cornish *et al*, 1997; Cornish *et al*, 2001).

The aims of this project were:

- i) to characterise the expression of ADM, in comparison to TGF- β 1, during key stages of rodent tooth development using immunohistochemical analysis

ii) to study ADM's effect on developmentally derived dental cell numbers and extracellular secretion indicative of mineralisation *in vitro* which may indicate its potential role(s) in tooth development and,

iii) to analyse the effects of ADM, using μ CT technology, in adult mice to determine its effects on dental and craniofacial mineralised tissue *in vivo*.

The data generated should provide valuable insight into the role of ADM in the dental and craniofacial mineralised tissues both developmentally and post-natally and may indicate its potential application for dental regenerative therapy.

1.2 Teeth in Oral Function during Health and Disease

Teeth have many functions. The primary and most commonly associated being that of mastication. In many animals, teeth also play a major role in attack and defence whilst in humans, teeth also aid speech (Ten Cate, 1998). During oral and dental disease, e.g., periodontal diseases and caries, oral function may be compromised.

Traditionally, oral function has been restored by simple surgical procedures to the dentition and periodontium, often using inert dental materials to replace lost tissue (Schröder, 1985; Murray and Garcia-Godoy, 2004). Currently, there is much interest in biological approaches to restore function by tissue regeneration and a deep understanding of the cellular and molecular processes involved in oral and dental tissue behaviour is required for effective clinical translation of such approaches (Smith 2003; Nakashima, 2005). The following sections of this Introduction aim to provide a background to the understanding of cell behaviour in teeth as a basis for future clinical exploitation of various bioactive molecules for dental regeneration.

1.3 Tooth Structure

There are three structurally distinct components that constitute a tooth which include the enamel, dentine and pulp (**Figure 1.1**). The enamel is the acellular layer that covers the exposed surface of the tooth (**Figure 1.1**) and is formed by ameloblasts during development that subsequently apoptose when the tooth erupts into the oral cavity (Kondo *et al*, 2001). Enamel is the most mineralised tissue and hardest substance found in the body. Although biologically “dead”, this layer is permeable, allowing ion exchange between the enamel and the oral cavity, in particular those ions present in saliva which aid remineralisation. Enamel is highly susceptible to demineralisation by bacterial acids, and once lost to wear or caries it cannot be replaced by cellular activity due to the absence of its formative cells (Ten Cate, 1998).

Dentine is an avascular, hard, connective tissue, which makes up the majority of the tooth (**Figure 1.1**). It consists of a complex compound of type I collagenous fibres and an apatite mineral phase, providing rigidity and strength, while the tubular nature of dentine provides the flexibility required to support the enamel, especially during mastication (Ten Cate, 1998; Kinney *et al*, 1999). Dentine is synthesized and maintained by odontoblasts, which secrete structurally distinct forms of dentine depending on their maturity. Between the odontoblasts and mineralised dentine is an unmineralised newly secreted predentine layer, 10–30µm wide, consisting of type I collagen and proteoglycans (Linde & Goldberg, 1993; Torneck, 1994). The principal component of dentine is the primary dentine, which is relatively rapidly synthesised up to root formation at which point secondary dentine is subsequently laid down at a much slower rate. Dentine is tubular in structure due to the mode by which it is deposited and the tubules contain the odontoblast processes, collagen fibrils, peritubular dentine and a complex mixture of proteins (Thomas, 1979; Linde &

Goldberg 1993; Torneck 1994). In the crown of the tooth the tubules extend from the dentine-enamel junction to the odontoblast layer, giving rise to the permeability of the dentine (Torneck 1994). Inside these tubules, the peritubular dentine can become hypermineralised and ultimately occlude the tubules thereby reducing permeability (Torneck 1994). At the outermost region of the primary dentine, just beneath the enamel, a narrow zone termed mantle dentine exists. This has a different composition to primary dentine, generally being less mineralised, and is produced by the newly differentiated odontoblasts (Linde & Goldberg, 1993; Torneck, 1994). Once the tooth is fully formed, i.e. after root formation, the odontoblasts continue to deposit secondary dentine at a significantly slower rate resulting in a reduction of the pulp chamber. Secondary dentine resembles primary dentine in structure but is less regular although the tubules are generally continuous (Linde & Goldberg, 1993; Torneck, 1994). Tertiary dentine is formed in response to trauma, such as dental caries, by odontoblasts or newly derived odontoblast-like cells beneath the site of injury to protect the underlying soft tissue of the pulp (for further description of this see **Section 1.5**) (Lesot *et al*, 1994; D'Souza *et al*, 1995). Unlike primary dentine, the morphology of the tertiary dentine varies greatly and it is often irregular, with permeability reduced as a result of a reduction of tubular structure and/or continuity (Tziafas *et al*, 2000).

The pulp, at the core of the tooth, comprises of soft connective tissue (**Figure 1.1**). Its primary functions are to form, repair and nourish the dentine. The majority of the dental pulp is made up of a heterogeneous cell population of fibroblasts (Tsukamoto *et al*, 1992) which, amongst other activities, secrete an extracellular matrix (ECM) composed primarily of type I and III collagenous fibrils responsible for maintaining its structural integrity (Goldberg and Smith, 2004; Killough *et al*, 2009).

Also within the pulp are undifferentiated mesenchymal cells known as dental pulp stem cells (DPSC) (Gronthos *et al*, 2000) that have a similar gene expression profile to bone marrow stem/stromal cells (BMSC) (Shi *et al*, 2001) and are thought to reside in the perivascular niche region of the pulp (Shi and Gronthos, 2003). DPSCs have the potential to differentiate down several cell lineages including adipocytes (Gronthos *et al*, 2002), neural-like cells (Gronthos *et al*, 2002), osteoblasts (Otaki *et al*, 2007) and notably, odontoblasts (Gronthos *et al*, 2002). Recent studies have also demonstrated that in response to dental tissue injury perivascular DPSCs exhibit increased proliferation, can migrate to the site of tissue damage and can secrete reparative dentine ECM (About *et al*, 2000; Téclès *et al*, 2004). Notably, residing within the dental pulp immuno-responsive cells are also present, these include dendrocytes, macrophages, lymphocytes and mast cells, which mediate the inflammatory reaction in response to cellular or tissue insults arising due to dental trauma or disease, e.g. dental caries (Jontell *et al*, 1998; Goldberg and Smith, 2004). Also present within the pulp is a complex network of capillaries and sensory nervous tissue (plexus of Raschkow), which provide nutritive and sensory support to the dentine-pulp complex (Goldberg and Smith, 2004).

To enable the tooth to perform its primary functions and to retain its position within the jaws, it is attached to the alveolar bone by two specialised supporting tissues, namely the periodontal ligament (PDL) and cementum (**Figure 1.1**). The PDL is a specialised connective tissue consisting of collagen fibre bundles synthesised by dental follicle-derived fibroblasts. These collagen fibres form a gel-like matrix, embedding themselves into the cementum and alveolar bone enabling the tooth to adapt to the forces applied during mastication. The PDL contains several cell lineages that are capable of (re)generating and maintaining the ligament itself as well as the

cementum and the alveolar bone adjacent to it. Cells resident in this tissue include fibroblasts, capable of collagen secretion, (McCulloch *et al*, 1989), cementoblasts and cementoclasts capable of remodelling the cementum (McCulloch *et al*, 1989; Seo *et al*, 2004), osteoblasts and osteoclasts (Basdra and Komposch, 1997) which maintain the alveolar bone. In addition, within the PDL are a population of progenitor/stem cells that have the potential to differentiate into all of these specific cell types to enable regeneration of the PDL fibres, alveolar bone and cementum following disease or trauma (Seo *et al*, 2004).

Cementum is the hard, mineralised connective tissue, which is attached to the root dentine (Ten Cate, 1998). There are three distinct types of cementum, acellular afibrillar cementum, acellular extrinsic fibre cementum and cellular intrinsic cementum (Saygin *et al*, 2000; Grzesik and Narayanan, 2002). Acellular afibrillar cementum is present at the cemento-enamel junction and is made up of a mineralised matrix lacking in collagenous fibres and embedded cells (Sagyin *et al*, 2000; Grzesik and Narayanan, 2002). Acellular extrinsic fibre cementum is the primary cementum involved in attachment to the tooth and consists of dense collagenous fibres, primarily type I collagen, perpendicularly implanted into the dentine matrix (Sagyin *et al*, 2000; Grzesik and Narayanan, 2002). The cellular intrinsic cementum plays a reparative role and therefore contains cementocyte cells embedded in mineralised matrix and collagenous fibrils (Sagyin *et al*, 2000; Grzesik and Narayanan, 2002).

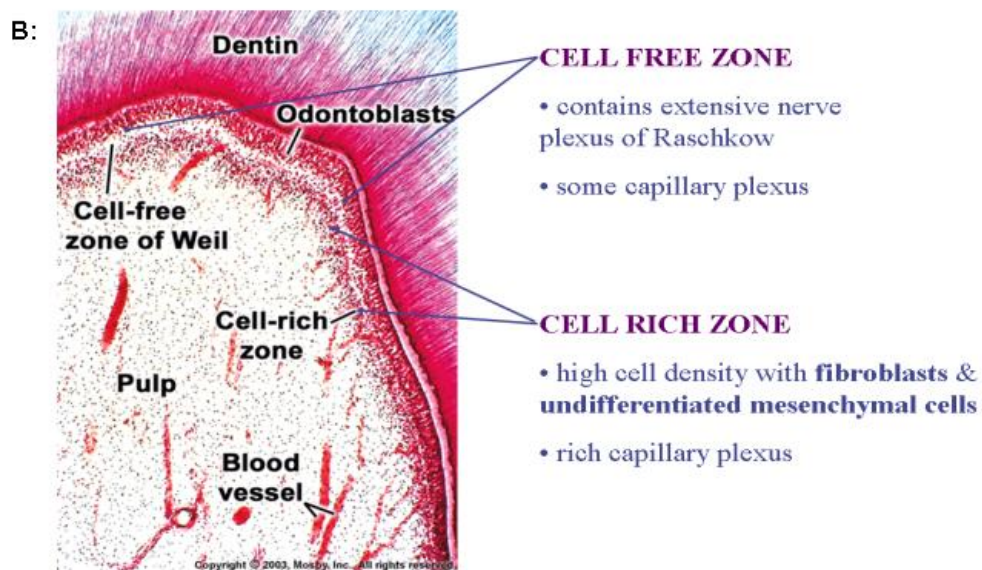


Figure 1.1: A: Diagram of a mammalian tooth, showing the positions of the main structural components. **B:** Histological image of mammalian tooth showing finer structures of the dental pulp. Adapted from Thesleff, 2003.

1.4 Craniofacial development

1.4.1 Development of the mandible

Mammalian development is a multifaceted process involving an intricate network of cell-cell signalling and is dependent on numerous epithelial-mesenchymal interactions. Craniofacial development is especially complex due to the diverse nature of the tissues involved (Thesleff *et al*, 1995).

Development of the craniofacial tissues is initiated as soon as the antero-posterior axis of an embryo is established and corresponds with the acquisition of two cell populations, the neural crest and the ectodermal placodes (Basch *et al*, 2004; McCabe *et al*, 2004). The neural crest comprises a pluripotent cell population derived from the neural plate during early stages of embryogenesis and in addition to giving rise to craniofacial structures, it also gives rise to the peripheral nervous system and connective tissues associated with the facial muscles (Noden, 1988; Couly *et al*, 1992; Kontges and Lumsden, 1996; Osumi-Yamashita *et al*, 1997).

Following initiation of craniofacial development, neural crest cells disperse from the dorsal surface of the neural tube and undergo epithelial-mesenchymal transformation, where the epithelial cells dissociate from the tissue they originate from and become mesenchymal in nature, migrating ventro-laterally as they populate the craniofacial region. These cells then interact with, and are instructed by, the pharyngeal endoderm, ectoderm, and mesoderm before giving rise to the fronto-nasal process and the discrete swellings that distinguish each branchial arch (Chai and Maxson, 2006). It is the ventral region of the first branchial arch that eventually gives rise to both maxillary and mandibular processes (Cerny *et al*, 2004; Lee *et al*, 2004).

The mandibular processes are bilaterally symmetrical structures located below the future oral cavity and composed of mesenchymal tissue derived from neural crest cells, enclosed by an epithelial cell layer of ectodermal and endodermal origin. Mandibular bone formation commences with the condensation of the mesenchymal cells (Hall and Miyake, 2000; Helms and Schneider, 2003; Eames *et al*, 2004) which then differentiate into osteoblasts and form bone through the intramembranous deposition and calcification of mineralized matrix (Tyler and Hall, 1977). After their initial formation, these processes undergo considerable outgrowth along 3 axes, fusing in the midline region to give rise to the triangular-shaped lower jaw (Mina, 2001). This fusion is a result of epithelial cell migration and the merging of the mesenchymal cells from the neighbouring processes (Shuler *et al*, 1992; Shuler, 1995; Chai *et al*, 1997; McGonnell *et al*, 1998).

The processes involved are dependent on epithelial-mesenchymal interactions. This was demonstrated by tissue recombination studies suggesting that signals derived from mandibular epithelium regulate growth of the underlying mesenchyme (Wedden, 1987; Richman and Tickle, 1989; Hall and Coffin-Collins, 1990; Mina *et al*, 1994). Similar to that seen during tooth development (see **Section 1.4.2**), these interactions are known to involve key growth factors, such as members of the Transforming Growth Factor- β superfamily, such as Bone Morphogenic Proteins (BMP), Fibroblast Growth Factors (FGFs), Wnt and Hedgehog (Hh) families, as demonstrated either by their temporo-spatial expression patterns (Chai *et al*, 1994; Chai *et al*, 1997; Trumpp *et al*, 1999; Ito *et al*, 2002; Liu *et al*, 2005) or in rodent genetic knockout studies (Chiang *et al*, 1996; Sanford *et al*, 1997; Nomura and Li, 1998; Liu *et al*, 2005). Key transcription factors involved in this process include *Msx1* and *Msx2*, and members of the *Dlx* family and *Pitx2* families, once again similar studies as used for growth

factors have shown their involvement in mandibular epithelium development (Davidson, 1995; Maas and Bei, 1997; Davideau *et al*, 1999; Kraus and Lufkin, 1999; Meijlink *et al*, 1999; Lin *et al*, 1999; Satokata *et al*, 2000).

1.4.2 Development of the Tooth

1.4.2.1 Initiation of Tooth Development

Tooth development is a reciprocal series of epithelial-mesenchymal interactions with both the epithelium and mesenchyme each being dominant at different stages throughout tooth development (Thesleff *et al*, 1995). Initiation of tooth development has been demonstrated to begin in the dental epithelium, with the molecules expressed interacting with the dental mesenchyme in such a way that there is a shift in the odontogenic potential, resulting in the mesenchymal cells being responsible for tooth development. In mouse embryos this shift occurs at approximately embryonic day 12.5 (E12.5), as shown in experiments by Mina and Kollar (1987) and Lumsden (1988). In these studies, only dental epithelium extracted before E12.5 initiated tooth formation when recombined with neural-crest-derived, second branchial arch mesenchyme. Conversely, only dental mesenchyme extracted after E12.5 carried odontogenic potential when recombined with second arch epithelium (Mina and Kollar, 1987; Lumsden, 1988).

At a molecular level, initiation and odontogenic potential are regulated by protein signalling molecules, in particular by members of several growth factor families (Smith and Lesot, 2001). These molecules act by inducing intracellular pathways in the target tissue to activate transcription factors and increase gene and protein expression, which subsequently affect cellular phenotype. Prominent growth

factors demonstrably involved in tooth development are similar to those involved in the development of the mandible (**Section 1.4.1**) and include members of the Transforming Growth Factor- β superfamily, such as Bone Morphogenic Proteins (BMPs), Fibroblast Growth Factors (FGFs), Wnt and Hedgehog (Hh) families (Hardcastle *et al*, 1998; Jernvall *et al*, 2000; Sarkar *et al*, 2000; Thesleff *et al*, 2002). Whilst transcription factors that are induced by these growth factors and have been shown to be instrumental in tooth development include *Msx1*, *Msx2*, *Dlx2*, *Pax9*, *Pitx1 and 2*, and *Barx1* (Dassule and McMahon, 1998; Grigoriou *et al*, 1998; Tucker *et al*, 1998; Peters *et al*, 1999; St Amand *et al*, 2000).

Members of the TGF- β superfamily play key roles in organogenesis throughout the developing embryo. The best characterised member being TGF- β 1, which is discussed in further detail in **Section 1.8**. Another prominent subfamily of the TGF- β superfamily are BMPs, and several of these are expressed during tooth development, although BMP4 in particular has been demonstrated to play a central role in this process (Thesleff *et al*, 2002). BMP4 is expressed in the dental epithelium prior to E12.5, and in the mesenchyme after E12.5, coinciding with the shift in odontogenic potential in mice (Vainio *et al*, 1993; Tureckova *et al*, 1995). BMP4 is known to regulate several dental development processes, including the restriction of transcription factor expression (e.g. *Pax9*, *Pitx2* and *Barx1*) to sites of tooth initiation (Tucker *et al*, 1998; Peters *et al*, 1999; St Amand *et al*, 2000). BMP4 also induces expression of other transcription factors in the mesenchyme, including *Msx1*, *Msx2*, *Dlx2* and *Lef1* (Dassule and McMahon, 1998). However, the precise role of BMP4 during tooth development has yet to be fully elucidated as mice deficient in BMP4 fail to survive before tooth formation is initiated (Winnier *et al*, 1995).

Several FGF family members exhibit a similar temporo-spatial expression pattern to that observed for BMPs during tooth formation and their functions range from tooth initiation to cusp formation regulation (Jernvall *et al*, 2000). Notably, FGF8 is expressed at significant levels in the dental epithelium prior to and during tooth development and is known to play a role in the induction of many transcription factors, including *Pax9*, *Pitx1 and 2*, *Barx1*, *Lhx6 and Lhx7* (Grigoriou *et al*, 1998; Tucker *et al*, 1998; Peters *et al*, 1999; St Amand *et al*, 2000).

Among the Hh family of growth factors in mammals only Sonic Hedgehog (Shh) is expressed in teeth (Johnson and Tabin, 1995). During tooth initiation Shh is thought to regulate the epithelial thickening and invagination required during bud formation, by stimulating proliferation in the epithelial cells (Cobourne *et al*, 2001). Studies have shown that Shh is required for early tooth germ development as blocking of Shh using neutralising antibodies at E10.5 resulted in tooth development arrest at the lamina stage (Cobourne *et al*, 2002). Double mutants of the Shh downstream signalling molecules *Gli2* and *Gli3* also resulted in the arrest of tooth development prior to bud stage (Hardcastle *et al*, 1998).

The Wnt gene family encode a large group of signalling proteins involved in the proliferation and differentiation of several organs and cell types (Cadigan & Nusse, 1997). One of the predominant Wnt genes involved in tooth development is Wnt7b which is expressed in the oral epithelium and is thought to interact with Shh in determining tooth pattern formation (Sarkar *et al*, 2000).

1.4.2.2 Bud, Cap and Bell Stages during Tooth Development

During development, the tooth goes through three morphological stages, which are named according to their histological appearance. These stages are used for descriptive purposes and represent a continuum of change with the end of one stage often overlapping with the beginning of the next (Ten Cate, 1998; Tucker and Sharpe, 2004) and therefore making it difficult to distinguish morphologically the distinct stages.

The first stage of tooth development is that of the bud stage. This begins with the thickening of the oral epithelium in what becomes known as the dental lamina. This ‘thickening’ begins to invaginate into the underlying neural crest-derived mesenchyme as the epithelial cells proliferate (**Figure 1.2**), whilst showing little or no change in shape or function (Ten Cate, 1998). As the epithelial cells transcend into the ectomesenchyme, the ectomesenchymal cells become condensed, surrounding the epithelial “bud” (Tucker and Sharpe, 2004).

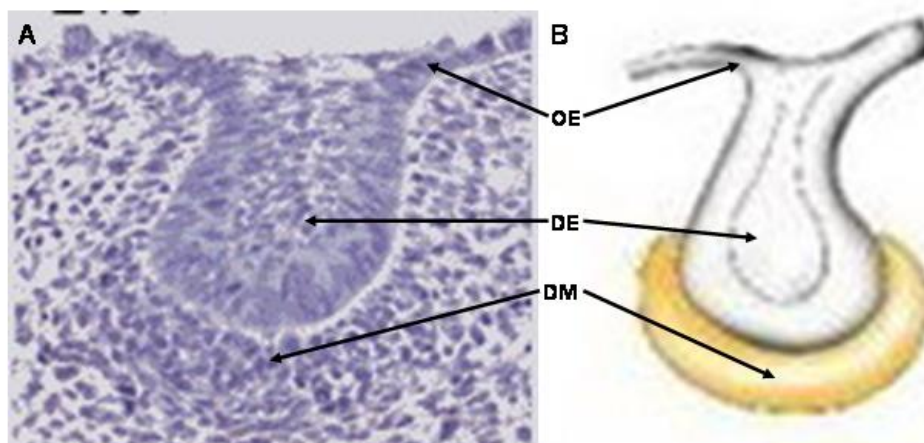


Figure 1.2: **A:** Histological image of developing rat molar in bud stage of development. Adapted from Hosoya *et al*, 2006. **B:** Schematic diagram of developing tooth at bud stage. Adapted from Thesleff, 2003. **OE** = Oral epithelium. **DE** = Dental epithelium. **DM** = Dental mesenchyme.

During the second stage of development, the cap stage (**Figure 1.3**), the density of ectomesenchymal cells beneath the epithelial bud increases significantly as cells fail to separate due to the pressure of the migrating “bud”. These mesenchymal cells become known as the dental papilla, which forms the pulp and dentine forming odontoblasts of the mature tooth (Tucker and Sharpe, 2004). This ability of dental papilla cells to differentiate into dentine forming odontoblasts has recently been elegantly demonstrated by Kikuchi *et al*, 2004, where dental papilla cells incubated in a three-dimensional model, encompassed by an artificial extracellular matrix, differentiated into tubular process forming columnar odontoblast-like cells. Atop the condensed, mesenchyme-derived dental papilla, the epithelial ingrowth continues to proliferate, surrounding the dental papilla to resemble a cap on the papilla’s “head”. This epithelial ingrowth becomes known as the dental organ (**Figure 1.3**), which, amongst other things, will provide the ameloblast cells which form the tooth enamel (Sasagawa and Ishiyama, 2005).

Surrounding the dental papilla and tip of the dental organ is a condensed lining of ectomesenchyme known as the dental follicle. Once the tooth is fully formed the cells of the dental follicle express key chemotactic agents which cause an influx of mononuclear cells, these cells fuse to become osteoclasts, which resorb the overlying alveolar bone to provide an eruptive pathway for the tooth (Marks *et al*, 1983; Wise *et al*, 1985). Once this process is finalised, the dental follicle gives rise to the periodontal ligament and cementum (Morsczech *et al*, 2005).

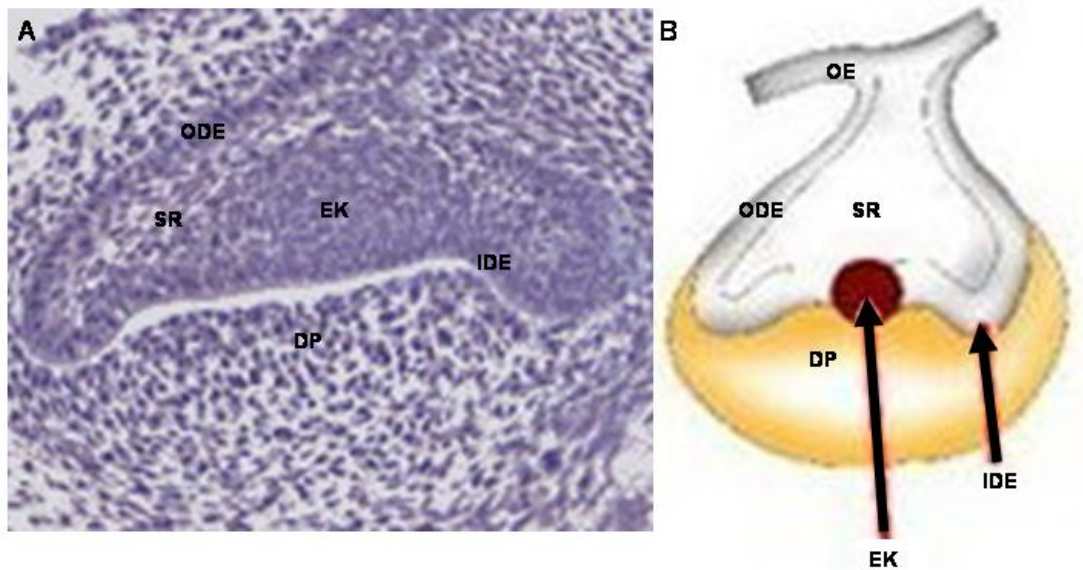


Figure 1.3: **A:** Histological image of developing rat molar in cap stage of development. Adapted from Hosoya *et al*, 2006. **B:** Schematic diagram of developing tooth at cap stage. Adapted from Thesleff, 2003. **OE** = Oral epithelium. **IDE** = Inner dental epithelium. **ODE** = Outer dental epithelium. **SR** = Stellate reticulum. **EK** = Enamel knot.

The final morphological stage of tooth development is known as the bell stage (**Figure 1.4**). It is during this stage that the cells of the dental organ begin to undergo histodifferentiation. The central area of the dental organ differentiates into a population of large, star shaped cells with large extracellular regions known as the stellate reticulum (Sasaki, 1990), and the cells in contact with the dental papilla differentiate into inner dental epithelium cells following a highly controlled signalling cascade originating from the basement membrane. These cells in turn differentiate into ameloblasts, the cells responsible for the formation of enamel, following the growth factor signals received from a layer of cells separating them from the stellate reticulum known as the stratum intermedium (Ten Cate, 1998; Sasagawa and Ishiyama, 2005). It is also during this stage that the tooth “bell” disassociates from the oral epithelium and the future crown shape becomes apparent (histologically resembling a bell shape), due to the ingrowth of the inner dental epithelial cells into the dental organ.

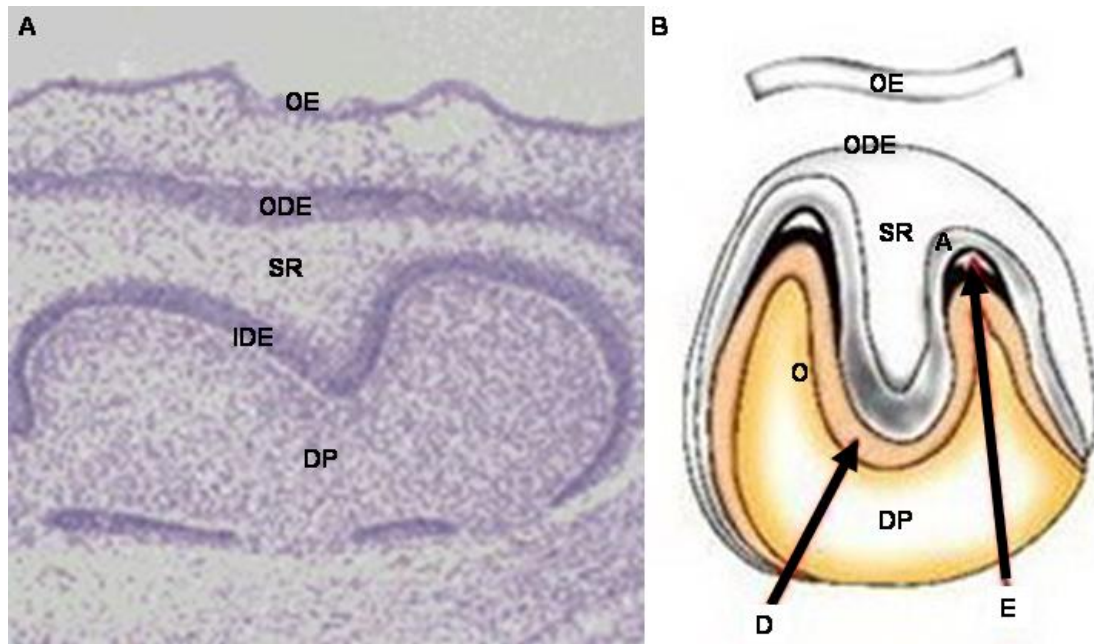


Figure 1.4: **A:** Histological image of developing rat molar in early bell stage of development. Adapted from Hosoya *et al*, 2006. **B:** Schematic diagram of developing tooth at late bell stage. Adapted from Thesleff, 2003. **OE** = Oral epithelium. **IDE** = Inner dental epithelium. **ODE** = Outer dental epithelium. **DP** = Dental pulp. **SR** = Stellate reticulum. **E** = Enamel. **D** = dentin.

1.4.2.3 Odontogenesis

Following the formation of the future crown shape, the next stage of tooth development results in the generation of the tooth's hard tissues, dentine and enamel (**Figure 1.5**). This is initiated as the cells of the inner dental epithelium cease to proliferate at the future cusp tip of the tooth. As the cells stop proliferating they begin to differentiate into tall, columnar cells with their nuclei positioned at the dental organ end of the cell and are now ameloblasts, the cells responsible for enamel formation. As they are differentiating, they release a series of signalling molecules to the cells of the dental papilla, which subsequently differentiate into odontoblasts, which synthesise and secrete dentine.

As the odontoblasts differentiate they initially produce unmineralised type I collagen and proteoglycans (Linde & Goldberg, 1993; Torneck, 1994), which is deposited between the odontoblast and the ameloblast cell layers, forming a type of pre-dentine with a ground substance present by the basal lamina. This process is

followed by the secretion of mantle dentine, which mineralises within matrix vesicles formed from buds that develop from the membrane of the odontoblast processes (Stratmann *et al*, 1995). Mantle dentine is less mineralised than primary dentine and resides at the periphery of the dentine, at the dentino-enamel junction. As dentine deposition continues, the odontoblasts secrete dentine whilst migrating towards the centre of the papilla, as they migrate they create cytoplasmic, odontoblast processes around which primary dentine is secreted. These remain embedded within the dentine giving rise to the tubular nature of the dentine matrix. Inside these dentine tubules peritubular dentine is formed, as has been demonstrated through ultrastructural, electron microscope studies of human molars (Thomas, 1979; Linde & Goldberg, 1993; Torneck, 1994).

As the first dentine is being secreted (mantle dentinogenesis), the fully differentiated ameloblasts begin secreting their own partially mineralised organic matrix against the newly formed dentin. This rapidly mineralises to form enamel, and as the enamel begins to form the ameloblasts begin to migrate away from the dental papilla, depositing increasing amounts of enamel.

Once the tooth is fully formed the odontoblasts once again undergo a series of morphological changes that are associated with a pronounced down-regulation in dentine production. In this state the odontoblasts produce relatively low amounts of dentine whilst staying viable throughout the tooth's life (Linde & Goldberg, 1993; Torneck, 1994; Ten Cate, 1998).

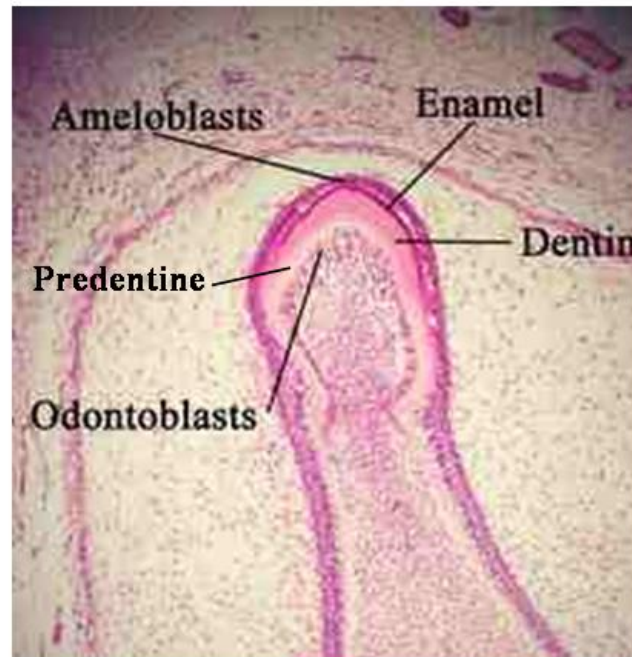


Figure 1.5: Histological image of developing molar during the deposition of the tooth's hard tissue, dentine and enamel.

1.4.2.4 Molecular Regulation of Odontoblast Differentiation

Odontoblast differentiation is a complex process controlled by cells of the inner dental epithelium, through a series of cell-cell signalling events. Therefore, despite the majority of dental papilla cells having the potential to differentiate, only those cells in contact with the basement membrane at its interface with the inner dental epithelium become odontoblasts (Ruch, 1998).

The exact molecular interactions involved in odontoblast differentiation are, as yet, not completely understood. Research has however demonstrated that several growth factors, including members of the TGF- β , IGF and FGF families, have been implicated in signalling this process. Many of these molecules are demonstrably expressed in the cells of the inner dental epithelium, the odontoblasts, or both, at the time of differentiation (Cam *et al*, 1992; Bégue-Kirn *et al*, 1994; Helder *et al*, 1998; Russo *et al*, 1998). In addition, *in vitro* studies have demonstrated the involvement of

TGF- β 1, TGF- β 3, BMP2 and IGF-1 in odontoblast differentiation (Bégue-Kirn *et al*, 1992; Bégue-Kirn *et al*, 1994; Sloan and Smith, 1999; Ruch and Lesot, 2000).

The precise role of these growth factors and their signalling inter-relationship is still undetermined due to their simultaneous expression, their functional redundancy, and due to relevant genetic knock-out animal models arresting during, or prior to, tooth development (Bégue-Kirn *et al*, 1994; Helder *et al*, 1998).

1.5 Dental Tissue Disease - Caries

Dental caries affects 60-90% of school children and the majority of adults in industrialised countries, whilst it is increasingly prevalent in developing countries. It is now estimated that approximately 5 billion people of all ages worldwide suffer from some form of caries which not only causes pain but also inevitably a reduction in quality of life due to impairment of function (Rohr Inglehart and Bagramian, 2002; Petersen, 2003). Caries treatment in children alone is currently beyond the resources of some developing countries (Petersen, 2003; Yee and Sheiham, 2002).

Pathologically dental caries is characterized by the progressive destruction of dental hard tissues due to bacterial infection. Currently clinical treatment for restoring the tooth utilises materials that share few of the natural characteristics of a tooth, often resulting in a high proportion of restorations failing mechanically (Murray and Garcia-Godoy, 2004). In severe cases of dental caries, when the pulp is exposed, direct pulp capping utilising a protective agent, such as calcium hydroxide, is often applied which can induce natural dental repair process (Schröder, 1985), thought to be a result of the solubilisation of growth factors such as TGF- β 1 from the dentine matrix (Smith and Smith, 1998). It is therefore desirable for future dental treatments to develop a modality that promotes the natural reparative processes. Current opinions

suggest that such an approach would likely involve the use of growth factors to stimulate specific cellular responses in the dentine-pulp complex, similar to those seen during tooth development and repair, that would result in a directed enhancement of the natural healing process and somewhat restore tooth structure, rather than the simplistic mechanical treatments currently utilised. Thereby preserving pulpal tissue function, providing a long-term clinical solution and reducing the number of restorations failing (Smith 2003; Nakashima, 2005).

1.6 Molecular and Cellular Components of Dental Tissue Regeneration

Currently there are two characterised mechanisms of natural tooth regeneration that depend upon the intensity of injury sustained. These dental tissue regeneration mechanisms are termed reactionary and reparative dentinogenesis (**Figure 1.6**). Both mechanisms result in the formation and secretion of tertiary dentine matrix, which varies in structure from primary dentine and is often irregular with a reduction of tubular dentine (Tziafas *et al*, 2000). Tertiary dentine provides a barrier between the injury and the underlying dental tissue (Lesot *et al*, 1993; Smith *et al*, 1995).

During mild injury to the tooth, the undamaged odontoblasts are stimulated by molecular signals, understood to involve a cocktail of growth factors sequestered into the dentine matrix during dental tissue development. Following demineralisation by bacterial acids and other metabolites during caries these molecules are released, which subsequently result in an up-regulation in formation and secretion of dentine (Smith *et al*, 1995; Smith, 2003). Signals sequestered in the dentine matrix which are thought to play a role in the up-regulation of dentine secretion include IGF-1 (Bégué-Kirn *et al*, 1994), TGF- β 1 and TGF- β 3 (Sloan and Smith, 1999), and BMP7 (Sloan *et al*, 2000), all of which are capable of up-regulating dentine secretion *in vivo*. Notably, many of

these molecules involved in this mechanism are also important in dental tissue development (see **Section 1.4**). In addition, reactionary dentinogenesis has also been stimulated *in vivo* following implantation of dentine fragments into prepared, exposed cavities providing further evidence that the molecules sequestered within dentine during development are key to modulating post-natal repair mechanisms (Smith *et al*, 1994).

Reparative dentinogenesis occurs when the injury to the tooth is more intense, often exposing the pulpal tissue, causing death of the primary odontoblast layer. In this case a new generation of odontoblast-like cells are signalled to differentiate from pulp progenitor/stem cells, a process involving cell recruitment, cell differentiation and an up-regulation of dentin synthesis (Lesot *et al*, 1993; Smith *et al*, 1995).

Induction of odontoblast-like cell differentiation from progenitor cells involves several growth factors, once again those sequestered and released from the dentine matrix following demineralisation, including TGF- β isoforms, BMPs and IGFs (Finkleman *et al*, 1990; Bégue-Kirn *et al*, 1994; Cassidy *et al*, 1997; Butler, 1998; Sloan and Smith, 1999; Roberts-Clark and Smith, 2000; Smith, 2003).

Despite the differing odontoblast phenotype and dentine structure, the process of stem cell recruitment, odontoblast differentiation and the induction of dentine secretion from the new generation odontoblasts that occurs during reparative dentinogenesis are thought to closely mimic those of tooth development (Smith and Lesot, 2001) with the release of signalling molecules from the demineralised dentine imitating the signalling events of the inner dental epithelium. Whilst there are a number of molecules known to be common to both processes further work is required to elucidate their individual roles, as a number of the growth factors involved have similar functions, often overlapping with each other and each interacting with each

other in a complex manner. As well as the release of this bio-active cocktail from the dentine there is likely a co-ordinate release of growth factors by pulpal and inflammatory cells that could also aid the reparative response (Sloan *et al*, 2000).

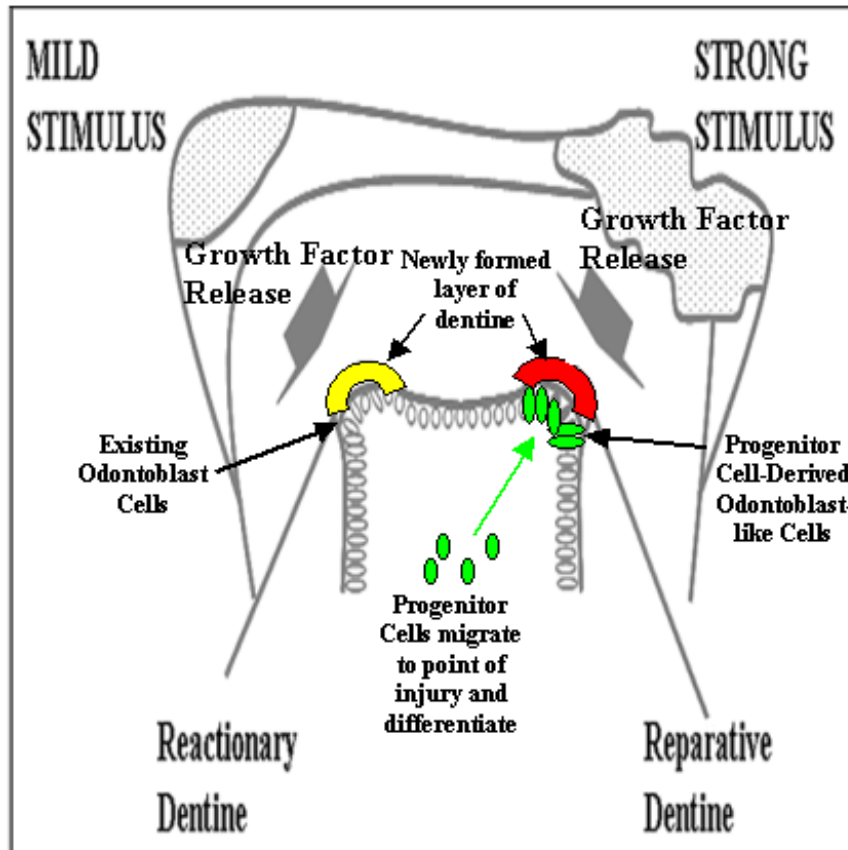


Figure 1.6: Schematic diagram showing the reactionary and reparative dentine deposition in response to mild and strong stimuli. Adapted from Smith *et al*, 1995.

1.7 Adrenomedullin (ADM) and its Potential Role in Dental Tissues

In a recent study analysing the genes differentially regulated in carious compared to healthy pulpal tissue, the ADM transcript was identified as being significantly up-regulated (McLachlan *et al*, 2002). In addition studies have now also demonstrated that ADM can be released from human dentine, at levels comparable or potentially higher than those of TGF- β 1, by dental cavity etchants and acids similar to those from cariogenic bacteria (Tomson *et al*, 2007; L. Graham - PhD Thesis). This data indicates that ADM is likely expressed during tooth development by odontoblasts and deposited into the dentine matrix, this is somewhat supported by data presented by Montuenga *et al* (1997), who published a paper studying ADM's expression pattern during embryogenesis which included an image of a developing tooth expressing ADM. It's release from the dentine matrix during tooth injury may therefore promote repair processes potentially in synergy with other dentine matrix signalling molecules.

ADM is a pleiotropic molecule known to be up-regulated in several diseased states (Bunton *et al*, 2004) such as congestive heart failure (Kobayashi *et al*, 1996), sepsis (Hirati *et al*, 1996), myocardial infarction (Asakawa *et al*, 2001) and renal impairment (Ishihara *et al*, 1999), where it potentially may function in several distinct ways. Notably ADM been demonstrated to act as a regulator of i) inflammation, including inducing ocular inflammation through increasing inflammation cell number in rabbits (Clementi *et al*, 2000) and reducing glomerular inflammation by reducing monocyte chemoattractant protein-1 (MCP-1) expression and subsequently glomerular monocyte infiltration (Plank *et al*, 2005) (for full review of ADM's role in inflammation see Elsasser and Kahl, 2002), ii) apoptosis, where ADM can act as both antiapoptotic and proapoptotic, promoting cell survival in vascular endothelial cells

(Kato *et al*, 1997) and astrocytes, an effect reversed by the addition of an ADM antagonist, (Xia *et al*, 2004), while inducing apoptosis in glomerular mesangial cells (Parameswaran *et al*, 1999) (for review see Filippatos *et al*, 2001), iii) cell migration, where Xia *et al*, (2004) demonstrated that ADM dose dependently enhanced astrocyte migration in modified Boyden chambers and iv) angiogenesis and vasodilation, enhancing capillary-like tube formation and blood vessel formation, an effect reversed by the addition of an ADM antagonist (Ribatti *et al*, 2003) and increasing arteriole diameter and lowering blood pressure in streptozotocin induced rats (Kaneko *et al*, 2006) (for review see Ribatti *et al*, 2007). In addition, it can function as an inducer of osteoblastic activity, increasing osteoblast cell number *in vitro* and increasing indexes of bone formation and mineralized bone area of mouse calvaria *in vivo* (Cornish *et al*, 1997). Furthermore, both immunohistochemical and *in situ* hybridisation studies have demonstrated a co-localisation of ADM and TGF- β 1 protein and mRNA during embryogenesis, including the giant trophoblastic cells of the early placenta and later in the developing cardiovascular, neural, lung, kidney, intestinal and skeletal-forming tissues (Montuenga *et al*, 1998).

ADM's up-regulation in carious teeth (McLachlan *et al*, 2002) could conceivably relate to its role(s) in inflammatory regulation, vasodilation and angiogenesis or cell survival promotion. However, data demonstrating that it is expressed during tooth development (Montuenga *et al*, 1997) combined with its ability to stimulate bone formation (Cornish *et al*, 1997) also suggests that ADM could be an important regulator of dental tissue development and regeneration.

1.7.1 ADM and ADM Receptors.

ADM is a 52 amino acid, pleiotropic peptide, initially isolated from human brain pheochromocytoma (Kitamura *et al*, 1993). It is part of the calcitonin gene-related peptide (CGRP) family and is known to be expressed in various adult and developing tissues including heart, lung, kidney and brain (Washimine *et al*, 1996; Cameron & Fleming, 1998; Montuenga *et al*, 1997; Montuenga *et al*, 1998).

ADM acts through two ADM-specific receptors (AM-1 and AM-2) which are comprised of a dimer of calcitonin receptor-like receptor (CRLR) and receptor activity modifying proteins 2 and 3 (RAMP-2 and RAMP-3, respectively) (McLatchie *et al*, 1998; Aiyar *et al*, 2001; Muff *et al*, 2001; Oliver *et al*, 2001), although no pharmacological difference with respect to ligand preference or signalling pathways stimulated has been identified between the two (Hay *et al*, 2003). ADM also exhibits affinity for the CRLR and RAMP1 complex however binding to this receptor is significantly weaker and this receptor is generally regarded as a CGRP receptor (Buhlmann *et al*, 1999).

CRLR is a member of the family-B G-protein coupled receptors (GPCRs) which contain seven transmembrane domains and share approximately 50% homology to the calcitonin receptor. CRLR was first cloned in 1993 by Chang *et al*, and was initially considered an orphan receptor until McLatchie *et al* (1998) discovered that, in the presence of RAMPs, the CRLRs were transported to the cell surface and became active receptors for the CGRP family.

Studies have suggested that binding of the ADM ligand to its receptors appears reliant on the cyclic structure formed by ADM's disulfide bridge and the C-terminal residue (Eguchi *et al*, 1994). This observation potentially explains how the ADM antagonist, ADM₂₂₋₅₂ (Eguchi *et al*, 1994; Hay *et al*, 2003) functions, as this

molecule retains the C-terminal residue allowing it to partially bind the receptor without leading to its activation, hence acting as a low affinity competitive inhibitor (Eguchi *et al*, 1994; Hay *et al*, 2003). Once ADM has bound to its receptor it can reportedly stimulate two signalling pathways involving either cAMP and/or Ca²⁺, in order to induce its cellular physiological affects (Shimekake *et al*, 1995; Xu and Krukoff, 2005).

1.7.2 ADM in Development.

Mammalian development and organogenesis is a complex process involving a series of instructive and permissive cell-cell interactions (Wessells, 1977) and whilst some signalling pathways are well characterized, for example chick embryo limb bud pathways (Johnson and Tabin, 1997), the majority of mammalian regulatory pathways are still unknown.

Adrenomedullin is thought to play an important role in mammalian development (for review see Garayoa *et al*, 2002). ADM signalling has been indicated in a number of embryonic tissue during rat and mouse development. It's expression is limited to small regions of the embryo at the early stages of embryogenesis such as the giant trophoblastic cells of the ectoplacental cone, during early placenta development (Montuenga *et al*, 1997; Yotsumotu *et al*, 1998). This is thought to be important in fetoplacental vasculogenesis and for providing nutrition and oxygen from maternal blood during early postimplantation (Yotsumotu *et al*, 1998). During the latter stages of development and organogenesis, it is expressed in the majority of tissues and organs. It's expression is first detected in the developing heart, which remains the most immunoreactive organ for ADM expression throughout development, notably in the walls of the atrial and ventricular walls and in the

differentiating smooth muscle cells of the large arteries (Montuenga *et al*, 1997; Montuenga *et al*, 1998). Other organs demonstrating ADM expression during development include the nervous system, where ADM expression has been suggested to appear parallel to sensory neuron maturation, the skeletal-forming tissues, with osteoblasts of the developing bone continuously expressing ADM and maturing cartilage becoming increasingly immunoreactive for ADM. Interestingly, regions in which epithelial-mesenchymal interactions occur such as the lung, kidney, tooth and intestines also demonstrate ADM expression at key developmental time points, particularly the meschyme surrounding developing brochi in the lungs, the epithelium of the metanephric duct and the metanephric collecting tubules of the kidney, what appears to be the odontoblasts of the developing tooth and in the mesenchymal cells that will form the gut muscle layer during early intestine development and later in the differentiated simple columnar intestinal epithelium (Montuenga *et al*, 1997; Montuenga *et al*, 1998).

The exact mechanism(s) of action(s) of ADM during development has yet to be entirely elucidated, partially due to ADM knockout mice being embryonically lethal (Ando and Fujita, 2003). However, ADM's activity is thought to regulate embryogenesis by controlling cell proliferation, differentiation and migration. Supporting data is provided from ADM's expression patterns (Montuenga *et al*, 1997; Montuenga *et al*, 1998), it's known mitogenic affect on many embryonic and neonatal derived cell lines, including those derived from rat osteoblasts (Cornish *et al*, 1997), rat cardiac fibroblasts (Tsuruda *et al*, 1999) and other embryonic-derived fibroblasts (Isumi *et al*, 1998; Coppock *et al*, 1999), ADM's expression in embryonic tissues and organs apparently coinciding with the onset of the differentiation process, for example in bone, the cells of the nervous tissue and areas of placental vasculogenesis

(Montuenga *et al*, 1997) and with a number of chemotactic cell processes present in the embryo, for example neural crest-derived cell migration (Montuenga *et al*, 1997) and its ability to enhance cell migration *in vivo* (Xia *et al*, 2004).

Notably ADM's spatio-temporal expression pattern is somewhat similar to that of other growth factors known to be important in mammalian development. For example in the developing kidney ADM appears to share very specific spatial and temporal expression patterns with insulin growth factors (IGFs), platelet – derived growth factor (PDGF) and members of the TGF- β family (Hammerman, 1995; Montuenga *et al*, 1997). The embryonic expression of members of the latter of these growth factor families was directly comparable to that of ADM. In particular it was reported that TGF- β 1 and ADM exhibited an overlapping expression pattern as both were concurrently present in several developmental tissues within the same cell types, indicating a potential inter-relationship between the two (Montuenga *et al*, 1998). Recently it has been shown that TGF- β 1 and ADM can act to suppress the expression of each other, with ADM also acting through the intracellular signal transducer Smad6 (Huang *et al*, 2005). While, studies using TGF- β 1 null mutant mice demonstrate a reduction in embryonic ADM expression (Bodegas *et al*, 2004), also indicating that a positive feedback mechanism may exist between the two molecules.

Overall, ADM's potential to induce proliferation, differentiation and migration in developmental cell-lines, coupled with its apparent abundant expression in areas involving key epithelial-mesenchymal interactions occurring during development suggest that ADM's role in tooth development warrants further investigation.

1.8 Transforming Growth Factor-Beta 1 (TGF- β 1)

TGF- β 1 was initially isolated from human platelet cells (Assoian *et al*, 1983) and is a multifunctional member of the TGF- β -superfamily of cytokines. TGF- β 1 plays important roles in regulating cell proliferation, inducing proliferation in the human osteoblast cell lines hMS(OB) and hOB (Kassem *et al*, 2000), while inhibiting proliferation in primary rabbit epithelial cells and rat heart endothelial cells, possibly through altering the cells' response to other growth factors (Takehara *et al*, 1987; Rotello *et al*, 1991), it's been demonstrated to both inhibit and induce the differentiation of osteoblasts and periodontal cells *in vitro* (Erlebacher *et al*, 1998; Chien *et al*, 1999; Spinella-Jaegle *et al*, 2001), it increases fibroblast and glioma cell migration *in vitro* (Cordeiro *et al*, 2000; Platten *et al*, 2000), can induce apoptosis in lymphocytes and podocytes (Lomo *et al*, 1995; Schiffer *et al*, 2001), inhibit apoptosis in myofibroblasts (Zhang and Phan, 1999) and induces the secretion of extracellular matrix in fibroblasts (Ihn, 2002). It has also demonstrated both pro-and anti-inflammatory properties (Brandes *et al*, 1991; Echeverry *et al*, 2009) and is released during tissue injury by inflammatory cells exposed to bacteria (Wahl *et al*, 1993). During disease TGF- β 1 is key to modulating the immune response and is well characterized in this context for example in rheumatoid arthritis and periodontal disease (Wahl *et al*, 1993; Skaleric *et al*; 1997).

TGF- β 1 exerts its cellular activity via binding its receptors, TGF- β RI and TGF- β RII, which are members of a transmembrane serine/threonine kinase receptor family. There is also a TGF- β RIII betaglycan receptor which does not contain an intracellular signalling domain but is thought to be important in retaining TGF- β 1 on the cell surface for presentation to TGF- β RI and TGF- β RII (Massagué, 1992; Lin and Lodish, 1993; Lopez-Casillas *et al*, 1993; Massagué, 1996). TGF- β 1 binds to TGF-

β RII, which dimerises with TGF- β RI resulting in the phosphorylation of a group of intracellular messengers called Smads (Massagué *et al.*, 2000; He *et al.*, 2001; Xu *et al.*, 2003).

In embryogenesis, members of the TGF- β superfamily, including TGF- β 1, are expressed in specific temporo-spatial patterns and are important in regulating the formation of various craniofacial structures (Chai *et al.*, 1994; Kaartinen *et al.*, 1995; Proetzel *et al.*, 1995; Sanford *et al.*, 1997). Attempts to develop TGF- β 1 knock-out mice to study its role during embryonic development have invariably failed due to embryonic growth arrest. TGF- β 1 null mutant mice have resulted in defective organ and vascular development resulting in pre-natal lethality indicating the pivotal role TGF- β 1 plays in regulating cell differentiation and cellular modulation during early embryogenesis (Dickson *et al.*, 1995).

In mineralised tissues, TGF- β 1 plays a key role in proliferation, differentiation and mineralisation processes. In bone, it has been proven to increase rat calvarial and human osteoblast proliferation (Bonewald *et al.*, 1994), whilst also potentially being a key mediator of bone resorption and deposition (Chen and Bates, 1993). In tooth development TGF- β 1 is essential for maintaining the homeostasis of the dentine-pulp complex (D'Souza *et al.*, 1998). In the developing tooth, expression of TGF- β 1 has been detected within the cells of the inner dental epithelium. Once histodifferentiation begins expression switches to pre-odontoblasts where it continues to be expressed throughout dentine secretion (Vaahtokari *et al.*, 1991; Begue-Kirn *et al.*, 1994), expression then decreases once the odontoblasts reach maturity and down-regulate their dentine secretory activity (Begue-Kirn *et al.*, 1994). Furthermore, *in vitro* and *in vivo* studies have demonstrated TGF- β 1 has the ability to initiate odontoblast differentiation and stimulate the synthesis of extracellular matrix (Sloan and Smith;

1999; Sloan *et al*, 2000; Unda *et al*, 2001). TGF- β 1 is also present in the cocktail of bioactive molecules released from dentine (Cassidy *et al*, 1997), which have demonstrable ability to induce odontoblast differentiation and mineralisation (Smith *et al*, 1995; Smith and Lesot, 2001; Liu *et al*, 2007).

The expression of TGF- β 1 during tooth development along with ADM therefore warrant further characterisation. Their reported sharing of similar temporo-spatial expression patterns during embryogenesis (Montuenga *et al*, 1998) along with their ability to modulate each others activity (Huang *et al*, 2005) is suggestive of a possible synergistic or antagonistic relationship during tooth development.

1.9 Role of Glucocorticoids in Mineralisation

Dexamethasone is arguably the best-characterized synthetic member of the glucocorticoid family of steroid hormones. Therapeutically it is commonly used in a wide range of treatments including the reduction of meningitis associated inflammation (van de Beek *et al*, 2007), controlling side effects associated with chemotherapy (Ioannidis *et al*, 2000) and is also used in obstetrics to promote foetal lung development in premature babies (Bloom *et al*, 2001).

In vitro, dexamethasone also has well characterised ability to induce mineralisation processes (Cheng *et al*, 1996; Hildebrandt *et al*, 2009) and can promote the differentiation of MC3T3 cells, bone marrow stromal cells, umbilical blood mesenchymal stem cells and dental papilla-derived cells into osteoblasts (Quarles *et al*, 1992; Cheng *et al*, 1994; Kosmacheva *et al*, 2008; Park *et al*, 2009).

Dexamethasone is thought to elicit it's mineralising and differentiating effects through the expression of key matrix proteins Bone Sialoprotein (BSP), Osteocalcin (OCN) and Osteopontin (OPN) (Cheng *et al*, 1996; Mikami *et al*, 2007), regulated through

the transcription factor *Runx2* (Mikami *et al*, 2007). Notably when dexamethasone is used in concordance with TGF- β 1 it promotes the differentiation of umbilical blood mesenchymal stem cells into chondrocytes (Kosmacheva *et al*, 2008).

In relation to dental effects, interestingly, long term treatment with glucocorticoids have been implicated in the narrowing of the pulpal chamber in humans and rats, thought to be a result of increased stimulation of the secretion of a new layer of dentine (Näsström *et al*, 1985; Näsström, 1996; Symons *et al*, 2000). Paradoxically, glucocorticoids have also demonstrated an ability to induce rapid bone loss and are thought to increase the risk of osteoporosis (Canalis, 2005), a result of decreased calcium levels caused by reduced absorption in the small intestines (Weiler *et al*, 1995).

Dexamethasone is a known regulator of ADM expression as well as the ADM-related receptors, CRLR, RAMP-2 and RAMP-3. Such regulation has been demonstrated in several different cell types including myocytes, smooth muscle cells, retinal pigment epithelial cells and osteoblasts (Nishimori *et al*, 1997; Hattori *et al*, 1999; Frayon *et al*, 2000; Udono-Fujimori *et al*, 2004 and Uzan *et al*, 2004). Notably, ADM and the ADM receptor, calcitonin gene related peptide (CRLR) have now been identified as containing a glucocorticoid receptor element in their regulatory sequences (Nikitenko *et al*, 2003; Zudaire *et al*, 2005) suggesting a potential for a component of dexamethasone's cellular effects to be mediated via regulation of ADM signalling mechanisms. Hence the regulation of ADM and associated cellular, biochemical, molecular and mineralisation responses due to dexamethasone in dental cells and tissues warrants further investigation.

1.10 *In vivo*, *ex vivo* and *in vitro* approaches used for studying mineralised tissue biology

1.10.1 *In vivo* experimental models

In vivo research approaches are generally the preferred method of biological study as they allow determination of the relevant systemic impact of the experimentations.

However, such studies can be incredibly complex and are constrained by ethical considerations in humans. Therefore this work in general utilises animals, primarily rats and mice, as alternative relevant model systems. This also carries specific ethical issues and experiments involving animals are subject to individual scrutiny by the home office and can only be used if the expected benefit outweighs the adverse effects and if there is no alternative research technique. The breeding and supply of animals for scientific use is also regulated by the home office, with the Animals (Scientific Procedure) Act 1986 (Home office website). Such analyses however also present limitations in particular due to inter-species differences in genetic make-up.

One of the most common methods of *in vivo* study involves the use of gene knockout mice which utilises genetically engineered mice in which one or more genes are inactivated, this is a reliable experimental model of *in vivo* study as it allows researchers to study the exact systemic role of each knock-out gene. Technologically, they are generated by the introduction of a DNA vector into embryonic stem cells harvested from early stage mouse embryos. Subsequently homologous recombination events are used to inactivate the target gene(s) and the embryonic stem cells generated are cultured for several days before being injected into blastocyst mouse embryos prior to implantation in a surrogate female mouse for further development. The implanted embryos contain both engineered and normal embryonic stem cells,

resulting in heterozygous knockouts, which are subsequently crossbred to produce homozygous mutant animals (Melton, 1994; Bedell *et al*, 1997).

Limitations which associate with this technology predominantly include early embryonic lethality which affects approximately 15 percent of gene knockouts made and which make it impossible to study the effects of the mutations in the adult animal or even at late stages of embryonic development. This problem can however be overcome by the use of conditional mutants whereby genes can be inactivated at later stages of development. The resulting phenotype using this approach, however, is not necessarily representative of the full effect of gene deletion. Other limitations of this technology include differing roles of genes during development and adulthood, making the study of gene knockouts in adults troublesome if the gene is important in developmental processes, and varying effects in different species, meaning the role a gene might play in the development of a mouse may not correspond to its role in humans. Despite these limitations, knockout mice are still a key tool for determining gene function *in vivo* (Hardouin & Nagy, 2000).

In mineralised tissue development, knockout mice have been used to study the role of several growth and transcription factors, including members of the TGF- β family (D'Souza and Litz, 1995; Letterio and Roberts, 1996; Atti *et al*, 2002), BMPs (Bandyopadhyay *et al*, 2006; Retting *et al*, 2009), FGFs (Naganawa *et al*, 2008), Msx-1 and -2 (Satokata *et al*, 2000; Han *et al*, 2007) and Pitx2 (Lin *et al*, 1999). Notably Adrenomedullin knockout mice were found to be embryonic lethal, however ADM^{+/-} heterozygous mice were viable and fertile (Ando and Fujita, 2003). Unfortunately, subsequent studies have focused on ADM's effect on vascular tissues (Ando and Fujita, 2003) and as such no information is reported on the development of mineralising tissues in ADM^{+/-} mice.

Other experimental models utilised to study the *in vivo* effects of growth factors on mineralising tissues include injection supplementation and, in dental tissues, the introduction of cavities to study tooth regeneration (Goldberg *et al*, 2001; Zhang *et al*, 2006; Simon *et al*, 2008), discussed in the next paragraph. Injection supplementation involves dosing the animal with the molecule via a series of local or systemic injections over a designated time period. An example of this approach used for mineralised tissue research is that described by Cornish *et al* (1997; 2001). In their initial study (Cornish *et al*, 1997), adult mice were subjected to local injections of ADM directly over the calvaria for a five-day period. Subsequent analysis revealed that indices of bone formation and mineralised bone area within the calvaria were increased. In the second study Cornish *et al*, (2001) administered subcutaneous injections of ADM into the loose skin at the nape of the neck over a four-week period. This approach enabled the study of the systemic effect of ADM on bone growth and identified an increase in the indices of osteoblast activity, osteoid perimeter, osteoblast perimeter, cortical width, trabecular bone volume and bone strength (Cornish *et al*, 2001). A limiting factor in the use of systemic injections as a means to study growth factors *in vivo* is their stability within the vascular system, which will vary depending on liver metabolism of the individual animals. Notably degradation of the growth factor will therefore significantly reduce the amount present in the target tissue.

A method used to study tooth regeneration *in vivo* involves the introduction of type V cavities into animal teeth. Type V cavities are defined as being of either i) moderate size and positioned in close proximity to gingival tissue, therefore in a position that is difficult to access and treat, or ii) severe carious lesions that results in a reduction in tooth structure (Mount and Hume, 1998). Significant research utilising

this experimental method involves the application of substances for pulp capping to the exposed cavities, such as calcium hydroxide and mineral trioxide aggregate (Zhang *et al*, 2006; Simon *et al*, 2008), dentine matrix proteins (Goldberg *et al*, 2001) and growth factor soaked beads (Goldberg *et al*, 2001). This approach provides a valuable method for studying tissue responses in physiological conditions however the use of relevant controls requires important consideration.

Methods for studying the effects of these *in vivo* experimental approaches include histological investigation, analysis of protein/mRNA expression, Fourier transform infrared spectroscopy (FTIR) and more recently micro-computed tomography analysis.

Histological investigations include any study of the tissues or cells as a whole. In mineralised tissues this generally involves the analysis of trabecular bone volume, dentine bridge formation and increases in osteoblast and odontoblast morphology (Cornish *et al*, 1997; Cornish *et al*, 2001; Simon *et al*, 2008; Six *et al*, 2000; Zhang *et al*, 2006).

Analysis of protein/mRNA expression is a fundamental tool in *in vivo* studies as it allows the researchers to determine what tissues/cells the protein of interest is expressed in, at what time point and by comparing them to control specimens they can determine whether the protein of interest is up- or down-regulated. Some histological methods that are employed to determine protein/mRNA expression include *in situ* hybridization and immunohistochemistry.

In situ hybridization is a method that utilises radio-, fluorescent- or digoxigenin-labelled cDNA or RNA probes to hybridize to complementary DNA or mRNA within tissues of interest (Schaeren-Wiemers and Gerfin-Moser, 1993; Jin and Lloyd, 1997). The use of fluorescent cDNA probes is generally used to determine the

integrity of chromosomes in medical diagnostics, for example the detection of trisomy in chromosome 21 (Pinkel *et al*, 1988). The hybridization of mRNA allows for the localisation of gene expression within the tissue of interest and has been utilised in mineralised tissue research to localise the expression of DMP-1 in the chondrocytes, cementoblasts, osteoblasts, ameloblasts and odontoblasts of embryonic and post-natal mice (Feng *et al*, 2003) and to localise the expression of osteopontin and bone sialoprotein to the osteoblasts, chondrocytes and cementoblasts of embryonic mice, the expression of osteonectin to the osteoblasts, chondrocytes and odontoblasts of embryonic mice and osteocalcin to the osteoblasts and odontoblasts of developing mice (Sommer *et al*, 1996).

Immunohistochemical approaches enable determination of the expression and localisation of specific proteins within the cells and tissues of interest. Briefly, this method uses a biotinylated primary antibody specific to the antigen of the protein of interest. This is then bound by a secondary enzyme-labelled antibody, which reacts with 3,3'-diaminobenzidine (DAB) to produce brown staining which can be visualised by light microscope, an alternative to this method is conjugating the secondary antibody to a fluorescent agent, or fluorophore, which allows visualisation using a fluorescent or confocal microscope (Ramos-Vara, 2005). This approach has been used to determine the expression pattern of ADM during embryogenesis where it was found to be expressed in the heart, lungs, kidney, skeletal forming tissues, neural system and developing teeth of embryonic mice (Montuenga *et al*, 1997; Montuenga *et al*, 1998).

Fourier transform infrared spectroscopy (FTIR) is an analytical technique that is used to measure the absorption of infrared radiation that is passed through an organic sample. Each sample will produce a unique wavelength, characteristic of its

molecular structure, allowing the identification and quantification of organic materials. In mineralised tissue research this technique is often used to quantify the presence of mineralised tissue, this is usually analysed through the measurement of apatite phosphates which produce a wavelength of approximately $900-1200\text{cm}^{-1}$ (Rey *et al*, 1991). An example of the application of this techniques was described for the analysis of variations in the quantity and quality of cortical and trabecular bone, by measuring mineral:matrix ratios (Paschalis *et al*, 1997).

Micro-computed tomography (μCT) can also be used to analyse mineralised tissue deposition *in vivo*, with a number of companies producing scanners of high quality including GE Healthcare (USA), Skyscan (Belgium) and Nanotom (US). μCT utilises X-ray technology to create 2-dimensional (2D) cross sectional images of 3-dimensional (3D) objects. μCT works in the same way as X-ray tomography systems (CAT scans) currently used in medicine, however the term ‘micro’ is used to indicate the pixel size of the 2D cross sectional images, i.e. pixels are in the μm range, enabling higher resolution images to be captured [e.g. $<1\mu\text{m}$ using the high resolution Skyscan 1172 (Skyscan, Belgium)] (Holdsworth and Thornton, 2002). Due to the high resolution images current μCT scanners are capable of generating they are often used to create reconstructions of relatively small objects [e.g. maximum sample size of 68mm in Skyscan 1172 (Skyscan, Belgium)] (Holdsworth and Thornton, 2002).

μCT analysis has been used in a variety of research areas for both quantitative and qualitative determinations. Examples include in palaeontology, where μCT provides a wealth of qualitative taxonomical data on fossils, especially those preserved in amber (Dierick *et al*, 2007), geology, where both qualitative and quantitative analyses have been studied, including quantitative analysis of the porosity of rocks (Cnudde *et al*, 2006), the study of composite materials, including quantitative

measurement of polymer fibre length and qualitative analysis of fibre distribution (Shen *et al*, 2004) and food studies where quantitative analysis includes measurement of apple porosity (Mendoza *et al*, 2007). More frequent application has been in the biomedical science areas of bone and tooth biology (Andreoni *et al*, 1997). In bone biology uses have ranged from quantitatively measuring trabecular bone thickness to qualitatively determining differences in the architecture of mandibular bone (Saha and Wehrli, 2004; Mulder *et al*, 2006). For dental research, applications have included structural evaluation of root canal treatments and restorative procedure success, while quantitative analyses have included determination of cavity size and measuring pulpal chamber volume (Bergmans *et al*, 2001; Oi *et al*, 2004, Amano *et al*, 2006; Magne, 2006). An example 2D image along with digitised analysis of a mouse mandible obtained from the present study, using a Skyscan 1172, is shown in **Figure 1.7** to demonstrate the high resolution analysis which can be performed using this technology.

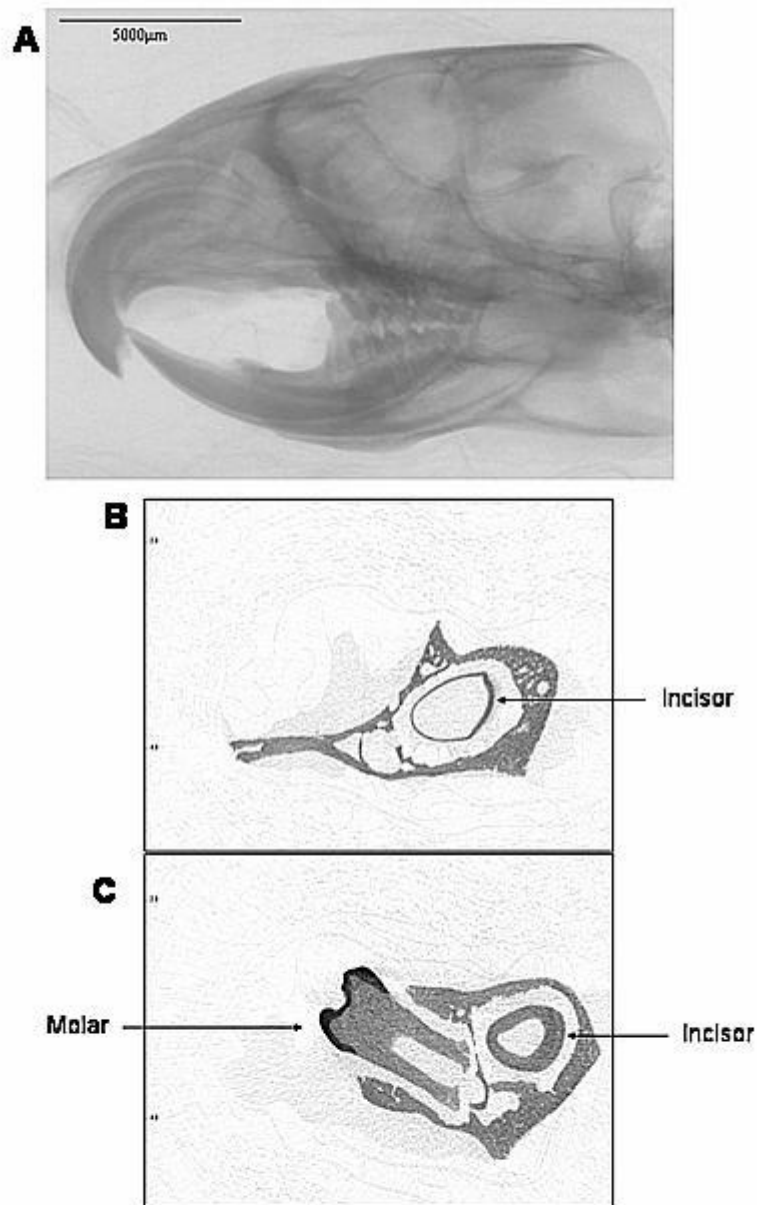


Figure 1.7: **A:** Two dimensional representative X-Ray image obtained from an adult male Swiss mouse crania-facial region using μ CT analysis. Scale bar is shown. **B & C:** 2D bitmap cross sectional images obtained from the reconstruction of the X-ray images CTRecon (Skyscan, Belgium).

1.10.2 *Ex vivo* experimental models

Ex vivo studies refer to experimental approaches that involve analysis of living cells or tissues taken from an organism and cultured in a laboratory. These studies provide a bridge between *in vitro* and *in vivo* studies as the cells or tissues used are generally more representative of the *in vivo* situation whilst being analysed under well-controlled laboratory conditions. *Ex vivo* differs from *in vitro* in that *ex vivo* involve cells/tissues extracted from organisms and experiments occur outside the organism with minimum alterations to natural conditions and are limited to a time period, usually no more than 24 hours, these are invariably multicellular and 3D in arrangement. While *in vitro* generally refers to experiments on cells in a controlled environment, which rarely mimic the natural environments, such as petri dishes.

Commonly used *ex vivo* models for mineralised tissue research include organ culture approaches, whereby slices of bone, usually the calvaria or tibia (Mueller and Richards, 2004; Mohammed *et al*, 2008), and teeth, primarily incisor (Sloan *et al*, 1998), are removed and maintained in growth media. This technique allows for direct stimulation of mineralised tissues with growth factors of interest in an environment that preserves much of the architecture and cellular diversity present *in vivo*, yet offers greater physiological relevance than cell cultures (see below section **1.10.3**). Such an approach is especially important in tooth biology where it has been demonstrated that odontoblasts require contact with the dentine matrix in order to retain their phenotypic morphology and secretory activity (Munksgaard *et al*, 1978; Heywood and Appleton, 1984). Organ culture approaches can be used for many purposes, including the determination of expression patterns of key mineralising mediators through immunohistochemical study (Mueller and Richards, 2004) and the effect of local

administration of growth factor soaked agarose beads on extracellular matrix secretion (Smith and Sloan, 1999; Sloan *et al*, 2000).

1.10.3 *In vitro* experimental models

Due to the complexity involved in studying mineralised tissues *in vivo*, *in vitro* model systems have also been developed which include the use of primary cell cultures and cell lines. Whilst providing a relatively easy method of studying cell activity they have limitations which include alterations to cell phenotype that result from removal from their natural environment and therefore subsequent interpretation of data needs to be placed in context (Tjäderhane *et al*, 1998).

In mineralised tissue research a number of immortalised cell lines have been developed and are frequently used. There are an extensive number of cell generated for study of mineralisation tissue behaviour *in vitro*, a small sample of cells derived from bone lineages include the osteoblast-derived cell lines MC3T3-E1 cells (Kodama *et al*, 1981), adult human osteoblast (hOB) cells (Keeting *et al*, 1992), human fetal osteoblast (hFOB) cells (Harris *et al*, 1995) and osteosarcoma derived cell lines used as osteoblast-like cells such as SAOS-2 cells (Fogh and Trempe, 1975) and MG-63 cells (Heremans *et al*, 1978); while dentally derived cell lines include the odontoblast-like MDPC-23 cells (Hanks *et al*, 1998) and pulp-like OD-21 cells (Hanks *et al*, 1998) used in this study and a number of other odontoblast-like cells, including the immortalised MO6-G3 cell line (George *et al*, 1996). Murine skin fibroblast-derived 3T3 cells (Todaro and Green, 1963) are also often used as a control in this study as they frequently used in a range of diverse studies. More detailed application of some of these cell lines will be discussed below

MC3T3 cells are inherently pre-odontoblast cells derived from newborn mouse calvaria (Kodama *et al*, 1981), their name is derived from the tissue they are isolated from, mouse calvaria (MC) and their general growth pattern of tripling in number every three days (3T3) (Kodama *et al*, 1981). They are characterised by high alkaline phosphatase activity, their ability to respond to parathyroid hormone (PTH) and inducible collagen secretion (Kumegawa *et al*, 1994). Since this cell line was initially established, numerous sub-types have been isolated, some with an osteoblast-like ability to induce mineralisation while others remained inherently non-mineralising cells (Leis *et al*, 1997; Wang *et al*, 1999). MC3T3 cells are therefore still primarily used as a pre-osteoblast cell line with recent studies demonstrating their ability to mineralise following stimulation using low-intensity ultrasound (Unsworth *et al*, 2007) and the ability of dexamethasone and growth and transcription factors to initiate their differentiation into osteoblast-like cells (Quarles *et al*, 1992; Bergeron *et al*, 2007; Sun *et al*, 2008).

The hOB cell line was isolated from a 68 year old female and immortalised following transfection with the SV40 large and small T antigens (Keeting *et al*, 1992). These cells closely represent a mature osteoblast phenotype and are characterised by their expression of procollagen- α I, osteopontin, TGF- β 1, and interleukin-1 β (IL-1 β). Notably they have the ability to secrete a mineralised matrix following exposure to β -glycerophosphate (Keeting *et al*, 1992). hFOB cells were isolated from a spontaneous miscarriage and immortalised in a similar manner to hOB cells (Harris *et al*, 1995). hFOB cells are also characterised by their high alkaline phosphatase activity and prevalent expression of osteopontin, osteonectin, bone sialoprotein (BSP) and type I collagen (Harris *et al*, 1995). Studies using these cell lines have examined the effect

of growth factors on osteoblast differentiation and mineralisation (Eichner *et al*, 2002; Zhang *et al*, 2003).

Originally isolated from the osteosarcoma tumour of an 11 year old girl (Fogh and Trempe, 1975), SAOS-2 cells are well characterised in their osteoblast-like characteristics (Rodan *et al*, 1987; McQuillan *et al*, 1995). Indeed, these cells have demonstrated high alkaline phosphatase activity (Murray *et al*, 1987) and when compared to primary osteoblast cultures, a study of the expression profile of fifty eight cytokines, growth factors and their receptors showed high similarities between the two, although they do lack the expression of IL-1 β and IL-6 (Bilbe *et al*, 1996). These cells are often used in mineralised research, demonstrating the release of mineralisation forming matrix vesicles (Fedde, 1992), specifically from their microvilli (Thouverey *et al*, 2009), they have been used to study the role of interleukins in glucocorticoid-induced osteoporosis (Dovio *et al*, 2003) and have been used to study the efficacy of a number of plate coatings for potential use in implantation, showing increased cell integration and mineralisation on biosilica coated plates and RGD/bisphosphonate coated titanium compared to non-coated materials (Schröder *et al*, 2005; Beuvelot *et al*, 2009). However, it should be noted that there are doubts over their phenotypic stability when cultured over long periods (Hausser and Brenner, 2005).

MG-63 cells were first isolated from the osteosarcoma tumour of a 14 year old male (Heremans *et al*, 1978). Unlike the osteosarcoma derived SAOS-2 cell line, their alkaline phosphatase activity is not representative of primary osteoblast cultures (Clover and Gowen, 1994). However, a study into the expression profile of fifty eight cytokines, growth factors and their receptors, compared to primary osteoblast cultures, found them to be largely representative of said primary cells, although some

indiscretions were present, such as MG-63 expressing PDGF- β and a number of cytokine receptors, including TNF IR and IIR and IGF IIR, while primary osteoblast cells do not (Bilbe et al, 1996). MG-63 cells have been utilised in a number of mineralised research studies including the potential role of interleukins on glucocorticoid-induced osteoporosis (Dovio et al, 2003), the effect of glucose on MG-63 cell mineralisation, providing knowledge into diabetic osteoporosis (Wang *et al*, 2009) and have been used to study the efficacy of bone tissue regeneration scaffolds, determining that 3D microporous/macroporous magnesium-calcium phosphate scaffolds produce a higher level of attachment, proliferation and alkaline phosphatase activity in MG-63 cells than both macroporous and calcium phosphate cement scaffolds (Wei *et al*, 2010)

The MDCP-23 cell line represents cloned odontoblast-like cells derived from dental papilla cells from embryonic day 18 – 19 (E18-19) mouse mandibular molars (Hanks *et al*, 1998). These cells share characteristics with odontoblasts *in vivo*, including high alkaline phosphatase activity, similar morphology with multiple processes, and they are known to express several dental-specific molecular markers, including dentin sialoprotein (DSP) and dentin phosphoprotein (DPP) (Hanks *et al*, 1998; Sun *et al*, 1998). MDPC-23 cells have often been used in experiments *in vitro* as representative odontoblast models. Recently they have been used for studies on the biocompatibility of pulpal capping agents (Mantellini *et al*, 2005) and also as models for the analysis of the effects of growth factors, such as TGF- β 1, on odontoblasts (He *et al*, 2004; He *et al*, 2005). MDPC-23 cells do however exhibit limitations, including their lack of ability to express Dental matrix protein-1 (DMP-1), which is known to be produced by odontoblasts *in vivo* (Hanks *et al*, 1998). Furthermore, a characteristic of odontoblast cells *in vivo* is their cell cycle arrest. Therefore an odontoblast cell line

that is constantly undergoing cellular proliferation is inherently un-odontoblast-like in behaviour.

MO6-G3 cells are an immortalised odontoblast-like cell line (George *et al*, 1996) that is well characterised in its role in dentinogenesis research (MacDougall *et al*, 2001). It has been used to demonstrate the effect of growth factors on odontoblast cell lines, showing that TGF- β 1 is capable of downregulating DMP-1 and DSPP expression (Unterbrink *et al*, 2002). While recently, an ultrastructural analysis and immunocytochemical determination of dentine sialoprotein, alkaline phosphatase, type I collagen and actin filaments in MO6-G3 cells demonstrated that, over a period of 42 days, these cells retain their odontoblast phenotype and the characteristic morphodifferentiation pattern of polarized odontoblasts (Mesgouez *et al*, 2006).

OD-21 cells are a developmentally derived, pulp-like cell line, often used as an *in vitro* model for undifferentiated pulp cells (Hanks *et al*, 1998). These cells are also frequently used in similar experiments as the MDPC-23 cells, for example as a model for the analysis of the effects of pulpal capping agents (Mantellini *et al*, 2005) and the effect of bacterial invasion during caries (Botero *et al*, 2003). Due to the abundance of cell types within the dental pulp, experimental results often vary between primary pulp derived cultures, depending on which lineages are isolated (Goldberg and Smith, 2004), therefore the application of a well characterized cell line is often preferred.

The 3T3 cell line is a fibroblast-like culture established from the tissue of an albino Swiss mouse (*mus musculus*) embryo (Todaro and Green, 1963). Mouse 3T3 cells are frequently used in research as both a fibroblast-like cell line and as a developmental cell line. Notably several studies have analysed the effects of ADM on these cells, with findings demonstrating that ADM induces proliferation and regulates

cytokine release (Isumi *et al*, 1998). It has also been shown that 3T3 cells express both ADM and its related receptors (Withers *et al*, 1996; McLatchie *et al*, 1998).

In addition to the use of immortalised cell lines in mineralised tissue studies, primary cell lines are also commonly used. Primary cell cultures for mineralised tissue research often involve the isolation of dental pulp or bone marrow cells. The isolation of dental pulp cells is generally considered problematic due to their heterogeneity (Huang *et al*, 2006). The approach used involves the removal of the pulpal tissue from healthy teeth then cells are isolated using either out-growth by adherence to tissue culture plastic from explant tissue (Park *et al*, 2004) or using an enzyme digestion approach (Gronthos *et al*, 2000), whereby minced pulp tissue is digested with collagenase type I and dispase and passed through a cell strainer before seeding on tissue culture plastic. Interestingly, it has been demonstrated that each method produces phenotypically variable cell lines (Huang *et al*, 2006). Studies utilising primary dental pulp cells have demonstrated the ability of such cells to differentiate into odontoblast-like cells and produce mineralised matrix *in vitro* (Tsukamoto *et al*, 1992; About *et al*, 2000) Notably, primary cells when seeded onto human dentine surfaces secreted a reparative-like dentine (Batouli *et al*, 2003).

1.10.4 *In vitro* mineralisation analyses

Determination of mineralisation *in vitro* generally utilises the measurement of markers of mineralisation. These rely upon chemicals or antibodies binding to substrates that are indicative of mineralisation, whether they are proteins involved in the process of mineralisation or the components of mineralised deposits. Some methods that utilise these techniques include high alkaline phosphatase activity, alizarin red staining or von Kossa staining.

High alkaline phosphatase activity is one of the most commonly used markers for assaying mineralisation. It is an enzyme that is localized on the plasma membrane of cells and on the membrane of matrix vesicles from which mineralised deposits are secreted (Golub and Boesze-Battaglia, 2004). It is thought to act by increasing calcium phosphate levels, which facilitates the mineralisation process (Golub and Boesze-Battaglia, 2004). The presence of alkaline phosphatase in tissues can be determined using a biochemical assay or by histochemical staining (Sartoris, 1996).

Alizarin red staining utilizes direct binding to calcium ions present in the cells and is subsequently characterised by the presence of an orange-red stain (**Figure 1.8**). This approach allows the evaluation of calcium distribution and inspection of mineralised nodule formation by microscopic analysis (Putchler *et al*, 1969). Staining for alizarin red also allows for relative quantification of mineral deposits through dye extraction and spectrophotometric analysis (Gregory *et al*, 2004).

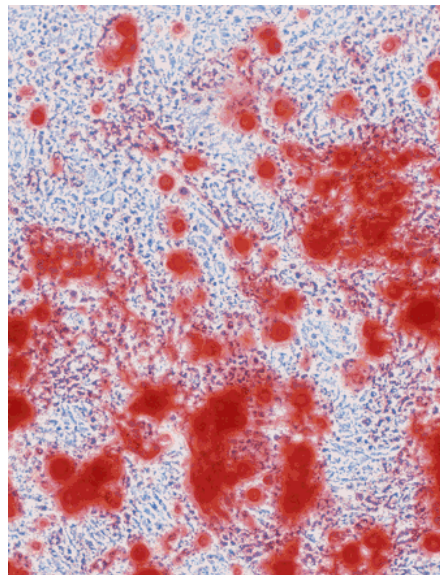


Figure 1.8: Positive alizarin red staining for the presence of calcium ions in a murine periodontal ligament cell line culture. Adapted from Saito *et al*, (2002).

The von Kossa staining method is also used to detect the presence of calcium deposits. This approach utilizes metal substitution of calcium deposits, whereby silver ions, usually in the form of silver nitrate, bind to the phosphate and carbonate groups of calcium deposits subsequently producing black staining (**Figure 1.9**). Despite limitations associated with this method, such as false-positive staining (Putchler and Meloan, 1978), studies have demonstrated a good correlation between positive von Kossa staining and calcium in the extracellular matrix of osteoblast cultures determined using electron microscopy (Kassem *et al*, 1998). More recently a study compared the efficacy of von Kossa staining to electron microscopy, X-ray diffraction and Fourier transform infrared spectroscopy (FTIR) (Bonewald *et al*, 2003). Whilst von Kossa staining was not as accurate as the other methods tested, it provided adequate data and was the simplest and cheapest method used. Its relative ease and inexpense therefore indicate why this approach is one of the most commonly used methods used for assaying mineralisation *in vitro* (Hakki *et al*, 2009; Park *et al*, 2009).

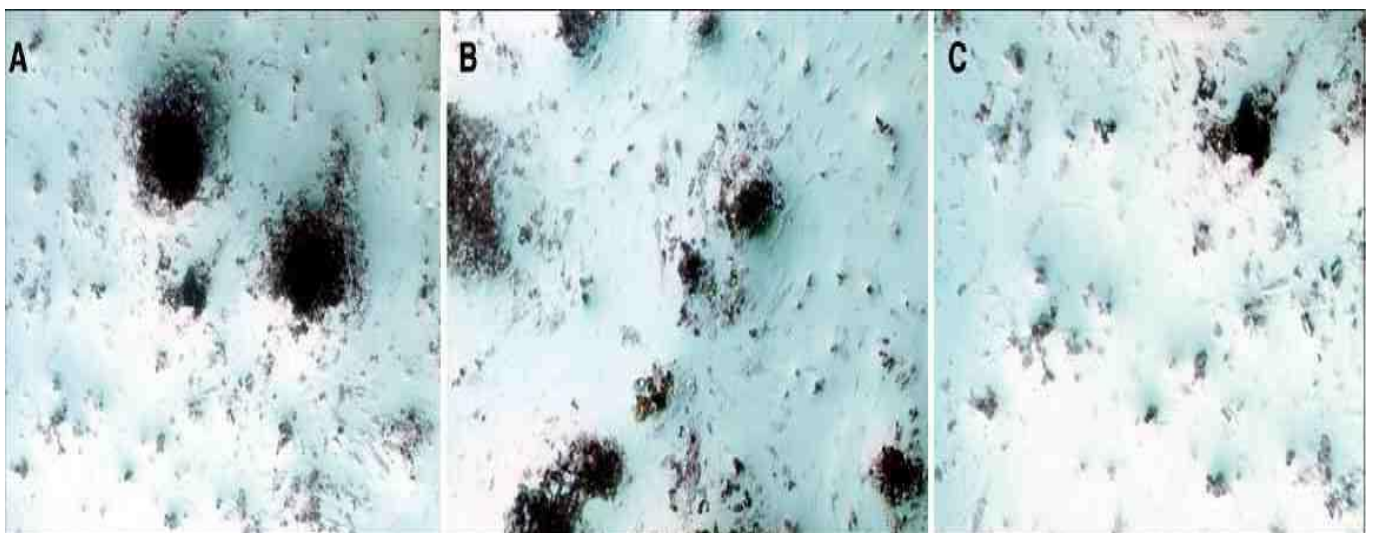


Figure 1.9: A-C: Von Kossa staining of adipocyte stem cells following osteogenic differentiation. Black staining denotes presence of calcium. (Downloaded from http://www.ijps.org/viewimage.asp?img=ijps_2008_41_1_8_41104_3.jpg)

2.0 Materials and Methods

2.1 Histology

2.1.1 Tissue specimens

Male Wistar rats between the ages of embryonic day (E) 16 – 20 were obtained from Charles River Laboratories, UK. They were sacrificed by cervical dislocation in the Pharmacy Department, Aston University, UK. Rats were decapitated using a sterile scalpel and the heads were de-skinned and bisected longitudinally prior to histological processing.

2.1.2 Fixing and demineralisation

Rat heads were fixed for 24 – 48 hours, depending upon age and size, in 10% (w/w) neutral buffered formalin (Surgipath Europe Ltd). Samples were demineralised in 10% formic acid (VWR) for at least 48 hours, with the end point measured using a chemical decalcification end-point test as described below.

2.1.3 Test for decalcification end-point

Five ml of used decalcifying fluid were removed, and placed in a test-tube containing litmus paper (BDH Ltd, UK). 29% concentrated ammonia (Sigma, UK) was subsequently added dropwise with constant agitation until the litmus paper indicated the solution to be alkaline. 0.5ml of this solution was then added to 5ml of saturated 5% ammonium oxalate (VWR), and agitated. If, after 30 minutes, a precipitate was formed, this indicated that calcium was still present and therefore the decalcification process was continued for a further 24 hours and the end-point test repeated.

However, if the fluid was clear after 30 minutes, the decalcification was determined to be complete and samples remained in decalcification fluid for a further 24 hours before further processing (see below).

2.1.4 Tissue processing and embedding

Following fixation and decalcification, samples were processed for histological analysis. Samples were submersed in 70% Industrial Methylated Spirits (IMS 99) (Genta Medical, UK) overnight, prior to being washed twice in 95% IMS 99 for 60 minutes each. Specimens were then washed four times in 100% IMS 99 for 90 minutes each and remained in 100% IMS 99 overnight. Subsequently, samples were washed twice for 90 minutes in xylene (Genta Medical, UK), followed by a further 120 minute wash in xylene. Samples were then transferred to a 68°C oven where they were imbibed with hot wax (Sakura Finetek Europe, NL) for 90 minutes. After 90 minutes, the hot wax was replaced with fresh wax and incubated for a further 90 minutes. Samples were incubated in a fresh batch of hot wax overnight. Following processing, samples were mounted into a mould with the inner surface orientated downwards prior to embedding in paraffin wax (Sakura Finetek Europe, NL).

2.1.5 Tissue sectioning

For each category of specimen age, a mandible was histologically analysed from each of 6 rats to provide a representative sample. Tissue sections of 5µm thick were cut from all samples using a rotary microtome (Leica DM 2135). Sections containing dental tissue were transferred to water at room temperature and then to warm water (50°C) before mounting on a SuperFrost® Plus slide (VWR International, DE) and

then dried in a 56°C oven for 120 minutes, then overnight at 37°C (Stuart scientific, UK).

2.1.6 Tissue staining

Sections for histology were stained with Haematoxylin and Eosin using an automated tissue stainer (Shandon Linistain, GLX). In the tissue stainer, sections were passed through xylene (Genta Medical, UK), a series of graded alcohols (Genta Medical, UK) and then water; before being stained with Gills (III) haematoxylin (Surgipath Europe Ltd). Sections were washed in distilled water, then in Scott's tap water (Surgipath Europe Ltd) to "blue", before being placed in 0.3% acetic acid (VWR) and counterstained in 0.125% buffered eosin (Surgipath Europe Ltd). Following staining, sections were washed in water, dehydrated through a series of graded alcohols (Genta Medical, UK) and finally cleared in xylene (Genta Medical, UK). Once stained, sections were mounted using a coverslip (Surgipath Europe Ltd) and Xam (a xylene based mountant) (BDH, UK) before being viewed by light microscopy (Leitz, UK) (see **Section 2.1.8**).

2.1.7 Immunohistochemistry (IHC)

Sections were de-waxed in xylene (Genta Medical, UK), re-hydrated through a series of graded alcohols (Genta Medical, UK) and then hydrated in phosphate buffered saline (PBS, pH 7.6) (Sigma, UK). Sections were digested in freshly made 0.1% Trypsin (150mg in 150ml PBS, Difco, UK) for 13 minutes with gentle agitation for antigen exposure. Trypsin was removed by rinsing in water for 5 minutes before sections were immersed in 3% hydrogen peroxide buffer (H₂O₂) (Sigma, UK) for 15 minutes to block endogenous peroxidase activity. Sections were washed in PBS and

then overlaid with diluted goat serum (1:5, Sigma, UK) in order to block non-specific protein binding. After 30 minutes, excess goat serum was removed and the appropriately diluted antibody, either ADM positive [1/3500 anti-ADM (Bachem, UK)], ADM blocking control [1/3500 anti-ADM (Bachem, UK) pre-incubated for 24 hours with 20x Molecular Weight ADM (Bachem, UK)], TGF- β 1 Positive [1/300 anti-TGF- β 1 (Santa Cruz Biotechnology, USA)], TGF- β 1 blocking control [1/300 Anti-TGF- β 1 (Santa Cruz Biotechnology, USA) + 20x Molecular Weight TGF- β 1 peptide (Santa Cruz Biotechnology, USA)], pre-bleed rabbit control (1/3500 pre-bleed rabbit serum (Sigma, UK)), negative control (PBS/BSA (Sigma, UK) only) (see **Table 2.1** for more details) was applied for 120 minutes, before being washed in PBS. Sections were then treated with 1:50 Multilink (Biogenex, USA) for 60 minutes (made up 60 minutes before use), washed in PBS and overlaid with Multi-label (Biogenex, USA) for a further 60 minutes; these contain a biotinylated secondary antibody, which binds to the primary antibody, and the enzyme streptavidin horseradish peroxidase which reacts with the diaminobenzidine (DAB) (Sigma, UK) to produce a brown staining wherever primary and secondary antibodies are attached. Sections were then washed again in PBS before being overlaid with the freshly prepared DAB (Sigma, UK) substrate reagent (10mg in 20ml PBS, filtered with 25ml H₂O₂ added) for 5 minutes, prior to rinsing in water. Sections were then overlaid with copper sulphate (0.5% w/v in NaCu, BDH, UK) to enhance the brown reaction product, rinsed in water, counterstained with Mayer's haematoxylin (VWR) for 50 seconds and 'blued' in water. Once stained, sections were dehydrated in graded alcohols (Genta Medical, UK), cleared in xylene (Genta Medical, UK) and then mounted using a coverslip (Surgipath Europe Ltd) and Xam (DBH, UK) as previously described.

Treatment	Antibody concentrations
ADM Positive	1µl Anti-adrenomedullin (Bachem, UK) in 3499 PBS/BSA (Sigma, UK)
ADM Blocking Control	1µl Anti-adrenomedullin (Bachem, UK) in 3499 PBS/BSA (Sigma, UK) + 20x Molecular weight ADM (Bachem, UK)
TGF-β1 Positive	1µl Anti-TGF- β1 (Santa Cruz Biotechnology, USA) in 299µl PBS/BSA (Sigma, UK)
TGF-β1 Blocking control	1µl Anti-TGF- β1 (Santa Cruz Biotechnology, USA) in 299µl PBS/BSA (Sigma, UK) + 20x mol. weight TGF-β1 peptide (Santa Cruz Biotechnology, USA)
Negative control	1000µl PBS/BSA (Sigma, UK)
Pre-bleed rabbit control	1µl Pre-bleed rabbit serum in 3499µl PBS/BSA (Sigma, UK)

Table 2.1 Antibody specifications used for immunohistochemistry. All antibodies were diluted in PBS/BSA (Sigma, UK) 12 hours prior to performing the procedure.
ADM = adrenomedullin, TGF-β1 = transforming growth factor – beta1.

2.1.8 Image analysis

Slides were viewed under a Dialux 22 light microscope (Leitz, UK), with images captured using a Coolpix 950 digital camera (Nikon, UK). All captured images had their blank, background images, taken at the same magnification as the original image, removed using the calculator plus plug-in with Image J software (downloaded from <http://rsbweb.nih.gov/ij/>) to give clearer images. Measurements of developing

teeth were made from images of scale bars obtained at the same magnification as H&E sections, using ImageJ software.

2.2 Cell culture

2.2.1 Cell lines

Cell culture experiments were performed using three developmentally derived murine cell lines. These were 3T3 fibroblasts (Todaro and Green, 1963), MDPC-23 odontoblast-like cells (Hanks *et al*, 1998) and OD-21 undifferentiated pulp cells (Hanks *et al*, 1998). Mouse 3T3 fibroblasts were cultured in 75cm² flasks (Appleton Woods, UK) in Dulbecco's Modified Eagle Media (DMEM) (Labtech International, UK) containing 10% foetal calf serum (FCS, Labtech International, UK), 2.5 HEPES (pH 7.4, filter sterilised, Labtech International, UK) and 1% Penicillin-Streptomycin (combined stock solution; Sigma, UK). Mouse OD-21 pulp-like cells and MDPC-23 odontoblast-like cells were cultured in 25cm² flasks (Appleton Woods, UK) in DMEM growth media (Labtech International, UK), containing 10% FCS (Labtech International, UK) 1mM L-glutamine (Sigma, UK) and 1% Penicillin-Streptomycin (combined stock containing 10,000 units penicillin and 10mgs streptomycin per ml; Sigma, UK). All cell lines were cultured in a MCO 175 CO₂ Incubator (Sanyo) with 5% CO₂, at 37°C.

2.2.2 Cell culture procedures for analysis of ADM, dexamethasone and dentine matrix protein extracts exposure

Confluent cell cultures were released from culture surfaces using 0.25% trypsin with 0.38g/l EDTA (Sigma, UK) and cells transferred to a 15ml tube (NUNC™, Denmark) for centrifugation at 1000rpm for 5mins, to pellet the cells. Cells were re-suspended in growth medium and seeded into 24-well, flat bottomed, sterile, micro-well plates (NUNC™, Denmark) at a density of 5×10^4 cells/well. After 24 hours incubation, media was removed and replaced with fresh media containing a range of concentrations of ADM (Pheonix Laboratories, US) (10^{-7} , 10^{-9} , 10^{-11} , 10^{-13} or 10^{-15} M), dexamethasone (Sigma, UK) (10^{-7} , 10^{-8} , 10^{-9} , 10^{-10} or 10^{-11} M) or EDTA extracted Dentine Matrix Proteins (DMPs) (0.00001, 0.001, 0.1, 10, 1000ng/ml) for 24 hours. DMPs were provided as a kind gift (Mrs G. Smith, Oral Biology, University of Birmingham) and were extracted as previously described (Graham *et al*, 2006). Cell counts were performed by releasing cells from wells using 0.5ml 0.25% trypsin with 0.38g/l EDTA (Sigma, UK) and transferring to a 2ml tube (Appleton Woods, UK) containing 0.5ml growth media. Tubes were gently vortexed (Vortex Genie-2 (Scientific Industries, UK)) before 10µl of the suspension was removed, mixed with 2µl trypan blue (Sigma, UK) and placed onto a standard Neubauer haemocytometer. Viable cell numbers were counted over the entire haemocytometer grid following observation using a variable relief contrast (VAREL) microscope (Zeiss Axiovert 25). Briefly, cells stained with trypan blue were regarded as non-viable, as the dye is taken up due to damaged cell membranes, therefore non-stained cells were counted over the large square grid area. The number of viable cells counted was subsequently multiplied by 10,000 to give cell number per ml of original dilution. Cell viability

data not presented due to insignificance of non-viable cell number (non viable cells < 1%).

For antagonist studies, cells were pre-treated with a range of concentrations of ADM₂₂₋₅₂ (10^{-14} M, 10^{-12} M, 10^{-10} M, 10^{-8} M and 10^{-6} M) (Bachem, UK) for 20 minutes prior to the addition of ADM as described previously.

2.3 Analysis of cell culture mineralisation

2.3.1 Cell culture

Cell lines, as described previously (see **section 2.2.1**), were seeded into 35mm Petri dishes (NUNC™, Denmark) at a density of 7.15×10^4 cells/cm². Following 24 hours culture, media were removed and replaced with either a medium containing 50mg/ml Ascorbic Acid (A.A) (Sigma, UK) and 10mM β -glycerophosphate (β -G) (Sigma, UK), medium containing 50mg/ml Ascorbic Acid (A.A) (Sigma, UK), 10mM β -glycerophosphate (β -G) (Sigma, UK) plus range of concentrations of ADM (Pheonix Laboratories, US) (10^{-7} , 10^{-9} , 10^{-11} , 10^{-13} or 10^{-15} M), standard mineralising medium [50mg/ml A.A (Sigma, UK), 10mM β -G (Sigma, UK) and 10^{-8} M Dexamethasone (Sigma, UK)] or standard mineralising medium including a range of concentrations of ADM (Pheonix Laboratories, US) (10^{-7} , 10^{-9} , 10^{-11} , 10^{-13} or 10^{-15} M). Ascorbic acid is known to increase alkaline phosphatase (ALP) levels and β -glycerophosphate is a substrate of ALP. Standard culture growth medium was also used as a control for each sample. Cultures were incubated for periods of 3, 7, 11, 14 and 21 days, with media changed every third day. Following the designated incubation time, cultures were von Kossa stained to detect mineral deposition (**Section 2.3.2**).

2.3.2 Von Kossa staining

Medium was removed from culture dishes and replaced with 10% formalin (Surgipath Europe Ltd) in PBS (Sigma, UK) for 30 minutes to fix the cells. Once fixed, the solution was removed and cells were washed in distilled water three times. Cells were stained with freshly made 5% silver nitrate solution (BDH Ltd, UK) for 30 minutes. Residual silver nitrate was subsequently removed by washing in distilled water. Staining was developed using fresh 5% sodium carbonate (BDH Ltd, UK) in 25% formalin (Surgipath Europe Ltd) for 3 minutes, washed with distilled water and finally fixed in 5% sodium thiosulphate (BDH Ltd, UK) for two minutes. Cells were then washed and covered in distilled water for viewing and digital analysis as described below (see **section 2.4.2**).

2.3.3 Digital analysis of von Kossa stained cultures

Images of the von Kossa stained cultures were captured following illumination on a light box (Hancocks, UK). Regions surrounding the culture dish were blacked out using a standard opaque card re-usable template. All images were captured from a distance of 20cm on a Coolpix 950 digital camera (Nikon, UK) using standard settings.

Images were analysed using ImageJ software (downloaded from <http://rsbweb.nih.gov/ij/>) following the image of the plate being isolated from the remainder of the image. Using ImageJ software captured images were adjusted to binary mode resulting in all stained sections appearing black and the non-stained regions white. The total binary area was measured using the analyse particles function on ImageJ, thereby providing a percentage value for the total area of mineral deposition as a function of plate area.

2.4 Gene expression analysis

2.4.1 Exposure of cell cultures to ADM for gene expression analysis

Cell lines were seeded into T25 flasks (Appleton Woods, UK) at a density of 2×10^4 cells/cm². When cultures reached ~90% confluency, media was replaced with growth medium containing a range of concentrations of ADM (Pheonix Laboratories, US) (10^{-7} , 10^{-9} , 10^{-11} , 10^{-13} or 10^{-15} M). Cultures were incubated for 24 hours under treatment to allow growth of a confluent monolayer of cells, following which RNA extraction was performed (see **Section 2.4.2**). Cell cultures grown in the absence of ADM were used as controls.

2.4.2 RNA isolation and extraction

All RNA isolations were performed with a SV Total RNA Isolation System using the procedure as recommended by the manufacturer (Promega, UK). Cell samples were directly collected from culture dishes in 175µl SV RNA lysis buffer (containing β-mercaptoethanol) (Promega, UK) and subsequently mixed by inversion in 1.5ml microcentrifuge tubes (Eppendorf, UK). Samples (and buffers) were then incubated at 70°C for 3 minutes. Following heating, samples were centrifuged for 10 minutes at 10,000 rpm (Centrifuge 5415D, Eppendorf) to pellet cell debris and the cleared lysate was transferred to a fresh Eppendorf tube, where 200µl 95% ethanol (Genta Medical, UK) was added and mixed by pipetting. The mixture was transferred to a spin basket assembly, centrifuged for 1 minute to capture the RNA on the spin basket membrane and the eluate discarded. 600µl SV RNA wash solution (Promega, UK) was added to the spin basket assembly, which was then centrifuged for 1 minute. Whilst centrifuging, a DNase incubation mix was prepared containing 40µl Yellow Core

Buffer (Promega, UK), 5µl 0.09m MnCl₂ (Promega, UK) and 5µl DNase I (Promega, UK). After centrifugation, the eluate was discarded and the DNase incubation mix was placed directly on the spin basket membrane and incubated at room temperature for 15 minutes. This procedure was used to degrade any DNA contaminants that might be present, ensuring that pure RNA was isolated. The reaction was subsequently stopped by the addition of 200µl DNase Stop Solution (Promega, UK) and centrifugation at 100000 rpm for one minute. The eluate was discarded, and two further washes with SV RNA wash solution (Promega, UK) were performed before the spin basket was transferred to a collection tube. 30µl nuclease-free water (Promega, UK) was added to the membrane and centrifuged at 100000 rpm for one minute to collect the RNA prior to storage at -80°C (-86°C Ultralow Freezer, Nuaire).

2.4.3 Reverse transcription

Reverse transcription was performed using an Omniscript Reverse Transcriptase kit (Qiagen, UK), following the protocol supplied in the handbook. This reaction was performed on ice, unless otherwise stated.

Previously obtained RNA was thawed on ice and 1-2 µg were added to 2µl 10mM Oligo DT primer (Ambion, UK), this mix was then made up to a total volume of 14µl using molecular grade water (Merck, UK) in a 0.2ml PCR tube (Appleton Woods, UK). The mix was incubated for 10 minutes at 80°C to minimise RNA secondary structures, such as hairpins, before being chilled on ice for 5 minutes. Whilst still on ice, 2µl RT buffer (Qiagen, UK), 2µl dNTP mix (Qiagen, UK), 0.3µl RNase inhibitor (Promega, UK) and 1µl Reverse Transcriptase enzyme (Qiagen, UK) were added. Following the addition of these components, the solution was incubated

at 37°C for 60 minutes, and then for a further 5 minutes at 93°C to remove enzyme activity, before storage at -20°C.

2.4.4 Purification of cDNA

To clean the cDNA and remove unincorporated nucleotides and other chemical contaminants, the cDNA solutions from the RT procedure described previously (**Section 2.4.3**) were transferred to YM-30 microcons (Millipore, UK), diluted to 500µl with molecular grade water (Merck, UK) and centrifuged for 7 minutes at 10,000 rpm (Centrifuge 5415D, Eppendorf). This process was repeated and centrifuged until approximately 30µl cDNA mix was remaining. The cDNA mix was collected in an Eppendorf tube by inverting the microcon and centrifuging at 1000rpm (Centrifuge 5415D, Eppendorf) for 3 minutes.

2.4.5 Quantification of RNA and cDNA

Following RNA extraction and reverse transcription, it was necessary to quantify the RNA and DNA concentrations and determine the purity of the RNA sample. This was performed using a Biophotometer (Eppendorf, UK). 1µl of the samples were diluted with 69µl molecular grade water (Merck, UK) in an Uvette (Eppendorf, UK) and the absorbance of the samples were read at 260nm (A₂₆₀). An absorbance value of 1 denotes 40µg/µl of RNA and cDNA.

The spectrophotometer was also used to determine RNA purity and degree of protein contamination. The purity was measured from a ratio of readings at 260nm and 280nm, with pure RNA giving a reading of 1.8 – 2.1. RNA quality was also confirmed by agarose gel electrophoresis (see **section 2.4.7**).

2.4.6 Polymerase chain reaction (PCR)

PCR was performed using reagents from the REDTaq™ ReadyMix™ PCR Reaction Mix with MgCl₂ (Sigma, UK). PCRs were prepared on ice to prevent degradation or premature annealing of primers. Individual PCR tubes (0.2ml volumes) (Appleton Woods, UK) contained a solution comprising of 100ng cDNA, 30µm forward and reverse primers (Invitrogen, UK) (see **Table 2.2** for primer details) and 12µl REDTaq™ ReadyMix™ (Sigma, UK) containing 20mM Tris-HCl (pH 8.3), 100mM KCl, 3mM MgCl₂, 0.002% gelatine, 0.4mM dNTP mix, stabilizers and 0.06 unit/µl Taq DNA Polymerase. This solution was then made up to a total volume of 25µl using PCR grade water (Sigma, UK).

The PCR tubes containing reaction solutions were transferred to a thermal cycler (Mastercycler Gradient, Eppendorf, UK) at the correct starting temperature (94°C, lid at 105°C) and thermocycled for the required number of cycles depending upon the primer conditions required (for a full list of conditions see **Table 2.2**)

A typical PCR programme used was as follows:

	Temperature.	Time.	Process.
1.	94°C	5 minutes	Denaturation
2.	94°C	30 seconds	Denaturation
3.	*	30 seconds	Annealing
4.	72°C	20 seconds	Elongation
5.	72°C	10 minutes	Elongation

Steps 2-4 are repeated for the required number of cycles

* = Annealing temperature varied depending on primers used (see **Table 2.2**)

Gene Symbol	Primer sequences (5'→3')	Annealing temp. (°C)	Cycle no.
GAPDH	F - cccatcaccatcttccaggagc R- ccagtgagcttcccgttcagc	60.5	19
ADM	F- atataggtgcgggtgacagc R- acctttggctggacaacaag	60	33
CRLR	F- tcttcgctgacagtgttcgt R- ccaggaggctggtttatca	60	43
RAMP-2	F- cattacagcgacctgcgaaa R- acaggtctgtgggaaggatg	55	32
PCNA	F- ttggaatcccagaacaggag R- cgatcttgggacccaataa	60.5	25
TGF-β1	F- ctgtccaaactaaggctcga R- cgtcaaaagacagccactca	60	28
BMP-2	F- tggaagtggcccatttagag R- catgccttagggatttga	60	27
Coll-1α	F- aaaagggtcatcgtggcttc R- actctgcgctctttgatatt	60	23

Table 2.2: Primers and PCR conditions used for gene expression analysis. GAPDH = glyceraldehydes-3-phosphate-dehydrogenase, ADM = adrenomedullin, CRLR = calcitonin receptor like receptor, RAMP-2 = receptor activity modifying protein-2, PCNA = proliferating cell nuclear antigen, TGF-β1 = transforming growth factor – beta1, BMP-2 = bone morphogenic protein – 2, Coll-1α = collagen - 1α.

To enable comparison of relative gene expression levels between samples, the routinely used glyceraldehydes-3-phosphate-dehydrogenase (GAPDH) expression was used to normalise the samples as this housekeeping gene is reportedly expressed at relatively equal levels in a significant number of cells lines and under similar growth conditions (Silver *et al*, 2006). Following agarose gel electrophoresis (see **section 2.4.7.**) GAPDH densitometric intensity of amplified products was determined using AIDA software (Fuji, UK) and cDNA amounts were modified until densitometric values were within 10% of each other (see **section 2.4.8.**).

2.4.7 Agarose gel electrophoresis

Non-denaturing agarose gels were prepared by adding agarose powder (Helena Biosciences, UK) to 1X TAE buffer [10X Tris acetate EDTA buffer, pH ~8.3, (Helena Biosciences UK,) diluted to 1X with distilled water]. The weight of agarose and volume of TAE buffer used depended on the percentage of agarose required in the gel to enable high resolution of sample separation. RNA samples were analysed using 1% agarose gels, whilst PCR products required 1.5 – 2.0% agarose gels.

Agarose was completely dissolved in TAE buffer by heating the mixture in a microwave (Samsung, TDS) on full power for a suitable time period. The mixture was allowed to cool, but not solidify before either 0.5 ug/mL ethidium bromide [EtBr (Sigma, UK)] or 1X SYBR Gold nucleic acid gel stain (Molecular probes, UK) was added to enable visualisation of samples under ultra-violet light. The solution was poured into an appropriate sized gel tray and a comb added to form sample-loading wells prior to gel solidification at room-temperature.

Following gel solidification, well forming combs were removed and the gel placed into an electrophoresis tank and covered with 1X TAE buffer. 7 µl of PCR

products were directly loaded per well. 100 ng of RNA, DNA or cDNA was mixed with 2 μ L 6X bromophenol blue buffer (VWR, UK) and loaded into the formed wells; 3 μ L of an appropriate RNA (Promega, UK) or DNA (Bioline, UK) size ladder was also loaded into appropriate sample wells. Gel electrophoresis was subsequently performed for 20-40 min at 80 to 120 volts until sample separation was achieved. The size of PCR products could subsequently be determined by comparing the position of the separated sample band to the known size bands of the electrophoresed DNA ladder.

2.4.8 Image analysis

Following electrophoresis, gel images were captured using the Electrophoresis Documentation Analysis System [EDAS (Kodak, USA)] whilst exposing the gel to a ultra-violet light source (Vilber Lourmat, UK) to enable sample visualisation. Captured RT-PCR gel images were subsequently imported into AIDA image analysis software (FUJI, UK) and semi quantitative densitometric analysis performed. To obtain a semi quantitative value of the volume density of amplified products, a rectangular area of equal size was outlined around PCR products for each sample using AIDA software, and the local background (an area 0.1mm^2 surrounding the rectangle) subsequently subtracted. Prior to comparison of gene expression levels between samples, obtained volume density values for each sample were normalised to their respective GAPDH housekeeping gene, volume density control values. Normalisation was achieved by dividing the obtained sample volume density values for each assay by their respective GAPDH volume density values. Normalised expression levels for each sample were then expressed as either a percentage or as relative expression levels of the highest normalised volume density obtained.

2.5 Systemic administration of ADM

The following work was performed by Professor Cornish and members of the Bone Research Group, based at the University of Auckland, New Zealand and previously used in a published study to determine the effect of systemic administration of ADM on tibia bone length and strength (Cornish *et al*, 2001). The murine specimens (whole animals) were provided as a kind gift from Professor Cornish as part of a Universitas 21 funded collaborative project (<http://www.u21.bham.ac.uk/>).

Briefly, two groups of male adult Swiss mice aged between 40 and 50 days and weighing 25-32g were used. Each group were given daily subcutaneous injections into the nape of the neck for 5 days/week over a period of 4 weeks. The test group received injections contained 8.1µg ADM in 50µl of water, whilst the control group received sham injections of 50µl saline solution alone. Each group was provided with the same chow diet and allowed to feed *ad libitum*. Following the experimental test period of 4 weeks, the mice were terminated by cervical dislocation prior to mineralised tissue analysis (see Cornish *et al* 2001 for further details on experimental procedure).

2.6 Micro-Computed Tomography (MicroCT) analysis of dental and craniofacial structures from experimental animals from sham and ADM exposed mice

2.6.1 MicroCT scanning and specimen reconstruction

Mice heads were removed from bodies and boiled for one hour to detach any adherent soft tissue from the bony structures. Heads were frozen for transport to the department of Chemical Engineering, University of Birmingham. Subsequently, at location, heads were defrosted and securely placed into plastic bijoux tubes (Appleton Woods, UK).

Bijous were securely fixed onto the rotating analysis platform inside the Skyscan 1172 (Skyscan, Belgium) (**Figure 2.1**). The scanning parameters for this study were set at 100kV source voltage and 98 μ A source current. Samples were stationed 202mm from x-ray source and 95mm from the detector, giving a pixel size of 18.8 μ m. Subsequently, samples were rotated, enabling 600 X-ray images to be captured, one every 0.6°, to enable the building of a 3D X-ray reconstruction image of the specimen. This process is shown diagrammatically in **Figure 2.2**.



Figure 2.1: Skyscan 1172 (Skyscan, Belgium)

μ -CT Schematic

Aerial View

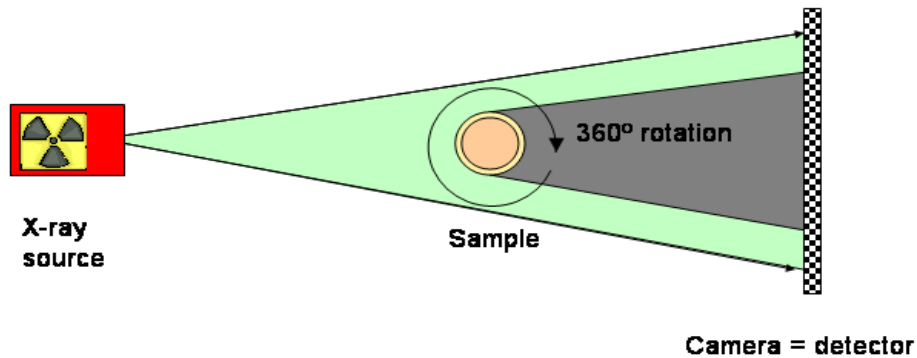


Figure 2.2: Diagrammatic representation of the scanning process used by the Skyscan 1172 (Skyscan, Belgium).

The images obtained from the scanning process were electronically transferred for the computer assisted reconstruction process (**Figure 2.3**). This analysis was performed using the CTrecon software (Skyscan, Belgium), which uses the 3D model to create 2D bitmap cross-sectional images of the hard tissue along the horizontal plane (as shown in **Figure 6.2**). Each scan provided approximately 920 2D slices, each measuring 1024x1024 pixels with a pixel size of 18.9 μ m.



Figure 2.3: Reconstruction process underway using CTrecon software (Skyscan, Belgium)

2.6.2 Volumetric measurements

2D bitmap images obtained from reconstruction stage (**Section 2.6.1**) were analysed using CT analysis software (CTan) (Skyscan, Belgium). Using CTan it was possible to create volumes of interest (VOIs) by manually isolating the tooth area on each cross sectional image, approximately 120 per molar, 215 per incisor and 750 per mandible. The software then provides a stack of images, measures each isolated area from the sections selected and enables determination of the total hard tissue volume (see **Figure 6.3**). Prior to the study each sham and ADM exposed animal was assigned a random number by a person unrelated to this study. When measurements were taken, the author was only aware of samples by their assigned number, therefore

removing any possibility of bias. This process was performed on each sample tooth and for the whole mandibles from sham and ADM exposed animals.

2.7 Digital analysis of heads from ADM treated mice

Ten mandibles from both test and control animals were removed. Digital images were taken against a background of standard graph paper from a fixed height of 10cm directly above using a Coolpix 950 digital camera (Nikon, UK) and accompanied by a standard ruler to provide scale. Key lengths were measured along the mandible, as proposed by Atchley *et al 1984*, who previously used this approach to study the effect of the muscular dysgenesis gene on mouse mandible development. Image analysis for craniofacial measurements was performed using ImageJ software (downloaded from <http://rsweb.nih.gov/ij/>). Prior to the study each sham and ADM exposed animal was assigned a random number by a person unrelated to this study. When measurements were taken the author was only aware of samples by their assigned number, therefore removing any possibility of bias.

2.8 Statistical analysis

The significance of the data presented was evaluated using one-way ANOVA and Dunnett's test to determine whether treated samples were significantly different from control samples. Data are presented as mean \pm standard error of the mean (s.e.m). A 5% significance level was maintained throughout.

3. Results chapter 1

3.1 Expression of ADM and TGF- β 1 in the developing tooth: An immunohistochemical study

Many growth factors are known to be important in regulating tooth development and associated dentinogenesis, with members of the TGF- β , BMP, IGF and FGF families implicated due to their expression patterns during tooth development (Vaah Tokari *et al*, 1991; Cam *et al*, 1992; Bégue-Kirn *et al*, 1994; Helder *et al*, 1998; Russo *et al*, 1998), while *in vitro* studies have demonstrated the involvement of these growth factors in odontoblast differentiation (Bégue-Kirn *et al*, 1992; Bégue-Kirn *et al*, 1994; Sloan and Smith, 1999; Ruch and Lesot, 2000). However, further molecular characterisation in this area is still required as the precise role of these growth factors and their inter-relationship is still undetermined due to their simultaneous expression and due to relevant genetic knock-out animal models arresting during, or prior to, tooth development (Bégue-Kirn *et al*, 1994; Helder *et al*, 1998) (**See Section 1.4.2 for further details**).

Previously published preliminary work has now indicated that ADM is expressed in the odontoblasts of the developing tooth at the approximate time of dentinogenesis onset, indicating that ADM may be important in regulating these processes (Montuenga *et al*, 1997). The role of the growth factor, TGF- β 1, is well established in regulating odontoblast differentiation and dentine secretion during tooth development (Begue-Kirn *et al*, 1992; Begue-Kirn *et al*, 1994; Smith *et al*, 1995; Sloan and Smith, 1999; Unda *et al*, 2001; Xu *et al*, 2003; Klopčic *et al*, 2007; Oka *et al*, 2007; Sassá Benedete *et al*, 2008) and now there is data that shows that ADM is co-expressed with TGF- β 1 during general mammalian embryogenesis (Montuenga *et*

al, 1998). In addition, a regulatory interrelationship between ADM and TGF- β 1 has been described, with studies showing that TGF- β 1 and ADM can act to suppress the expression of each other, while studies using TGF- β 1 null mutant mice demonstrate a reduction in embryonic ADM expression (Bodegas *et al*, 2004; Huang *et al*, 2005). The following study was therefore undertaken to characterize the temporo-spatial expression of ADM and TGF- β 1 during rat tooth development. This data may help clarify ADM's potential role during dental tissue development and may indicate whether a regulatory inter-relationship between these two molecules likely exists during tooth development.

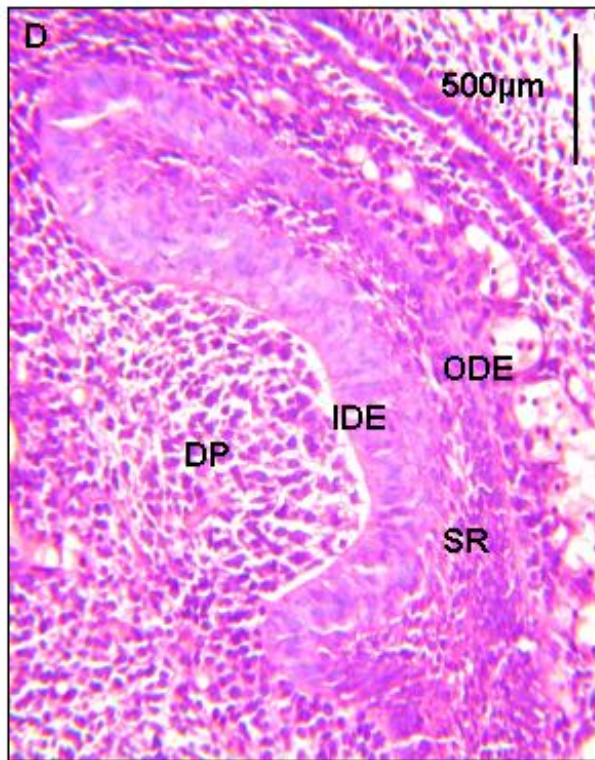
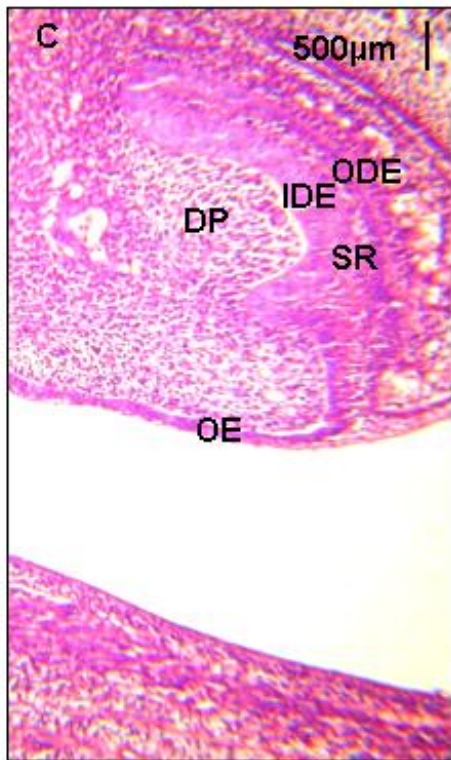
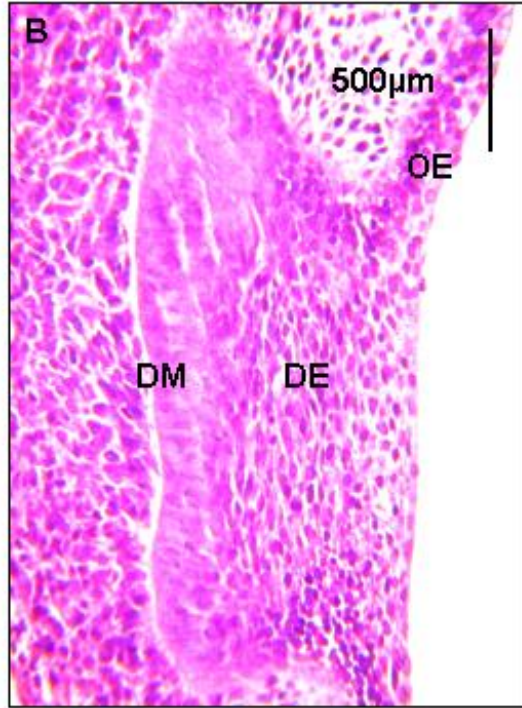
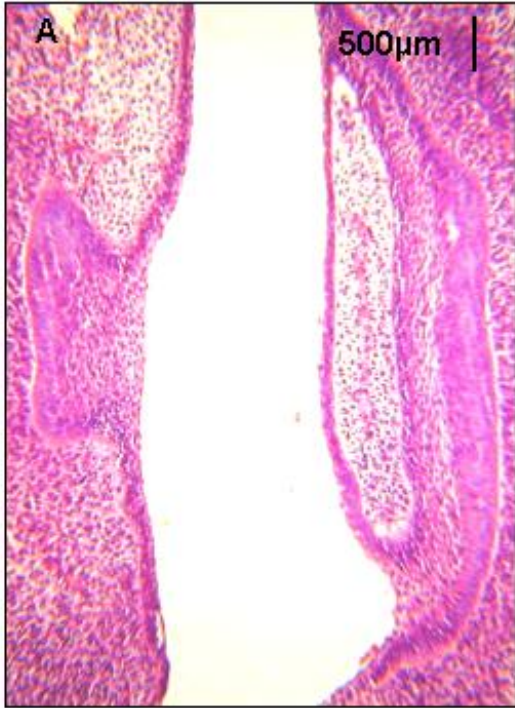
3.2 Histological study of tooth development in rats

Throughout this study it was often difficult to obtain exact times of conception for the rodents used. To initiate conception, male and female animals were placed together at the end of a working day and the following morning vaginal plugs were used to assess early signs of pregnancy. As conception time is taken from this timepoint, there remains a 14 hour period in which conception could have occurred this potentially contributes to slight inaccuracies with regards developmental age for the animals used in this study. Therefore to better assess the developmental age at which the rats used in this work underwent each stage of tooth development, a preliminary study was undertaken. During this study, sections of tooth germs of rat foetuses from embryonic day 16 (E16), embryonic day 18 (E18) and embryonic day 20 (E20) were stained with Haematoxylin and Eosin (H&E) (see **Section 2.1**). These images were then compared to the key stages of tooth development previously reported (Ten Cate, 1998). Furthermore, measurements of organ width, height and distance from oral epithelium were taken of the developing molars, using ImageJ software (see **Section 2.1.8**), as there appears to be no such information currently available. These measurements may act as useful guidelines for determining developmental stages in future study.

At the embryonic age of E16 it appeared that the 1st molars of the rats were in the bud stage of development (**Figure 3.1A & B**). When viewed under high magnification (x500) the cells of the dental mesenchyme, dental epithelium and oral epithelium were clearly visible (**Figure 3.1B**). Also visible was the apparent condensing of the ectomesenchyme around the dental membrane, caused by the epithelial 'ingrowth' (**As described in Section 1.4.2.2**). This histological event is a

key stage in the transition from bud to cap stage. As the molar is still in the bud stage it was only possible to measure the width of the tooth bud, which was 2.76mm.

The incisor tooth at E16 appeared to be in the cap stage of development (**Figure 3.1C**), as it can be seen that the developing tooth remains attached to the oral epithelium by the dental lamina, whilst at the higher magnification the dental papilla, inner and outer dental epithelium and the stellate reticulum are all visible. The only feature not visible, that is synonymous with the cap stage, is the enamel knot. However, as none of the cells appear to have begun histodifferentiation indicative of a tooth being in the bell stage, such as odontoblast and ameloblasts differentiation, and as the developing tooth is attached to the oral epithelium, it is reasonable to presume that this represents the cap stage of development (Ten Cate, 1998). The enamel knot is a relatively transient structural feature and thus, the fact it is not visible is perhaps unsurprising as its presence is very dependent on the exact time of observation.



E:

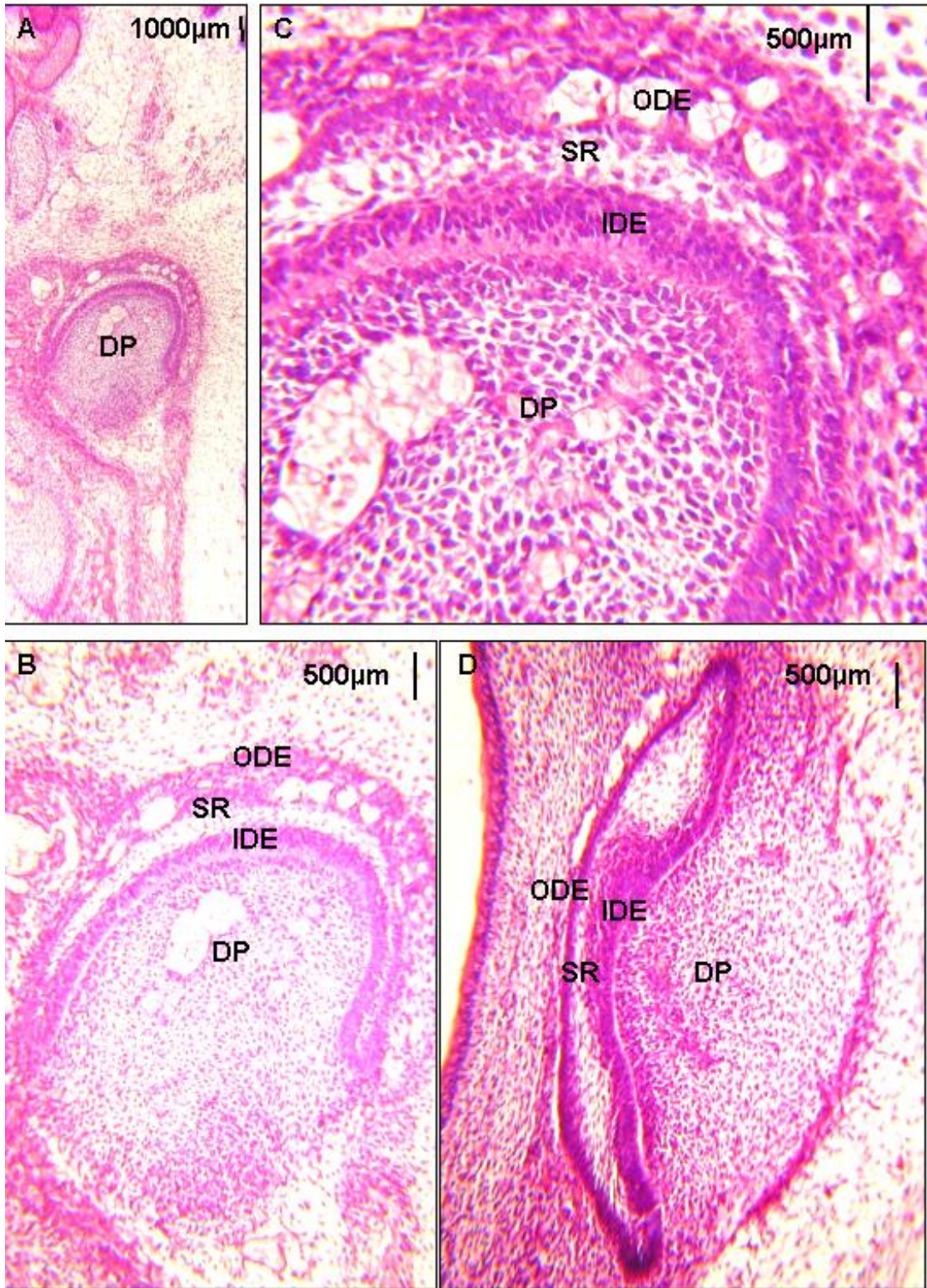
1 st Molar Measurement	Mean Length (mm)
Width	2.76
Height	N/A
Distance from epithelium	N/A

Figure 3.1: A – Representative image of developing rat 1st upper molar at E16 (x125 magnification) stained with H&E. **B** – Developing rat 1st upper molar at E16 (x500 mag) stained with H&E and with key features labelled. DM = Dental membrane. BM = Basement membrane. DE = Dental epithelium and OE = Oral epithelium. **C + D** – Developing rat incisor at E16 stained with H&E. Key feature dentoed: DP = Dental papilla. IDE = Internal dental epithelium. ODE = Outer dental epithelium. SR = Stellate reticulum and OE = Oral epithelium. **C** = x125 mag. **D** = x500 mag. **E** – Table showing key measurements taken from developing rat 1st molar at E16. These images are representative of six Wistar rats.

Histological evidence indicates that the developing incisor of a rat at E18 appeared to be on the boundary of cap and bell stage (**Figures 3.2A, B & C** provide representative images). At this stage, the developing tooth appears to be dissociated from the oral epithelium indicating entry into the bell stage (Ten Cate, 1998). Inspection of the image also provides morphological evidence indicative of a developing incisor (**Figure 3.2**). However, as yet there appears to be little of the histodifferentiation which is indicative of a developing tooth in the bell stage. It is often difficult to state with certainty which developmental stage a tooth is at due to stages overlapping, as appears the case here at embryonic age E18 (**Figure 3.2**).

The developing molar at E18 also appears to have dissociated from the oral epithelium, however, other apparent features indicate this section as being derived from the cap stage of development. The tooth has yet to gain the crown shape associated with a molar in bell stage and there appears to be no histodifferentiation indicative of bell stage occurring. Clearly visible are the dental papilla, inner dental epithelium, stellate reticulum and outer dental epithelium (**Figures 3.2D - H**) as would be expected for a tooth at the cap stage of development (Ten Cate, 1998).

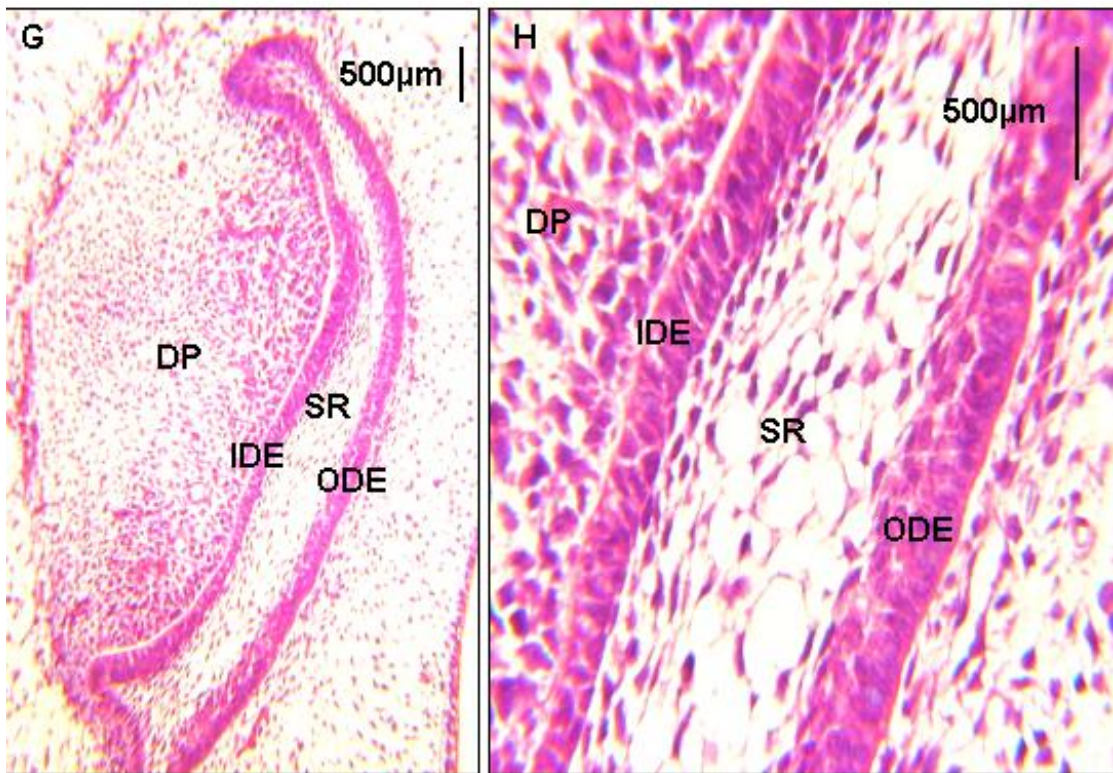
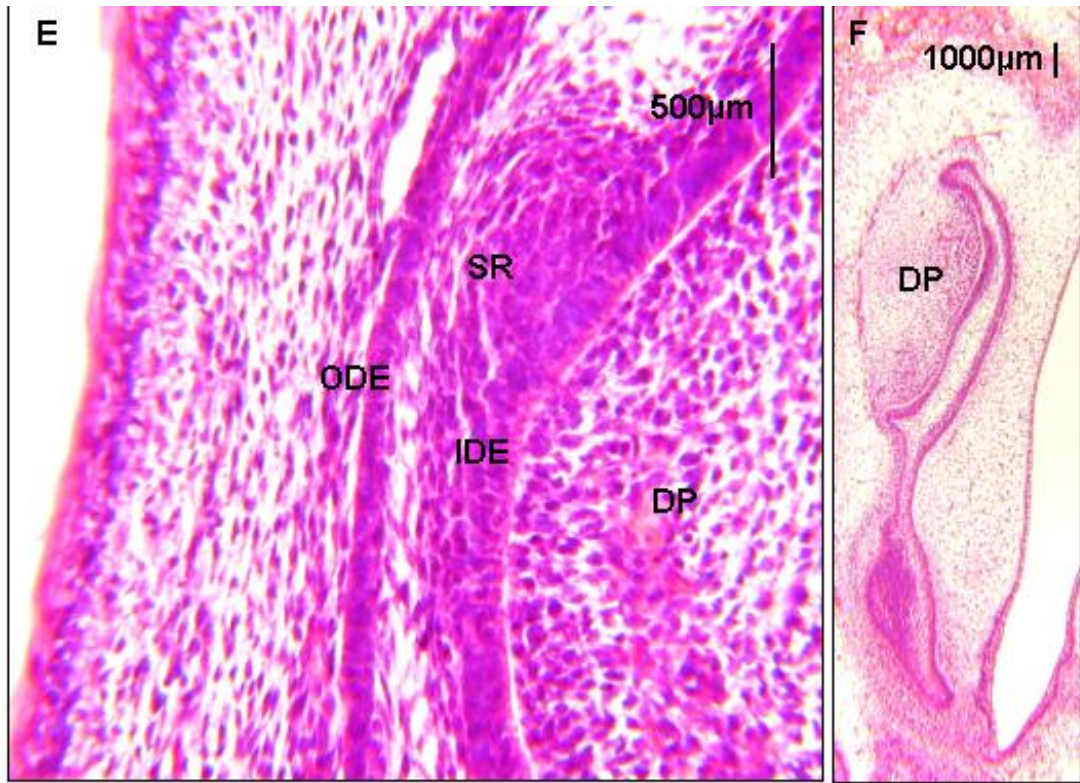
In **Figure 3.2F** it is also possible to observe the onset of the 2nd molar development. It is interesting to note that the dental epithelia of the 1st and 2nd molars appear to be attached. It also appears that the 2nd molar is currently developmentally between bud and cap stages as the developing organ has yet to take on the 'cap' appearance. At this stage, the width of the developing molar has now more than doubled as compared to the E16 derived tissue and now measures 6.98mm. The height of the developing tooth bud was 3.33mm and the distance from the oral epithelium was 1.08mm.



I:

1st Molar Measurement	Mean Length (mm)
Width	6.98
Height	3.33
Distance from epithelium	1.08

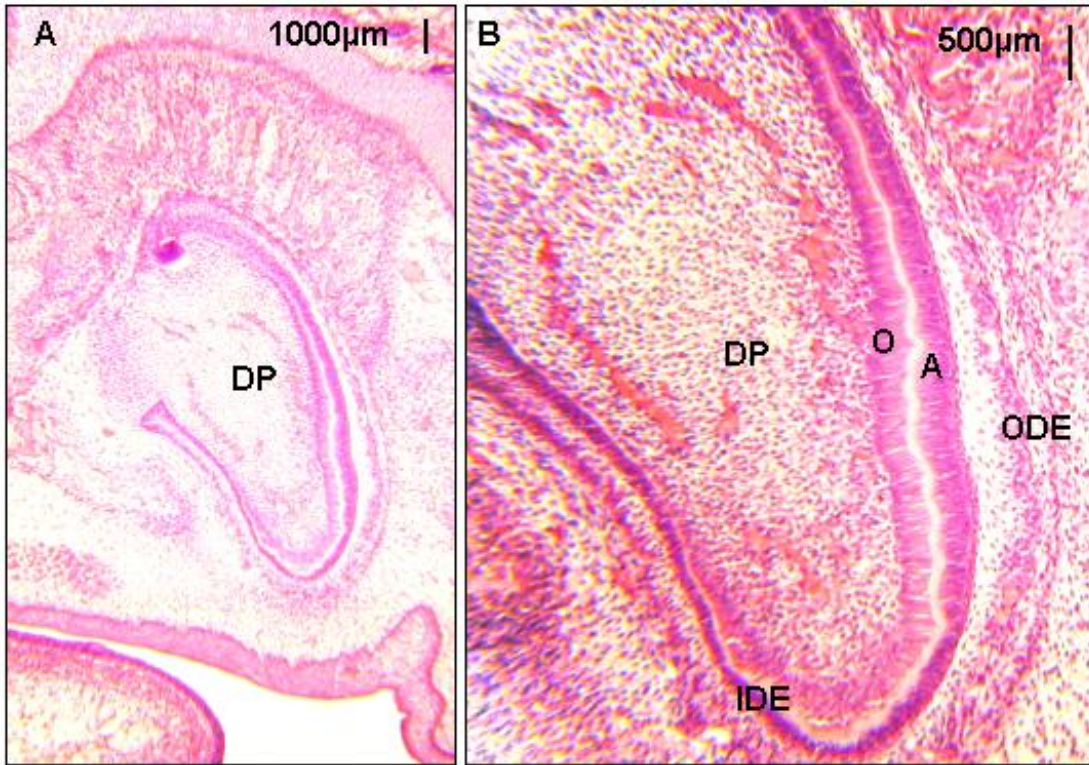
Figure 3.2: A – C: Representative image of developing rat incisor at E18 stained with H&E and with key features labelled. A = x50 mag B = x125 magnification C = x500 mag. D – H: Developing rat 1st molar at E18 stained with H&E. F = x 50mag D + G = x125 mag. E + H = x500 mag. Key features denoted: DP = Dental papilla. IDE = Internal dental epithelium. ODE = Outer dental epithelium and SR = Stellate reticulum I – Table showing key measurements taken from developing rat 1st molar at E18. These images are representative of five Wistar rats.



Once the rat reaches E20, the developing incisor appears to be in the bell stage of development (Ten Cate, 1998). The tooth is clearly forming its' predetermined shape, notably it has fully dissociated from the oral epithelium and the cells have begun to undergo histodifferentiation. **Figure 3.3C** clearly shows that the cells of the inner dental epithelium and stratum intermedium have differentiated into odontoblasts and ameloblasts, with the odontoblasts beginning to deposit dentine. The differentiation of these cells begins at the cusp of the developing crown, which signals to the neighbouring cells initiating a cascade of differentiation throughout the inner dental epithelium and stratum intermedium; as such not all cells of the inner dental epithelium and stratum intermedium have begun to differentiate (**Figure 3.3B**).

The 1st molar of the rat at E20 appears to be developmentally between the cap and bell stages. The developing organ has yet to undergo the histodifferentiation one would expect for a tooth in the bell stage, such as the differentiation of odontoblasts and ameloblasts, however, it had taken on the future crown shape of a molar. There also appears to be a mixture of structures from both cap and bell stage present, with the inner dental epithelium, outer dental epithelium and stellate reticulum indicative of cap stage visible and the stratum intermedium which is indicative of bell stage also visible. This suggests a general continuum from one stage to another (**Figure 3.3F**).

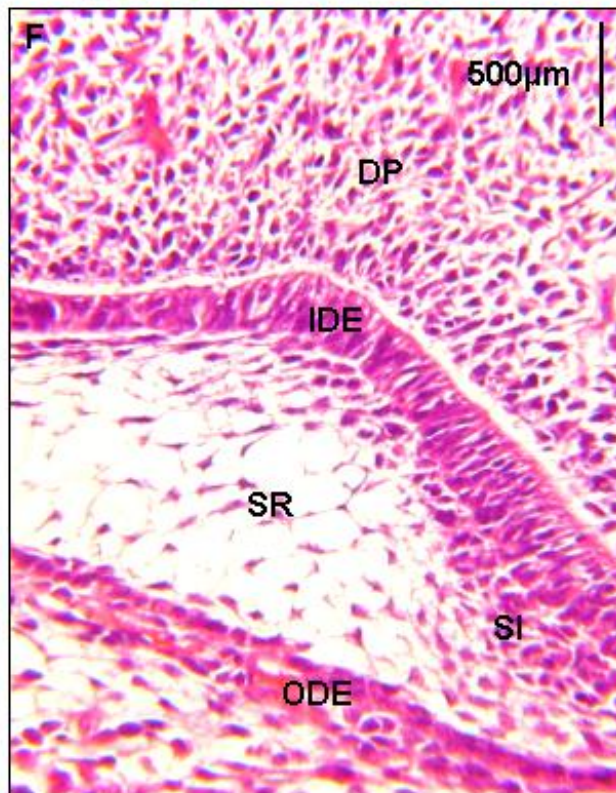
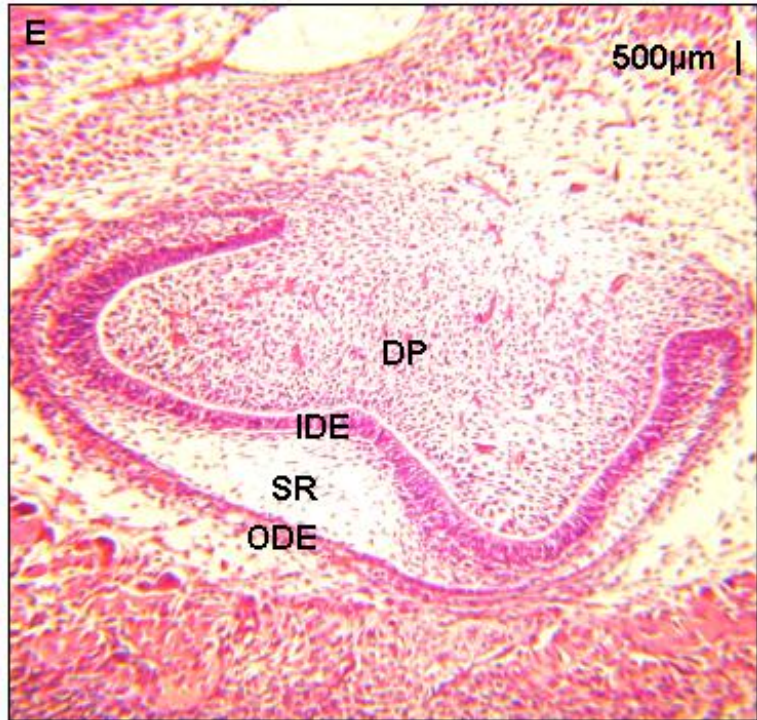
The size of the developing molar has changed minimally from the E18 time-point, with the width increasing by 0.21mm to 7.17mm and the height increasing by 0.16mm to 3.49mm. The distance from the oral epithelium has also increased between E18 and E20 from 1.08mm to 2.65mm.



G:

1 st Molar Measurement	Mean Length (mm)
Width	7.17
Height	3.49
Distance from epithelium	2.65

Figure 3.3: A – C: Representative image of developing rat incisor at E20 stained with H&E and with main features highlighted. A = x50 mag B = x125 magnification C = x500 mag. D – F: Developing rat 1st upper molar at E20 stained with H&E and with key features labelled. D = x50mag E = x125 mag. F = x500 mag. Key features denoted: DP = Dental papilla. IDE = Internal dental epithelium. ODE = Outer dental epithelium. SR = Stellate reticulum SI = Stratum intermedium O = Odontoblasts. D = Dentin and A = Ameloblasts. G – Table showing key measurements taken from developing rat 1st molar at E20. These images are representative of five Wistar rats.



3.3 Immunohistochemical analyses of ADM and TGF- β 1 in the developing tooth organ of male Wistar rats

Following the histological determination of the developmental ages at which male Wistar rats exhibit certain tooth developmental stages (**Section 3.2**), an immunohistochemical study was performed to determine in which histological locations and at what developmental ages ADM was detectable in the developing teeth. Previously published data is limited to a single image of ADM positive staining in a developing mouse tooth (Montuenga *et al*, 1997), therefore all immunohistochemical data obtained from the developing teeth of embryonic male Wistar rats in this study is novel and will increase our knowledge.

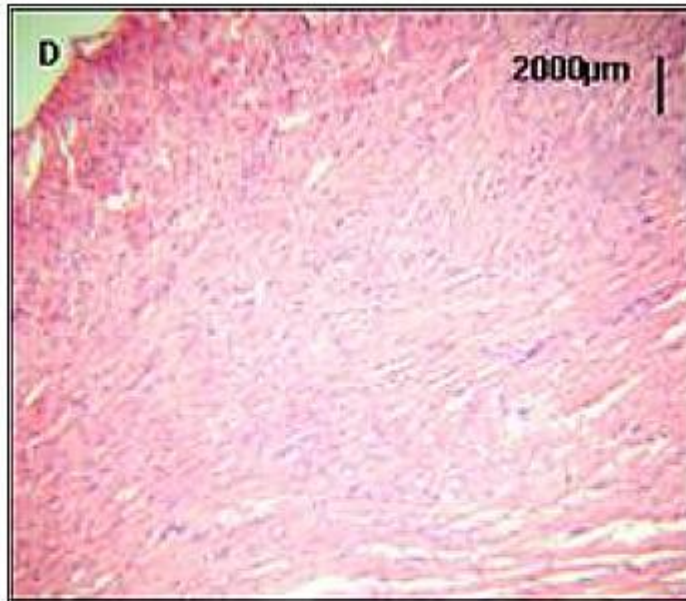
Initially adult male Wistar rat heart sections were used as a positive immunohistochemical staining control, as ADM is reportedly prevalently expressed in the heart (Jougasaki *et al*, 1995). Subsequently, 5 μ m sections of teeth from rats aged at embryonic day 16 (E16), embryonic day 18 (E18) and embryonic day 20 (E20) were obtained and stained for the presence of ADM (**Section 2.1**).

Furthermore, sections from male Wistar rats aged E20 were stained for the presence of TGF- β 1 to determine if concurrent expression with ADM exists in the developing tooth, as has previously been described during embryogenesis in other tissues (Montuenga *et al*, 1998).

Notably, ADM expression was confirmed to be prevalent throughout the heart tissue (**Figure 3.4A**), predominantly the smooth muscle cells, as previously described in literature (Jougasaki *et al*, 1995; Montuenga *et al*, 1997). The pre-incubation of an ADM peptide with the ADM antibody overnight (ADM blocking control) resulted in a reduction in staining for ADM (**Figure 3.4B**) indicating that the staining seen in Figure 3.4A was due to specific ADM antigen binding and confirming that the ADM antibody functions as expected. The absence of an ADM antibody (-ve control) resulted in no detectable staining (**Figure 3.4C**). **Figure 3.4D** provides an image of H&E staining of the heart tissue section.

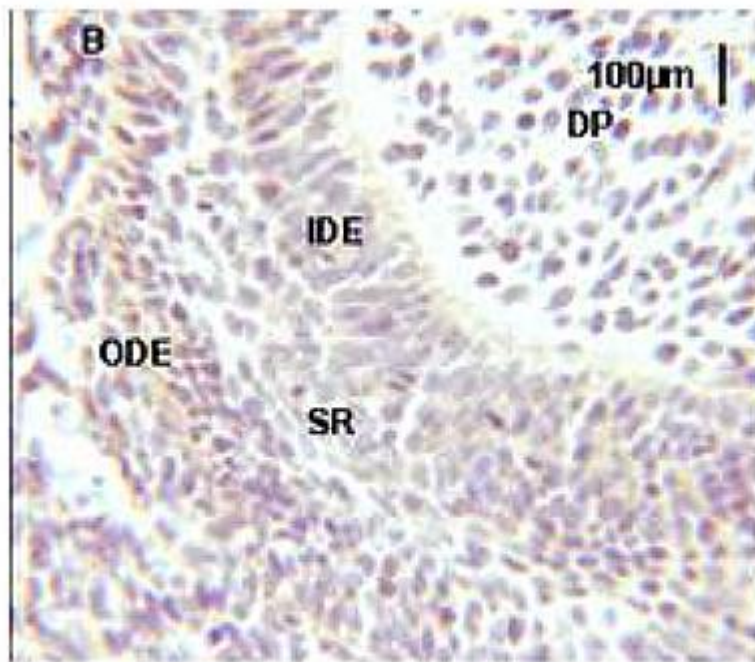
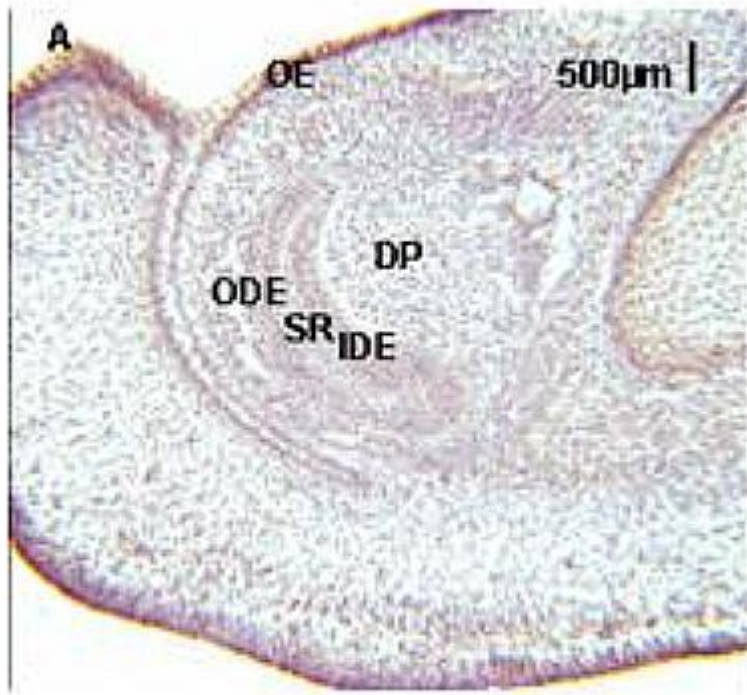


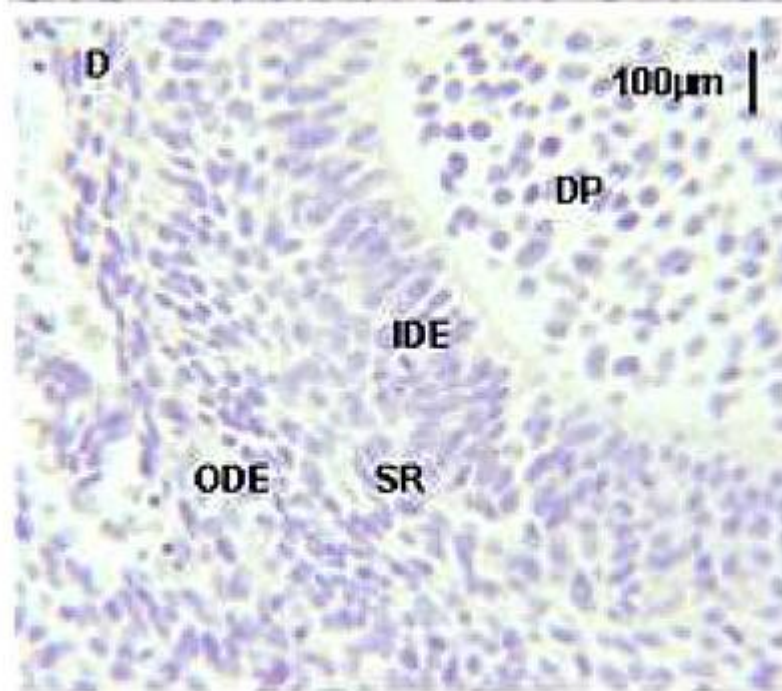
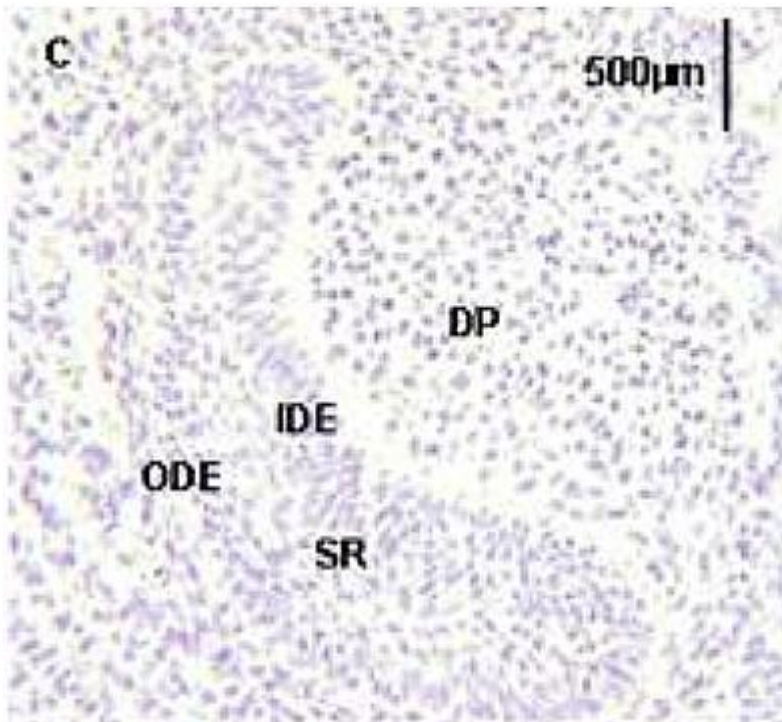
Figure 3.4: Representative images of an adult male Wistar rat heart (all x50 mag) stained with **A** – 1/3500 anti-ADM **B** – 1/3500 anti-ADM + ADM peptide (ADM blocking control) **C** – No antibody present (negative control) **D** – H&E. These images are representative of the staining seen in three Wistar rats.



At embryonic age E16, when the incisor was identified as being in the bud stage, a high intensity of staining was visible in the majority of oral epithelial cells throughout the developing jaw, whilst in the majority of mesenchymal cells there appeared to be a lower intensity of positively stained cells for the presence of ADM (**Figure 3.5A**). A higher magnification view (**Figure 3.5B**) demonstrated that in the developing incisor, positive staining for ADM appears to be present in the cells of both the internal and external dental epithelium.

In the pre-bleed control specimens (**Figures 3.5C & D**), there was no apparent positive staining for ADM in any of the cells of the developing jaw or tooth. Furthermore, there was no positive staining in the negative control (no ADM antibody) specimens (**Figures 5.3E & F**).





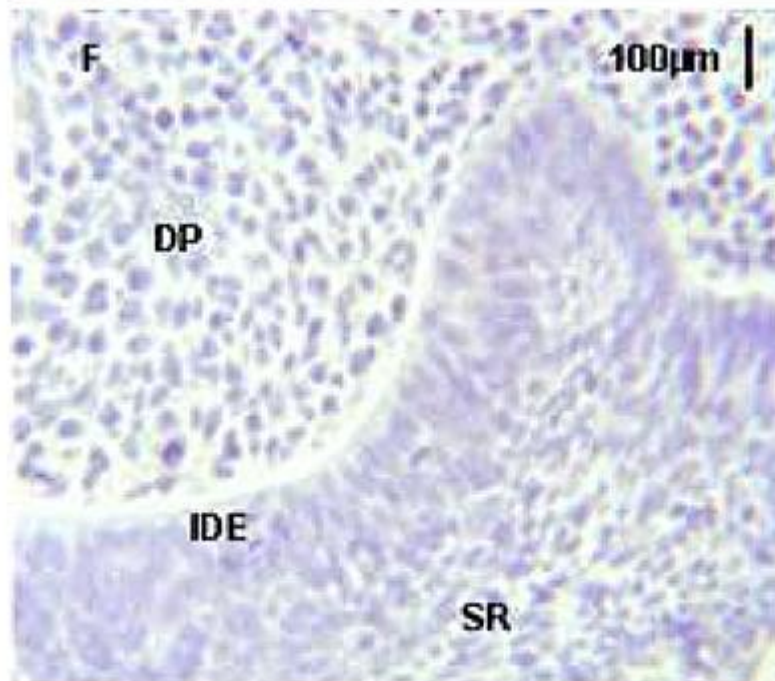
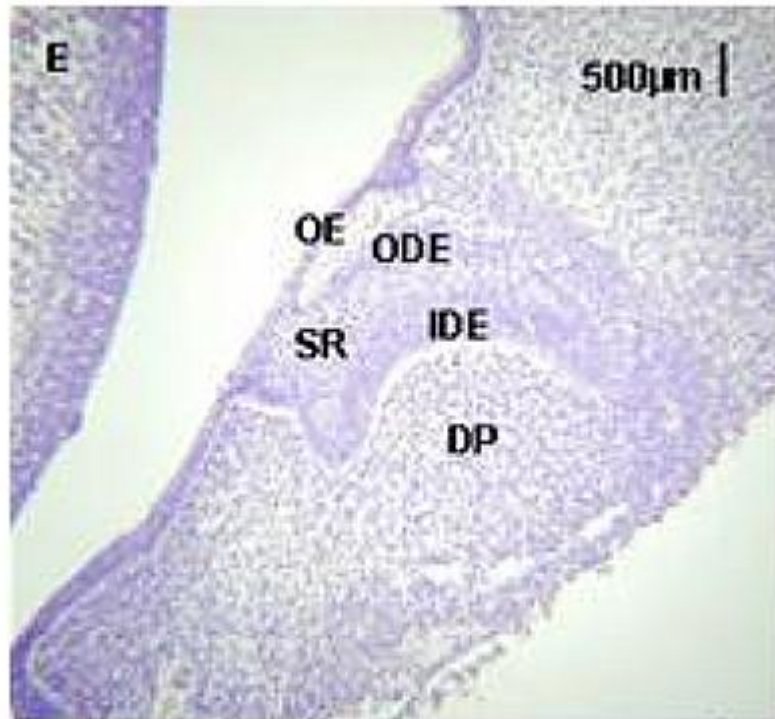
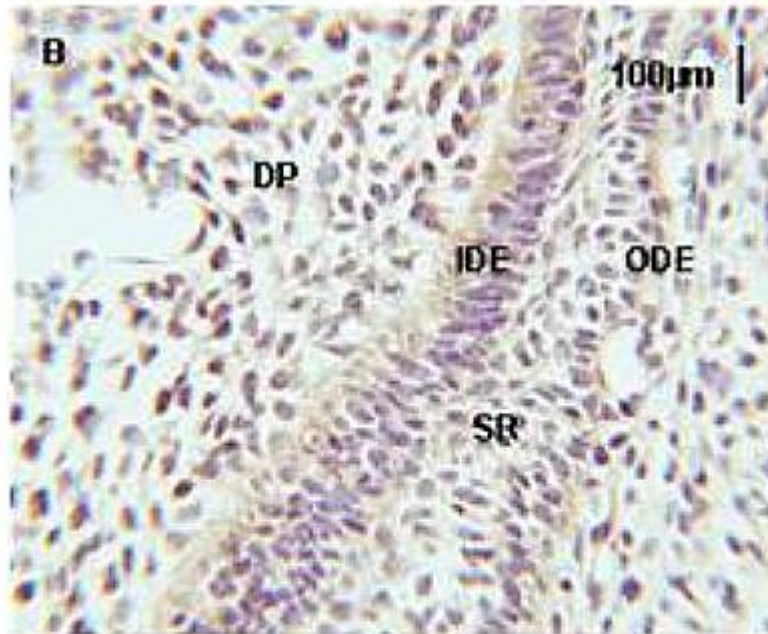
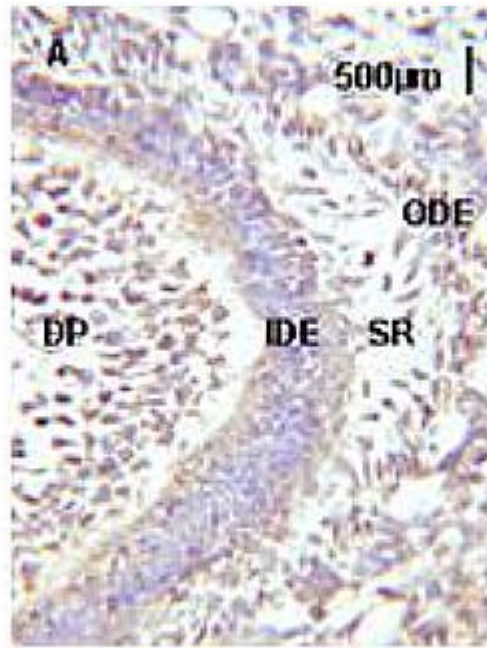
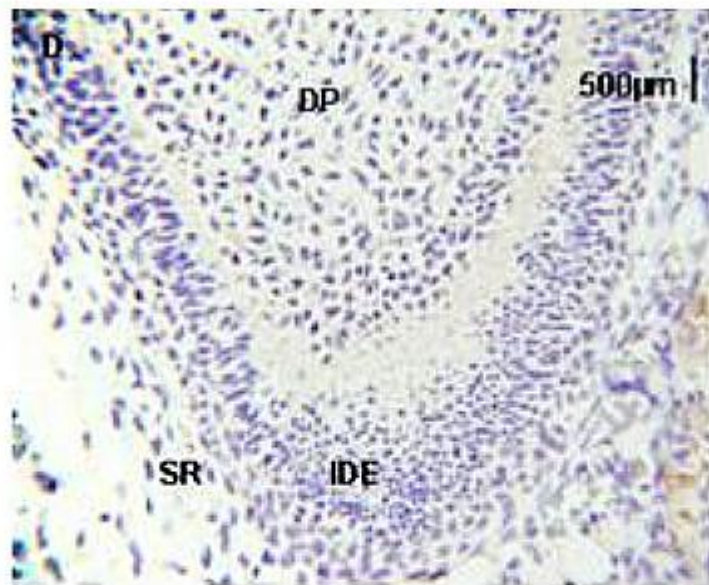
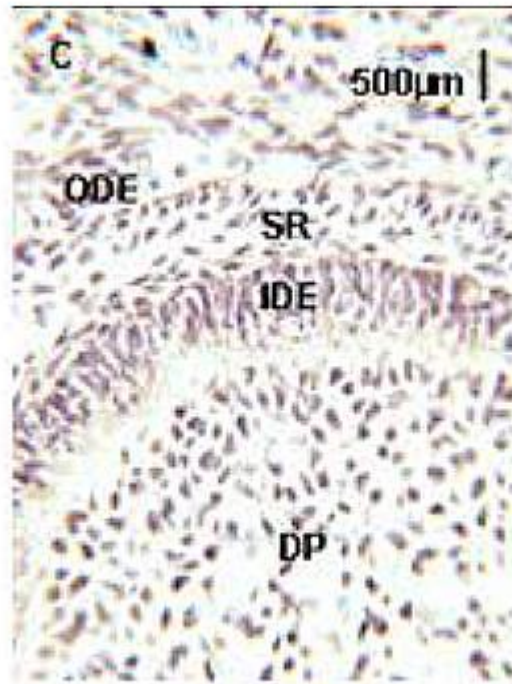


Figure 3.5: Representative immunohistochemical images of male Wistar rat developing incisors at E16. Specimens are stained with **A + B** – 1/3500 anti-ADM **C + D** – 1/3500 pre-bleed rabbit serum **E + F** – no antibody present (negative control). Key features denoted: DP = dental papilla. IDE = internal dental epithelium. ODE = outer dental epithelium. SR = stellate reticulum and OE = oral epithelium. Magnification – **A + E:** x125. **C:** x500. **B, D + F:** x787.5. These images are representative of six Wistar rats.

At E18 when the developing incisor was in transition from cap to bell stage (**Figure 3.6**), positive staining for the presence of ADM was visible in the cells of the internal dental epithelium, whilst there appears to be some pericellular positive staining indicating the presence of ADM in the cells of the dental papilla, stellate reticulum and outer dental epithelium, which could indicate paracrine signalling (**Figures 3.6 A & B**). The pre-incubation of an ADM peptide with the ADM antibody resulted in no detectable positive staining for the presence of ADM in any of the cells of the developing incisor (**Figure 3.6 C**). Similar results were observed with pre-bleed rabbit serum and the negative control samples, with no positive staining for ADM apparent (**Figures 3.6 D, E & F**).





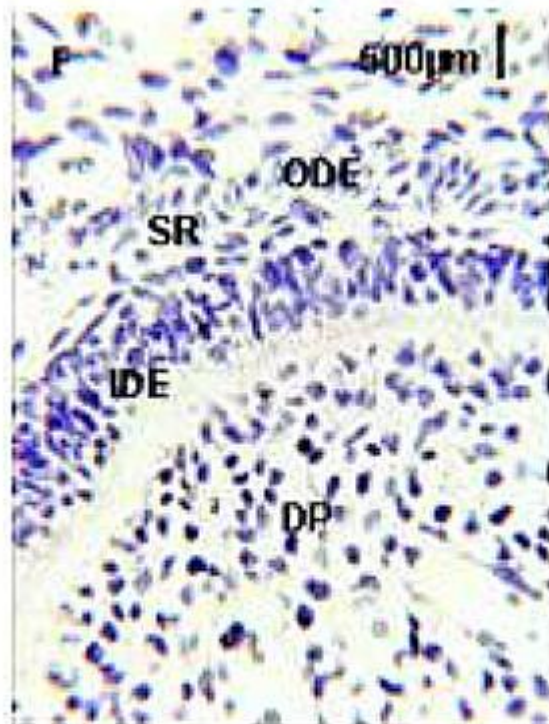
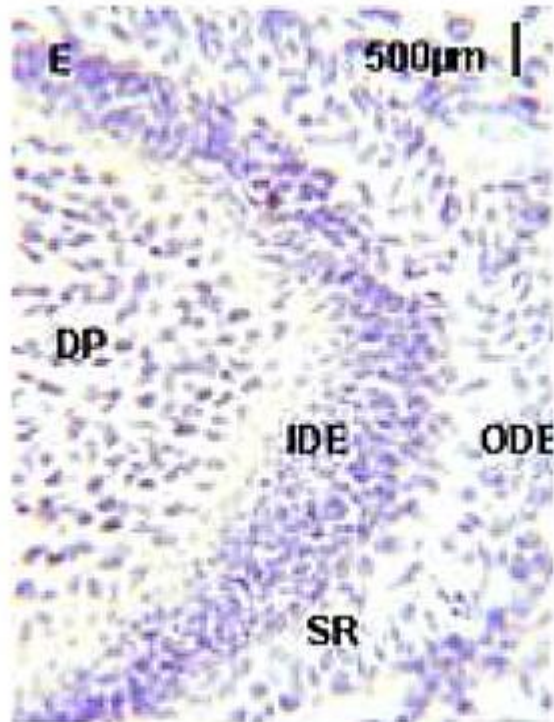
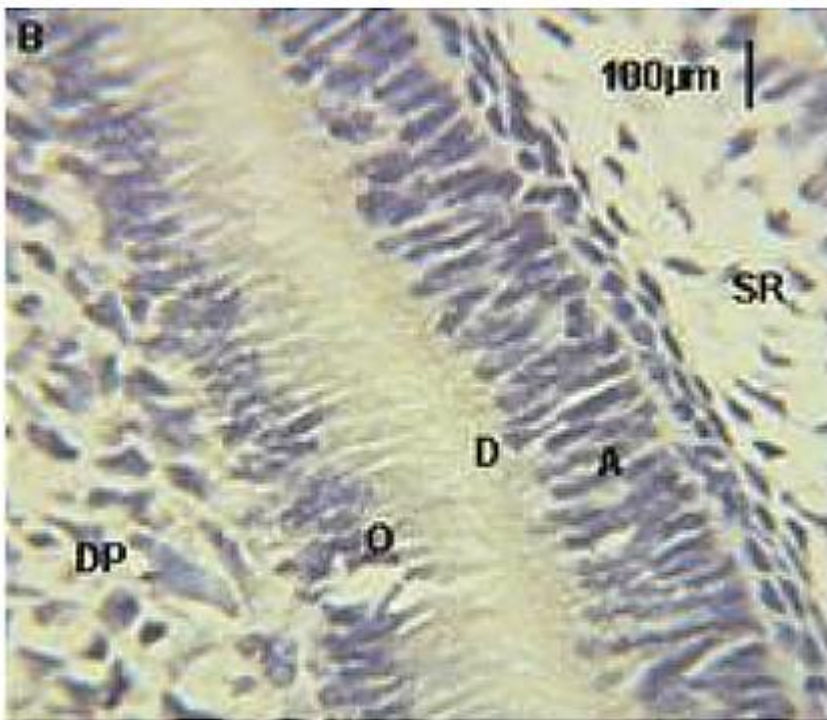
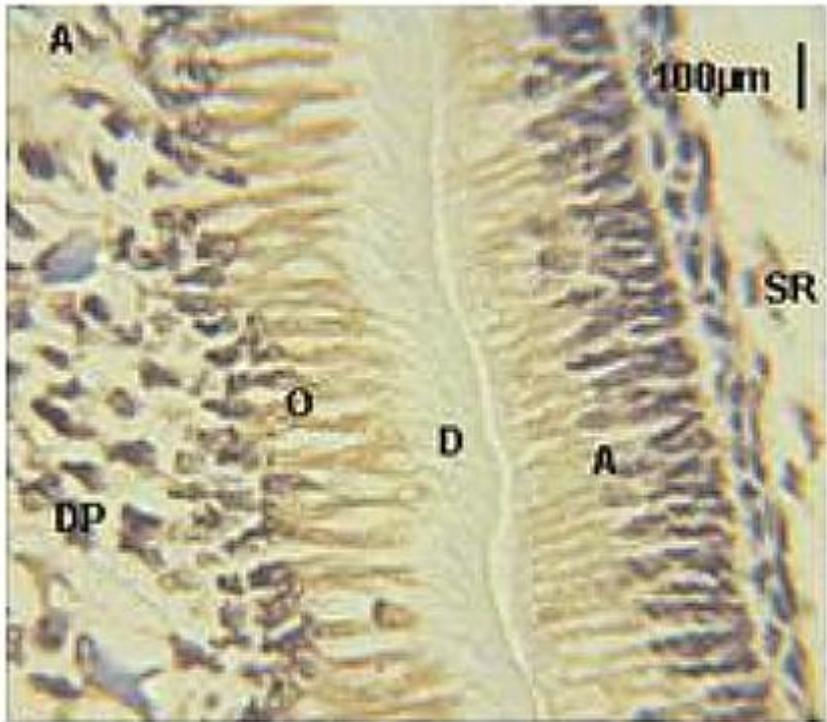


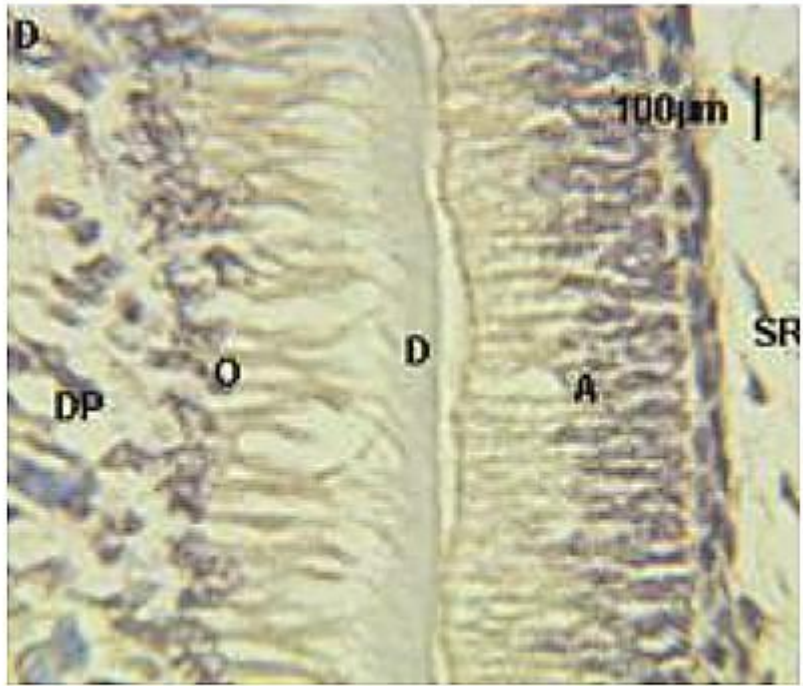
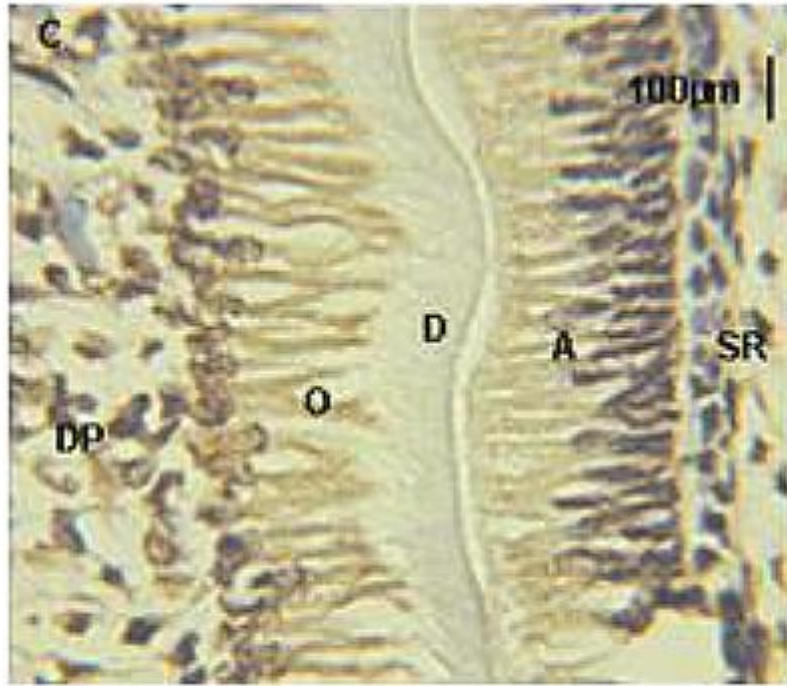
Figure 3.6: Representative immunohistochemical images of male Wistar rat incisors at E18. Specimens are stained with **A + B:** 1/3500 anti-ADM (mag. **A:** x500 **B:** x787.5). **C:** 1/3500 anti-ADM + ADM peptide (ADM blocking control) mag. x500. **D:** 1/3500 pre-bleed rabbit serum mag. x500. **E + F:** no antibody present (negative control) mag. x500. Key features denoted: DP = dental papilla. IDE = internal dental epithelium. ODE = outer dental epithelium. SR = stellate reticulum. These images are representative of six Wistar rats.

At E20, when the incisor was demonstrably in the bell stage, positive staining for ADM was observed in the odontoblasts and ameloblasts, predominantly in the processes where extracellular secretion occurs (**Figure 3.7 A**), suggesting that ADM may be involved in this process. The cells of the dental papilla appear to have some positive staining albeit at a lower intensity compared to the odontoblasts and ameloblasts, while in the stellate reticulum it appears that there was no immunoreactivity detected for ADM (**Figure 3.7 A**). In the ADM blocking control (**Figure 3.7 B**), there was no observable positive staining for ADM in any of the cells of the developing incisor.

Following staining of embryonic age E20 incisors using a TGF- β 1 antibody (**Figure 3.7 C**) positive staining was observed in the processes of the odontoblasts and ameloblasts, similar to that observed following staining for ADM (**Figure 3.7 A**), increasing our knowledge from previously published data showing co-expression of these two growth factors during embryogenesis. The inclusion of a TGF- β 1 peptide pre-incubation step blocked detectable immunoreactivity for TGF- β 1 (**Figure 3.7 D**).

Sections stained with pre-bleed rabbit serum and the negative control produced no observable positive staining in any cells of the developing incisor (**Figure 3.7 E & F**).





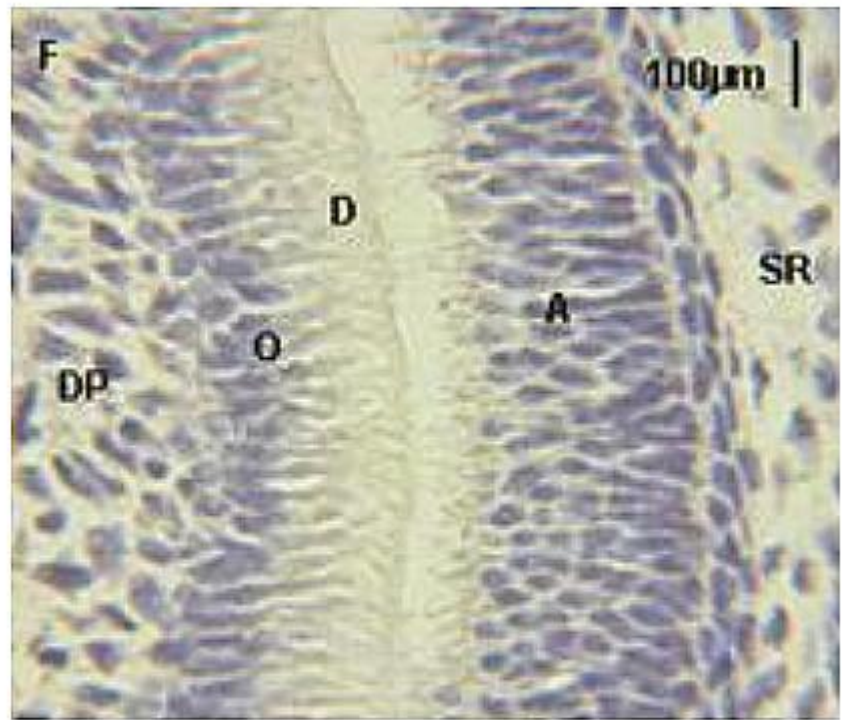
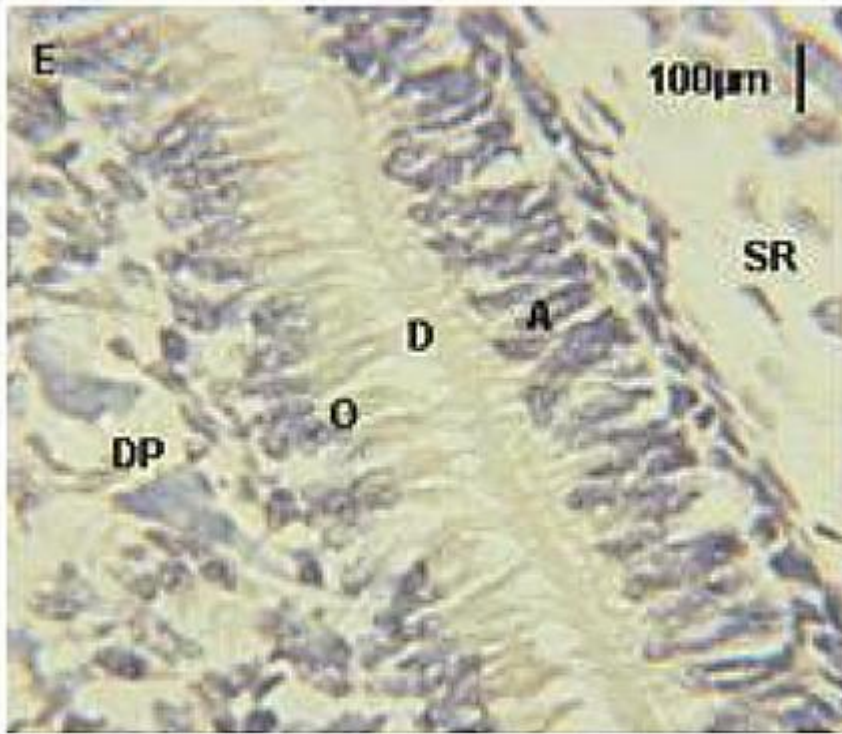


Figure 3.7: Representative immunohistochemical images of male Wistar rat incisors at E20. Specimens are stained with **A:** 1/3500 ADM antibody **B:** 1/3500 ADM antibody + ADM peptide (ADM blocking control) **C:** 1/300 TGF- β 1 antibody **D:** 1/300 TGF- β 1 antibody + TGF- β 1 peptide **E:** 1/3500 pre-bleed rabbit serum **F:** no antibody present (negative control). Key features denoted: DP = dental papilla. O = odontoblasts. D = dentin. A = ameloblasts. SR = stellate reticulum. These images are representative of six Wistar rats.

4. Results Chapter 2

4.1 Effect of ADM, Dexamethasone and DMPs on dental cell behaviour

Whilst published data (Montuenga *et al*, 1997), along with the histological studies reported in the previous chapter, implicate ADM in tooth development, its' mechanism of action in these cells is yet to be determined. Notably ADM has been shown to stimulate proliferation in several cell types, including Swiss 3T3 fibroblasts, skin and oral keratinocytes, thymocytes and osteoblasts (Martinez *et al*, 1997; Kapas *et al*, 1997; Isumi *et al*, 1998; Cornish *et al*, 2002; Hamada *et al*, 2002; Belloni *et al*, 2003). Conversely, in cardiac fibroblasts, hepatic stellate and rat mesangial cells, ADM suppresses cell growth (Jiang *et al*, 2004; Wang *et al*, 2005; Chini *et al*, 1995). The purpose of the following studies, therefore, was to determine whether ADM affected cell numbers in dental cells. The cell lines used were MDPC-23 cells and OD-21 cells, which are murine odontoblast-like and dental pulp-like cells isolated from foetal tissues, respectively (Hanks *et al*, 1998). The murine 3T3 skin fibroblast cell line was used as control, as ADM has been previously shown to induce proliferation in these cells (Isumi *et al*, 1998).

Initially, to determine whether these cell lines were likely to respond to ADM, gene expression analyses for the ADM receptors, along with the proliferation marker PCNA, were performed. ADM is known to signal through two ADM-specific receptors, namely AM-1 and AM-2, and these are made up of a dimer of calcitonin receptor-like receptor (CRLR) and either receptor activity modifying protein-2 or -3 (RAMP-2 and RAMP-3, respectively) (McLatchie *et al*, 1998; Aiyar *et al*, 2001; Muff *et al*, 2001; Oliver *et al*, 2001).

The effects of ADM on cell number were also compared to that of EDTA extracted dentine matrix proteins (DMPs) and dexamethasone. Notably, particular concentrations of DMPs have been shown to increase dental cell numbers (Graham, 2004) and these preparations are known to contain ADM, which is released along with other growth factors during dentine dissolution (Graham, 2004; Tomson *et al*, 2007). Dexamethasone is well characterized *in vitro* with regards to its mineralising induction action (Cheng *et al*, 1996; Hildebrandt *et al*, 2009) and is known to induce the differentiation of bone marrow stromal cells into osteoblasts (Cheng *et al*, 1994). Dexamethasone is thought to elicit its mineralising and differentiating effects through the expression of key matrix proteins Bone Sialoprotein (BSP), Osteocalcin (OCN) and Osteopontin (OPN) (Cheng *et al*, 1996; Mikami *et al*, 2007), regulated through the transcription factor *Runx2* (Mikami *et al*, 2007). It has also been shown to regulate expression of ADM and/or its receptors in several cell lines, including myocytes, smooth muscle cells, retinal pigment epithelial cells and osteoblasts (Nishimori *et al*, 1997; Hattori *et al*, 1999; Frayon *et al*, 2000; Udono-Fujimori *et al*, 2004 and Uzan *et al*, 2004). Markedly a glucocorticoid receptor element has been identified in the regulatory sequences of ADM and the ADM receptor, calcitonin receptor like receptor (CRLR) (Nikitenko *et al*, 2003; Zudaire *et al*, 2005). These results indicate the potential for a component of dexamethasone's cellular effects to be mediated via regulation of an ADM autocrine signalling mechanism.

To confirm that the responses observed were due to ADM specific interactions, an antagonist for ADM was also included in the experimental design. ADM₂₂₋₅₂ is known to act as a competitive antagonist for both the AM-1 and AM-2 receptors (Hay *et al*, 2004). ADM₂₂₋₅₂ is a partial fragment of the full ADM growth factor and is able to partially bind to the receptors as it retains the C-terminal residue,

however, it does not contain the disulfide bridge which would allow it to elicit a response, hence acting as a low affinity competitive antagonist (Eguchi *et al*, 1994; Hay *et al*, 2003). Initially, ADM₂₂₋₅₂ activity was analysed alone to determine whether it elicited agonistic effects and subsequently in the presence of ADM to determine if it modulated ADM activity.

4.2 Effect of ADM cellular exposure on ADM receptor and PCNA gene expression

In this study, MDPC-23, OD-21 and 3T3 cells were exposed to a range of concentrations of ADM for 24 hours. Cells were subsequently lysed and the RNA extracted. RT-PCR was performed to determine the effect of ADM exposure on the gene expression of CRLR, RAMP-2 and PCNA (see **Sections 2.2.4 and 2.5**). ADM is part of the calcitonin superfamily of regulatory peptides (Kitamura *et al*, 1993) and exerts its effect upon cells directly through interactions with CRLR/RAMP-2 (AM-1) or CRLR/RAMP-3 (AM-2) receptor complexes (McLatchie *et al*, 1998). ADM's effects upon CRLR and RAMP-2 gene expression were therefore examined to determine whether these receptor components were present in the target cell lines and whether ADM has a role in regulating their expression. PCNA is expressed in the nuclei of cells during DNA synthesis (Leonardi *et al*, 1992) and therefore transcript levels were also investigated as a surrogate marker for cell proliferation.

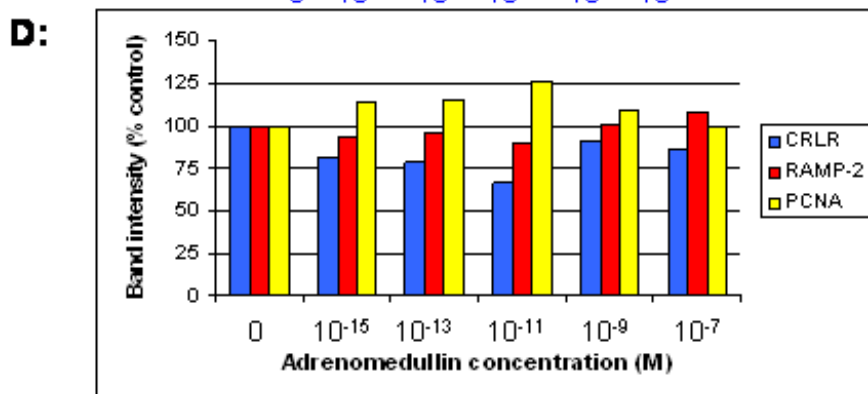
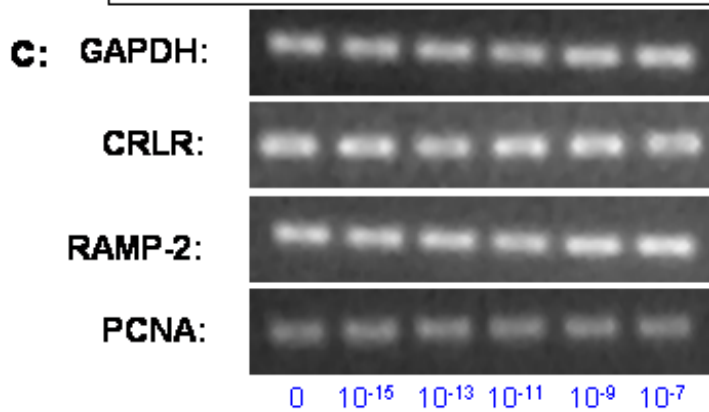
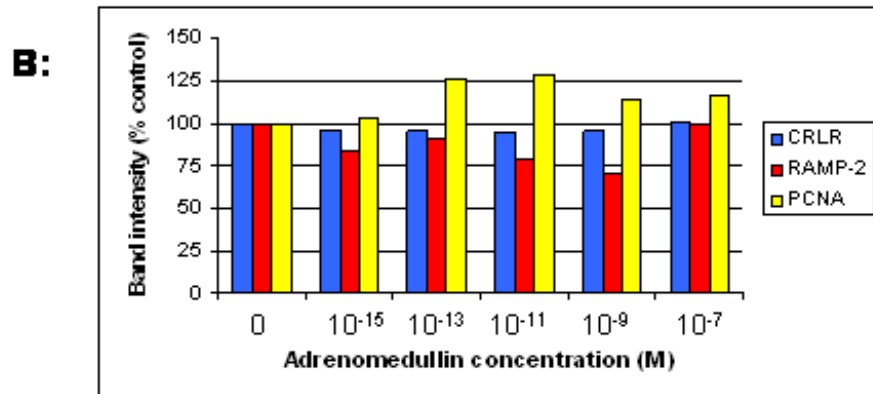
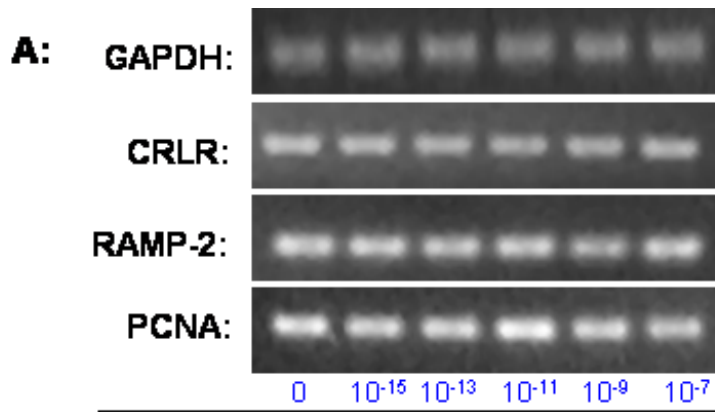
4.2.1 Analysis of CRLR, RAMP-2 and PCNA transcript levels in MDPC-23, OD-21 and 3T3 cells

Figure 4.1A provides representative gel images of GAPDH, CRLR, RAMP-2 and PCNA gene expression in MDPC-23 cells following 24 hour exposure to a range of concentrations of ADM. Figure 4.1B presents the mean band intensities obtained from these studies. The data indicate that CRLR gene expression appeared relatively unaltered following treatment with ADM. Expression levels decreased only minimally following treatment with 10^{-15} M, 10^{-13} M, 10^{-11} M and 10^{-9} M, while 10^{-7} M ADM had no observable effect on CRLR transcript levels. RAMP-2 expression appeared to minimally decrease following cell exposure to the ADM concentrations used.

PCNA gene expression marginally increased following exposure to all concentrations of ADM used, with potentially the greatest change observed at 10^{-11} M ADM.

The effect upon OD-21 cell gene expression levels of CRLR, RAMP-2 and PCNA following exposure to ADM is presented in Figures 4.1C and D with representative gel images and associated densitometric analysis provided. In OD-21 cells, the levels of CRLR mRNA appeared to show a dose dependent trend in reduction following exposure to ADM. ADM concentrations of 10^{-15} M, 10^{-13} M, 10^{-11} M, 10^{-9} M and 10^{-7} M decreased densitometrically derived values by 18%, 22%, 34%, 9% and 14%, respectively, compared to the untreated control. RAMP-2 levels also appeared to decrease in OD-21 cells following exposure to the lower three concentrations of ADM (10^{-15} M, 10^{-13} M and 10^{-11} M by 6, 4 and 11% densitometric reduction compared to control, respectively). Changes in PCNA expression in OD-21 cells exhibited a similar pattern to that observed for MDPC-23 cells. ADM appeared to marginally elevate expression as 10^{-15} M, 10^{-13} M, 10^{-11} M and 10^{-9} M increased the densitometric values by 14%, 15%, 26% and 9%, respectively.

ADM's effect on gene expression in 3T3 cells is presented in Figures 4.1E and F. In this cell line exposure to each concentration of ADM resulted in a marginal reduction in CRLR gene expression. A maximum reduction, as derived from densitometric values, of 10% was observed in CRLR expression following treatment with 10^{-7} M ADM. Other reductions observed in transcript levels were relatively minor. RAMP-2 gene expression generally appeared unaltered following ADM exposure, although 10^{-7} M ADM induced a RAMP-2 densitometric reduction of ~28%. PCNA expression appeared to marginally increase in 3T3 cells with a dose-dependant trend following ADM exposure. At the highest concentration used, 10^{-7} M ADM, a densitometric increase of 15% was calculated compared to the control cultures.



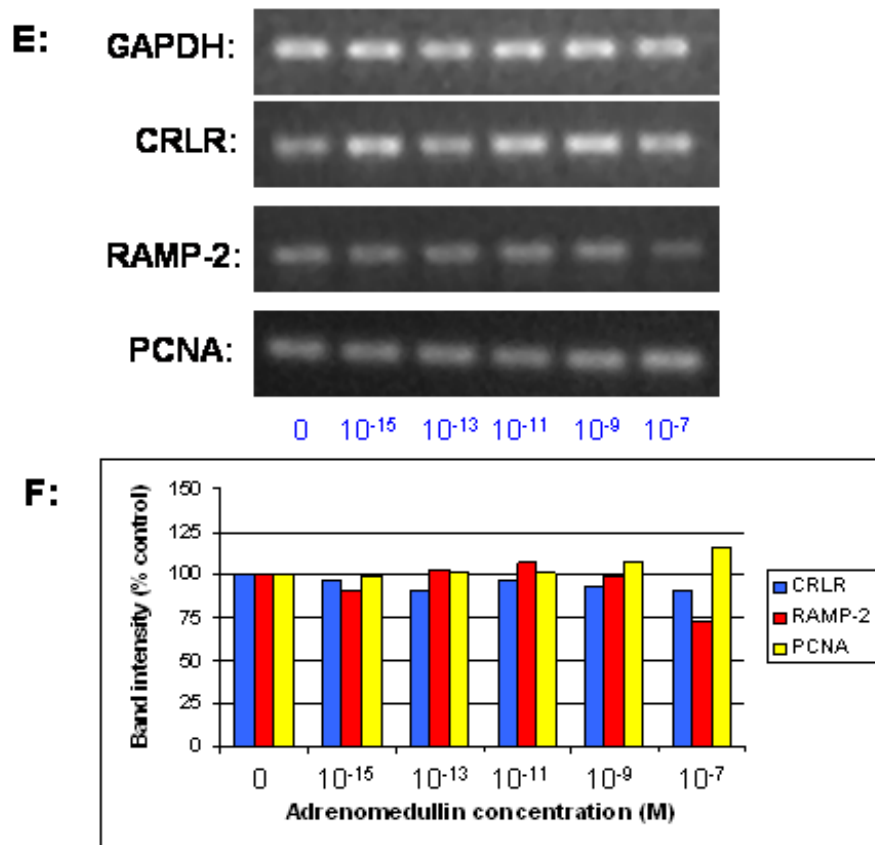


Figure 4.1: **A C** and **E** are representative gel images of effect of **A:** MDPC-23, **C:** OD-21 and **E:**3T3 cells exposed to a range of concentrations of ADM (10⁻¹⁵M, 10⁻¹³M, 10⁻¹¹M, 10⁻⁹M and 10⁻⁷M) for 24 hours on GAPDH, CRLR, RAMP-2 and PCNA gene expression. **B D** and **F** are graphical representations of the effect of treatment with the aforementioned ADM concentrations on CRLR, RAMP-2 and PCNA expression compared to the control in **B:** MDPC-23, **D:** OD-21 and **F:** 3T3 cells. Values obtained are averages from densitometric evaluation of the gel image bands, following normalisation to GAPDH. This experiment was done in duplicate.

4.3 Effect of ADM on MDPC-23, OD-21 and 3T3 cell number

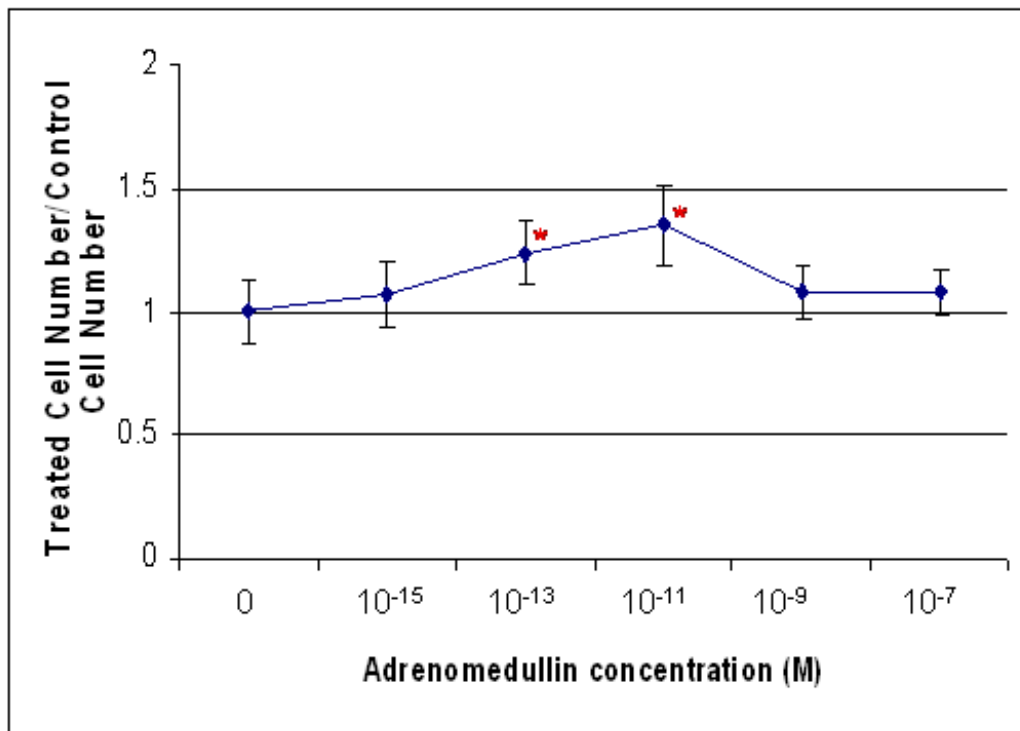
Following the identification of an ADM receptor component in the target cell lines and the increases in PCNA expression observed as a result of ADM exposure (**Section 4.2**), the effect of ADM upon MDPC-23, OD-21 and 3T3 cell number was assessed. Viable cell numbers (see **Section 2.2.2**) following 48 hour exposure to a range of concentrations of ADM were determined and compared to control unstimulated cultures. Statistical significance was measured using one-way ANOVA test ($P < 0.05$) (see **Section 2.9**). Cell viability data not presented as non-viable cell number was not affected by exposure to ADM (non viable cells $< 1\%$ for all concentrations studied).

Results presented in Figure 4.2A indicate the ratio of the average MDPC-23 cell number following treatment with a range of concentrations of ADM, in relation to the control. Data indicate ADM has a biphasic response on cell number in these cells. The relatively low concentrations of ADM, 10^{-13}M and 10^{-11}M , induced a statistically significant increase in cell number of 24% and 34%, respectively, compared to control. Whilst 10^{-9}M and 10^{-7}M ADM both increased cell numbers by $\sim 8\%$, these changes, however, were not statistically significant.

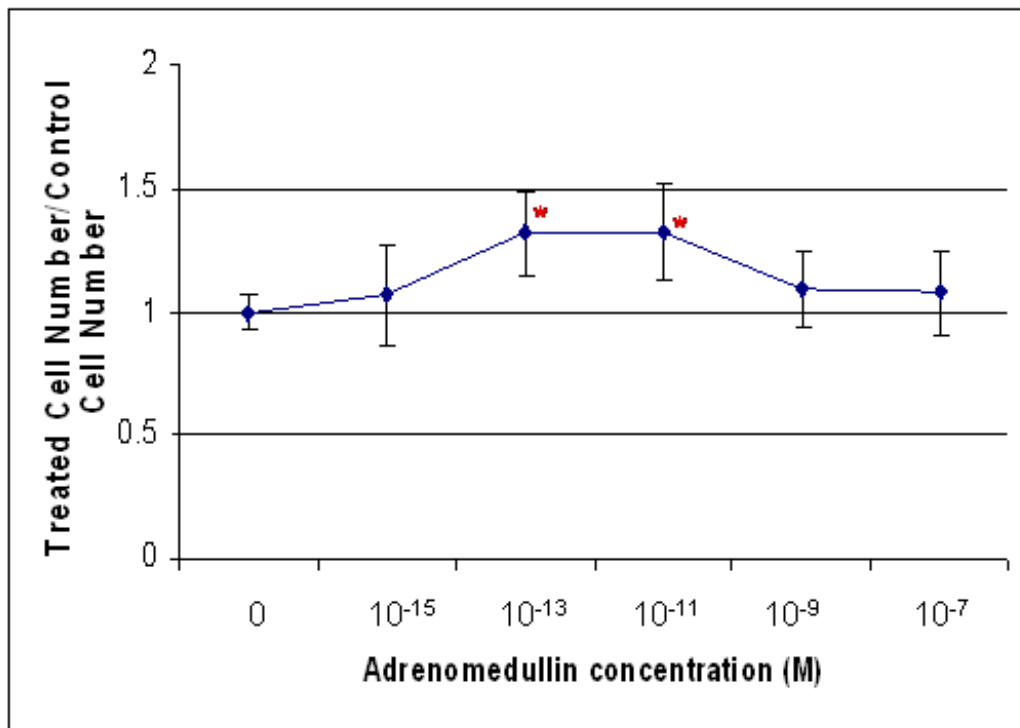
Interestingly a similar biphasic response to ADM exposure, as seen with the MDPC-23 cells, was observed in OD-21 cells (**Figure 4.2B**). Whilst ADM concentrations of 10^{-15}M , 10^{-9}M and 10^{-7}M all produced increases in viable cell numbers (7%, 9% and 8%, respectively), these were not found to be statistically significant. However 10^{-13}M and 10^{-11}M ADM, both elicited a statistically significant increase in cell number compared to the control, with both stimulating increases in cell numbers by $\sim 32\%$ as compared to the control.

The cell number profile of 3T3 cells in response to increasing concentrations of ADM is shown in Figure 4.2C. The relatively low concentrations of ADM, 10^{-15} M and 10^{-13} M, did not elicit a statistically significant change in 3T3 cell number compared to the control. Conversely 10^{-11} M, 10^{-9} M and 10^{-7} M ADM all statistically significantly increased 3T3 cell numbers by 24%, 24% and 50%, respectively. Notably the growth response profile observed for the 3T3 cultures was markedly different from that observed for the MDPC-23 and OD-21 cells (**Figures 4.1A & B**). This result, however, is comparable to that reported by Isumi *et al*, (1998), who also analysed the effect of ADM on Swiss 3T3 fibroblasts cell growth.

A:



B:



C:

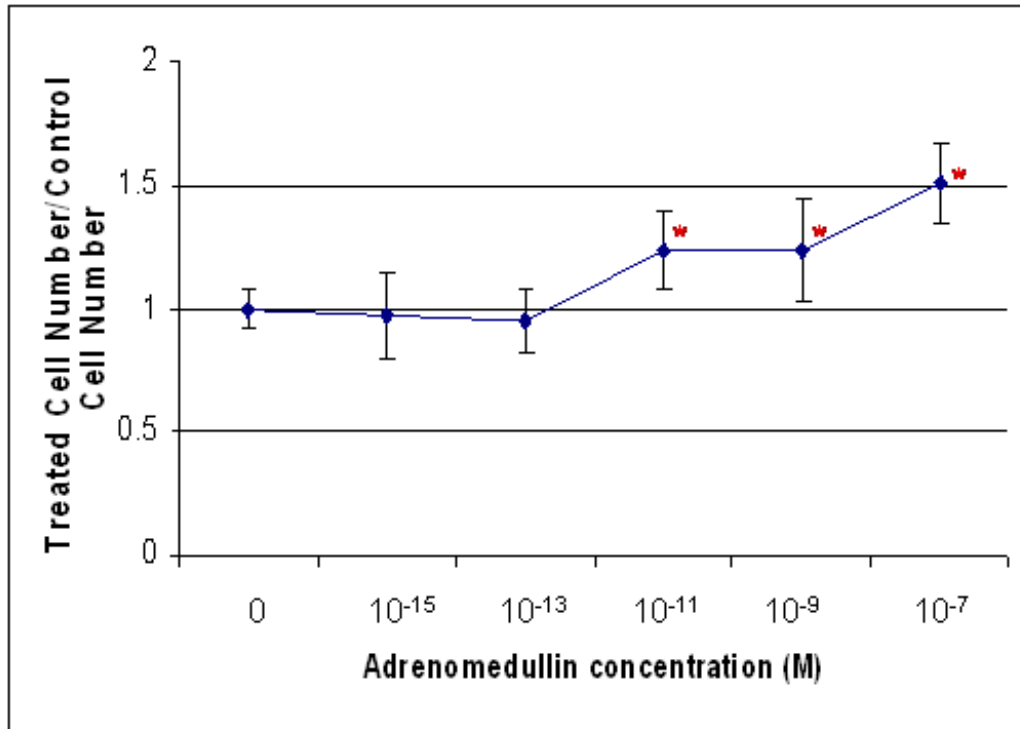


Figure 4.2: Changes in A: MDPC-23, B: OD-21 and C: 3T3 cell number following 48 hour stimulation with 0, 10^{-15} M, 10^{-13} M, 10^{-11} M, 10^{-9} M and 10^{-7} M ADM. This experiment was run in triplicate and repeated four times.

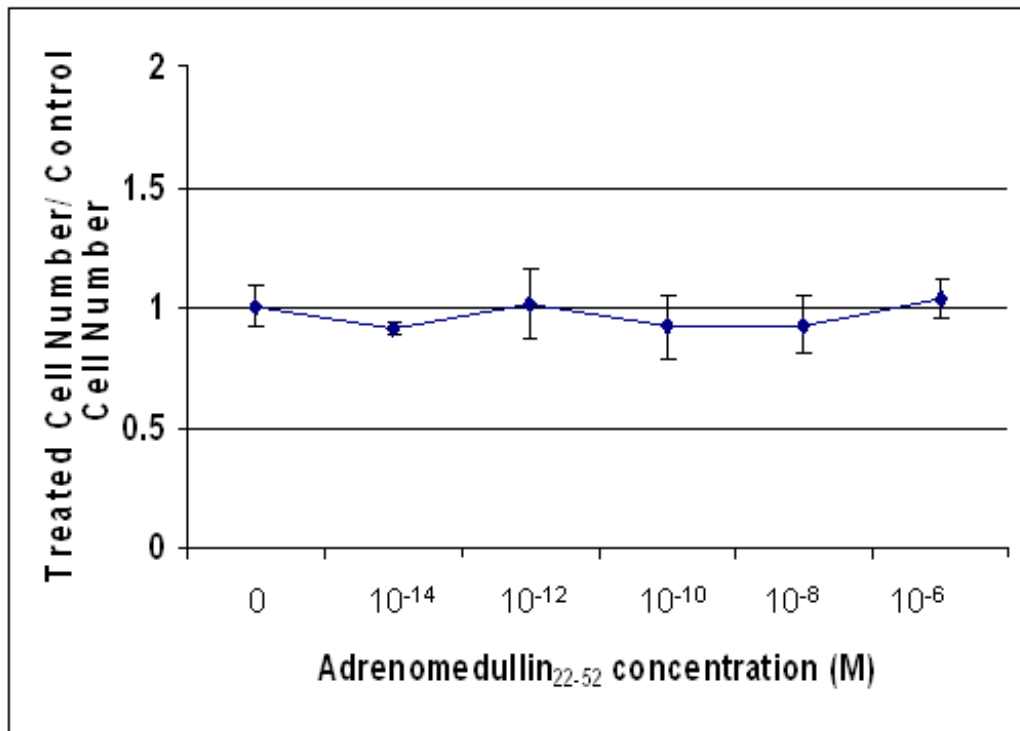
*** = Statistically significant difference compared to the control ($P < 0.05$).**

4.4 Analysis of the ADM₂₂₋₅₂ antagonist on MDPC-23, OD-21 and 3T3 cell number

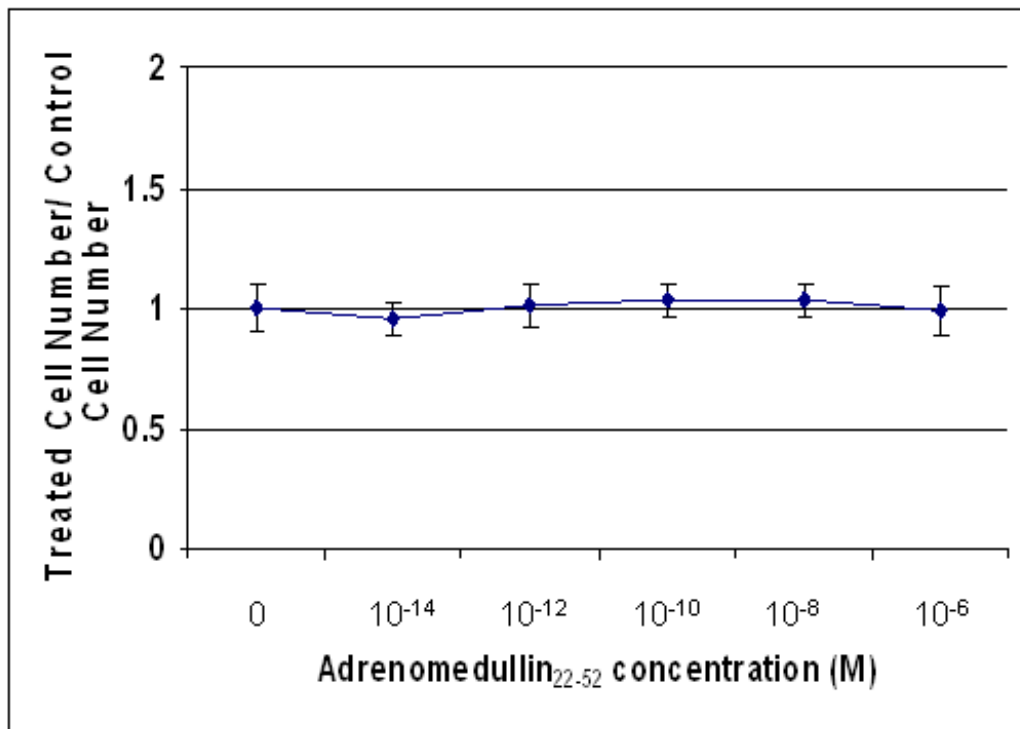
To determine if the ADM antagonist, ADM₂₂₋₅₂, affected numbers of the cell lines, cell counts were performed following treatment with a range of concentrations of ADM₂₂₋₅₂. Concentrations analysed were selected from studies, which previously used the ADM antagonist (Hay *et al*, 2003). Viable cell numbers were compared to those of the control unexposed samples (see **Section 2.2.2**). Cell viability data not presented as non-viable cell number was not affected by exposure to ADM₂₂₋₅₂ (non viable cells < 1% for all concentrations studied).

Data indicated that that ADM₂₂₋₅₂ had minimal effect on MDPC-23, OD-21 and 3T3 cell numbers at the concentrations used (**Figure 4.3**). Cell numbers varied minimally for all cell lines under the range of concentrations used, however, no changes were found to be statistically significant.

A:



B:



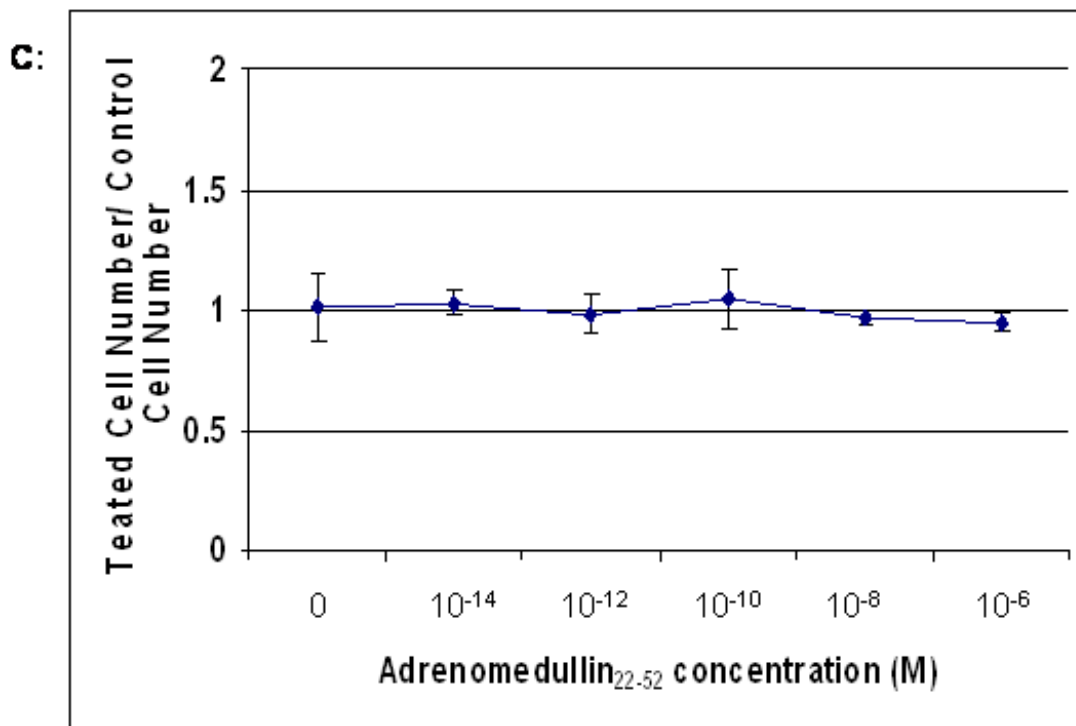


Figure 4.3: Changes in A: MDPC-23, B: OD-21 and C: 3T3 cell number following 48 hour stimulation with 0, 10⁻¹⁴M, 10⁻¹²M, 10⁻¹⁰M, 10⁻⁸M and 10⁻⁶M of the ADM antagonist ADM₂₂₋₅₂. This experiment was run in triplicate and repeated four times.

*** = Statistically significant difference compared to the control (P<0.05).**

4.5 Antagonistic effect of ADM₂₂₋₅₂ on ADM's ability to increase cell number

To determine whether the effect of ADM exposure on cell numbers in the cell lines studied in Section 4.3 was likely due to ADM specific receptor interactions, analyses were performed which included 20 minute pre-treatment of cells with a range of concentrations of the ADM antagonist, ADM₂₂₋₅₂ (10^{-12} M, 10^{-10} M, 10^{-8} M and 10^{-6} M), prior to stimulation with ADM at concentrations of 10^{-11} M, 10^{-11} M and 10^{-7} M. These ADM concentrations analysed were those previously identified as being optimal to increase cell number in the MDPC-23, OD-21 and 3T3 cells, respectively (**Figure 4.2**). The ADM₂₂₋₅₂ concentrations chosen for this study were the same as those in previously published reports (Hay *et al*, 2004). As previously described, viable cell numbers were determined and compared to those of the control (see **Section 2.2.2**). Statistical significance was determined using one-way ANOVA tests ($P < 0.05$) (see **Section 2.9**). Cell viability data not presented as non-viable cell number was not affected by exposure to ADM₂₂₋₅₂ or ADM (non viable cells $< 1\%$ for all concentrations studied).

4.5.1 Antagonistic effect of ADM₂₂₋₅₂ on the proliferative effect of ADM in MDPC-23, OD-21 and 3T3 cells

Data demonstrating the ability of ADM₂₂₋₅₂ to act antagonistically to ADM in MDPC-23 cells are provided in Figure 4.4A. In this study 10^{-11} M ADM alone statistically significantly increased cell numbers by 37% above those of the control. However, as the concentrations of the ADM₂₂₋₅₂ antagonist used increased, the cell numbers at 48 hours of growth decreased. Notably 10^{-8} M ADM₂₂₋₅₂ statistically significantly reduced the cell numbers from 37% with 10^{-11} M ADM alone down to 17% in the presence of the antagonist, as compared to control cultures. When the concentration of ADM₂₂₋₅₂

was increased to 10^{-6} M, cell numbers decreased by 47% compared to 10^{-11} M ADM exposure alone. This reduction in cell number was statistically significant.

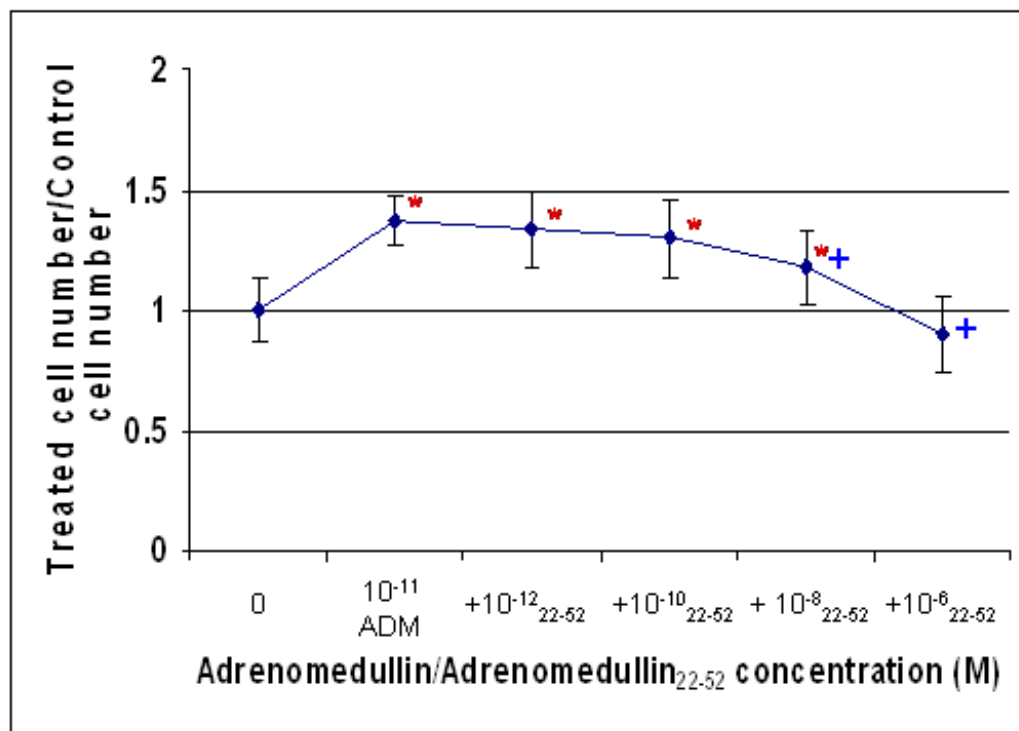
Data presented in Figure 4.4B demonstrated the antagonistic effect of ADM₂₂₋₅₂ on the ability of ADM to affect cell numbers in OD-21 cells. When the cells were treated with ADM alone cell numbers increased statistically significantly by 35%. Whilst this increase in cell number was decreased by the addition of 10^{-12} M and 10^{-10} M ADM₂₂₋₅₂ these reductions in cell number were not shown to be statistically significant. Similar to the data obtained for MDPC-23 cells, 10^{-8} M ADM₂₂₋₅₂ was the lowest concentration used which reduced cell number by a statistically significant amount (19%). The highest concentration of ADM₂₂₋₅₂ used, 10^{-6} M, reduced cell numbers by 54% compared to 10^{-11} M ADM stimulation alone, resulting in a statistically significant 20% reduction compared to the control.

In 3T3 cells, treatment with 10^{-7} M ADM alone increased cell numbers by 51% in this cell line and the relatively low concentrations of the antagonist, 10^{-12} M and 10^{-10} M ADM₂₂₋₅₂, resulted in minimal inhibition (**Figure 4.4C**). Whilst the addition of 10^{-8} M ADM₂₂₋₅₂ reduced cell numbers by 19% compared to 10^{-7} M ADM exposure alone, this result was not found to be statistically significant. Treatment with 10^{-6} M ADM₂₂₋₅₂ did however elicit a statistically significant reduction in 3T3 cell numbers by ~60% compared to 10^{-7} M ADM exposure alone.

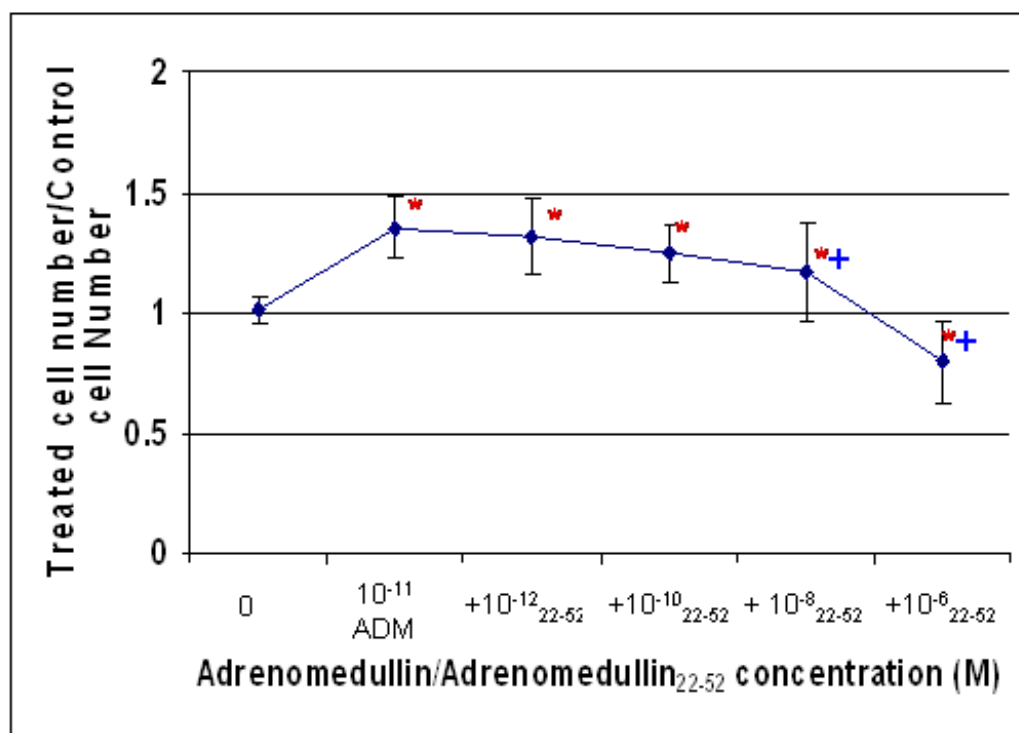
In each cell line the lower concentrations of ADM₂₂₋₅₂ failed to have an effect on cells exposed to 10^{-7} M ADM, but at higher concentrations of ADM₂₂₋₅₂ exposure, cell numbers are significantly reduced. This data is not surprising as ADM₂₂₋₅₂ acts as a low infinity competitive inhibitor to ADM (Eguchi *et al*, 1994; Hay *et al*, 2003). The fact that the higher concentrations of ADM₂₂₋₅₂ lowers cell numbers below that of the control could perhaps be explained by blocking the effect endogenous ADM,

however, this is unlikely as exposure to ADM₂₂₋₅₂ alone (**Section 4.4**) did not elicit such an effect. To fully elucidate why this reduction occurs, further pharmacological studies would be required.

A:



B:



C:

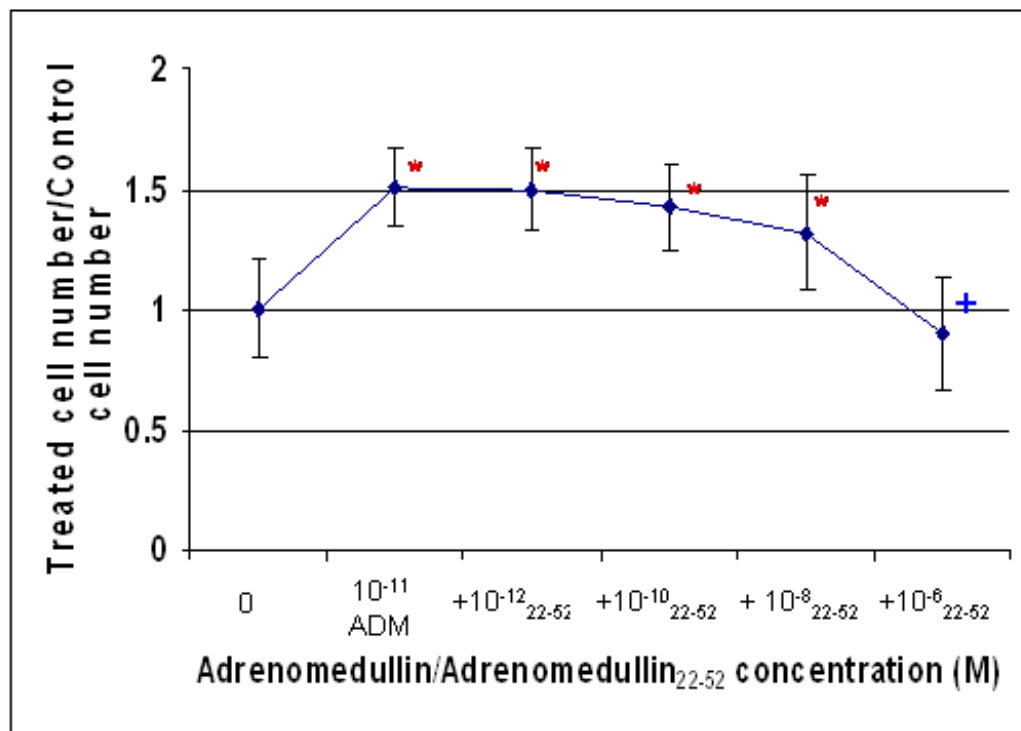


Figure 4.4: Changes in A: MDPC-23, B: OD-21 and C: 3T3 cell number following 48 hour stimulation with 0 ADM or A+B: 10⁻¹¹M and C: 10⁻⁷M ADM with 0, 10⁻¹²M, 10⁻¹⁰M, 10⁻⁸M and 10⁻⁶M of the ADM antagonist ADM₂₂₋₅₂. This experiment was run in triplicate and repeated four times.

*** = Statistically significant difference compared to the control (P<0.05). + = statistically significant compared to 10⁻¹¹M ADM (P<0.05)**

4.6 Effect of DMP exposure on MDPC-23, OD-21 and 3T3 cell numbers

Previous studies have demonstrated that amongst the growth factors sequestered in EDTA extracted DMPs (E-DMPs), ADM is present at relatively high concentrations (approximately 2.61pg/mg), especially when compared to other growth factors such as TGF- β 1 (MacLachlan *et al*, 2002; Graham, 2004; Tomson *et al*, 2007). In addition it has also been demonstrated that DMPs extracted using this method stimulate MDPC-23 and OD-21 cell growth (Graham, 2004).

In this study, MDPC-23, OD-21 and 3T3 cells were treated with a range of concentrations of DMPs using the same protocol as that described previously for ADM exposure (see **Section 4.3**). Cell numbers were subsequently compared to those obtained using ADM exposure alone to determine if there is a possibility that the proliferative effect previously found with DMPs might correlate with the concentration of its' ADM component. However, there are other growth factors, such as TGF- β 1, also released from E-DMPs and therefore, without antagonistic studies demonstrating a reduction in ADM induced cell number, this data should be viewed solely as an indication of ADM's potential involvement. Notably, no previous comparisons have been made between the effects of E-DMPs on cell number and the effects of it's constituent growth factors on cell number, providing interesting avenues for future study.

According to data obtained by Graham, (2004), there is ~2.61pg ADM contained within 1mg E-DMP. Therefore, the concentrations of DMPs utilised in this study were selected to enable relative comparative analysis with single ADM exposure as presented in Table 4.1.

E-DMP concentration (mg/ml)	ADM present in E-DMP (µg)	Concentration of ADM in E-DMP (M)	Concentration of ADM used in Section 4.2 (M)
0.00001	0.0000026	4.4×10^{-16}	1×10^{-15}
0.001	0.00026	4.4×10^{-14}	1×10^{-13}
0.1	0.026	4.4×10^{-12}	1×10^{-11}
10	2.6	4.4×10^{-10}	1×10^{-9}
1000	261	4.4×10^{-8}	1×10^{-7}

Table 4.1: Table showing concentrations of ADM sequestered from E-DMPs and those examined in Section 4.2.

Following cellular exposure to E-DMPs, viable cell number counts were determined and compared to that of the control (see **Section 2.2.2**). Statistical significance was determined using one-way ANOVA tests ($P < 0.05$) (see **Section 2.9**). Cell viability data not presented as non-viable cell number was not affected by E-DMP exposure (non viable cells $< 1\%$ for all concentrations studied).

4.6.1 Cell number characterisation following exposure of MDPC-23, OD-21 and 3T3 cells to DMPs and comparable concentrations of ADM

The data on the effect of E-DMPs on the cell number of MDPC-23 cells, with previous ADM data, are illustrated in Figure 4.5A. The graph indicates that the lower three concentrations of DMPs used (0.00001mg/ml, 0.001mg/ml and 0.1mg/ml) increased cell numbers in comparison to ADM. Exposure of MDPC-23 cells to 0.001mg/ml of DMPs increased numbers by 33%, while the nearest concentration of ADM (10^{-13} M) increased cell number by 24%. The optimal increase in cell number

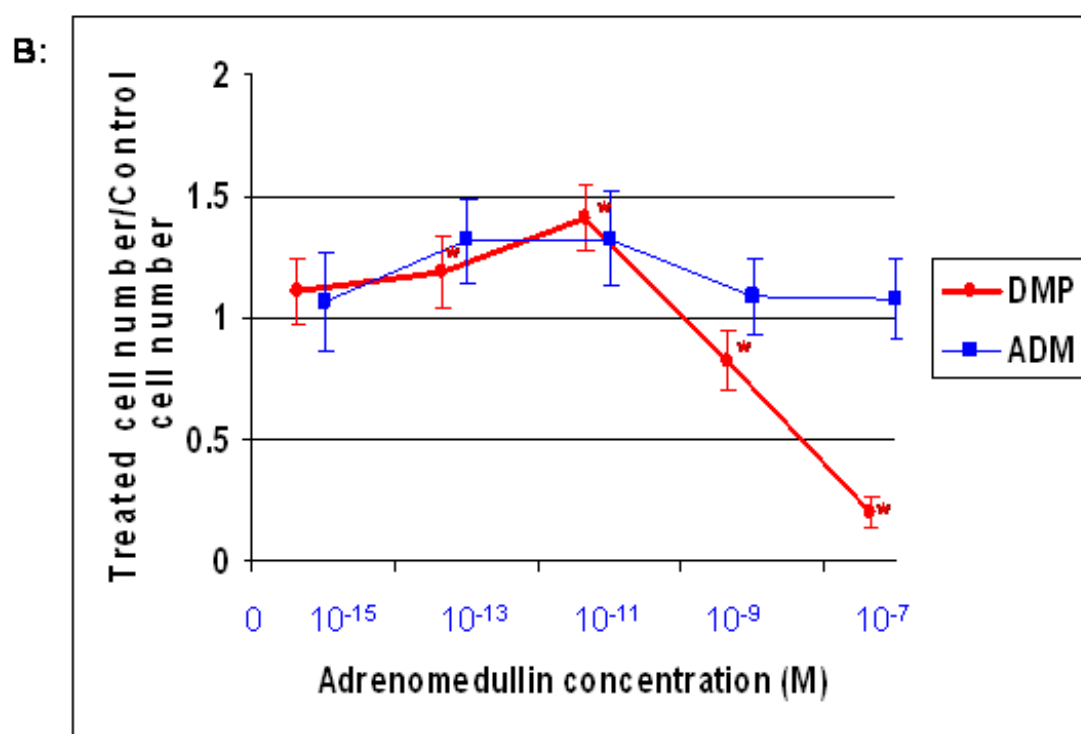
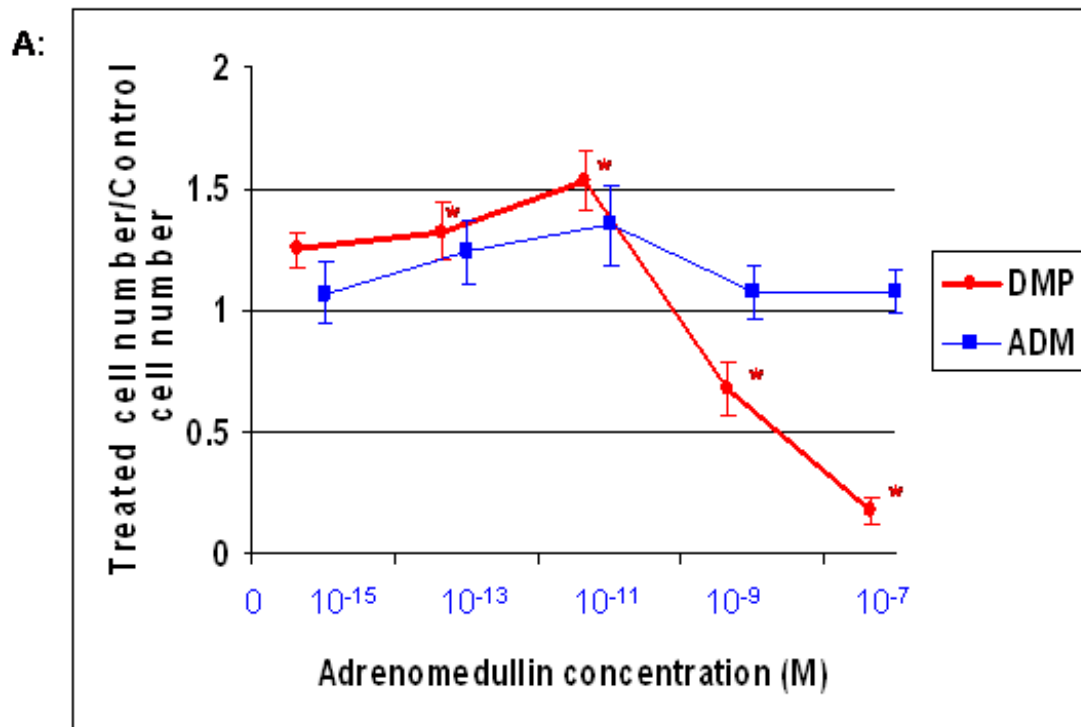
occurred at 0.1mg/ml DMP and 10^{-11} M ADM, which cell numbers increased by 54% and 35%, respectively, all of which were statistically significant increases compared to the unstimulated control.

At the higher two concentrations of DMPs examined (10mg/ml and 1000mg/ml), cell numbers decreased to below that of the control. Indeed 10mg/ml DMP decreased cell numbers to 68% whilst 1000mg/ml decreased numbers to 18% of the control. The higher concentrations of ADM (10^{-9} M and 10^{-7} M) produced non-significant increases in cell number compared to the control. The decreases in cell number seen with the higher DMP treatments (10mg/ml and 1000mg/ml) were statistically significant compared to the unstimulated control.

The effects of E-DMP and ADM treatment on the number of OD-21 cells were also studied (**Figure 4.5B**). In this cell line, increases in cell numbers were observed following exposure to 0.00001mg/ml DMP and 10^{-15} M ADM of 10% and 7%, respectively. Notably, cells exposed to 0.001mg/ml DMP exhibited a 19% increase in cell numbers whilst exposure to the nearest ADM concentration (10^{-13} M) increased cell numbers by 32%. Both increases were statistically significant compared to the control. Statistically significant increased cell numbers, above those of control, were also observed following 0.1mg/ml DMP and 10^{-11} M ADM exposure, which increased numbers by 41% and 32%, respectively.

Similar to the pattern observed for MDPC-23 cells, the higher two concentrations of DMP studied (10mg/ml and 1000mg/ml) statistically significantly decreased cell number by 18% and 80%, respectively. Conversely, the number of cells following treatment with the higher concentrations of ADM (10^{-9} M and 10^{-7} M) slightly increased cell number, although not statistically significantly, compared to the control; 9% with 10^{-9} M and 8% with 10^{-7} M.

Analysis of the effects of exposure to E-DMPs and the results obtained following ADM exposure to 3T3 cell numbers is presented in Figure 4.5C. Cell numbers increased with 3T3 cells exposed to 0.00001mg/ml DMP and the lowest ADM concentration. Neither of these increases were, however, statistically significant compared to the unstimulated control cultures. Cell numbers notably increased as the concentration of DMP used increased to 0.001mg/ml and 0.1mg/ml, with cell number increases of 24% and 51% above control, respectively. The nearest comparative ADM concentrations had differing effects with 10^{-13} M slightly decreasing cell number and 10^{-11} M increasing cell number by 23%. When the cells were subjected to relatively high concentrations of DMPs, cell numbers decreased, as seen previously for the two cell lines used. DMPs at concentrations of 10mg/ml and 100mg/ml decreased cell numbers by 12% and 45%, respectively, which were statistically significant compared to the unstimulated control. The higher concentrations of ADM used (10^{-9} M and 10^{-7} M) continued to produce statistically significant increases in cell numbers, 24% and 51%, respectively.



C:

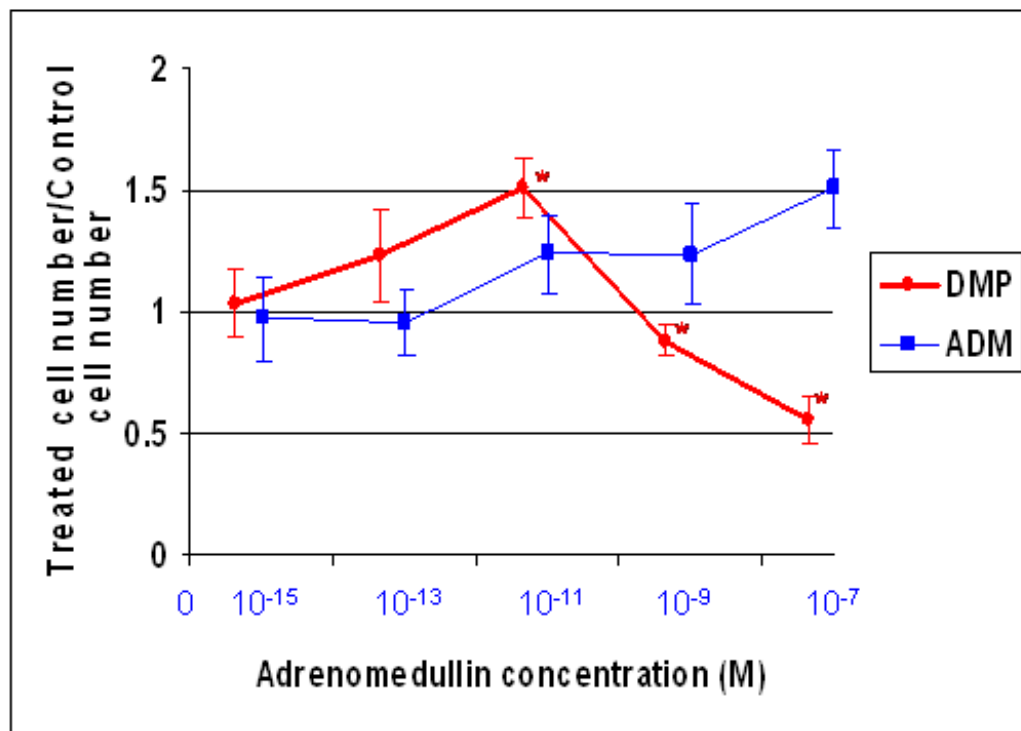


Figure 4.5: Changes in A: MDPC-23, B: OD-21 and C: 3T3 cell number following 48 hour stimulation with 0.00001, 0.001, 0.1, 10, 1000ng/ml E-DMP, compared with 0, 10⁻¹⁵M, 10⁻¹³M, 10⁻¹¹M, 10⁻⁹M and 10⁻⁷M ADM. This experiment was run in triplicate and repeated four times. x axis values denotes the ADM concentration found in the relative E-DMP concentrations (Graham *et al*, 2004)

*** = E-DMP cell counts that have a statistically significant difference compared to the control (P<0.05).**

4.7 Effect of Dexamethasone exposure on MDPC-23, OD-21 and 3T3 cell numbers

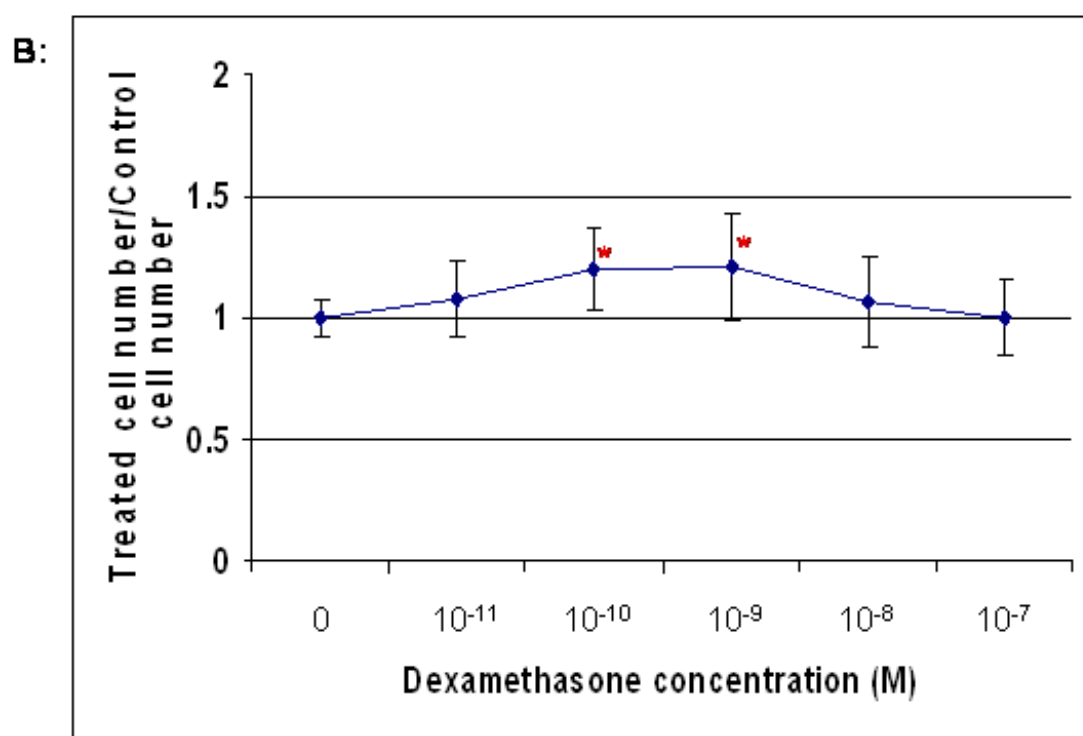
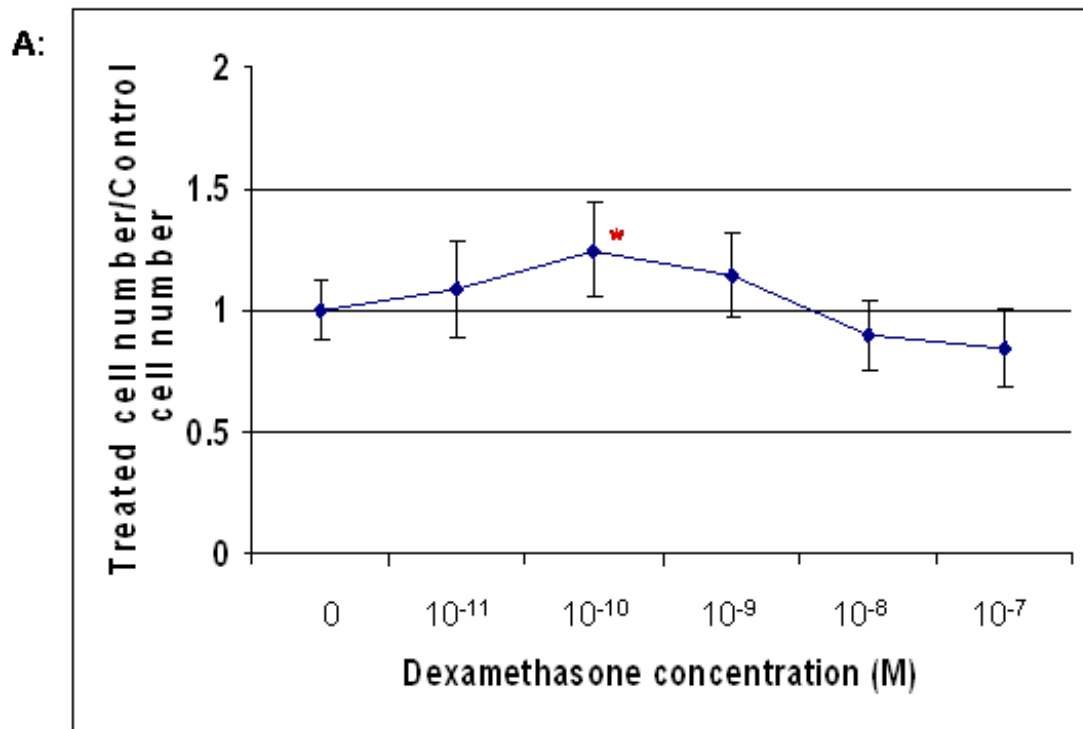
The ability of Dexamethasone (DEX) to increase cell numbers in MDPC-23, OD-21 and 3T3 cell lines was investigated. DEX has been shown to regulate expression of ADM and/or its receptors in several cell lines, including myocytes, smooth muscle cells, retinal pigment epithelial cells and osteoblasts (Nishimori *et al*, 1997; Hattori *et al*, 1999; Frayon *et al*, 2000; Udono-Fujimori *et al*, 2004 and Uzan *et al*, 2004), furthermore, the regulatory sequences of ADM and its receptor CRLR contain a glucocorticoid receptor element (Nikitenko *et al*, 2003; Zudaire *et al*, 2005) indicating the potential for a component of dexamethasone's cellular effects to be mediated via regulation of an ADM autocrine signalling mechanism.

The range of concentrations used in this study were similar to that previously described by Uzan *et al* (2004) when studying ADM's effect on ADM receptor expression in osteoblasts. The effect of DEX on cell number was assessed by determining viable cell number (see **Section 2.2.2**). Statistical significance was measured using one-way ANOVA test ($P < 0.05$) (see **Section 2.9**). Cell viability data not presented as non-viable cell number was not affected by DEX exposure (non viable cells $< 1\%$ for all concentrations studied).

The effect of DEX on MDPC-23 cell numbers is presented in Figure 4.6A. In this study, 10^{-11} M DEX increased MDPC-23 cell numbers after 48 hrs of growth by 9%. As the concentration increased to 10^{-10} M, cell numbers peaked with an increase of 25%. 10^{-9} M DEX also resulted in an increased cell number of 15%. 10^{-8} M and 10^{-7} M DEX reduced cell numbers by 10% and 15%, respectively. The increase in cell number seen as a result of exposure to 10^{-10} M DEX was the only one found to be statistically significant.

Figure 4.6B illustrates the effect of DEX on numbers of OD-21 cells following 48 hours of exposure. OD-21 cells that were exposed to 10^{-11} M DEX showed an increase in number of 8%, which was not found to be statistically significant. Both 10^{-10} M and 10^{-9} M DEX increased cell numbers by statistically significant amounts, 20% and 21%, respectively. Cells exposed to 10^{-8} M DEX had an increase in cell number of 7%, whilst treatment with 10^{-7} M DEX had no effect of the number of OD-21 cells when compared to that of the control.

The effect of DEX exposure on 3T3 cell number is presented in Figure 4.6C. In this study none of the concentrations of DEX used altered cell number by a statistically significant amount. Minor reductions (~6%) in cell number were observed at both 10^{-11} M and 10^{-10} M DEX exposure and 10^{-9} M, 10^{-8} M and 10^{-7} M DEX also slightly reduced cell numbers.



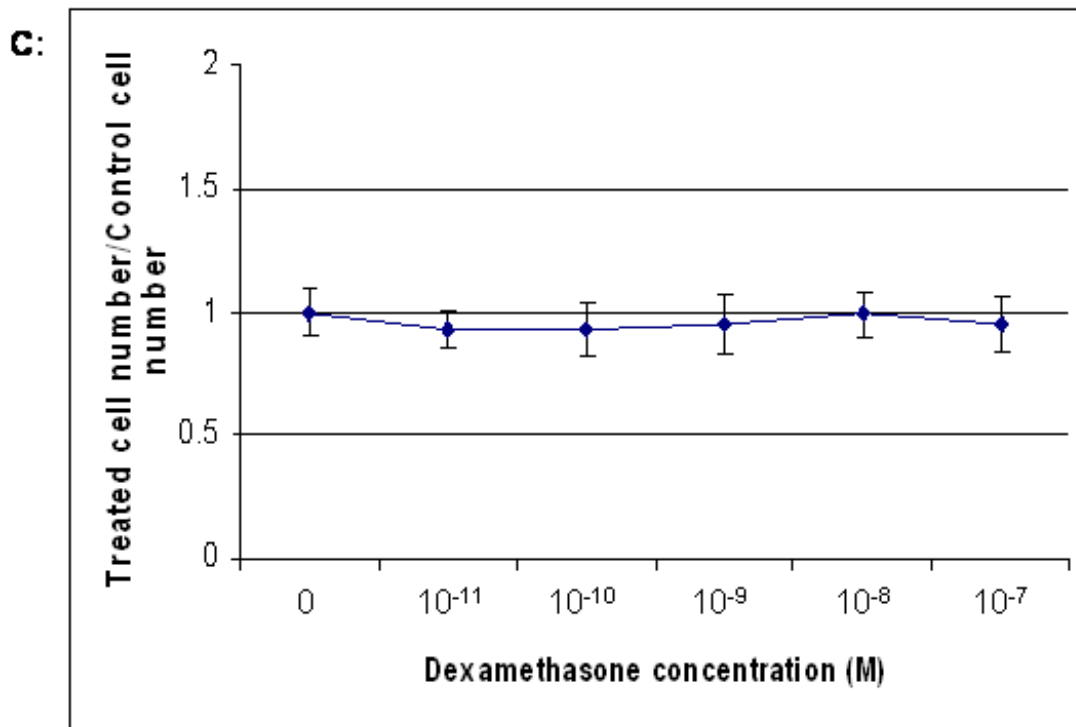


Figure 4.6: Changes in A: MDPC-23, B: OD-21 and C: 3T3 cell number following 48 hour stimulation with 0, 10^{-11} M, 10^{-10} M, 10^{-9} M, 10^{-8} M and 10^{-7} M Dex. This experiment was run in triplicate and repeated four times.

*** = Statistically significant difference compared to the control ($P < 0.05$).**

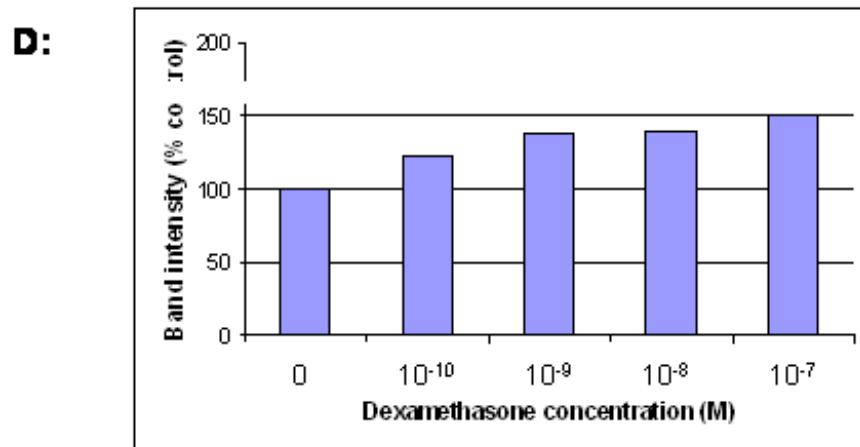
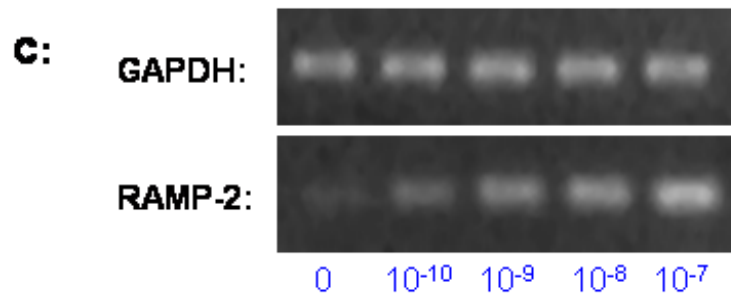
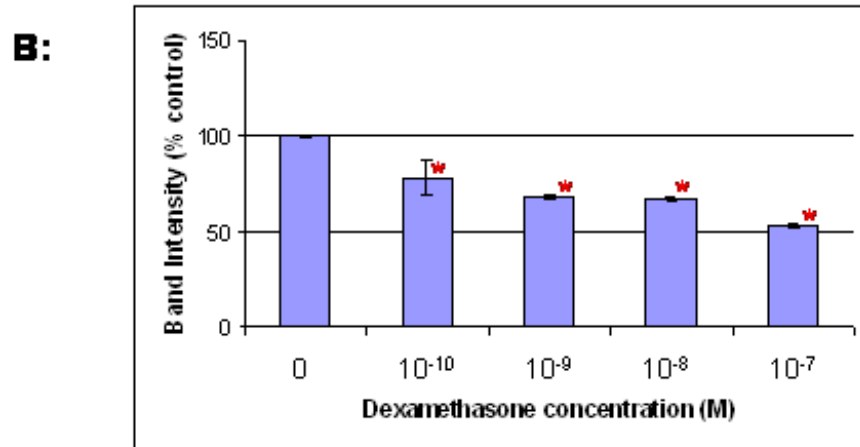
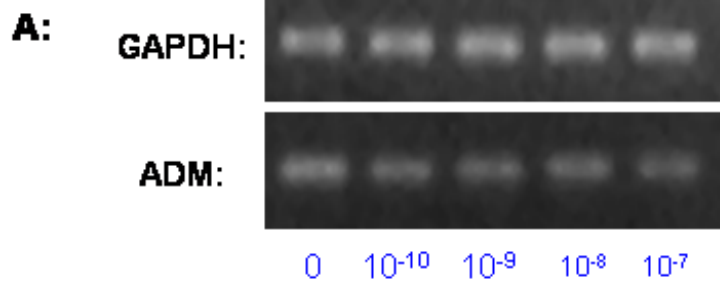
4.8 Effect of Dexamethasone exposure on ADM expression in MDPC-23 and OD-21 cells

As dexamethasone demonstrably affected dental cell numbers (**Section 4.7**) and as it has been previously reported to regulate ADM related transcripts in osteoblasts (Uzan *et al*, 2004), the effects of dexamethasone exposure on ADM gene expression was assessed in MDPC-23 and OD-21 cells. A preliminary study was also performed on RAMP-2 expression in MDPC-23 cells following exposure to dexamethasone. For these analyses, MDPC-23 and OD-21 cells were exposed to a range of concentrations of dexamethasone for 24 hours prior to cells being lysed and the RNA extracted for RT-PCR analysis.

In MDPC-23 cells, DEX appeared to induce a dose-dependant decrease in ADM expression (**Figures 4.7A & B**), with each concentration of DEX statistically significantly reducing the densitometric value of the ADM amplified product. Exposure to 10^{-10} M DEX reduced ADM expression by 22%, while both 10^{-9} M and 10^{-8} M DEX reduced ADM expression by 33% compared to the unstimulated control. The largest reduction in ADM expression in MDPC-23 cells was following 24 hour exposure to 10^{-7} M DEX, which reduced the densitometric value by 47%. This data suggests the possible negative feedback of ADM by DEX, particularly at higher concentrations.

The preliminary study regarding the effect of DEX exposure on RAMP-2 expression in MDPC-23 cells indicates that DEX may cause a dose-dependant increase in RAMP-2 levels following 24-hour exposure (**Figures 4.7C & D**). The densitometrically derived values increased with the increasing concentrations of DEX used. DEX concentrations of 10^{-10} M, 10^{-9} M, 10^{-8} M and 10^{-7} M increased RAMP-2 levels by 22%, 38%, 40% and 50%, respectively.

ADM transcript levels in OD-21 cells were reduced following 24 hour exposure to DEX (**Figures 4.7E & F**). 10^{-10} M DEX reduced ADM levels by 10% densitometrically, although this was not a statistically significant reduction. 10^{-9} M, 10^{-8} M and 10^{-7} M DEX did, however, reduce ADM levels by statistically significant amounts, reducing the densitometric-derived values by 43%, 38% and 26%, respectively. Similar to the effect seen in MDPC-21 cells, this data suggest that DEX is acting to suppress ADM expression in a negative feedback system.



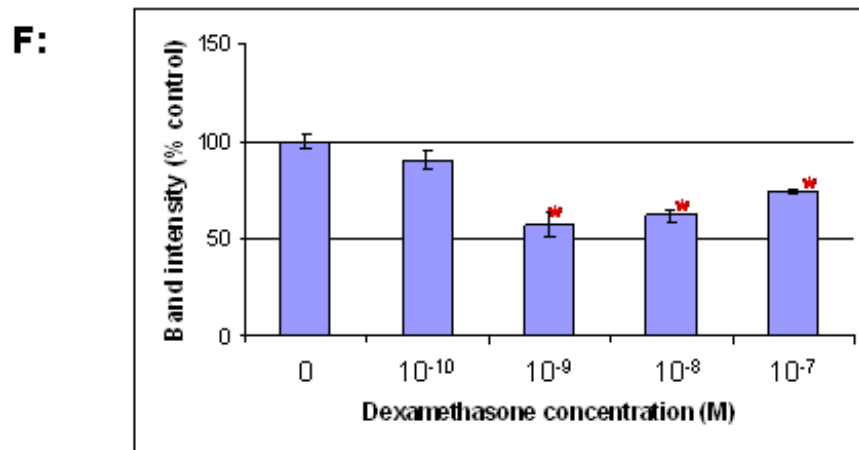
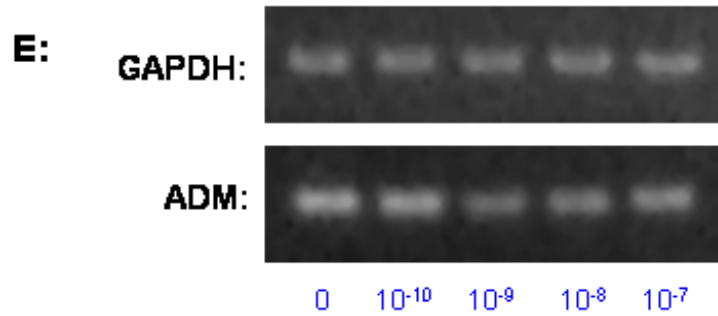


Figure 4.7: A + F - Representative gel images of the effect of a range of concentrations of DEX (10^{-10} M, 10^{-9} M, 10^{-8} M and 10^{-7} M) on ADM expression in **A** - MDPC-23 and **E** - OD-21 cell, with GAPDH acting as a housekeeping gene. **B + F** – Graphical representation of the aforementioned treatments on **B** – MDPC-23 and **F** – OD-21 cells. Values obtained by measuring band intensity from gel images, normalised to GAPDH. This experiment was repeated three times. **C** – Gel image showing the effect of a range of concentrations of DEX on the expression of RAMP-2 in MDPC-23 cells, normalised to GAPDH. **D** – Graphical representation of the expressional changes seen in figure **C**. Values obtained by measuring band intensity, normalised to GAPDH. This data is preliminary as no repeats were performed.

* = Statistically significant difference compared to the control ($P < 0.05$).

5. Results Chapter 3

5.1 Effect of ADM on mineral deposition in dental cells *in vitro*

Previous studies have demonstrated that *in vitro*, ADM can stimulate osteoblast proliferation (Cornish *et al*, 1997; Cornish *et al*, 2002) whilst *in vivo*, ADM supplementation can promote mineralised bone area, bone volume and strength (Cornish *et al*, 1997; Cornish *et al*, 2001). As the previous results (**Chapters 3 and 4**) indicated significant levels of ADM in odontoblast cells during tooth development and that ADM can stimulate increases of dental cell numbers *in vitro*, work was undertaken to determine whether ADM can also promote mineral deposition, indicative of mineralisation, from developmentally relevant dental tissue cell lines.

Subsequently, ADM was used as a substitute for the known mineralised tissue promoting agent dexamethasone, as well as in conjunction with it, to determine whether ADM can induce mineral deposition that is indicative of mineralisation in a similar manner to dexamethasone, or whether it can enhance mineral deposition in combination with it. For these analyses cells were exposed to two control media:

i) medium containing 50mg/ml Ascorbic Acid (A.A) and 10mM β -glycerophosphate (β -G) and,

ii) standard mineralising medium containing 50mg/ml A.A, 10mM β -G and 10^{-8} M DEX.

A range of concentrations of ADM (10^{-15} M, 10^{-13} M, 10^{-11} M, 10^{-9} M and 10^{-7} M, as in **Chapter 4**) were used in conjunction with both these control media. As in Chapter 4, the odontoblast-like MDPC-23 cells and pulp-like OD-21 cells were used for analysis together with the 3T3 skin fibroblast cell line, which was used as a negative control.

5.2 Effect of ADM exposure on the MDPC-23 cell mineral deposition

The mineralising effect of ADM *in vitro* was determined using von Kossa staining (**Section 2.4**). Briefly, cells were exposed to a range of conditions, as stated in Section 5.1, for 3, 7, 11, 14 and 21 days, following which, the medium was removed and the cells fixed. To visualise mineral deposition, cultures were exposed to the von Kossa stain and, following digital image capture, the area of mineral deposition was determined using ImageJ software analysis (see **Sections 2.2.5 and 2.4**). Statistical significance was measured using one-way ANOVA test ($P < 0.05$) (see **Section 2.9**).

Following 3 days of exposure under the conditions shown (**Figure 5.1**), only the MDPC-23 culture supplemented with ascorbic acid (A.A), β -Glycerophosphate (β -G) and 10^{-7} M ADM exhibited detectable mineral deposition. The area of mineral deposition detected was 1.6% of the culture area. However, there was no statistically significant difference in mineral deposition with this treatment, or any other, after 3 days of culture compared to the control, therefore any mineral deposition seen is more likely to be mere artefact (**Figure 5.1**).

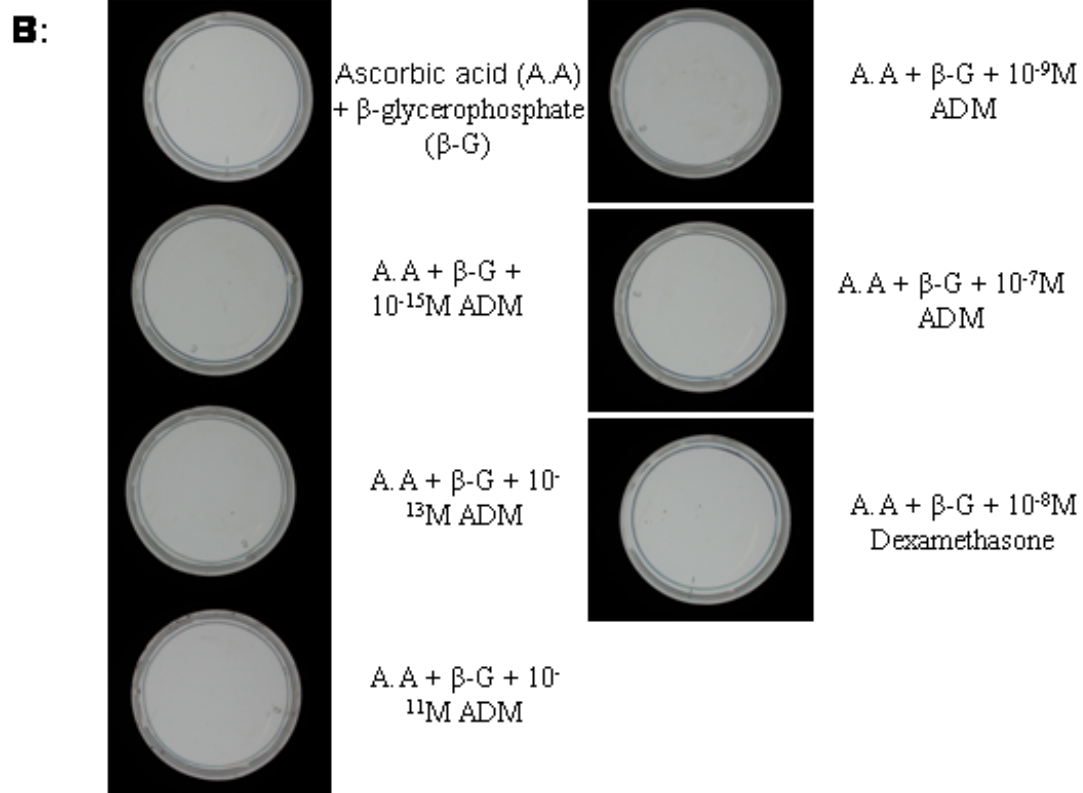
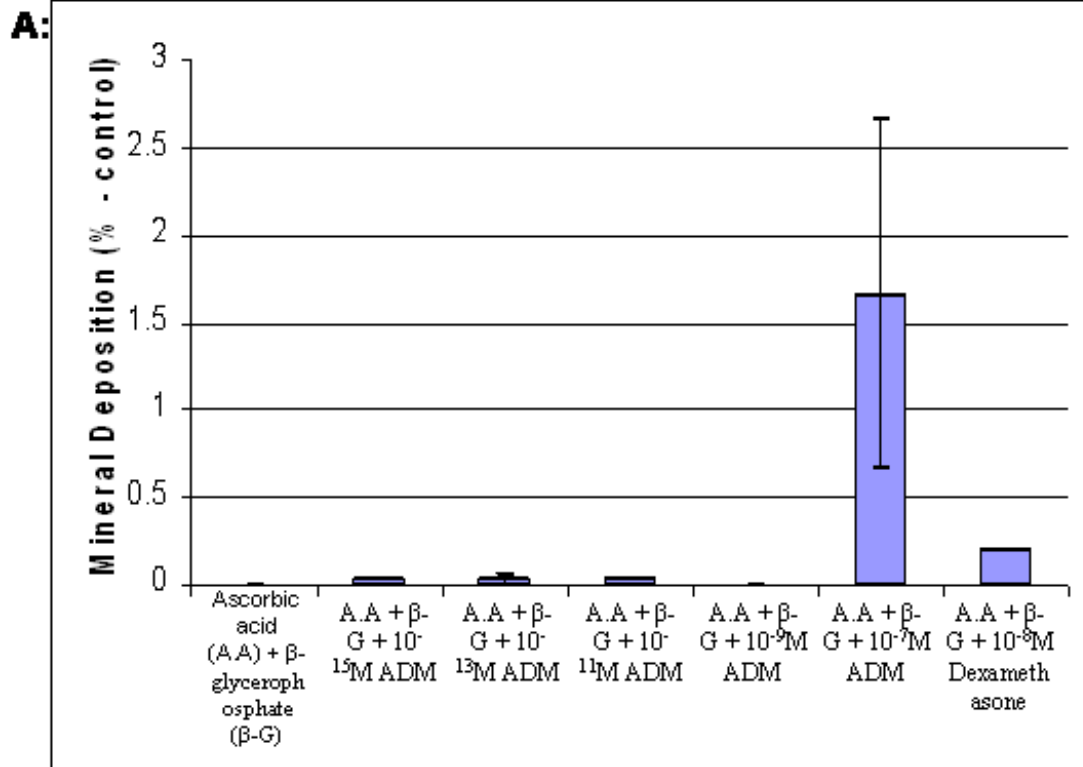
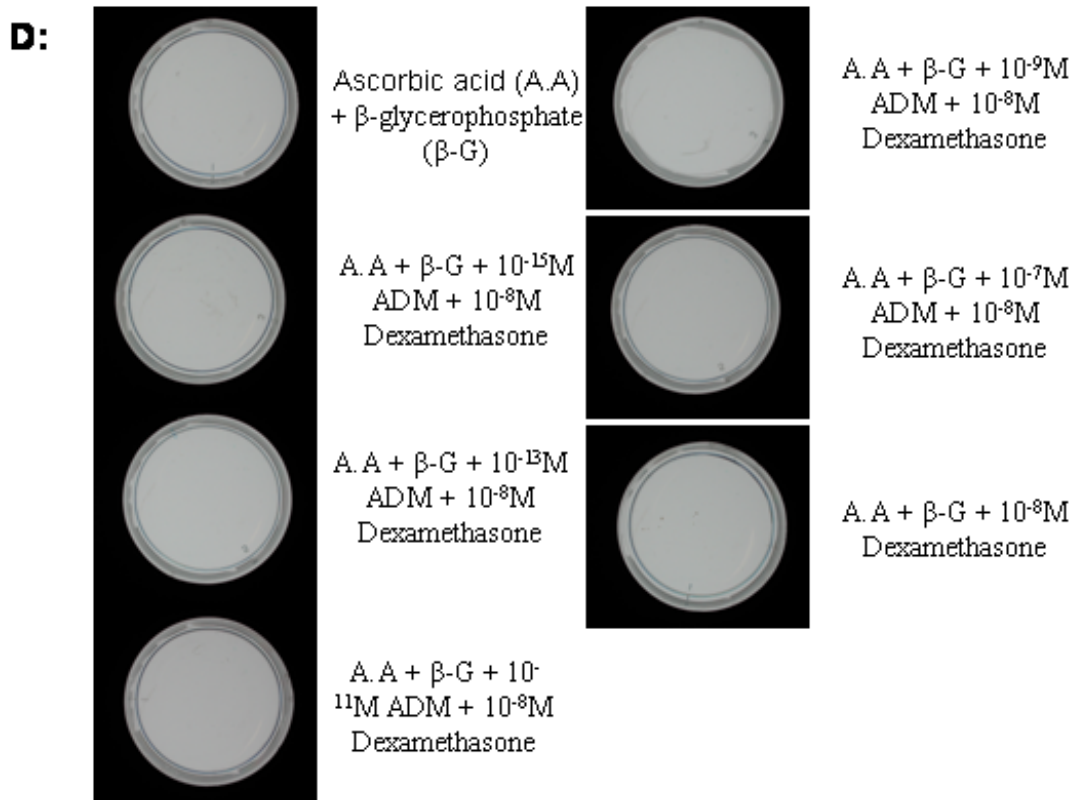
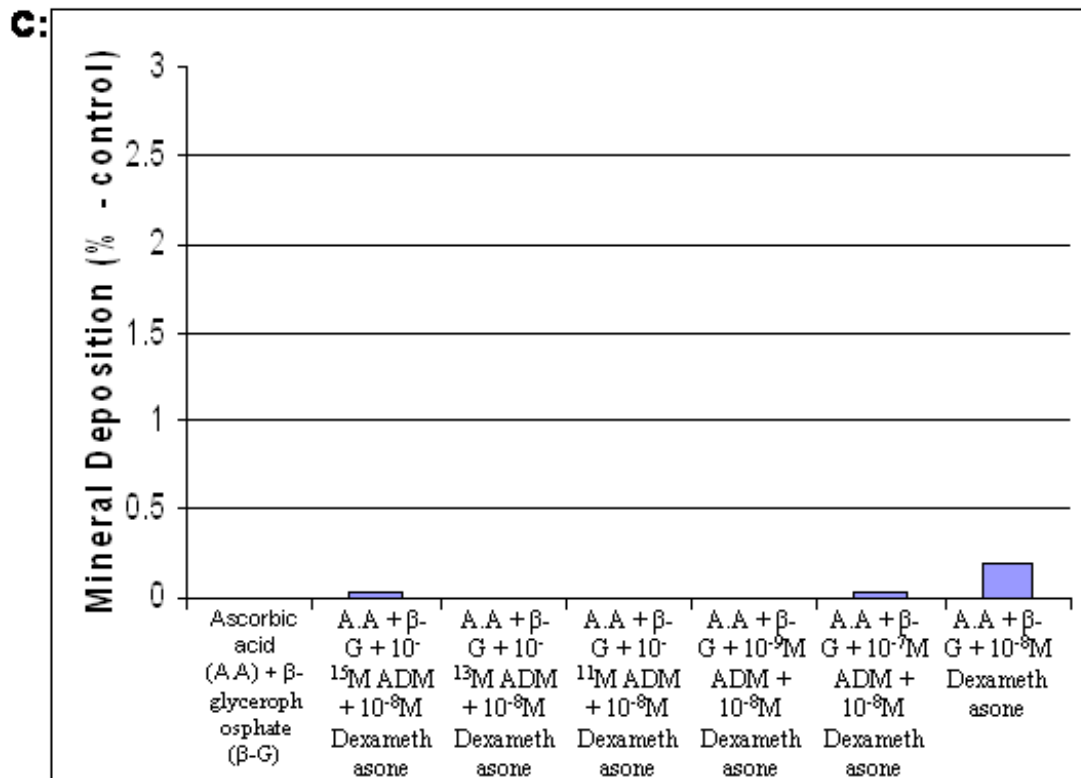


Figure 5.1: A + C – Mean mineral deposition in MDPC-23 cells following 3 day treatment with Ascorbic acid (A.A) and β -glycerophosphate (β -G), A.A, β -G and a range of concentrations of ADM (10^{-15} M, 10^{-13} M, 10^{-11} M, 10^{-9} M and 10^{-7} M ADM), A.A, β -G and 10^{-8} M dexamethasone and A.A, β -G, 10^{-8} M dexamethasone and a range of concentrations of ADM (10^{-15} M, 10^{-13} M, 10^{-11} M, 10^{-9} M and 10^{-7} M ADM). B + D: Representative images of the von Kossa stained cells from which the data presented in A + C was obtained.

*** = statistically significant difference compared to A.A and β -G treatment. * = statistically significant difference compared to A.A, β -G and 10^{-8} M dexamethasone treatment. This experiment was carried out three times.**



Following 7 days exposure of MDPC-23 cultures, greater areas of mineral deposition were detected (**Figure 5.2**). Notably, exposure to the mineralisation control medium resulted in a mineral deposition area of 5.7% being detected (**Figure 5.2A**). Similar results using the conditions of A.A, β -G and 10^{-13} M ADM; A.A, β -G and 10^{-9} M ADM; A.A, β -G and 10^{-7} M ADM were also obtained. The conditions of A.A, β -G and 10^{-15} M ADM and A.A, β -G and 10^{-11} M resulted in the detection of a mineral deposition area of 3.5%, A.A and β -G supplementation alone resulted in production of a relatively low detectable area of mineral deposition, 1.5%. ADM supplementation in addition to the mineralised control medium appeared to produce an increase in detectable mineral deposition in MDPC-23 cells when compared to the mineralised control medium alone (**Figure 5.2C**). Including 10^{-13} M, 10^{-11} M, 10^{-9} M ADM or 10^{-7} M ADM within the mineralised control medium increased the area of mineral deposition observed to 10.2%, 9.3%, 8.1% and 9.2%, respectively. Seven day exposure of MDPC-23 cells to 10^{-13} M, 10^{-11} M and 10^{-7} M ADM in addition to the mineralisation control medium produced a statistically significant difference when compared to A.A and β -G medium exposure alone.

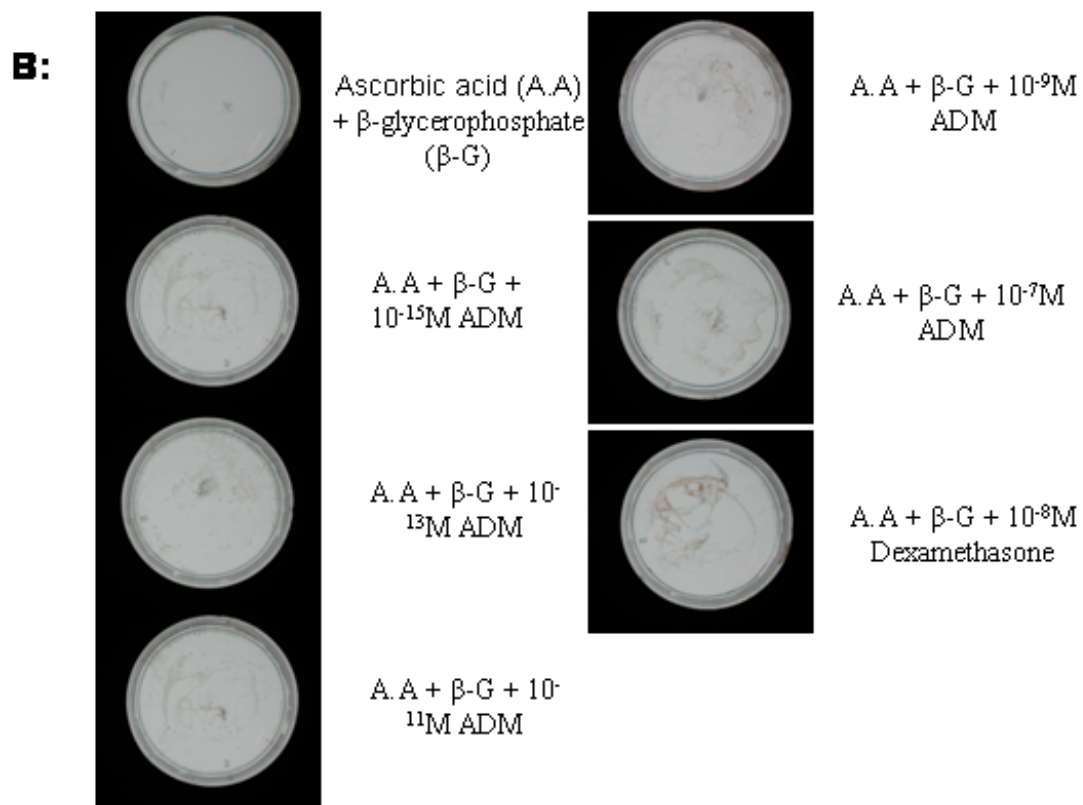
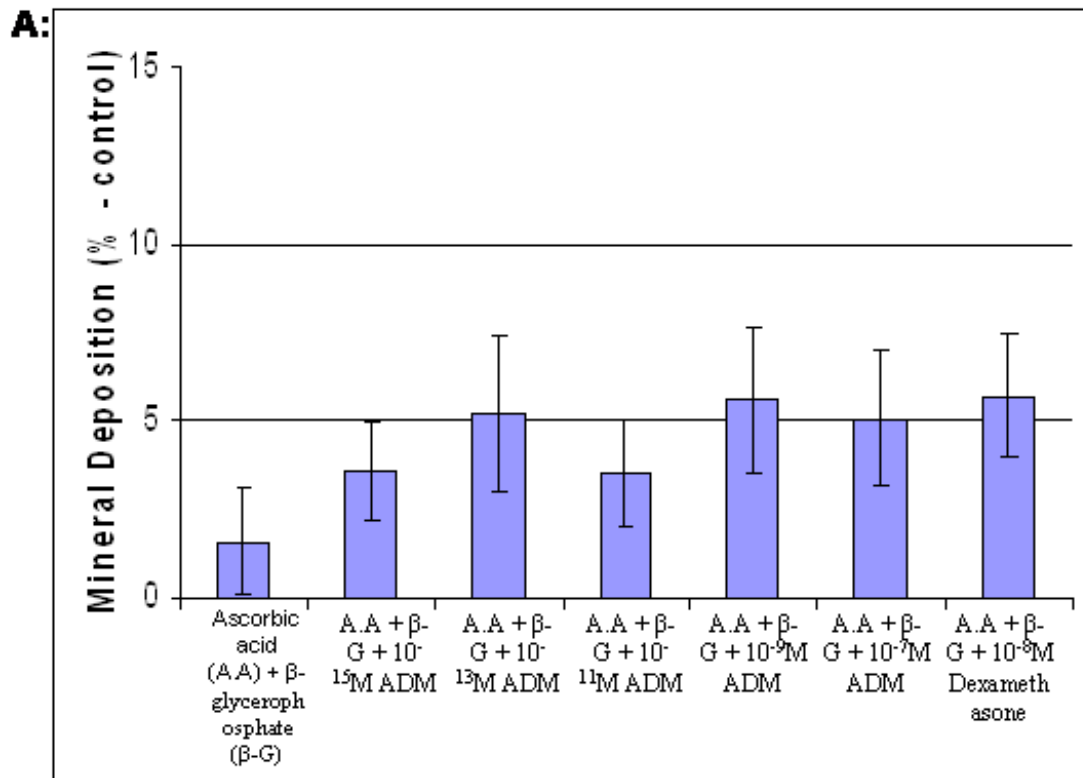
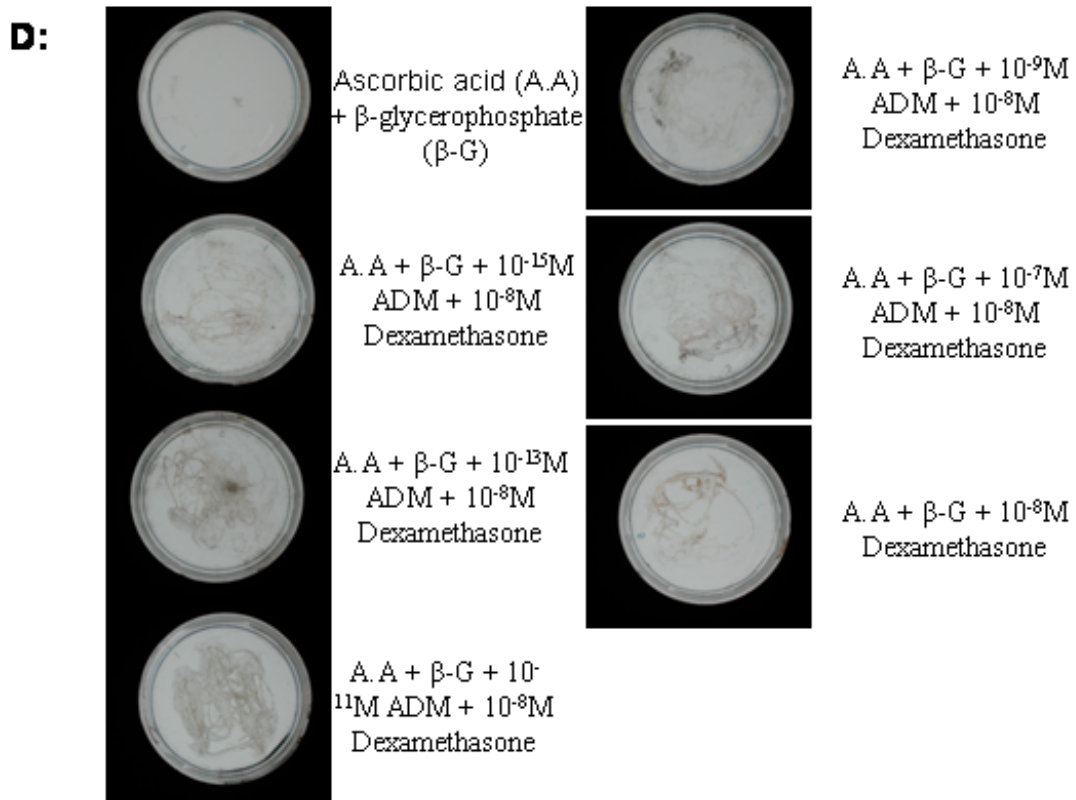
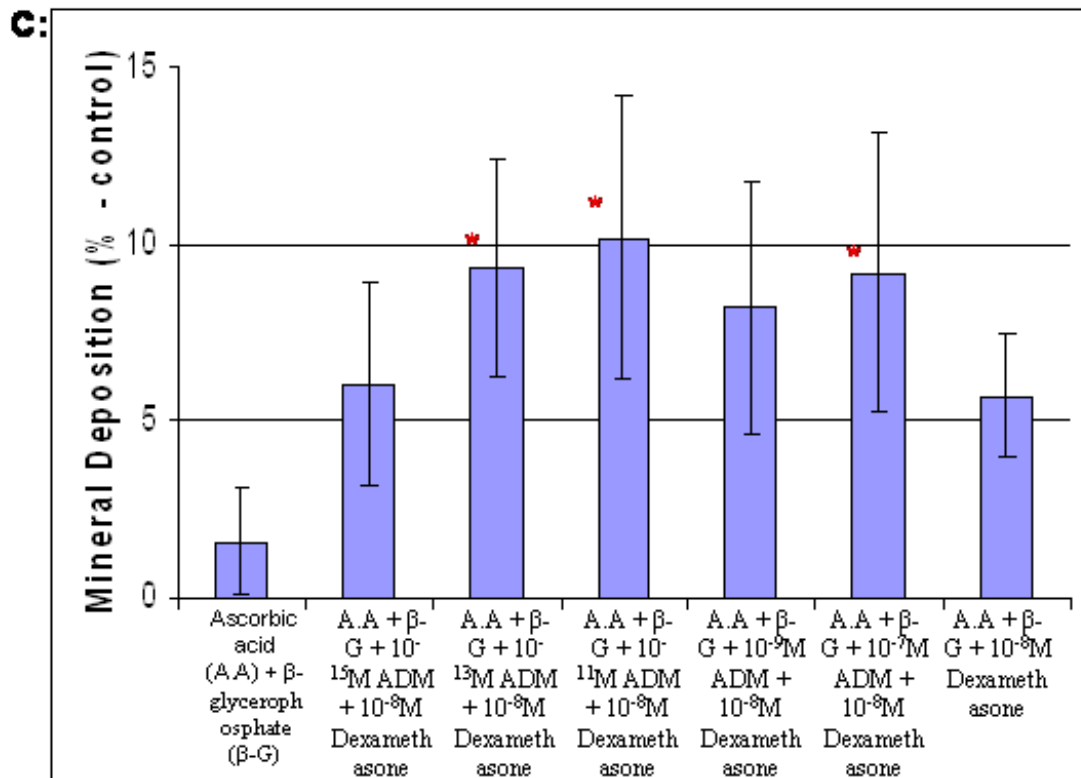


Figure 5.2: A + C – Mean mineral deposition in MDPC-23 cells following 7 day treatment with Ascorbic acid (A.A) and β -glycerophosphate (β -G), A.A, β -G and a range of concentrations of ADM (10^{-15} M, 10^{-13} M, 10^{-11} M, 10^{-9} M and 10^{-7} M ADM), A.A, β -G and 10^{-8} M DEX, and A.A, β -G, 10^{-8} M DEX and a range of concentrations of ADM (10^{-15} M, 10^{-13} M, 10^{-11} M, 10^{-9} M and 10^{-7} M ADM). B + D: Representative images of the von Kossa stained cells from which the data presented in A + C was obtained.

*** = statistically significant difference compared to A.A and β -G treatment. * = statistically significant difference compared to A.A, β -G and 10^{-8} M dexamethasone treatment. This experiment was carried out three times.**



The effects on *in vitro* mineral deposition following 11 days exposure of the differently supplemented media are presented in Figure 5.3. Exposure to all conditions resulted in a statistically significant increase in the mineral deposition area detected when compared to the control A.A and β -G supplemented medium alone. When ADM was used in addition to the A.A and β -G medium, the area of mineral deposition detected for the range of ADM concentrations used was between 6.9% and 7.5%. The area of mineral deposition detected following treatment with the standard mineralisation control medium was marginally higher at 8.2%. Supplementation with ADM in addition to the standard mineralisation control medium resulted in a statistically significant increase in detectable mineral deposition. Data presented in Figure 5.3C indicate that there is minimal variation in the area of mineral deposition detected between each concentration of ADM used which ranged from 11.5% for 10^{-15} M ADM to 12.2% for the 10^{-9} M ADM exposures.

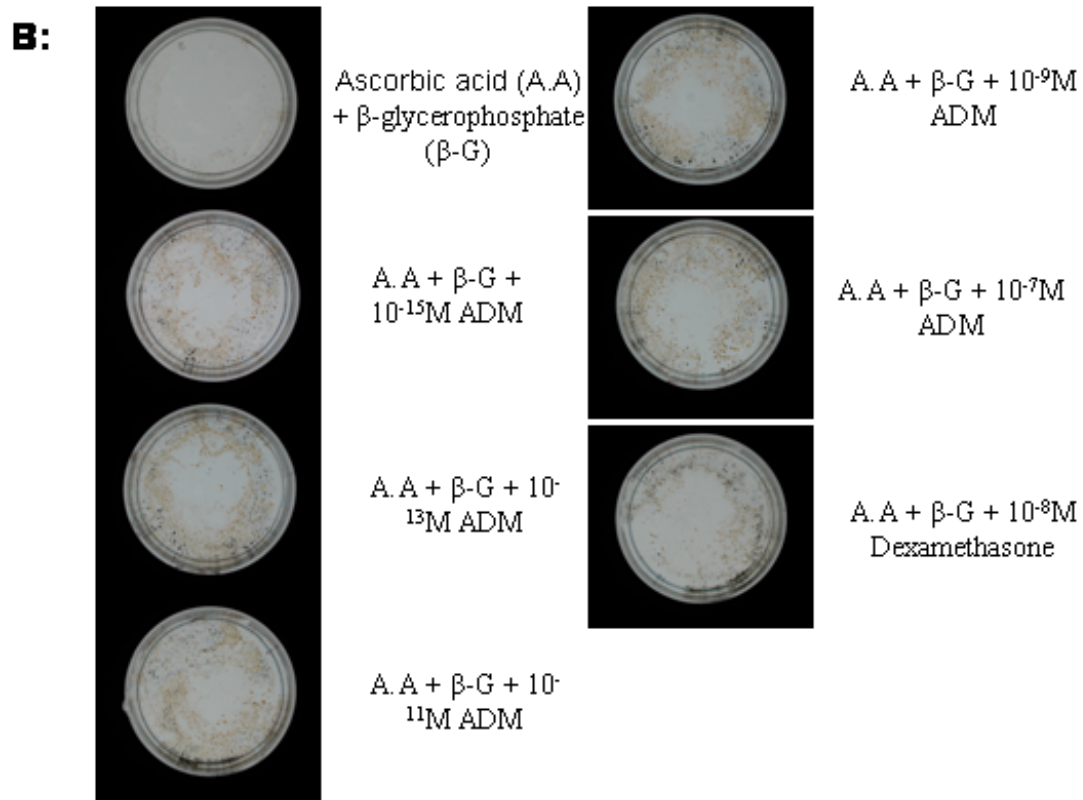
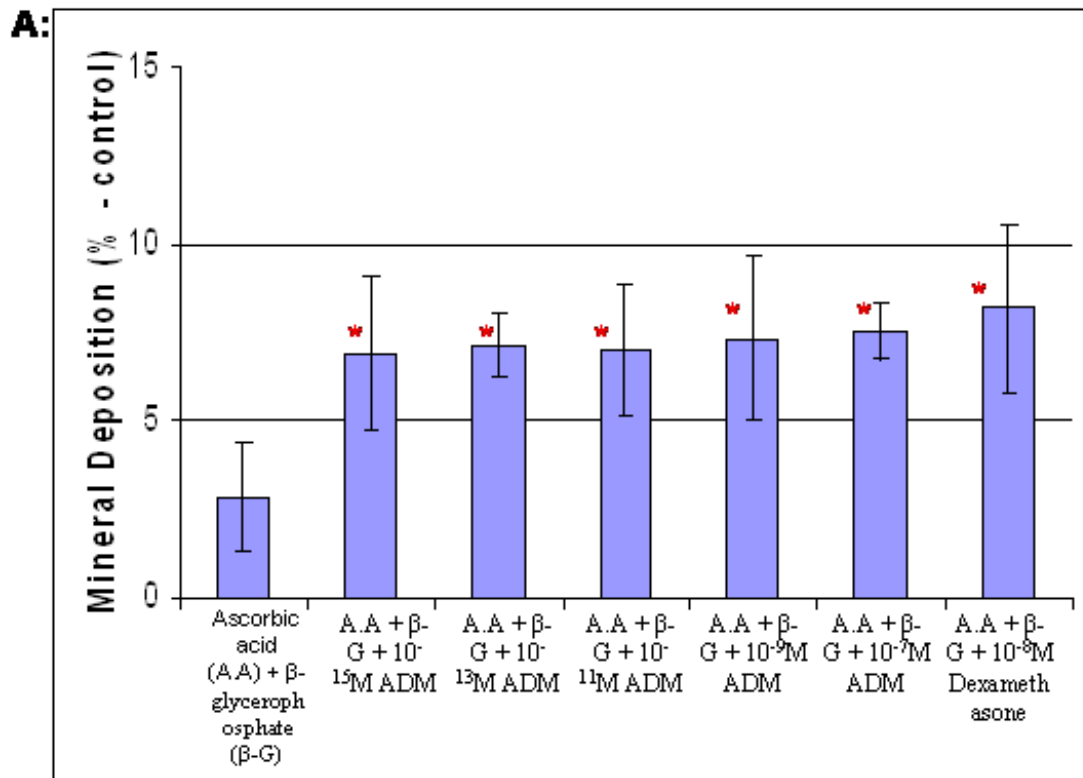
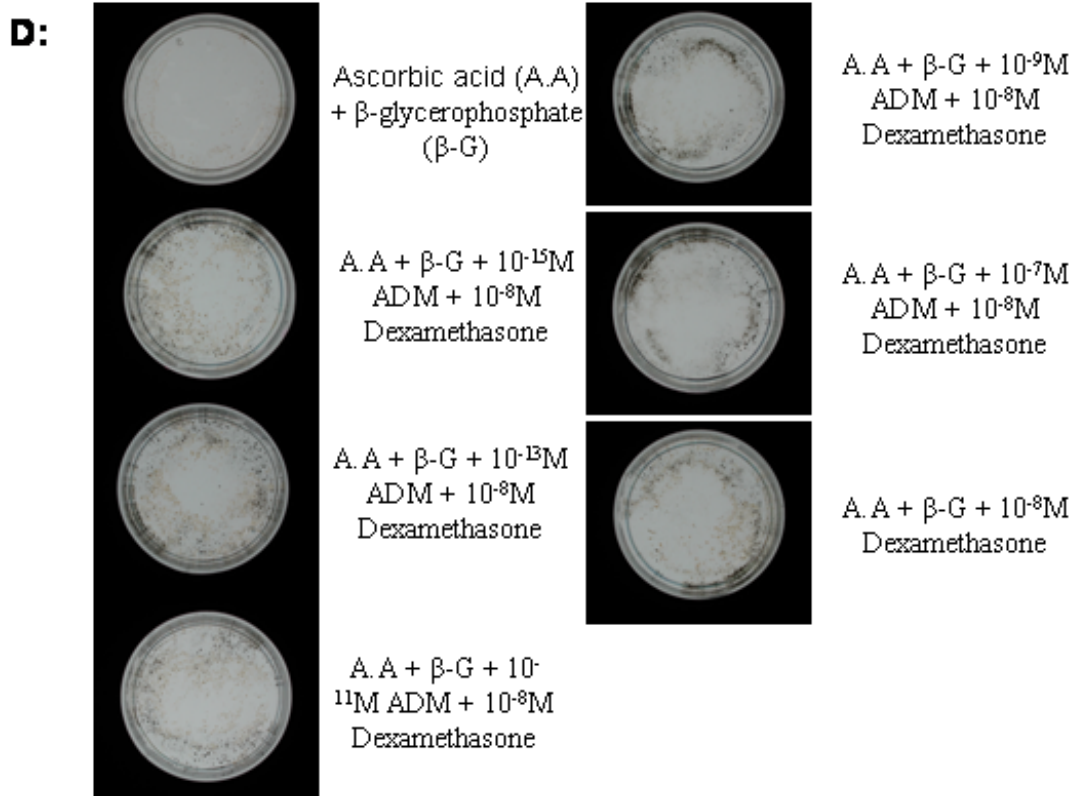
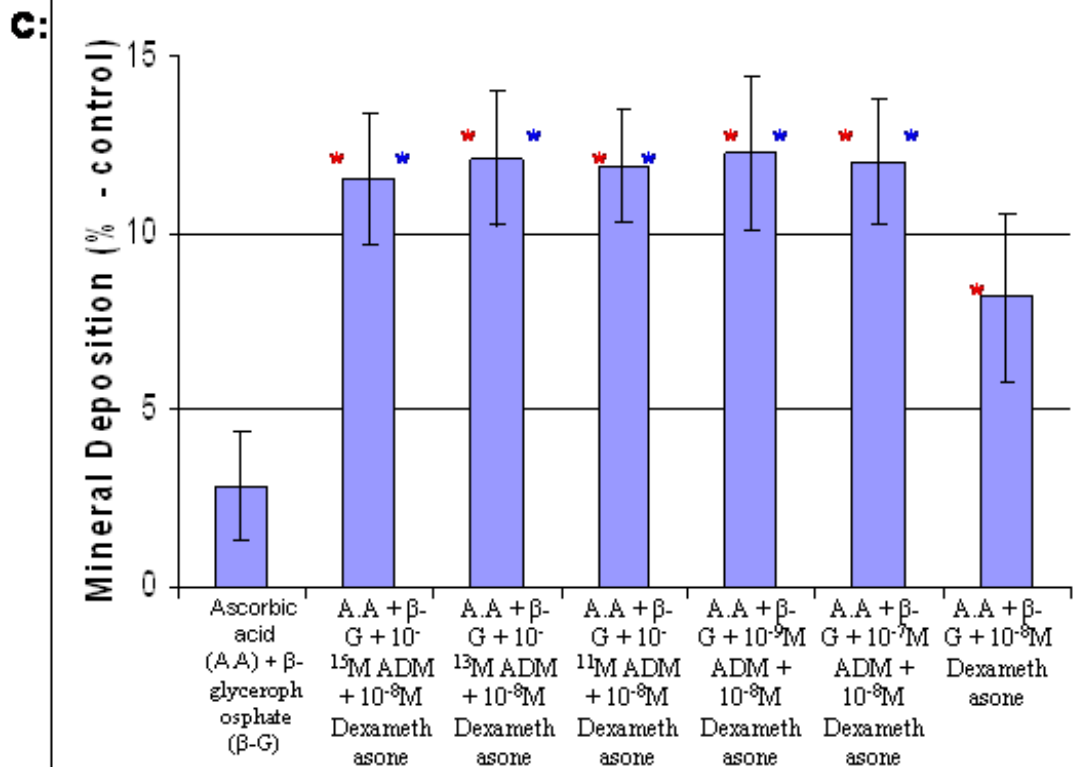


Figure 5.3: A + C – Mean mineral deposition in MDPC-23 cells following 11 day treatment with Ascorbic acid (A.A) and β -glycerophosphate (β -G), A.A, β -G and a range of concentrations of ADM (10^{-15} M, 10^{-13} M, 10^{-11} M, 10^{-9} M and 10^{-7} M ADM), A.A, β -G and 10^{-8} M DEX, and A.A, β -G, 10^{-8} M DEX and a range of concentrations of ADM (10^{-15} M, 10^{-13} M, 10^{-11} M, 10^{-9} M and 10^{-7} M). **B + D**: Representative images of the von Kossa stained cells from which the data presented in **A + C** was obtained.

* = statistically significant difference compared to A.A and β -G treatment. * = statistically significant difference compared to A.A, β -G and 10^{-8} M dexamethasone treatment. This experiment was carried out three times.



Following 14 days of culture, all test conditions analysed produced a statistically significant increase in the area of mineral deposition detected compared to A.A and β -G exposure alone (**Figure 5.4**). Medium containing A.A and β -G alone resulted in a minimal detectable area of mineral deposition, 3.5%. The addition of 10^{-15} M, 10^{-13} M, 10^{-11} M, 10^{-9} M and 10^{-7} M ADM increased the area of mineral deposition to 10.9%, 9.6%, 10.5%, 10.8% and 10.7%, respectively. Notably, none of these detectable areas were statistically significantly different from the mineralisation control medium samples. When the range of concentrations of ADM were supplemented into the mineralisation control medium, no statistically significant difference, compared to the mineralisation control medium alone, was observed although the area of mineral deposition detected was incrementally larger with each concentration of ADM used. Notably, the 10^{-15} M ADM concentration generated an area of mineral deposition of 14.2% and the higher concentration of ADM (10^{-7} M) resulted in a detectable area of mineral deposition of 15.7%.

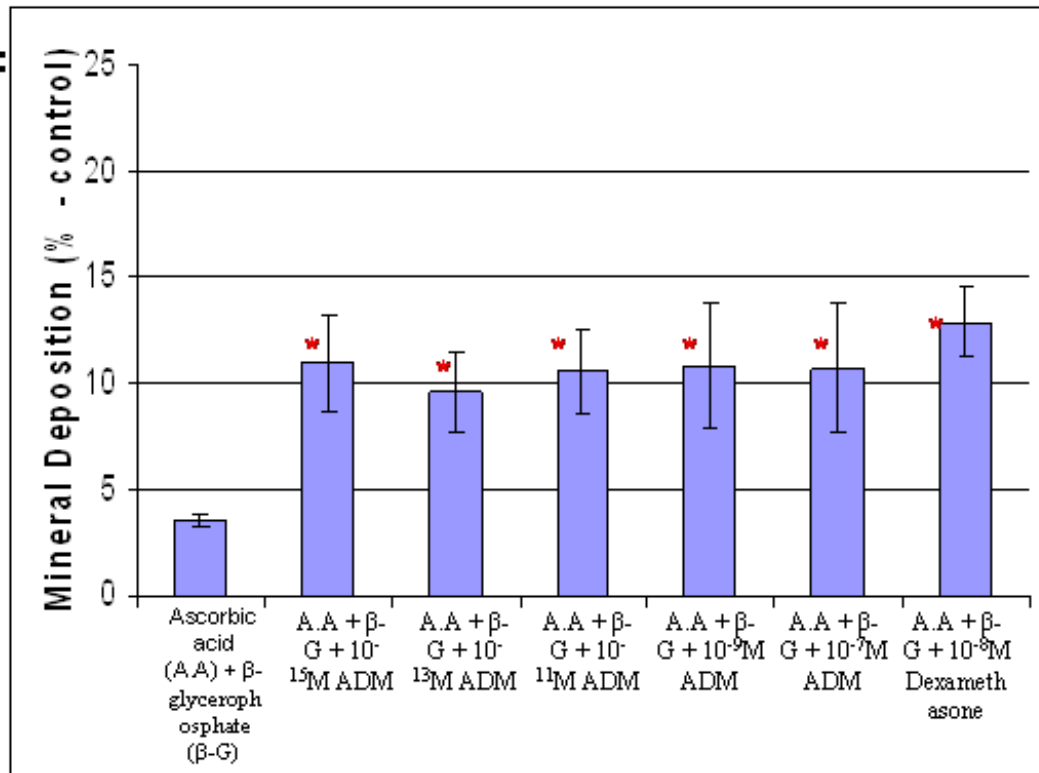
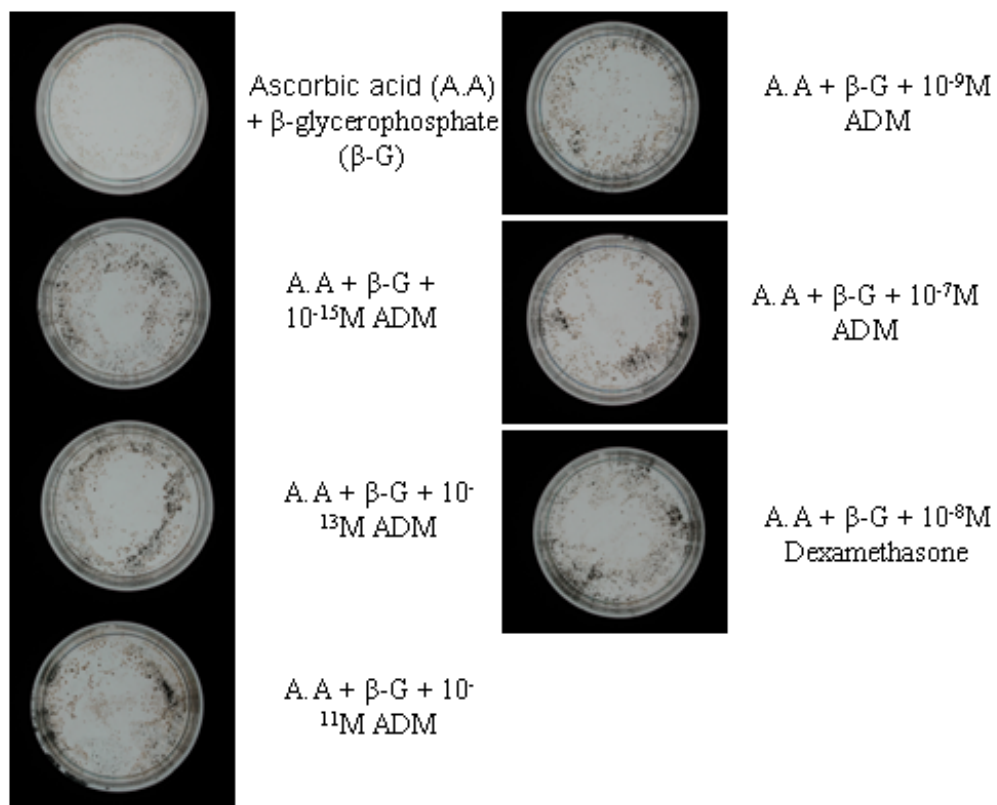
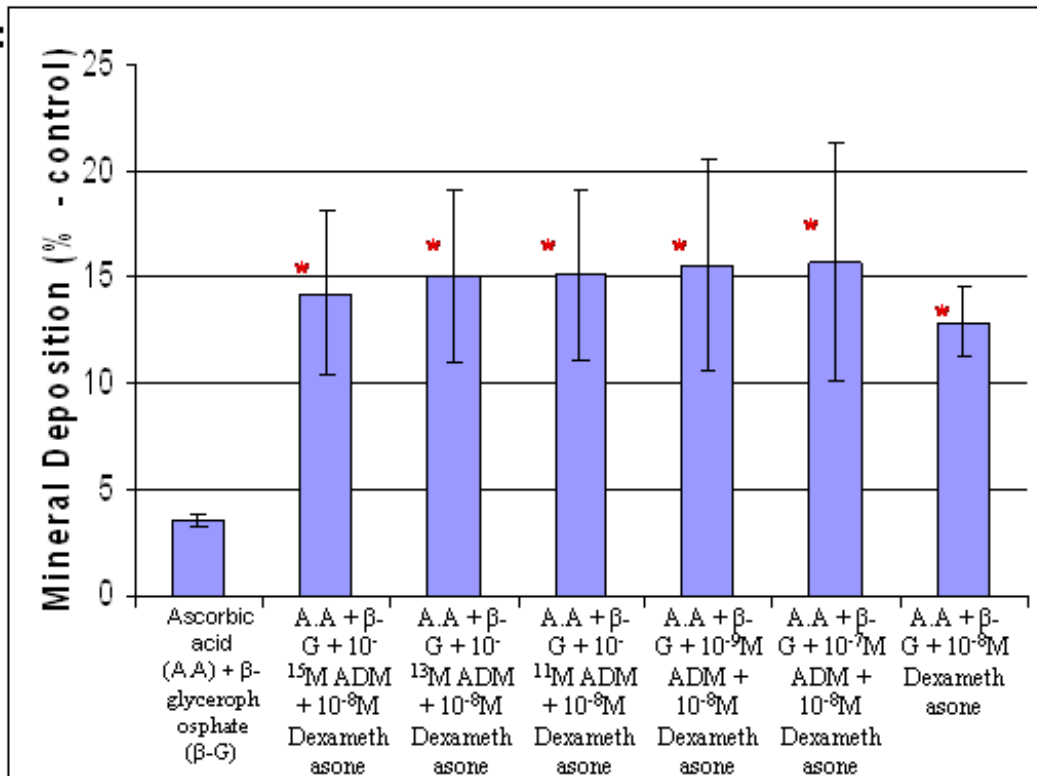
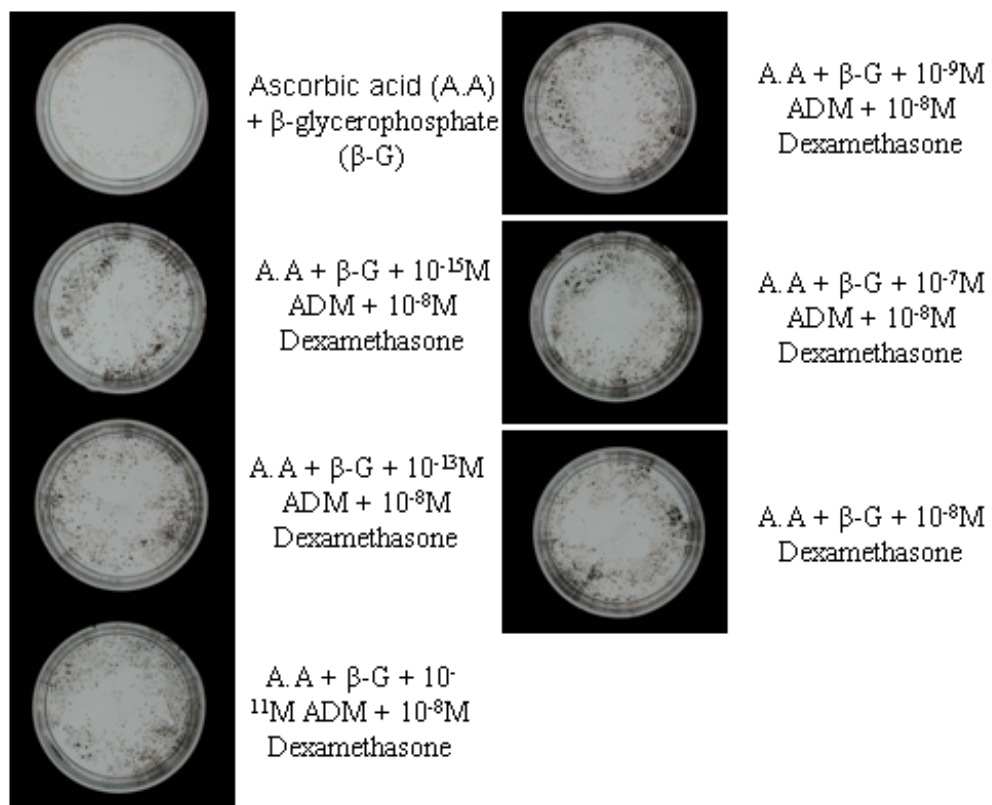
A:**B:**

Figure 5.4: A + C – Mean mineral deposition in MDPC-23 cells following 14 day treatment with Ascorbic acid (A.A) and β -glycerophosphate (β -G), A.A, β -G and a range of concentrations of ADM (10^{-15} M, 10^{-13} M, 10^{-11} M, 10^{-9} M and 10^{-7} M ADM), A.A, β -G and 10^{-8} M DEX, and A.A, β -G, 10^{-8} M DEX and a range of concentrations of ADM (10^{-15} M, 10^{-13} M, 10^{-11} M, 10^{-9} M and 10^{-7} M ADM). B + D: Representative images of the von Kossa stained cells from which the data presented in A + C was obtained.

*** = statistically significant difference compared to A.A and β -G treatment. * = statistically significant difference compared to A.A, β -G and 10^{-8} M dexamethasone treatment. This experiment was carried out three times.**

C:**D:**

Twenty-one days of exposure of MDPC-23 cultures to ADM resulted in greater areas of mineral deposition being observed (**Figure 5.5**). The data presented indicate that when treated with A.A and β -G alone, MDPC-23 cells produced an area of mineral deposition of 4.9%. When the cells were exposed to A.A, β -G and a range of concentrations of ADM there was a statistically significant increase in the area of mineral deposition compared to A.A and β -G alone. 10^{-15} M and 10^{-9} M ADM both produced a detectable area of mineral deposition of 22.2%, 10^{-13} M ADM yielded an area of 22.4% and 10^{-11} M ADM promoted an area of mineral deposition of 21.3%. The largest increase in mineral deposition resulted from exposure to 10^{-7} M ADM (+ A.A, β -G), which produced an area of 23.6%. This value, however, was marginally less than the mineralisation control medium, which produced an area of detectable mineral deposition of 25.2%. The effect of treatment with the mineralisation control and a range of concentrations of ADM were also analysed (**Figure 5.5C & D**). Data demonstrated (**Figure 5.5C**) that there were minimal differences between samples treated with the mineralisation control medium alone and those treated with the mineralisation control medium supplemented with the range of concentrations of ADM. Inclusion of 10^{-15} M, 10^{-13} M and 10^{-7} M ADM gave detectable areas of mineral deposition of 24.1%, 24.4% and 24.7%, respectively, whereas inclusion of 10^{-13} M (25.3%) and 10^{-9} M (26.5%) ADM produced marginal increases in the area of mineral deposition compared to the mineralisation control medium. These values represented statistically significant increases in area compared to the A.A and β -G medium used, but not to the standard mineralisation control medium (A.A, β -G & 10^{-8} M Dex).

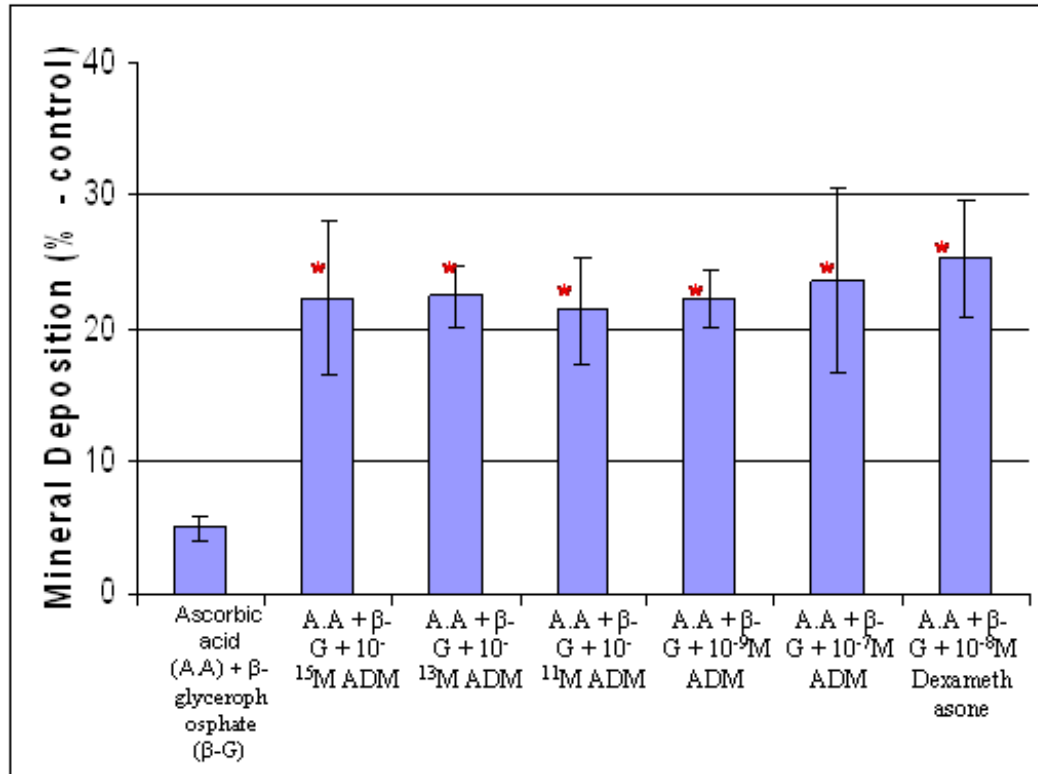
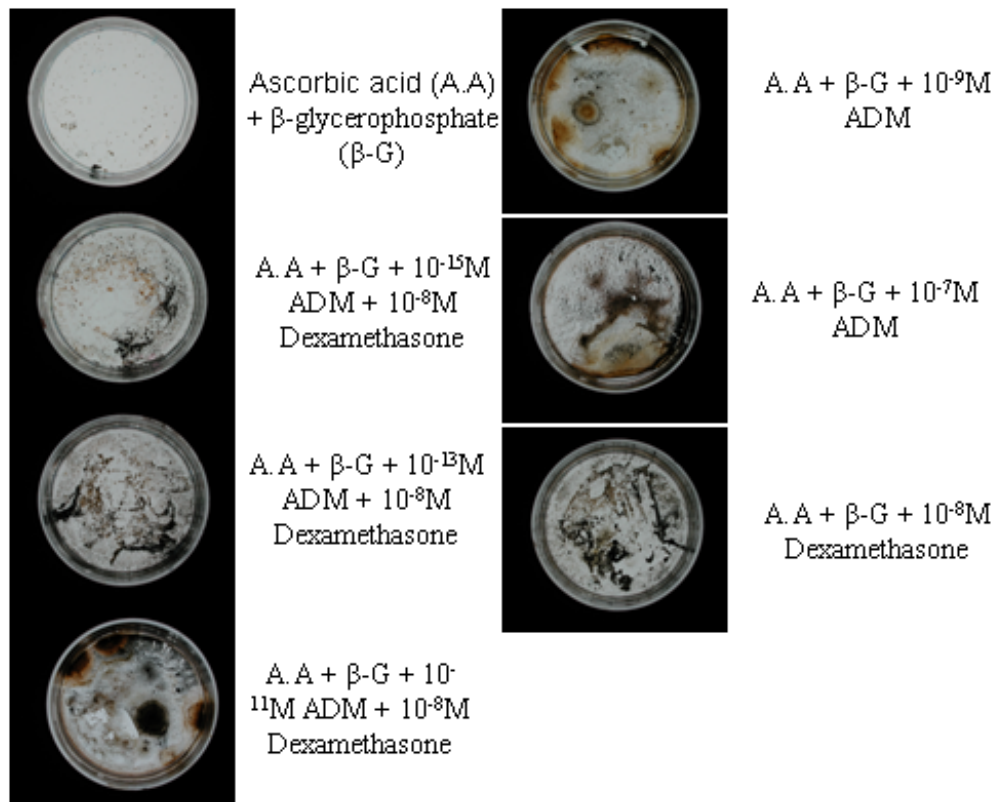
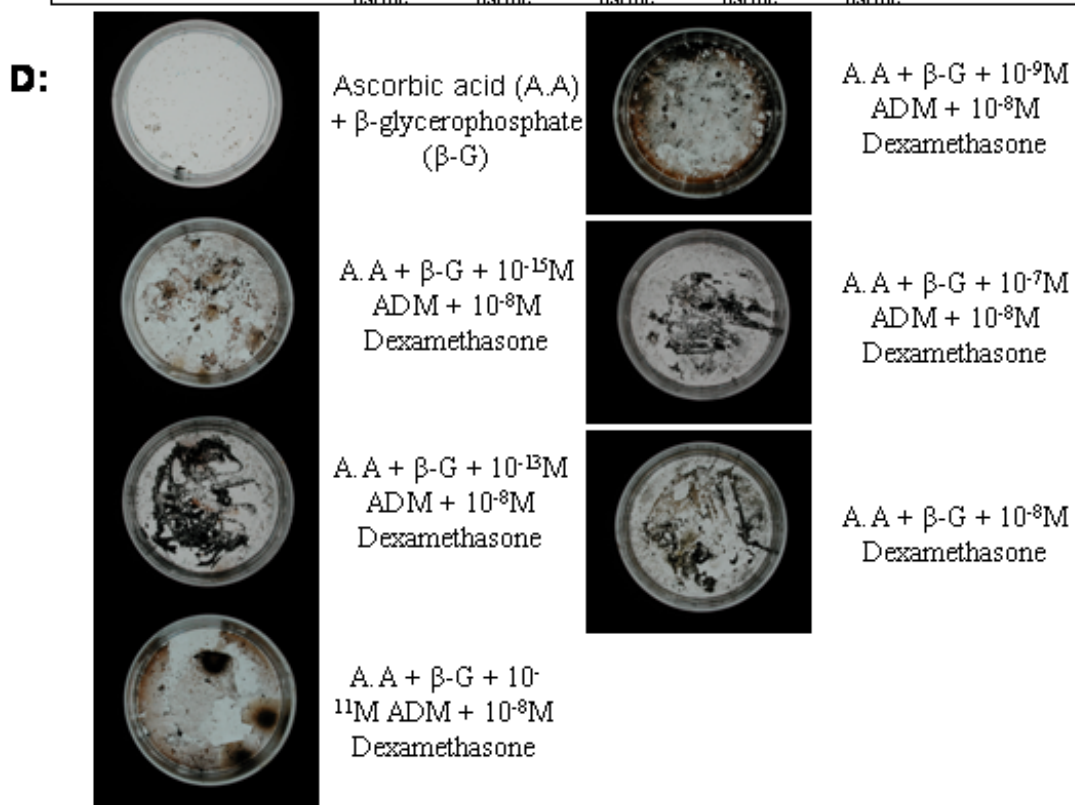
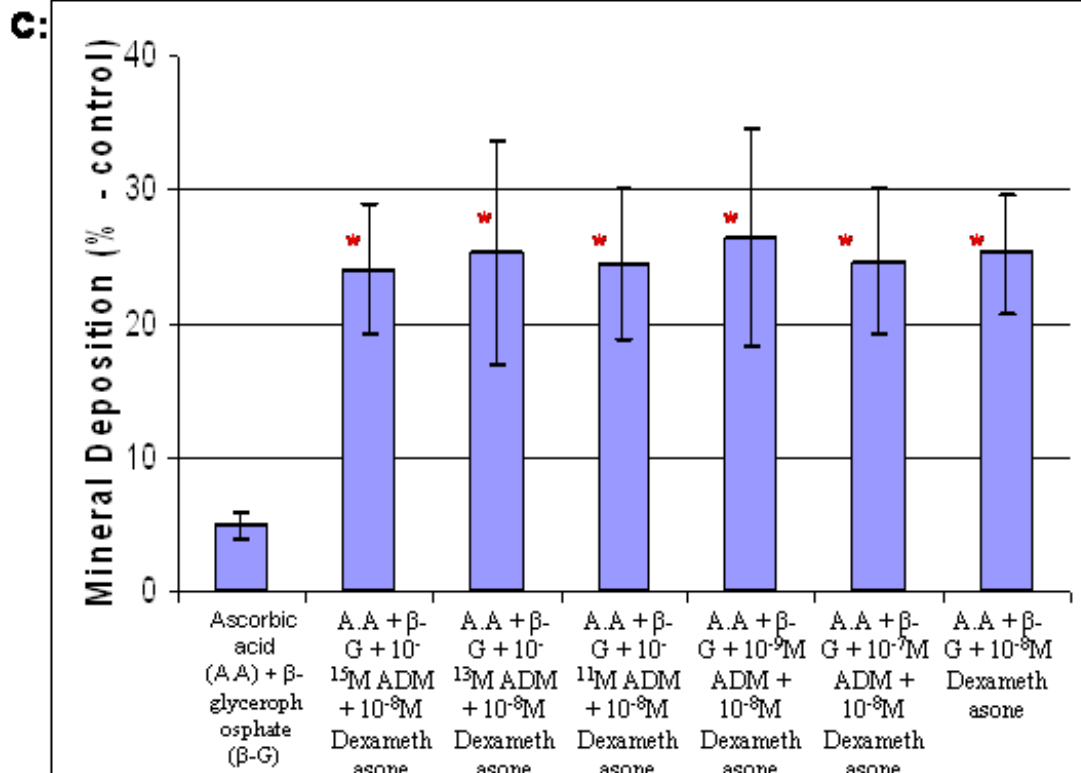
A:**B:**

Figure 5.5: A + C – Mean mineral deposition MDPC-23 cells following 21 day treatment with Ascorbic acid (A.A) and β -glycerophosphate (β -G), A.A, β -G and a range of concentrations of ADM (10^{-15} M, 10^{-13} M, 10^{-11} M, 10^{-9} M and 10^{-7} M ADM), 7: A.A, β -G and 10^{-8} M DEX, and A.A, β -G, 10^{-8} M DEX and a range of concentrations of ADM (10^{-15} M, 10^{-13} M, 10^{-11} M, 10^{-9} M and 10^{-7} M ADM). B + D: Representative images of the von Kossa stained cells from which the data presented in A + C was obtained.

*** = statistically significant difference compared to A.A and β -G treatment. * = statistically significant difference compared to A.A, β -G and 10^{-8} M dexamethasone treatment. This experiment was carried out three times.**



To provide a summary of the results presented thus far (**Figures 5.1 – 5.5**), a graph is presented in **Figure 5.6** demonstrating the changes in MDPC-23 cell mineral deposition over the period of 3, 7, 11, 14 and 21 days, following exposure to each pre-described treatment.

When looking at the results in full it appears that when MDPC-23 cells were exposed to A.A, β -G and differing concentrations of ADM (10^{-15} M, 10^{-13} M, 10^{-11} M, 10^{-9} M and 10^{-7} M), there is a uniform increase in mineral deposition from 7 days exposure through to 21 days exposure, when compared to A.A and β -G medium alone (**Figure 5.6A**). The exceptions to this are following exposure to 10^{-15} M and 10^{-7} M ADM after 7 days, which produced an increase in mineral deposition compared to A.A and β -G exposure that did not prove to be statistically significant (**Figure 5.6A**).

When MDPC-23 ECM secretion with these treatments [A.A, β -G and differing concentrations of ADM (10^{-15} M, 10^{-13} M, 10^{-11} M, 10^{-9} M and 10^{-7} M)] are compared to MDPC-23 cells exposed to the standard mineralising medium (A.A, β -G & 10^{-8} M Dex), it is clear that at 7 and 11 days there is generally very little difference in levels of mineral deposition, however, following 14 and 21 days exposure the standard mineralising medium increases mineral deposition to a higher level than all other treatments (**Figure 5.6A**). This suggests that ADM is capable of inducing a mineral deposition, indicative of mineralisation, at a similar rate to dexamethasone in MDPC-23 cells up to 11 days exposure, after which the rate of deposition slows compared to the standard mineralising medium.

MDPC-23 cells exposed to the standard mineralising medium plus a range of concentrations of ADM (10^{-15} M, 10^{-13} M, 10^{-11} M, 10^{-9} M and 10^{-7} M) appeared to produce a higher amount of mineral deposition compared to the standard mineralising medium following 7, 11 and 14 days exposure. However, this increase in mineral

deposition was only found to be statistically significant at 11 days exposure (**Figure 5.6B**). Following 21 days exposure, this increased rate of mineral deposition appears to be negated, with the standard mineralising medium marginally increasing the amount of mineral deposition compared to the standard mineralising medium plus a range of concentrations of ADM (10^{-15}M , 10^{-13}M , 10^{-11}M , 10^{-9}M and 10^{-7}M). This suggests that when used in coordination with Dex, ADM at all concentrations is capable of producing higher levels of mineral deposition compared to Dex alone during the early stages of mineralisation, while this effect is lost later in the mineralisation process. In **Section 4.6** Dex demonstrated an ability to reduce levels of ADM expression, particularly at 10^{-8}M . The loss of increased mineral deposition following exposure to ADM over the longer time points could relate to this. It would be interesting to look at time points over 21 days to determine whether this trend continues. It may be that any increases in mineral deposition following exposure to ADM were due to increased cell numbers, as described in **Section 4.2**, however, as the increased mineral deposition is roughly uniform for each concentration studied, while cell number increases were found to be biphasic, makes this unlikely.

A:

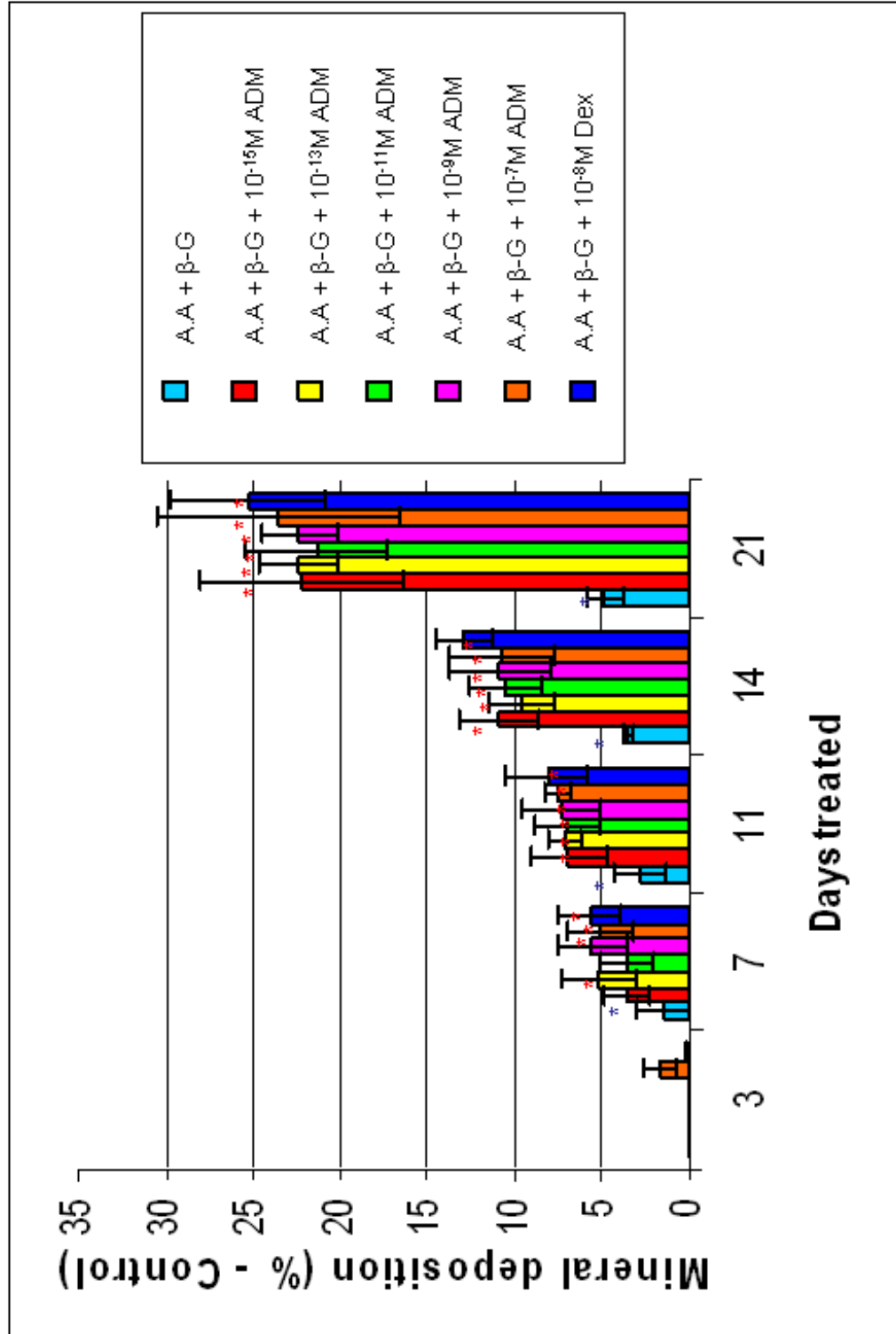
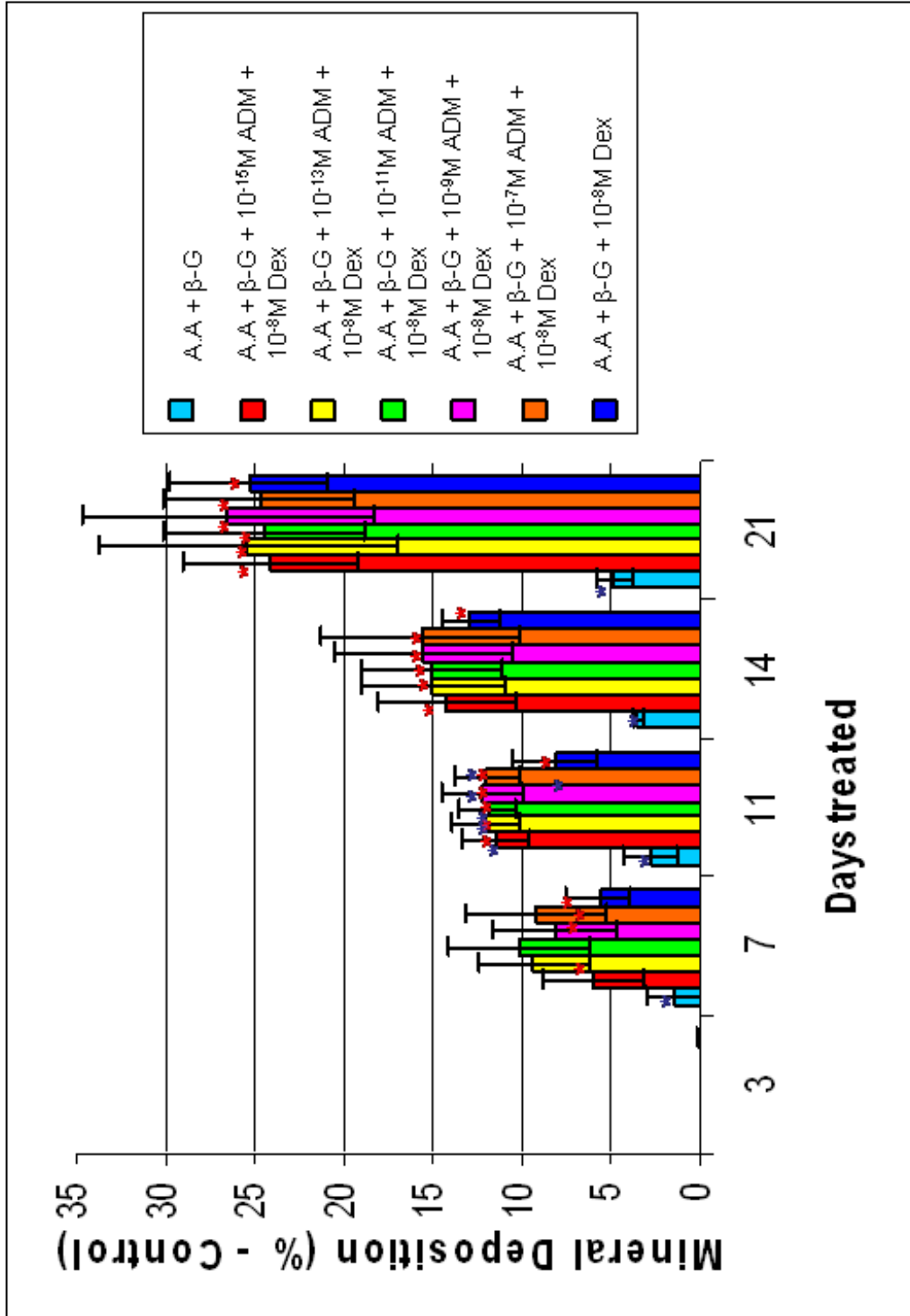


Figure 5.6: Mean mineral deposition in MDPC-23 cells treated with A: either 50µg/ml ascorbic acid (AA) and 10mM β-glycerophosphate (β-G), AA, β-G and a range of concentrations of ADM (10^{-15} M, 10^{-13} M, 10^{-11} M, 10^{-9} M and 10^{-7} M) or AA, β-G and 10^{-8} M Dex and B: either AA and β-G, AA, β-G and 10^{-8} M Dex or AA, β-G, 10^{-8} M Dex and a range of concentrations of ADM (10^{-15} M, 10^{-13} M, 10^{-11} M, 10^{-9} M and 10^{-7} M) for a period of 3, 7, 11, 14 and 21 days

*** = statistically significant difference compared to AA and β-G treated samples. * = statistically significant difference compared to AA, β-G and 10^{-8} M Dex. This experiment was carried out three times.**

B:



5.3 Effect of ADM exposure on OD-21 cell mineral deposition

The mineralising effect of ADM on the OD-21 pulp-like cell line cultured *in vitro* was determined using the von Kossa staining approach previously described, with cultures exposed to a range of conditions for 3, 7, 11, 14 and 21 days, following which, the medium was removed and the cells fixed. Analysis was performed as described previously in **Section 5.2**.

Figure 5.7 provides data demonstrating the effects of the supplementation of the control medium (A.A and B-G) and standard mineralising medium (A.A, B-G and DEX) with ADM on detection of mineral deposition in OD-21 cells following 3 days culture. No significant mineral deposition was detected after 3 days exposure to each of the conditions.

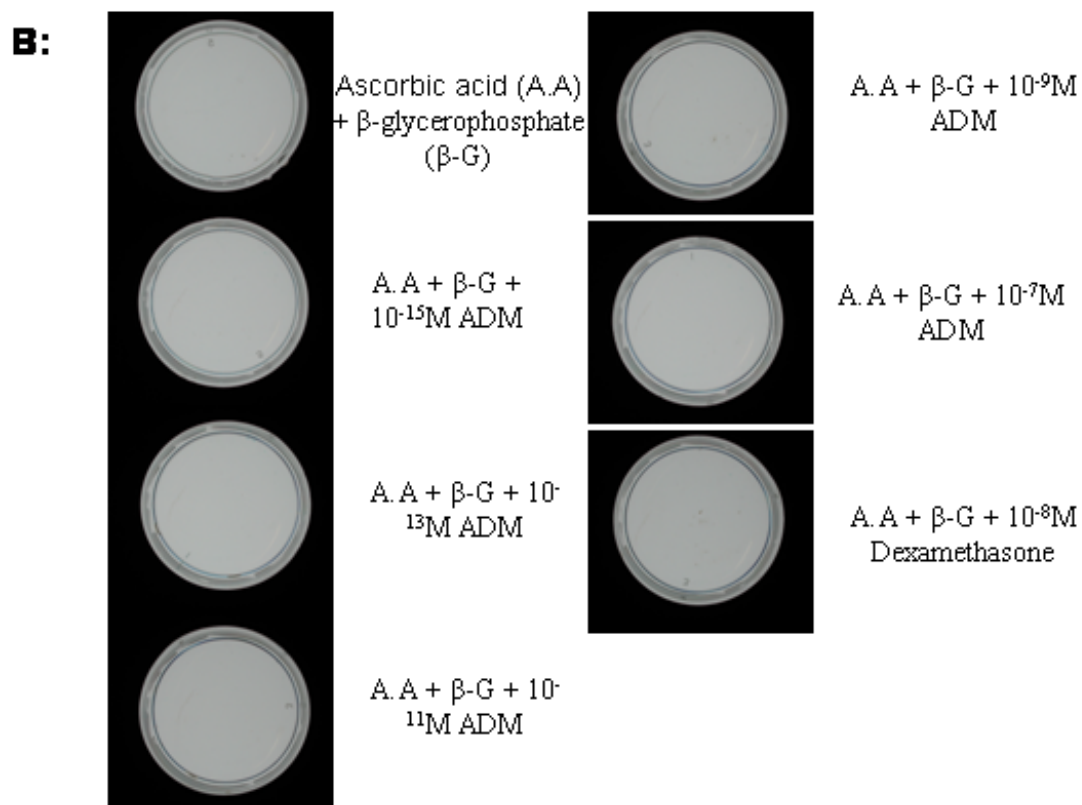
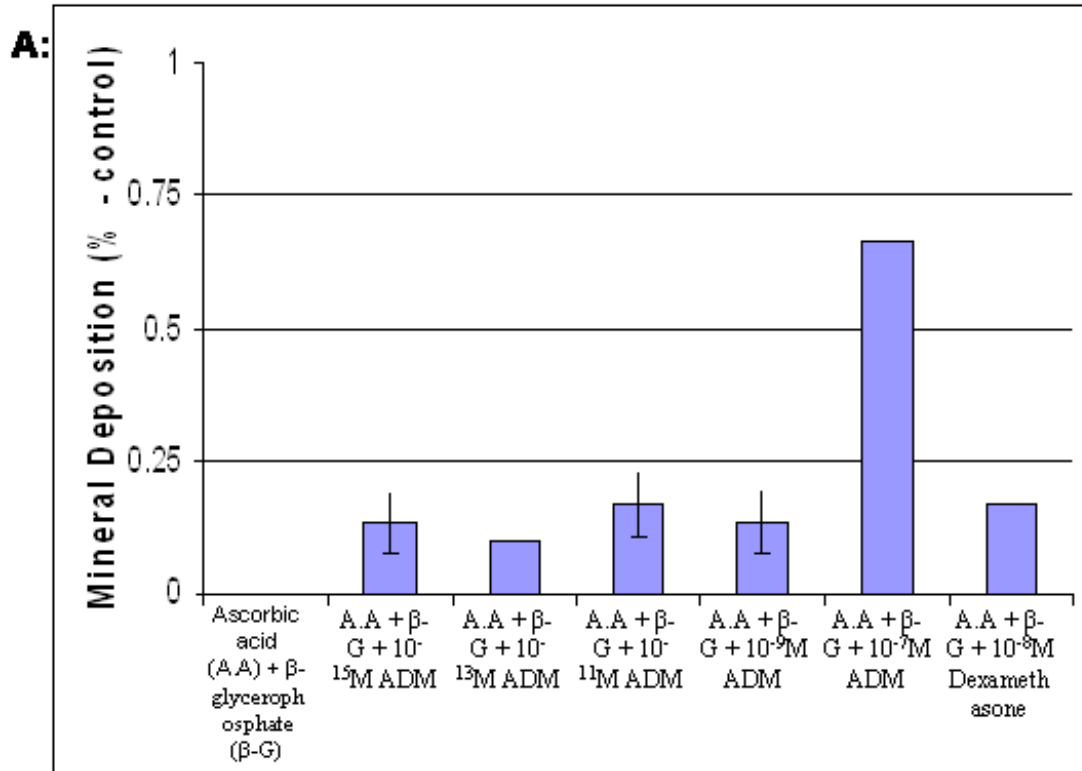
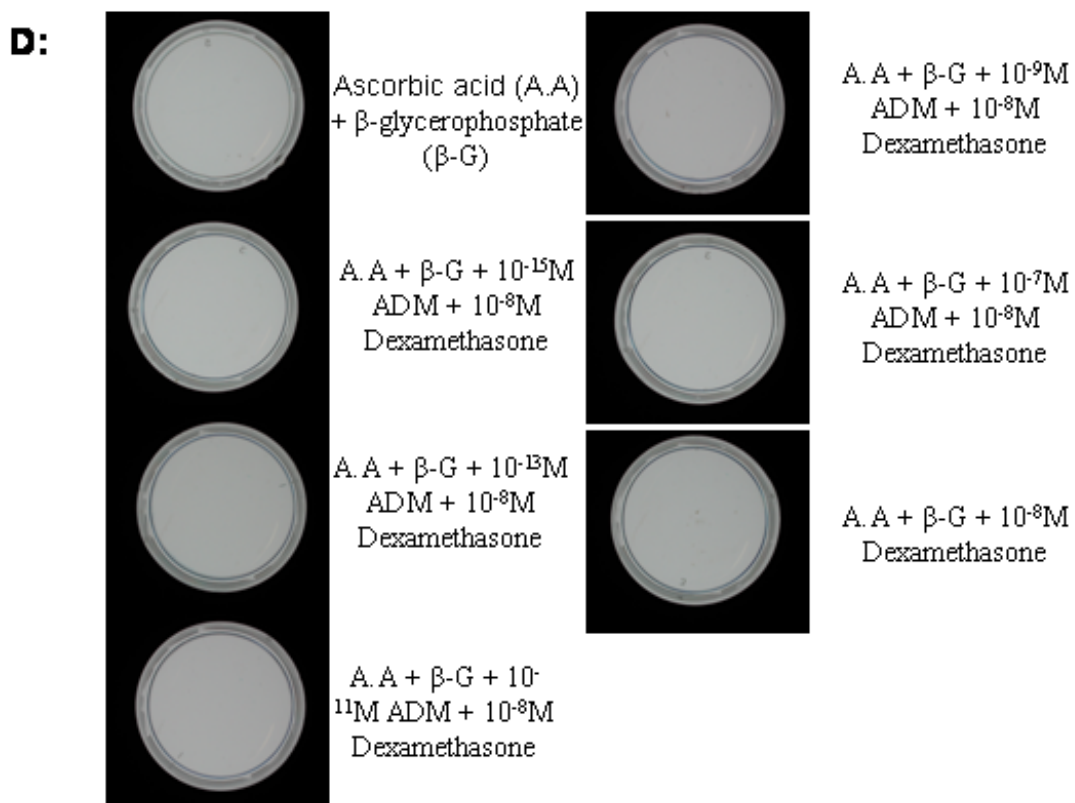
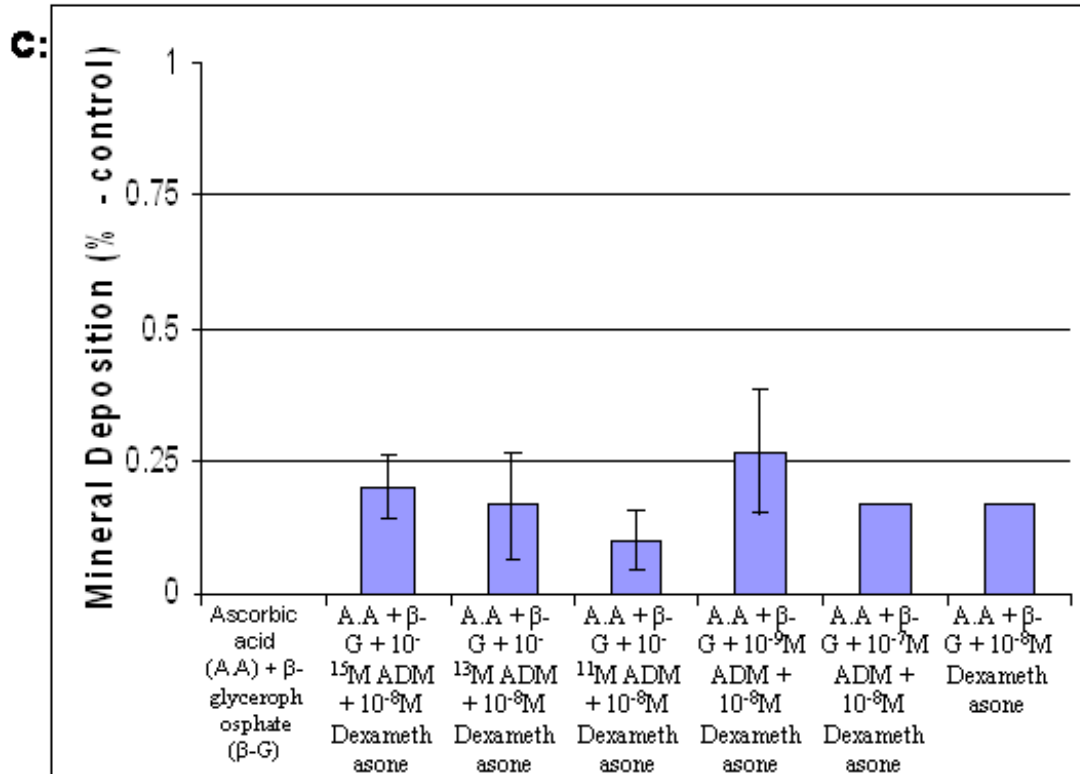


Figure 5.7: A + C – Mean mineral deposition in OD-21 cells following 3 day treatment with Ascorbic acid (A.A) and β -glycerophosphate (β -G), A.A, β -G and a range of concentrations of ADM (10^{-15} M, 10^{-13} M, 10^{-11} M, 10^{-9} M and 10^{-7} M ADM), A.A, β -G and 10^{-8} M DEX, and A.A, β -G, 10^{-8} M DEX and a range of concentrations of ADM (10^{-15} M, 10^{-13} M, 10^{-11} M, 10^{-9} M and 10^{-7} M ADM). **B + D**: Representative images of the von Kossa stained cells from which the data presented in **A + C** was obtained.

* = statistically significant difference compared to A.A and β -G treatment. * = statistically significant difference compared to A.A, β -G and 10^{-8} M dexamethasone treatment. This experiment was carried out three times.



The effect of ADM on mineral deposition in OD-21 cells after 7 days of culture was subsequently analysed (**Figure 5.8**). A.A and β -G treatment alone produced a minimal detectable area of mineral deposition (0.7%), as did medium containing A.A, β -G and 10^{-9} M ADM. Increases were evident following treatment with the mineralisation control medium, and with A.A, β -G and 10^{-11} M ADM medium. Other cell exposures to these supplements also generated minimally increased detectable areas of mineral deposition including A.A, β -G and 10^{-13} M ADM (1.7%), A.A, β -G and 10^{-15} M (2%) and A.A, β -G and 10^{-7} M (2%). Cells exposed to the standard mineralisation control medium supplemented with a range of concentrations of ADM also generated increased levels of mineral deposition. The addition of 10^{-15} M and 10^{-13} M ADM produced a 2.3% detectable area of mineral deposition, 10^{-11} M gave 1.7% and the additions of 10^{-9} M and 10^{-7} M ADM both resulted in detectable areas of mineral deposition of 2.7% for these treatments. None of these results however were statistically significantly different compared to the control medium.

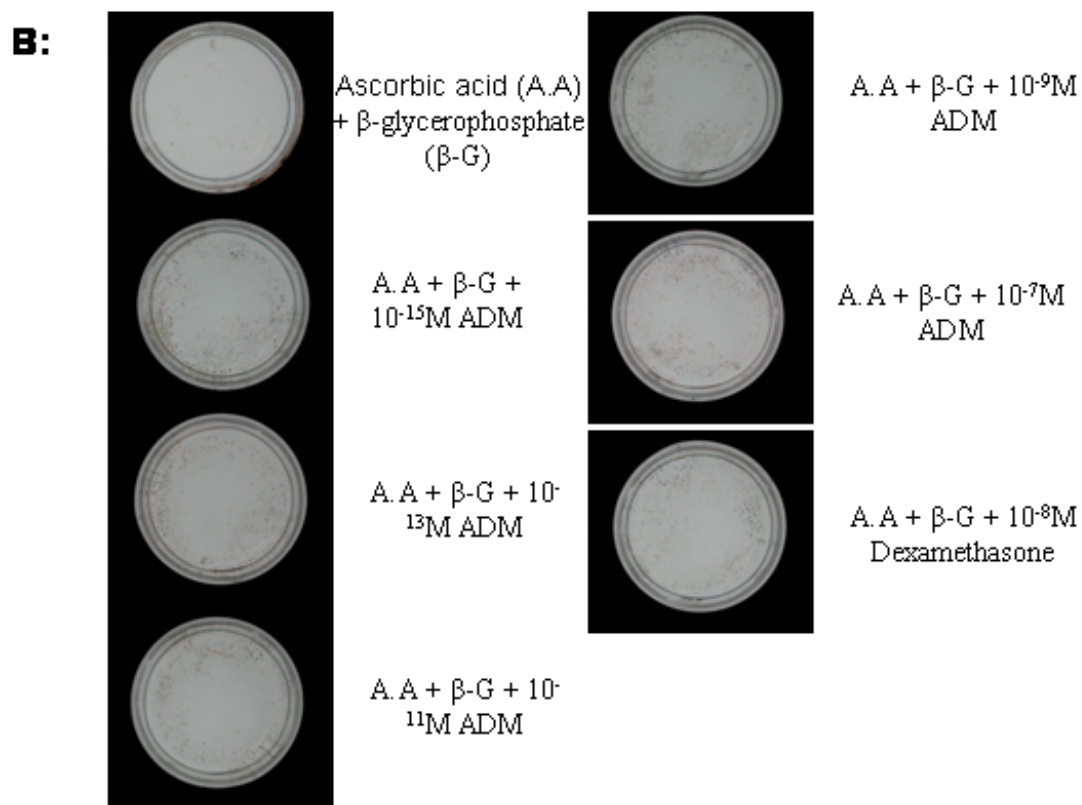
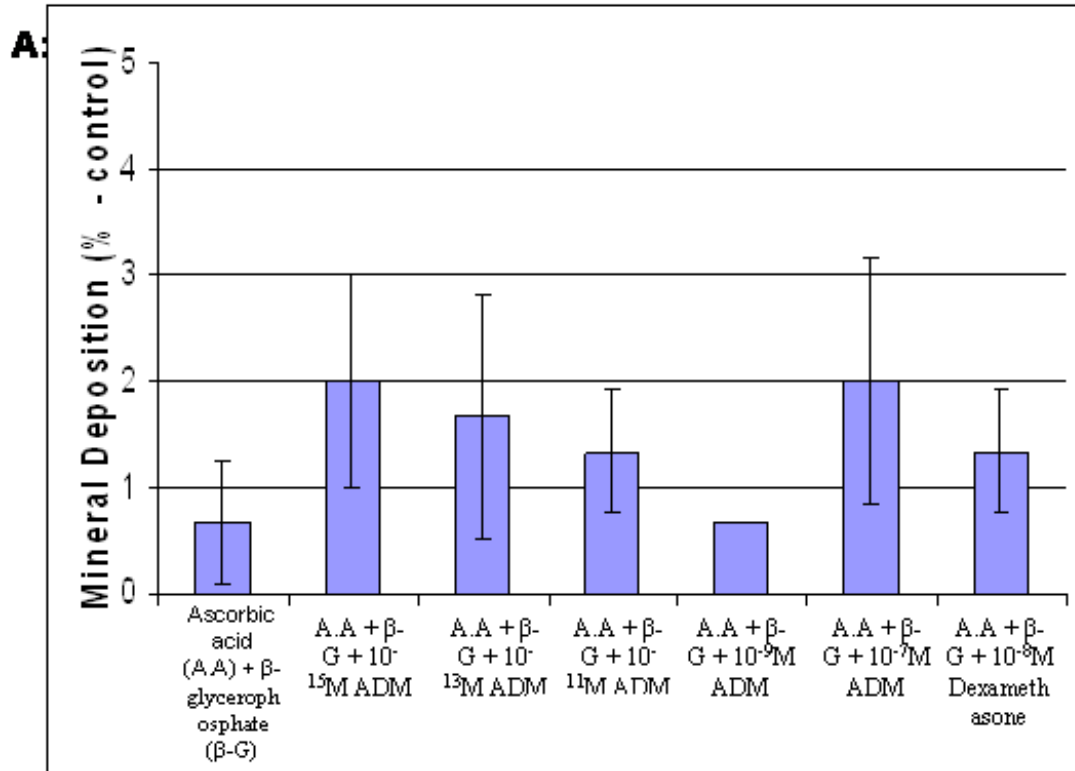
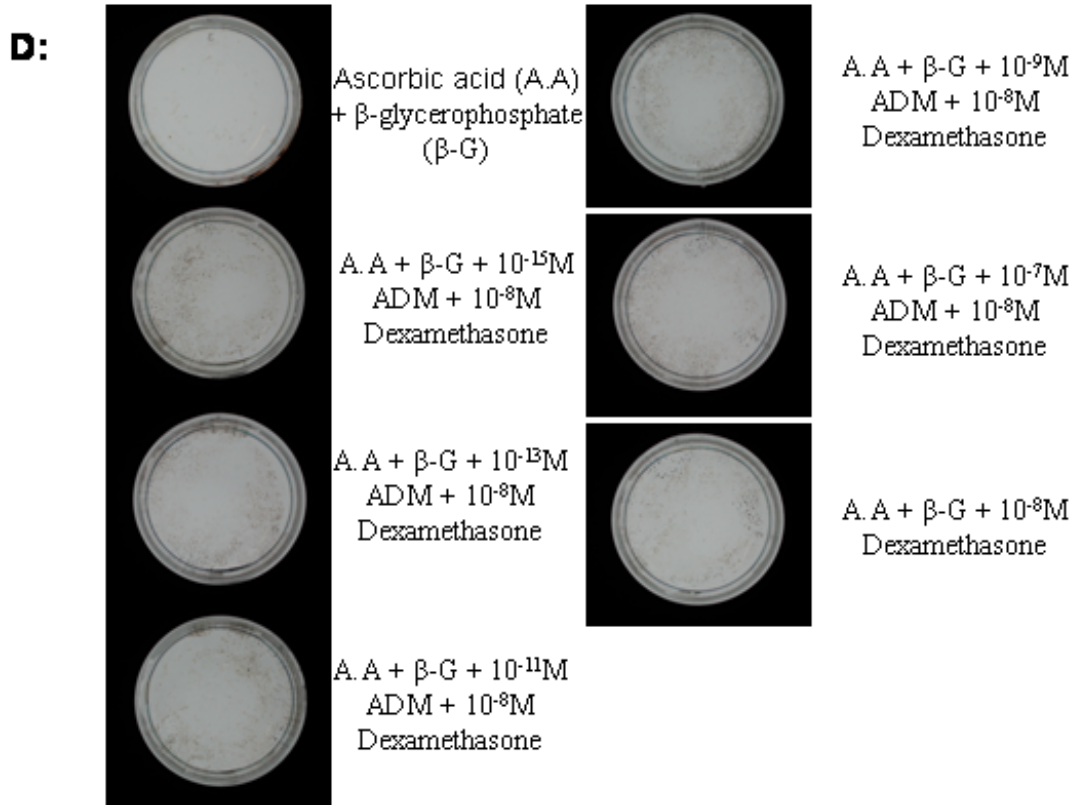
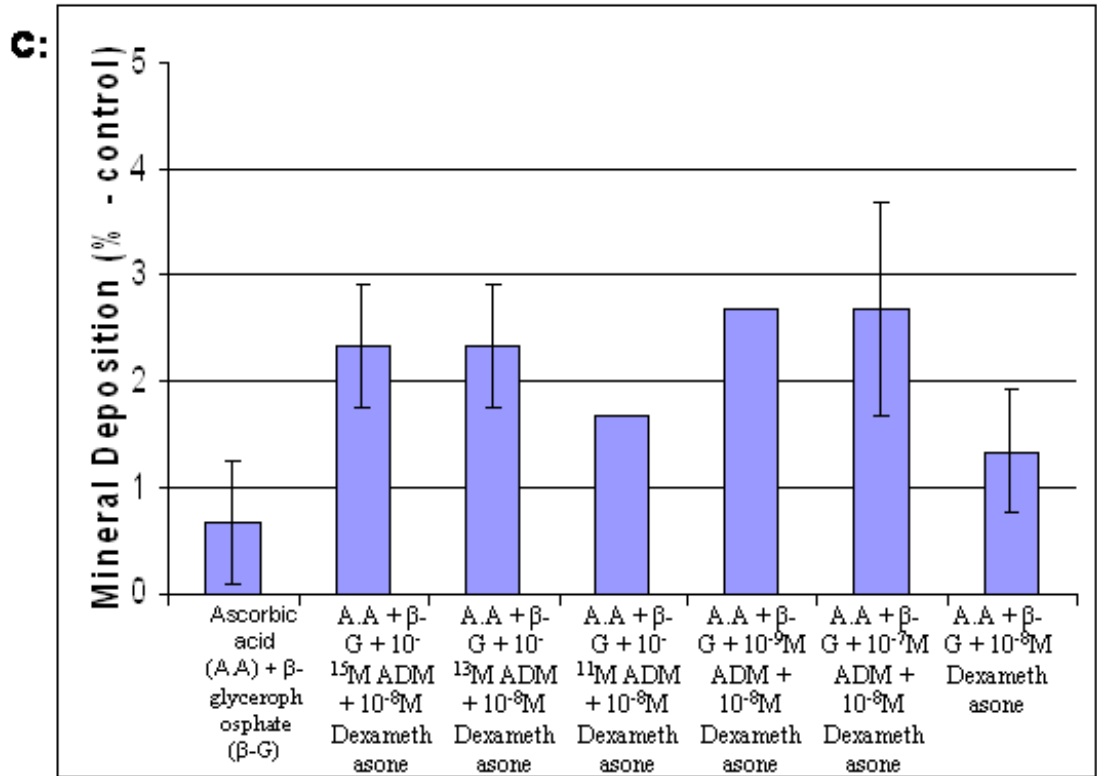


Figure 5.8: A + C – Mean mineral deposition in OD-21 cells following 7 days treatment with Ascorbic acid (A.A) and β -glycerophosphate (β -G), A.A, β -G and a range of concentrations of ADM (10^{-15} M, 10^{-13} M, 10^{-11} M, 10^{-9} M and 10^{-7} M ADM), A.A, β -G and 10^{-8} M DEX, and A.A, β -G, 10^{-8} M DEX and a range of concentrations of ADM (10^{-15} M, 10^{-13} M, 10^{-11} M, 10^{-9} M and 10^{-7} M ADM). **B + D**: Representative images of the von Kossa stained cells from which the data presented in **A + C** was obtained.

* = statistically significant difference compared to A.A and β -G treatment. * = statistically significant difference compared to A.A, β -G and 10^{-8} M dexamethasone treatment. This experiment was carried out three times.



Following 11 days treatment (**Figure 5.9**), A.A and β -G exposure resulted in a 0.47% detectable area of mineral deposition in OD-21 cell cultures. The data presented (Figure 5.8A) demonstrate that treatment with A.A, β -G and each concentration of ADM elicited a statistically significant increase in the area of mineral deposition compared to A.A and β -G containing media alone. The inclusion of ADM at all concentrations within this medium resulted in >4% increases in mineral deposition. Each of these exposures resulted in more mineral deposition than cells treated with the standard mineralisation control medium alone, which gave a detectable area of mineral deposition of 3.7%. However, none of these differences were statistically significant. Cells exposed to the mineralising medium control containing a range of concentrations of ADM also produced more mineral deposition than the standard mineralisation control medium alone. OD-21 cells exposed to the mineralisation control medium containing 10^{-15} M ADM, produced the greatest levels of mineral deposition after 11 days of exposure, exhibiting an area of 6.27%. The addition of 10^{-13} M ADM to the mineralisation medium control gave a detectable area of mineral deposition of 5.8%. Inclusion of 10^{-11} M, 10^{-9} M and 10^{-7} M ADM in the mineralisation control medium resulted in detectable areas of mineral deposition of 4.7 - 4.9% for the OD-21 cultures. Each treatment with ADM and the mineralisation control media gave a statistically significant difference in area of mineral deposition compared to A.A and β -G alone, however, there were no statistically significant differences when these values were compared with the standard mineralisation control medium (A.A, B-G & 10^{-8} M Dex) alone.

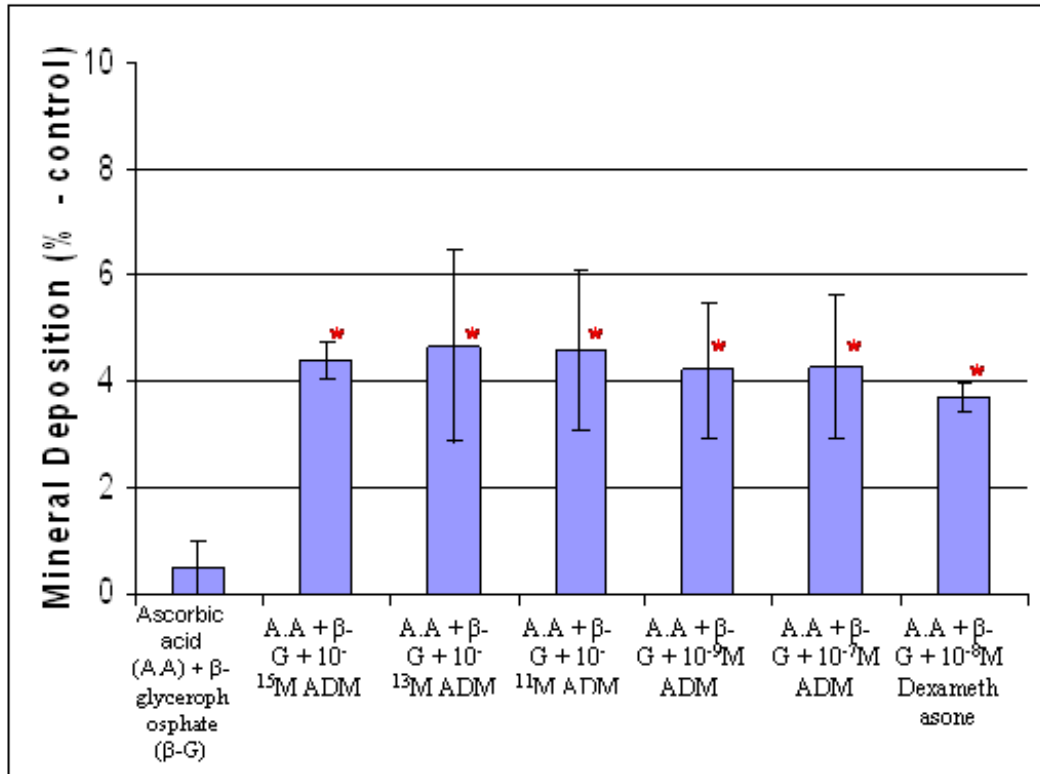
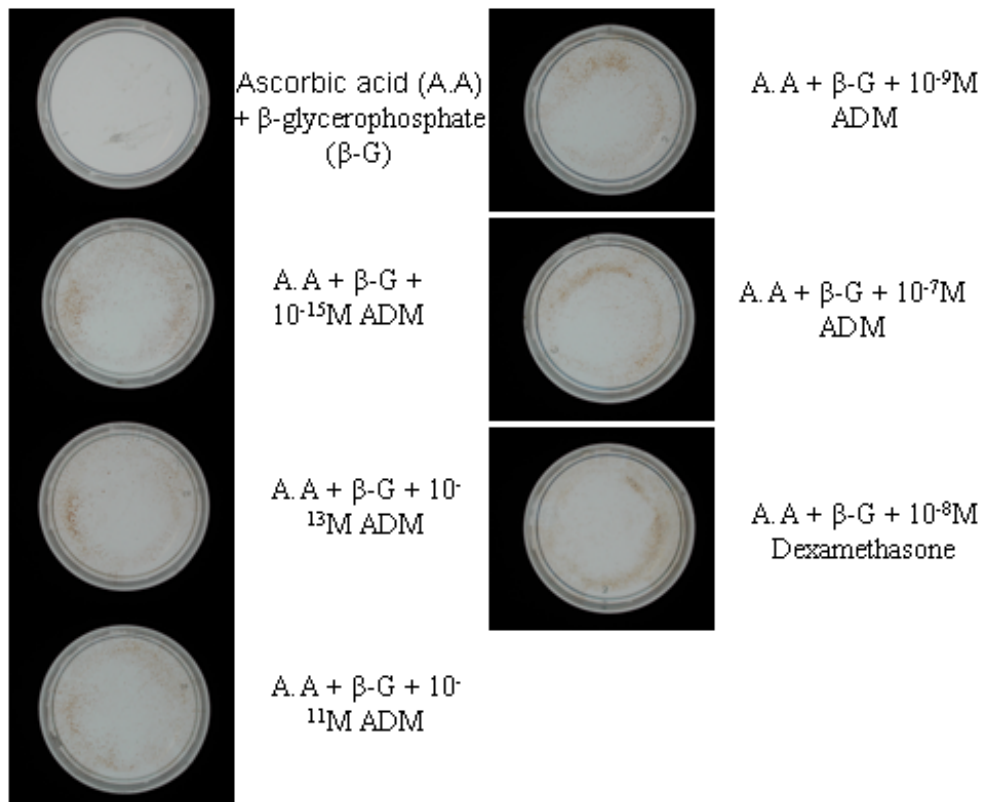
A:**B:**

Figure 5.9: A + C – Mean mineral deposition in OD-21 cells following 11 day treatment with Ascorbic acid (A.A) and β -glycerophosphate (β -G), A.A, β -G and a range of concentrations of ADM (10^{-15} M, 10^{-13} M, 10^{-11} M, 10^{-9} M and 10^{-7} M ADM), A.A, β -G and 10^{-8} M DEX, and A.A, β -G, 10^{-8} M DEX and a range of concentrations of ADM (10^{-15} M, 10^{-13} M, 10^{-11} M, 10^{-9} M and 10^{-7} M ADM). **B + D**: Representative images of the von Kossa stained cells from which the data presented in **A + C** was obtained.

* = statistically significant difference compared to A.A and β -G treatment. * = statistically significant difference compared to A.A, β -G and 10^{-8} M dexamethasone treatment. This experiment was carried out three times.

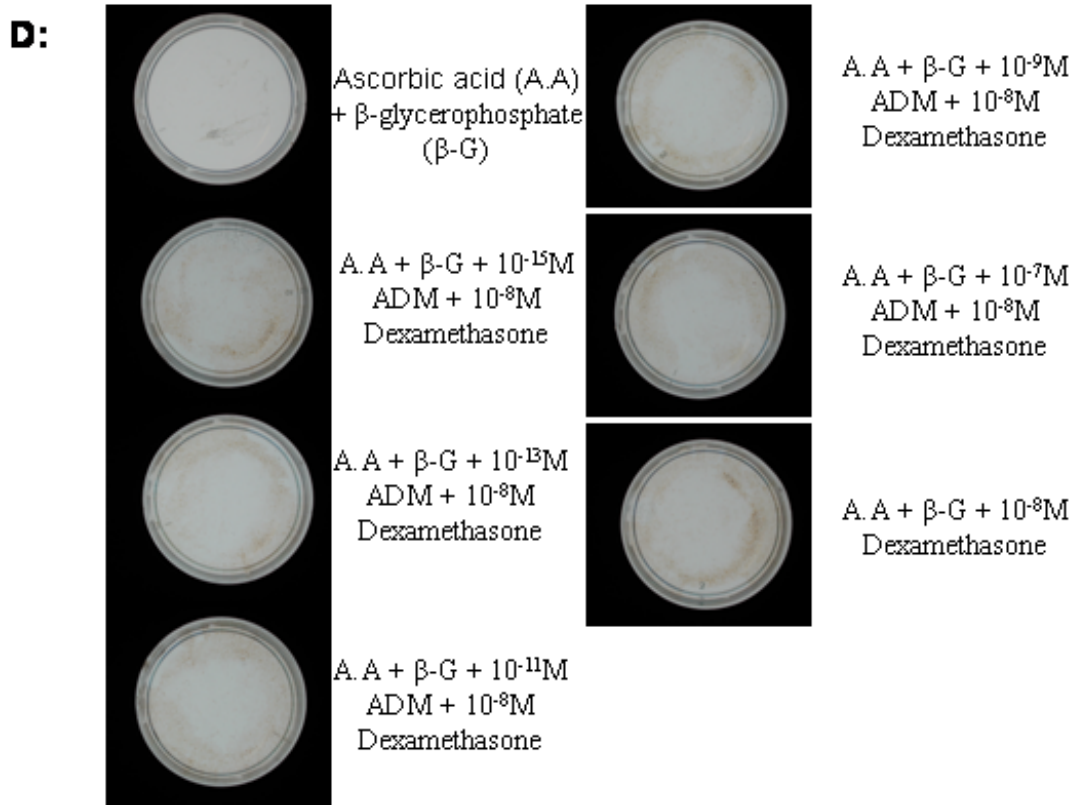
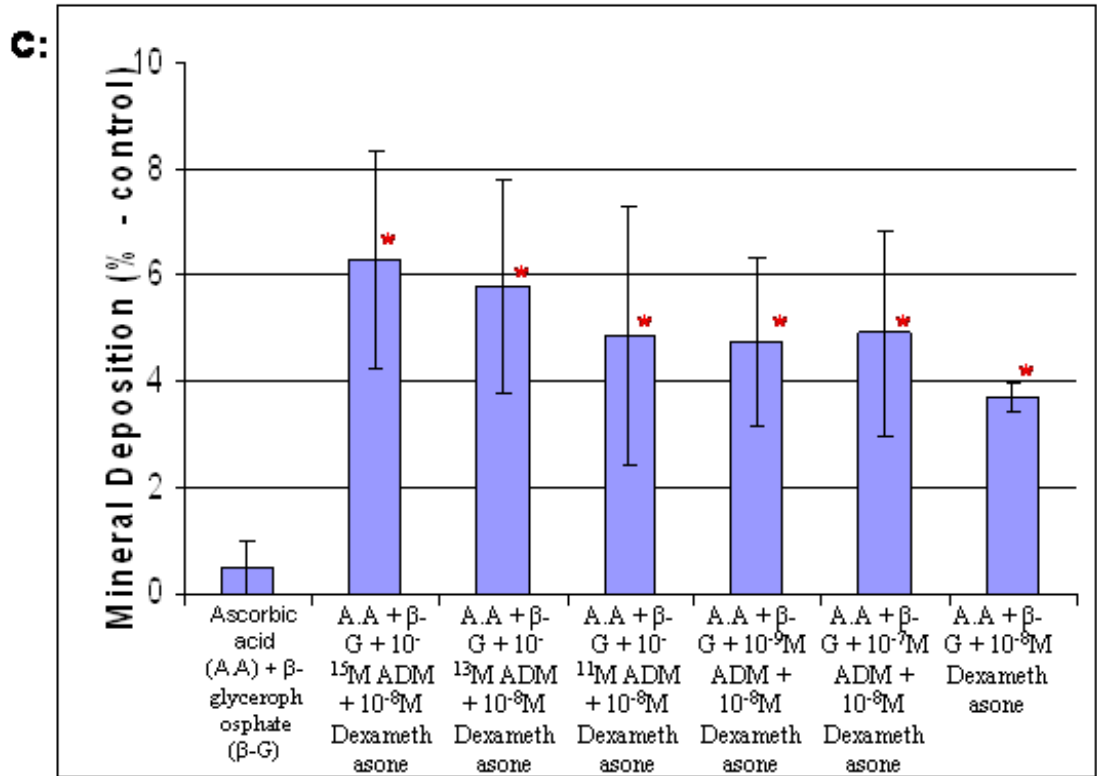


Figure 5.10A provides data demonstrating the effect of media containing A.A, β -G plus the range of concentrations of ADM on OD-21 cell mineral deposition following 14 days culture, compared to A.A and β -G medium use alone along with the standard mineralisation control medium. A.A and β -G alone induced a detectable area of mineral deposition of 3.9%, whilst exposure to A.A, β -G plus the range of ADM concentrations produced statistically significant increases in the areas of mineral deposition detected. 10^{-13} M ADM elicited the greatest increase in conjunction with A.A and β -G, stimulating a detectable area of mineral deposition of 6.37%. Inclusion of 10^{-15} M, 10^{-11} M, 10^{-9} M and 10^{-7} M ADM promoted detectable areas of mineral deposition of 5.7%, 6.3%, 5.2% and 6.3%, respectively. These percentage areas were lower than the cells treated with the mineralisation control medium, which stimulated an area of mineral deposition of 7.1%. This value was statistically significant when compared to A.A and β -G alone and A.A, β -G and 10^{-9} M ADM. When ADM was used in conjunction with the standard mineralisation control medium (**Figure 5.10C**), each concentration stimulated a greater area of mineral deposition compared to the mineralisation control medium except 10^{-9} M ADM, which resulted in an area of 7.0% of detectable mineral deposition. Cells exposed to the standard mineralisation control medium supplemented with 10^{-15} M ADM produced the greatest detectable mineral deposition with an area of 8.6%. Inclusion of 10^{-13} M, 10^{-11} M and 10^{-7} M ADM induced a detectable area of mineral deposition of $\sim 7.5\%$ in all cases. Each of these areas of mineral deposition was shown to represent a statistically significant increase compared to A.A and β -G alone.

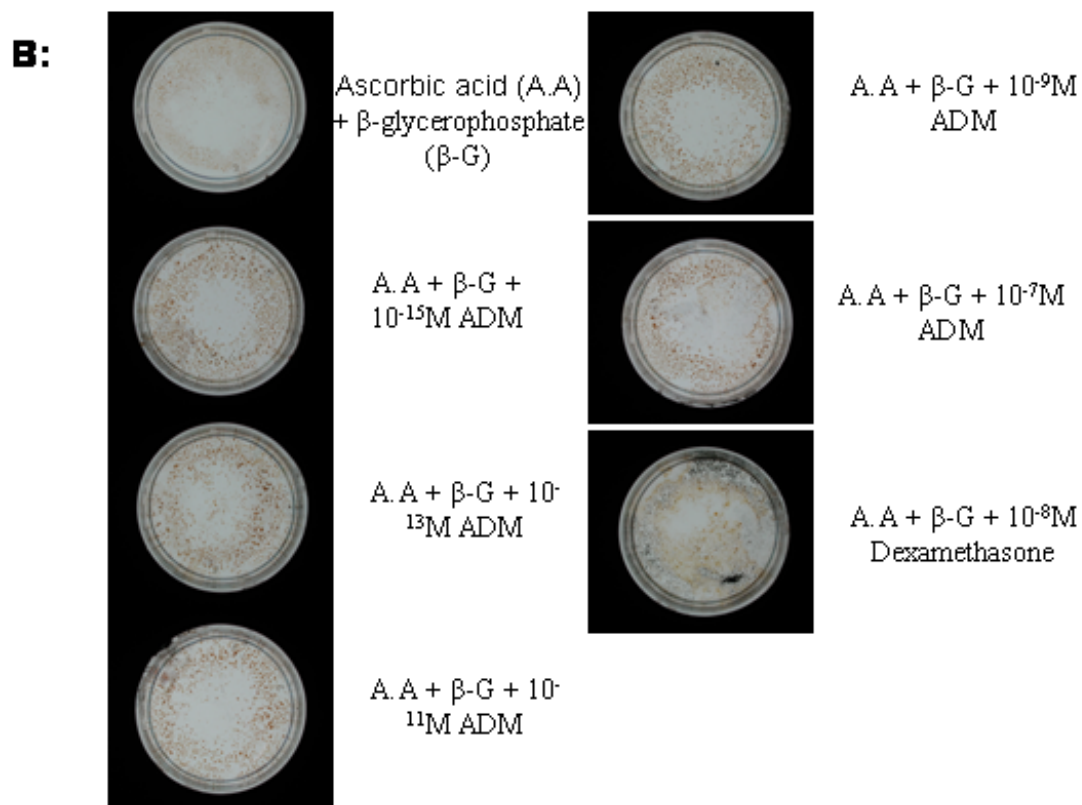
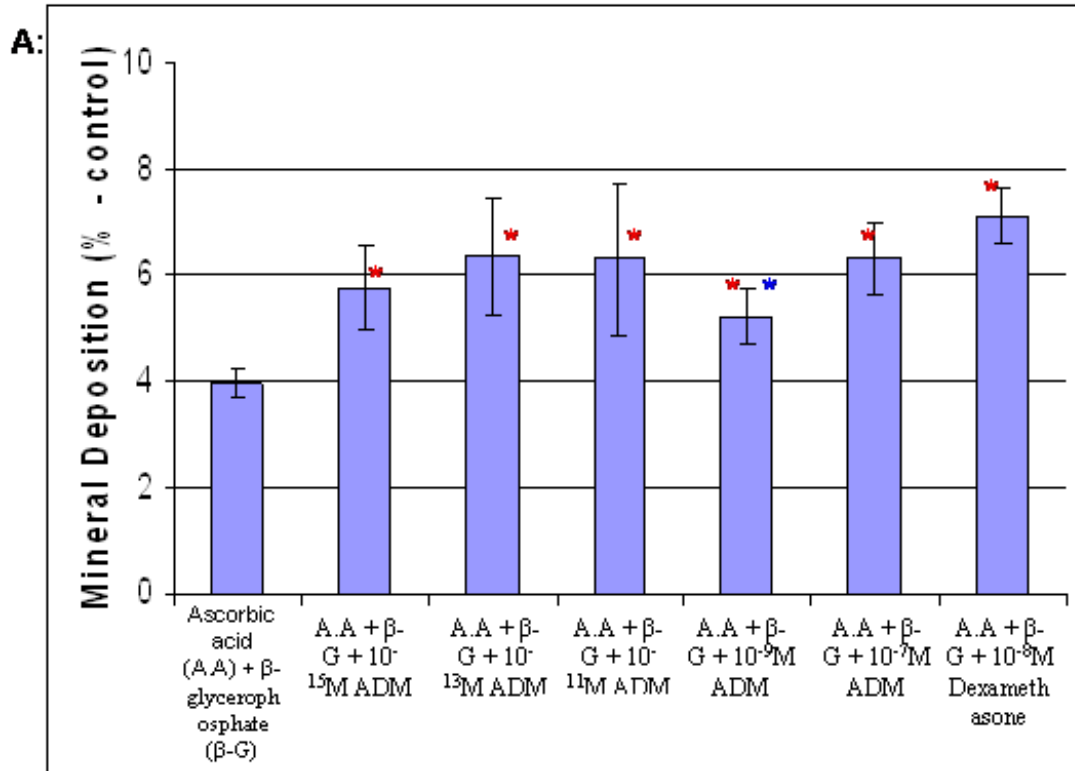
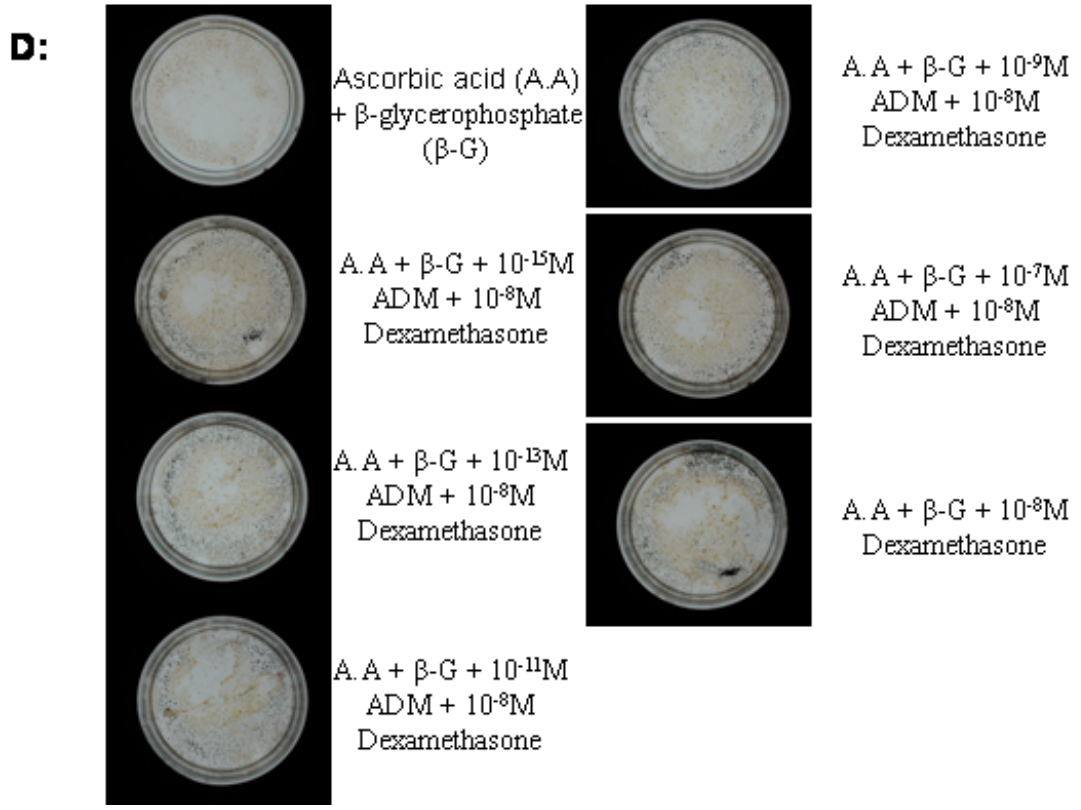
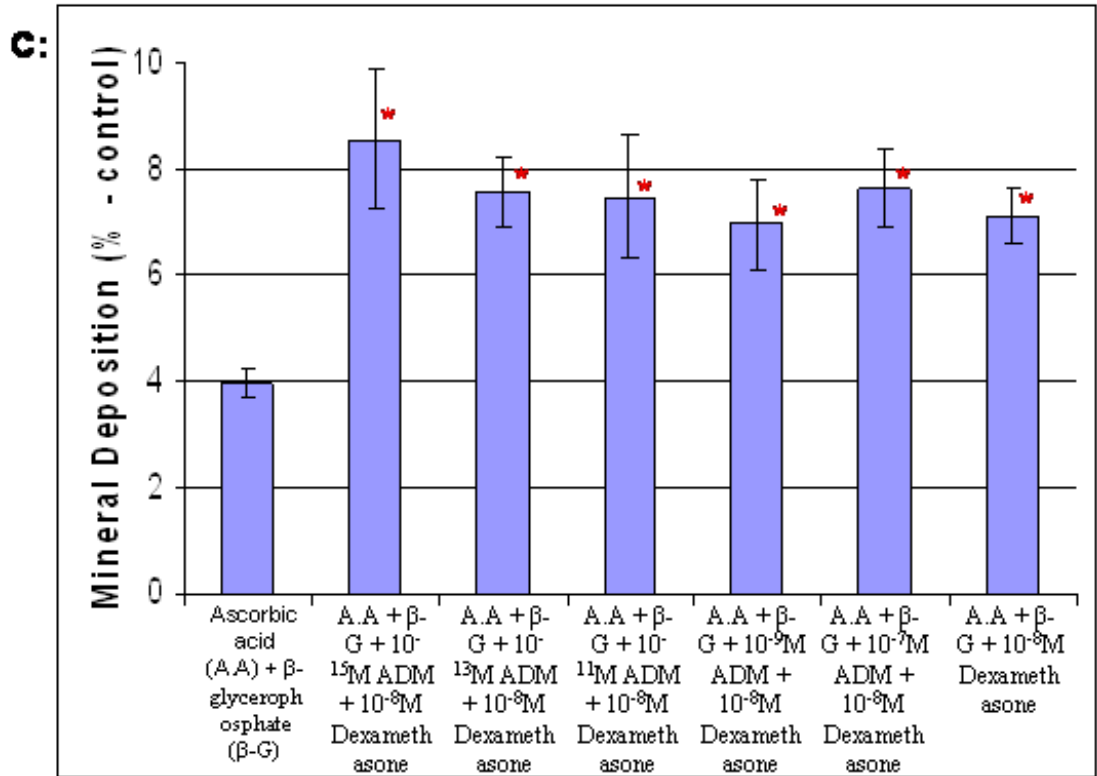


Figure 5.10: A + C – Mean mineral deposition in OD-21 cells following 14 day treatment with Ascorbic acid (A.A) and β -glycerophosphate (β -G), A.A, β -G and a range of concentrations of ADM (10^{-15} M, 10^{-13} M, 10^{-11} M, 10^{-9} M and 10^{-7} M ADM), A.A, β -G and 10^{-8} M DEX, and A.A, β -G, 10^{-8} M DEX and a range of concentrations of ADM (10^{-15} M, 10^{-13} M, 10^{-11} M, 10^{-9} M and 10^{-7} M ADM). B + D: Representative images of the von Kossa stained cells from which the data presented in A + C was obtained.

*** = statistically significant difference compared to A.A and β -G treatment. * = statistically significant difference compared to A.A, β -G and 10^{-8} M dexamethasone treatment. This experiment was carried out three times.**



Data indicating the effect of ADM on the OD-21 mineral deposition after 21 days culture are provided (**Figure 5.11**). Results presented (**Figure 5.11A**) demonstrate the effect of A.A, β -G and the range of concentrations of ADM on the OD-21 cell-line mineral deposition compared to A.A and β -G containing medium alone together with the standard mineralisation control medium (A.A., B-G & 10^{-8} M Dex). A.A and β -G medium exposure alone resulted in an area of mineral deposition of 4.9% detected whilst the standard mineralisation medium control induced an area of mineral deposition of 15.2%. The cells exposed to the A.A and β -G medium supplemented with the range of concentrations of ADM all gave results that were statistically significantly lower than the standard mineralisation control medium, whilst being significantly higher than the control A.A and β -G medium alone. The addition of 10^{-15} M, 10^{-13} M, 10^{-11} M, 10^{-9} M ADM to A.A and β -G resulted in promotion of mineral deposition in the ranges of 7.9 - 8.9%. The concentration of ADM that produced the greatest detectable mineral deposition in conjunction with A.A and β -G medium was 10^{-7} M, which stimulated a detectable area of mineral deposition of 10.2%. Cells exposed to ADM in conjunction with the standard mineralised control medium also gave a statistically significant increase in mineral deposition compared to A.A and β -G alone (**Figure 5.11C**). Minimal variation in detectable mineral deposition induction was evident between the range of concentrations of ADM studied, the smallest area of detectable mineral deposition was 13.5% for 10^{-13} M ADM with the highest area of mineral deposition detected being 14.1% following treatment with 10^{-7} M ADM. 10^{-15} M, 10^{-11} M and 10^{-9} M each produced detectable areas of mineral deposition of 13.8%, 13.7% and 13.9%, respectively. Each ADM treatment produced an area of mineral deposition that was

smaller than that observed with the standard mineralisation control medium alone, however, the differences were not statistically significant.

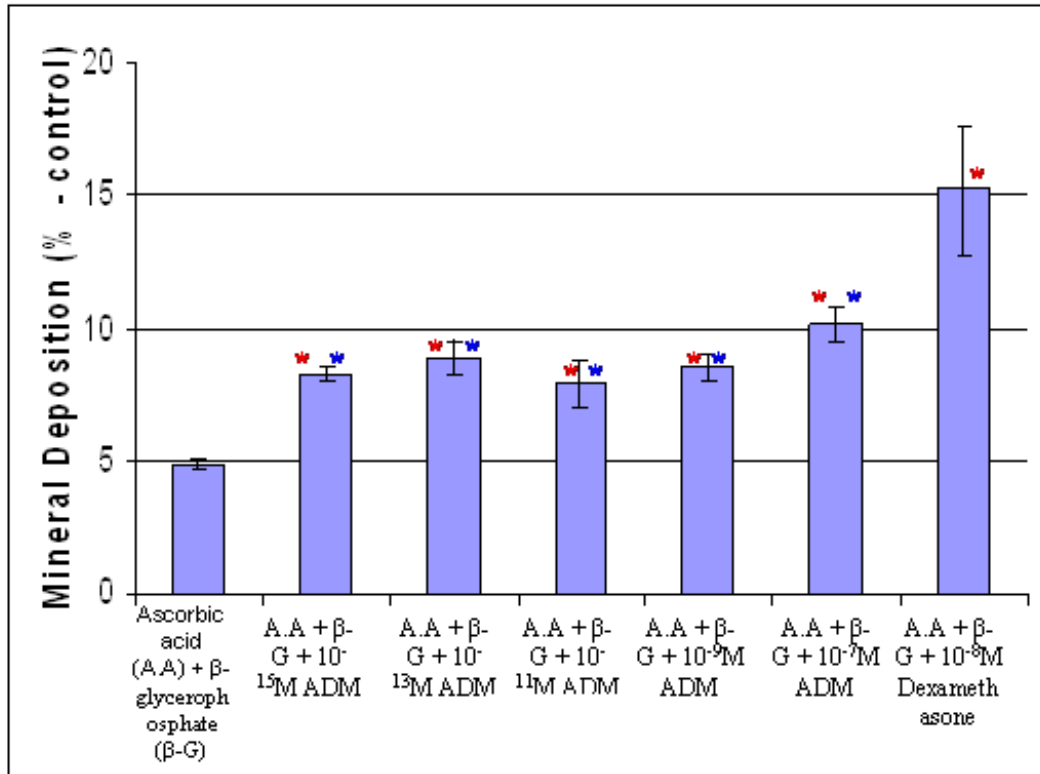
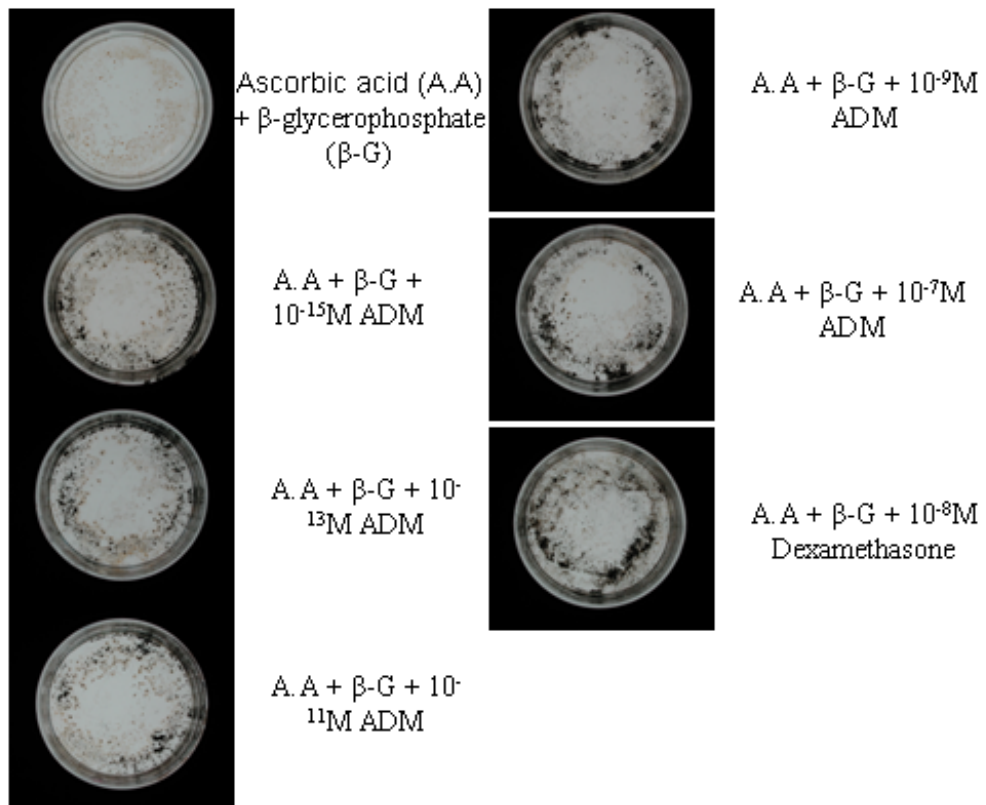
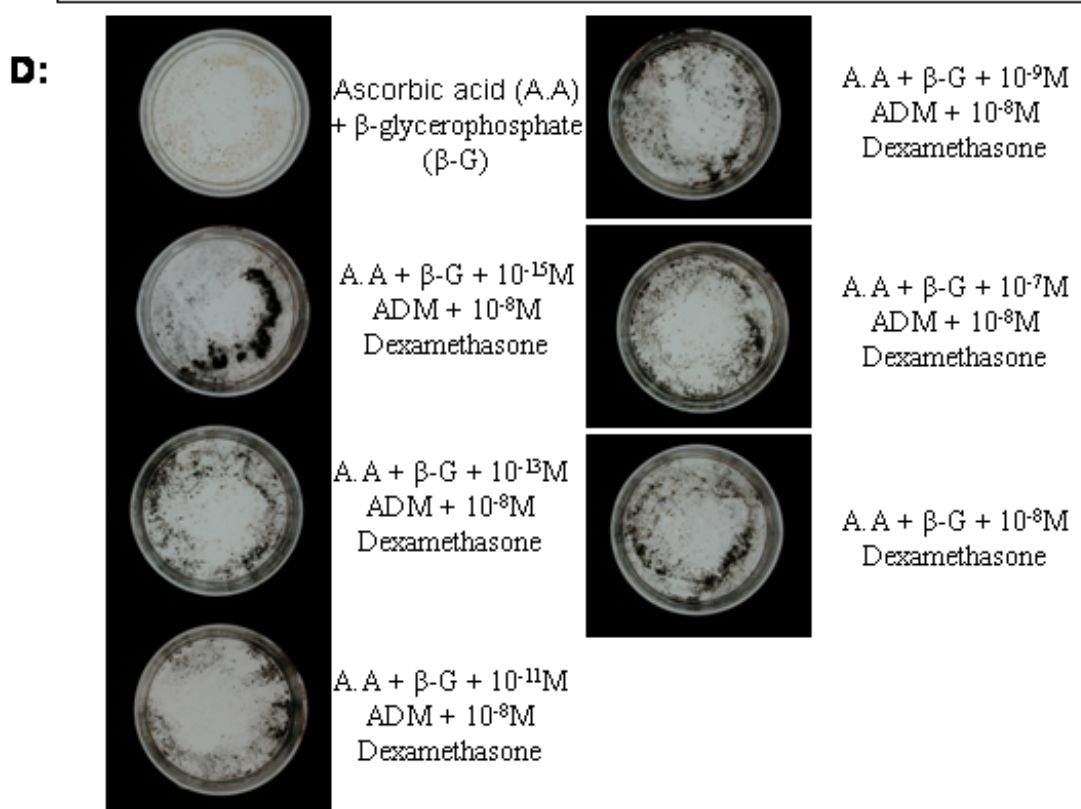
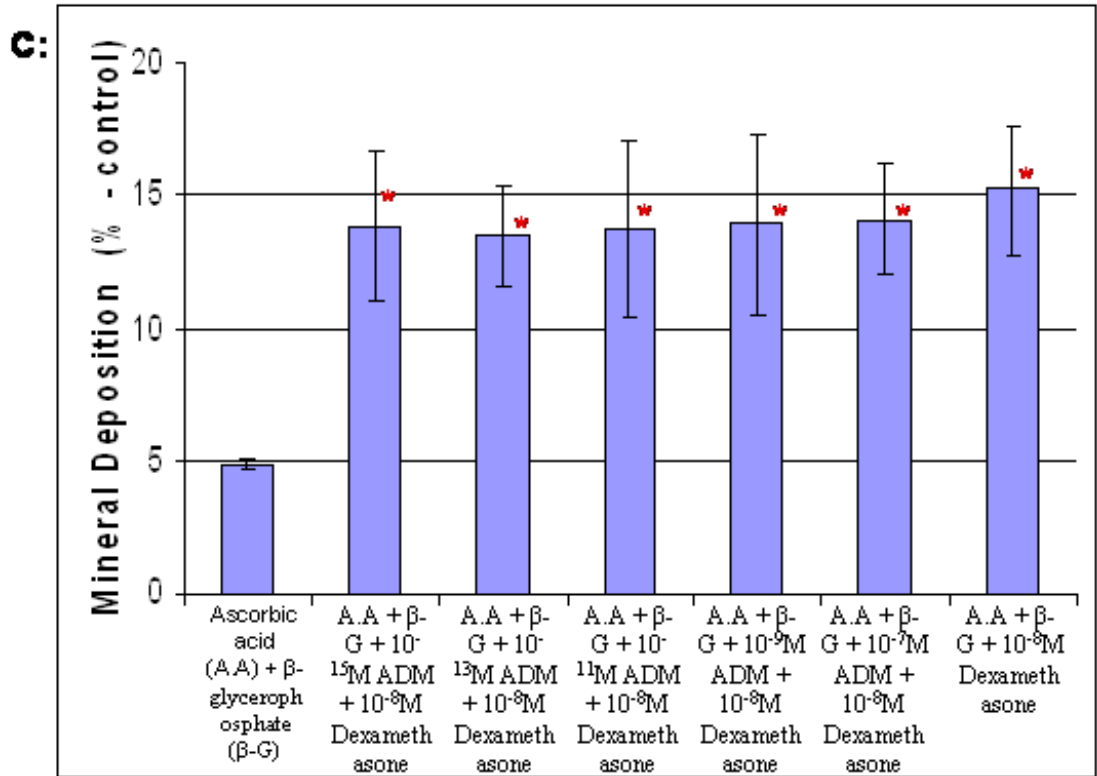
A:**B:**

Figure 5.11: A + C – Mean mineral deposition in OD-21 cells following 21 day treatment with Ascorbic acid (A.A) and β -glycerophosphate (β -G), A.A, β -G and a range of concentrations of ADM (10^{-15} M, 10^{-13} M, 10^{-11} M, 10^{-9} M and 10^{-7} M ADM), A.A, β -G and 10^{-8} M DEX, and A.A, β -G, 10^{-8} M DEX and a range of concentrations of ADM (10^{-15} M, 10^{-13} M, 10^{-11} M, 10^{-9} M and 10^{-7} M ADM). B + D: Representative images of the von Kossa stained cells from which the data presented in A + C was obtained.

*** = statistically significant difference compared to A.A and β -G treatment. * = statistically significant difference compared to A.A, β -G and 10^{-8} M dexamethasone treatment. This experiment was carried out three times.**



A graph is presented in **Figure 5.12** demonstrating the changes in OD-21 cell mineral deposition over the period of 3, 7, 11, 14 and 21 days, following exposure to each pre-described treatment, to provide a summary of the OD-21 cell results presented thus far (**Figures 5.7 – 5.11**).

OD-21 cells exposed to A.A, β -G and a range of concentrations of ADM (10^{-15} M, 10^{-13} M, 10^{-11} M, 10^{-9} M and 10^{-7} M) generally appeared to produce statistically significant increased mineral deposition compared to A.A and β -G exposure alone, from day 11 onwards (**Figure 5.12A**), suggesting that ADM is capable of inducing mineral deposition, indicative of mineralisation, in OD-21 cells. This increase is later than the increases seen in MDPC-23 cells, which increased mineral deposition from day 7 onwards (**Figure 5.6A**). These treatments [A.A, β -G and a range of concentrations of ADM (10^{-15} M, 10^{-13} M, 10^{-11} M, 10^{-9} M and 10^{-7} M)] generally increased mineral deposition in OD-21 cells to similar amounts as the standard mineralising medium (A.A, β -G & 10^{-8} M Dex) up to 14 days exposure, whilst at 21 days exposure there was a significantly larger amount of mineral deposition following treatment with the standard mineralising medium compared to the other treatments [A.A, β -G and a range of concentrations of ADM (10^{-15} M, 10^{-13} M, 10^{-11} M, 10^{-9} M and 10^{-7} M)] (**Figure 5.12A**). This is similar to the pattern of mineralisation observed in MDPC-23 cells (**Figure 5.6A**) suggesting that ADM is capable of inducing a mineral deposition, indicative of mineralisation, at a similar rate to dexamethasone in MDPC-23 cells during the early stages of mineralisation.

In a similar pattern to that observed in MDPC-23 cells, OD-21 cells exposed to the standard mineralising medium plus a range of concentrations of ADM (10^{-15} M, 10^{-13} M, 10^{-11} M, 10^{-9} M and 10^{-7} M) appeared to produce higher amounts of mineral deposition compared to the standard mineralising medium following 7 and 11 days

exposure. Although statistically significant increases were limited to 10^{-15} M and 10^{-13} M ADM after 11 days exposure (**Figure 5.12B**). Following 14 days exposure, treatments supplemented with ADM marginally increased levels of mineral deposition, while at 21 days the standard mineralising medium marginally increased mineral deposition compared to all other treatments (**Figure 5.21B**). Once again, this suggests that when used in coordination with Dex, ADM is capable of producing marginally higher levels of mineral deposition compared to Dex alone during the early stages of mineralisation, an effect that is lost later in the mineralisation process. This could relate to the potential negative feedback effect Dex has on ADM, as discussed in **Section 4.6** and the results surrounding **Figure 5.12**.

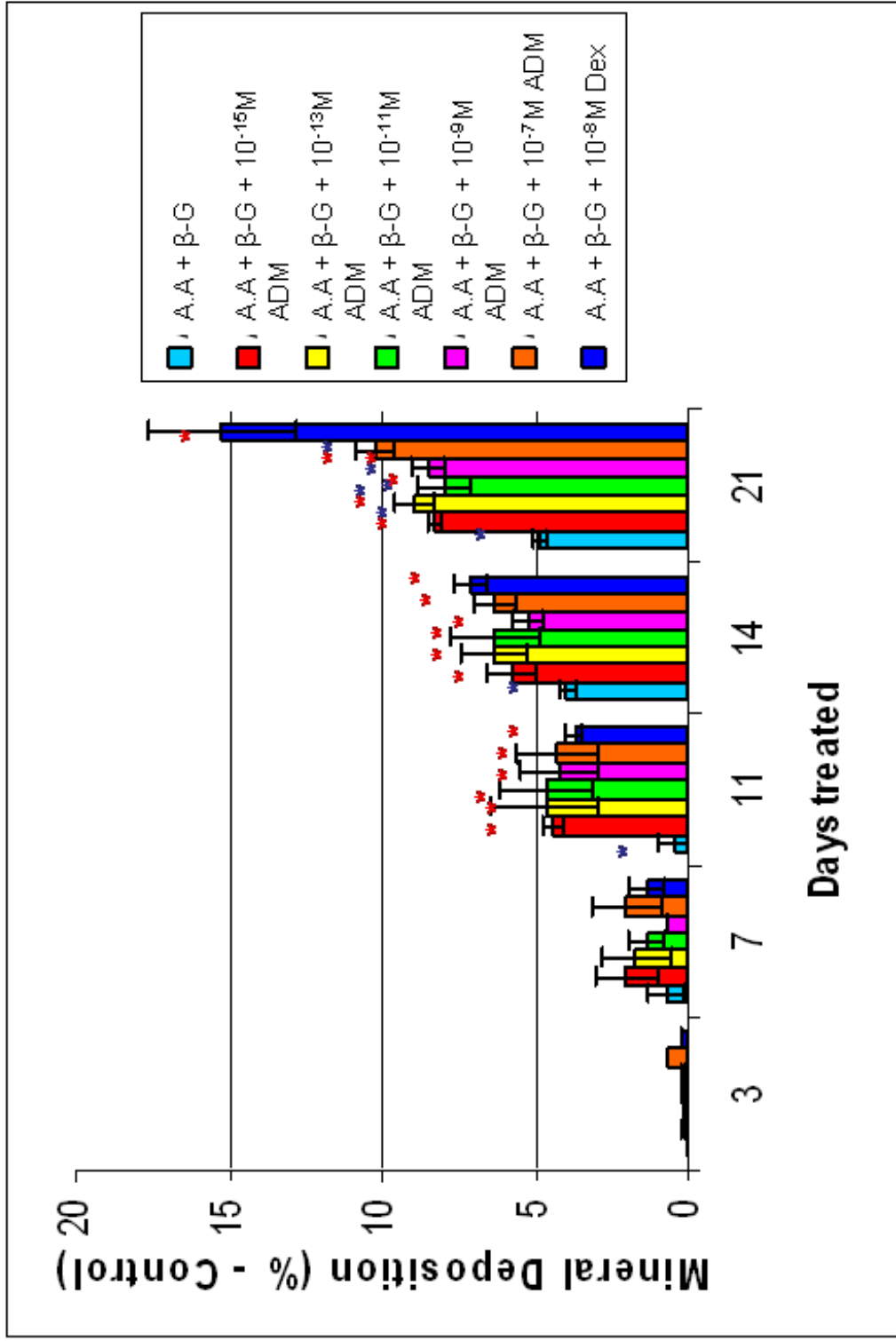
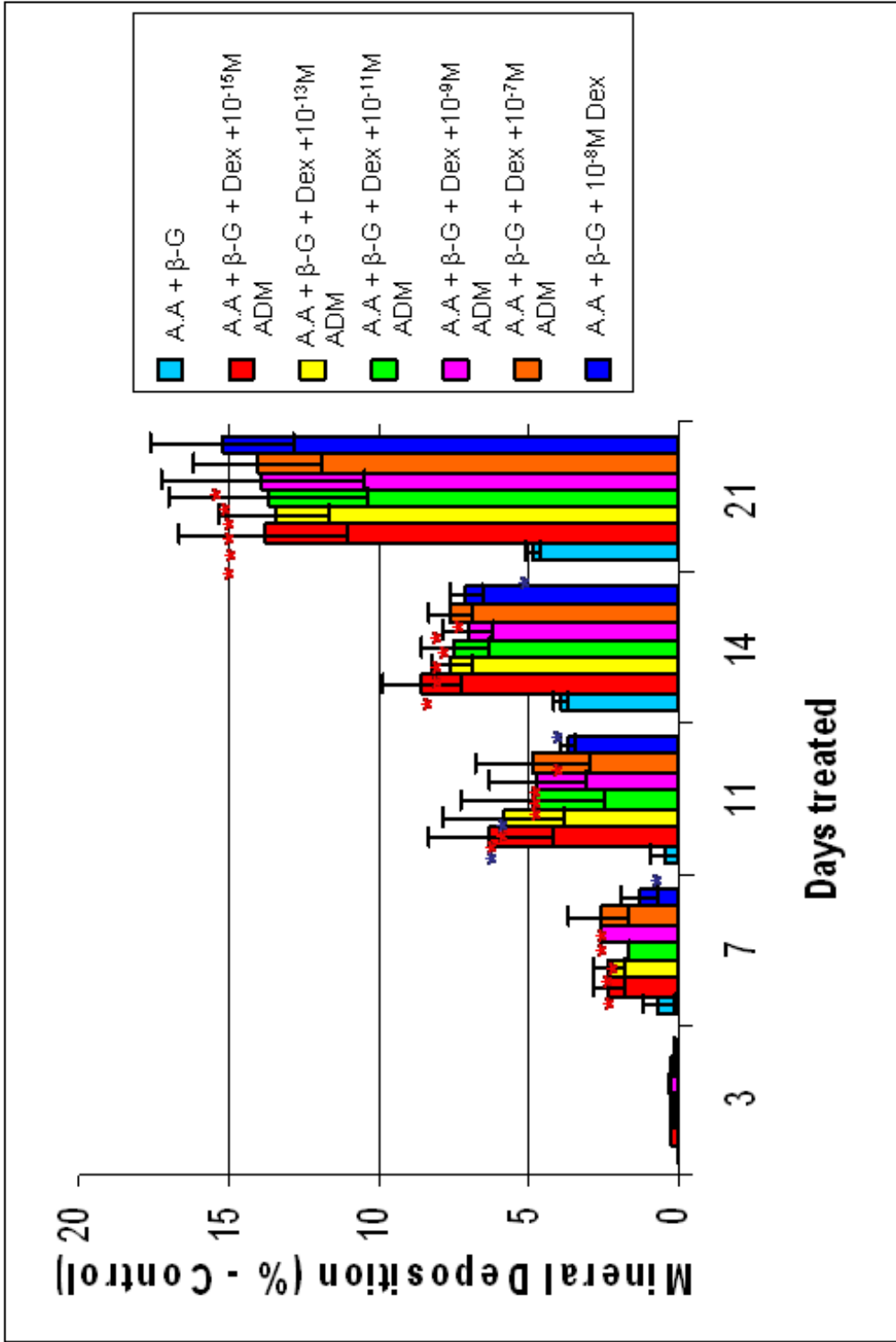


Figure 5.12: Changes in mineral deposition in samples of OD-21 cells treated with A: either 50µg/ml ascorbic acid (AA) and 10mM β-glycerophosphate (β-G), AA, β-G and a range of concentrations of ADM (10^{-15} M, 10^{-13} M, 10^{-11} M, 10^{-9} M and 10^{-7} M) or AA, β-G and 10^{-8} M Dex and B: either AA and β-G, AA, β-G and 10^{-8} M Dex or AA, β-G, 10^{-8} M Dex and a range of concentrations of ADM (10^{-15} M, 10^{-13} M, 10^{-11} M, 10^{-9} M and 10^{-7} M) for 3, 7, 11, 14 and 21 days.

*** = statistically significant difference compared to AA and β-G treated samples. * = statistically significant difference compared to AA, β-G and 10^{-8} M Dex. This experiment was carried out three times.**

B:



5.4 Analysis of mineral deposition in 3T3 fibroblast cultures exposed to ADM

The potential effect of ADM on mineral deposition in 3T3 cultures *in vitro* was determined with von Kossa staining as previously described. Cultures were exposed to a range of conditions for 3, 7, 11, 14 and 21 days, following which, the medium was removed and the cells fixed. Analysis was performed as described previously in **Section 5.2**.

The data for detectable 3T3 culture mineral deposition in response to exposure to the range of treatments described for 3, 7, 11, 14 and 21 days are shown in **Figures 5.13 and 5.14**. The representative images presented in **Figure 5.13** demonstrate that there was very little discernable mineral deposition detected in 3T3 cells following exposure to any treatment. As these cells are derived from a non-mineralising tissue, i.e. skin, it is perhaps not surprising that only minimal amounts of mineral deposition were detected, as compared to the dental cell line cultures.

3 Days exposure:



Ascorbic acid + β - glycerophosph hate	Ascorbic acid + β - glycerophosph ate +10 ⁻⁸ M DEX + 10 ⁻ 19M ADM	Ascorbic acid + β - glycerophosph ate +10 ⁻⁸ M DEX + 10 ⁻ 19M ADM	Ascorbic acid + β - glycerophosph ate +10 ⁻⁸ M DEX + 10 ⁻ 19M ADM	Ascorbic acid + β - glycerophosph ate +10 ⁻⁸ M DEX + 10 ⁻ 19M ADM	Ascorbic acid + β - glycerophosph ate +10 ⁻⁸ M DEX + 10 ⁻ 19M ADM	Ascorbic acid + β - glycerophosph ate +10 ⁻⁸ M DEX
---	--	--	--	--	--	---



Ascorbic acid + β - glycerophosph hate	Ascorbic acid + β - glycerophosph ate +10 ⁻¹⁵ M ADM	Ascorbic acid + β - glycerophosph ate +10 ⁻¹³ M ADM	Ascorbic acid + β - glycerophosph ate +10 ⁻¹¹ M ADM	Ascorbic acid + β - glycerophosph ate +10 ⁻⁹ M ADM	Ascorbic acid + β - glycerophosph ate +10 ⁻⁷ M ADM	Ascorbic acid + β - glycerophosph ate +10 ⁻⁶ M DEX
---	--	--	--	---	---	---

7 Days exposure:

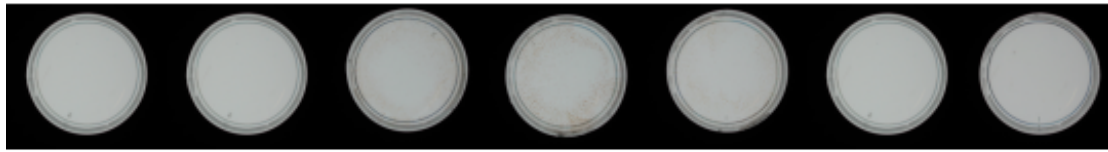


Ascorbic acid + β - glycerophosph hate	Ascorbic acid + β - glycerophosph ate +10 ⁻¹⁵ M ADM	Ascorbic acid + β - glycerophosph ate +10 ⁻¹³ M ADM	Ascorbic acid + β - glycerophosph ate +10 ⁻¹¹ M ADM	Ascorbic acid + β - glycerophosph ate +10 ⁻⁹ M ADM	Ascorbic acid + β - glycerophosph ate +10 ⁻⁷ M ADM	Ascorbic acid + β - glycerophosph ate +10 ⁻⁶ M DEX
---	--	--	--	---	---	---



Ascorbic acid + β - glycerophosph hate	Ascorbic acid + β - glycerophosph ate +10 ⁻⁸ M DEX + 10 ⁻ 19M ADM	Ascorbic acid + β - glycerophosph ate +10 ⁻⁸ M DEX + 10 ⁻ 19M ADM	Ascorbic acid + β - glycerophosph ate +10 ⁻⁸ M DEX + 10 ⁻ 19M ADM	Ascorbic acid + β - glycerophosph ate +10 ⁻⁸ M DEX + 10 ⁻ 19M ADM	Ascorbic acid + β - glycerophosph ate +10 ⁻⁸ M DEX + 10 ⁻ 19M ADM	Ascorbic acid + β - glycerophosph ate +10 ⁻⁸ M DEX
---	--	--	--	--	--	---

11 Days exposure:



Ascorbic acid + β - glycerophosph hate	Ascorbic acid + β - glycerophosph ate +10 ⁻⁸ M DEX + 10 ⁻ 1 ⁹ M ADM	Ascorbic acid + β - glycerophosph ate +10 ⁻⁸ M DEX + 10 ⁻ 1 ⁹ M ADM	Ascorbic acid + β - glycerophosph ate +10 ⁻⁸ M DEX + 10 ⁻ 1 ⁹ M ADM	Ascorbic acid + β - glycerophosph ate +10 ⁻⁸ M DEX + 10 ⁻ 1 ⁹ M ADM	Ascorbic acid + β - glycerophosph ate +10 ⁻⁸ M DEX + 10 ⁻ 1 ⁹ M ADM	Ascorbic acid + β - glycerophosph ate +10 ⁻⁸ M DEX
---	---	---	---	---	---	---



Ascorbic acid + β - glycerophosph hate	Ascorbic acid + β - glycerophosph ate +10 ⁻¹⁵ M ADM	Ascorbic acid + β - glycerophosph ate +10 ⁻¹³ M ADM	Ascorbic acid + β - glycerophosph ate +10 ⁻¹¹ M ADM	Ascorbic acid + β - glycerophosph ate +10 ⁻⁹ M ADM	Ascorbic acid + β - glycerophosph ate +10 ⁻⁷ M ADM	Ascorbic acid + β - glycerophosph ate +10 ⁻⁶ M DEX
---	--	--	--	---	---	---

14 Days exposure:



Ascorbic acid + β - glycerophosph hate	Ascorbic acid + β - glycerophosph ate +10 ⁻¹⁵ M ADM	Ascorbic acid + β - glycerophosph ate +10 ⁻¹³ M ADM	Ascorbic acid + β - glycerophosph ate +10 ⁻¹¹ M ADM	Ascorbic acid + β - glycerophosph ate +10 ⁻⁹ M ADM	Ascorbic acid + β - glycerophosph ate +10 ⁻⁷ M ADM	Ascorbic acid + β - glycerophosph ate +10 ⁻⁶ M DEX
---	--	--	--	---	---	---



Ascorbic acid + β - glycerophosph hate	Ascorbic acid + β - glycerophosph ate +10 ⁻⁸ M DEX + 10 ⁻ 1 ⁹ M ADM	Ascorbic acid + β - glycerophosph ate +10 ⁻⁸ M DEX + 10 ⁻ 1 ⁹ M ADM	Ascorbic acid + β - glycerophosph ate +10 ⁻⁸ M DEX + 10 ⁻ 1 ⁹ M ADM	Ascorbic acid + β - glycerophosph ate +10 ⁻⁸ M DEX + 10 ⁻ 1 ⁹ M ADM	Ascorbic acid + β - glycerophosph ate +10 ⁻⁸ M DEX + 10 ⁻ 1 ⁹ M ADM	Ascorbic acid + β - glycerophosph ate +10 ⁻⁸ M DEX
---	---	---	---	---	---	---

21 Days exposure:

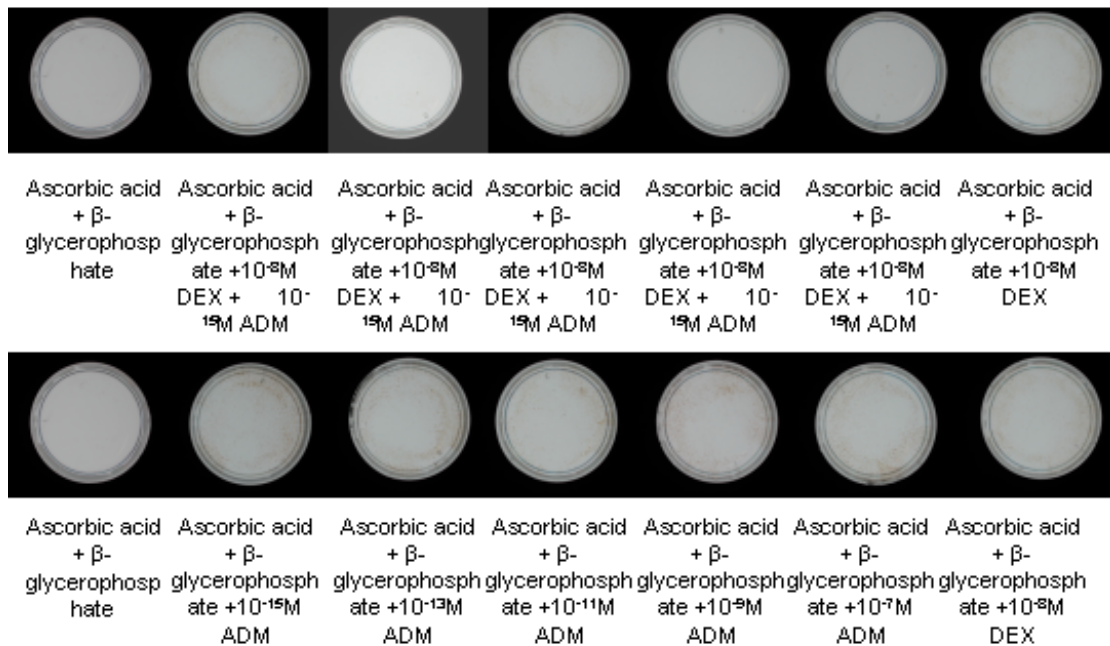


Figure 5.13: Representative images of von Kossa staining of 3T3 cells following exposure to Ascorbic acid (A.A) and β-glycerophosphate (β-G), A.A, β-G and a range of concentrations of ADM (10⁻¹⁵M, 10⁻¹³M, 10⁻¹¹M, 10⁻⁹M and 10⁻⁷M ADM), A.A, β-G and 10⁻⁸M dexamethasone or A.A, β-G, 10⁻⁸M dexamethasone and a range of concentrations of ADM (10⁻¹⁵M, 10⁻¹³M, 10⁻¹¹M, 10⁻⁹M and 10⁻⁷M ADM) for 3, 7, 11, 14 and 21 days.

This experiment was carried out three times.

A:

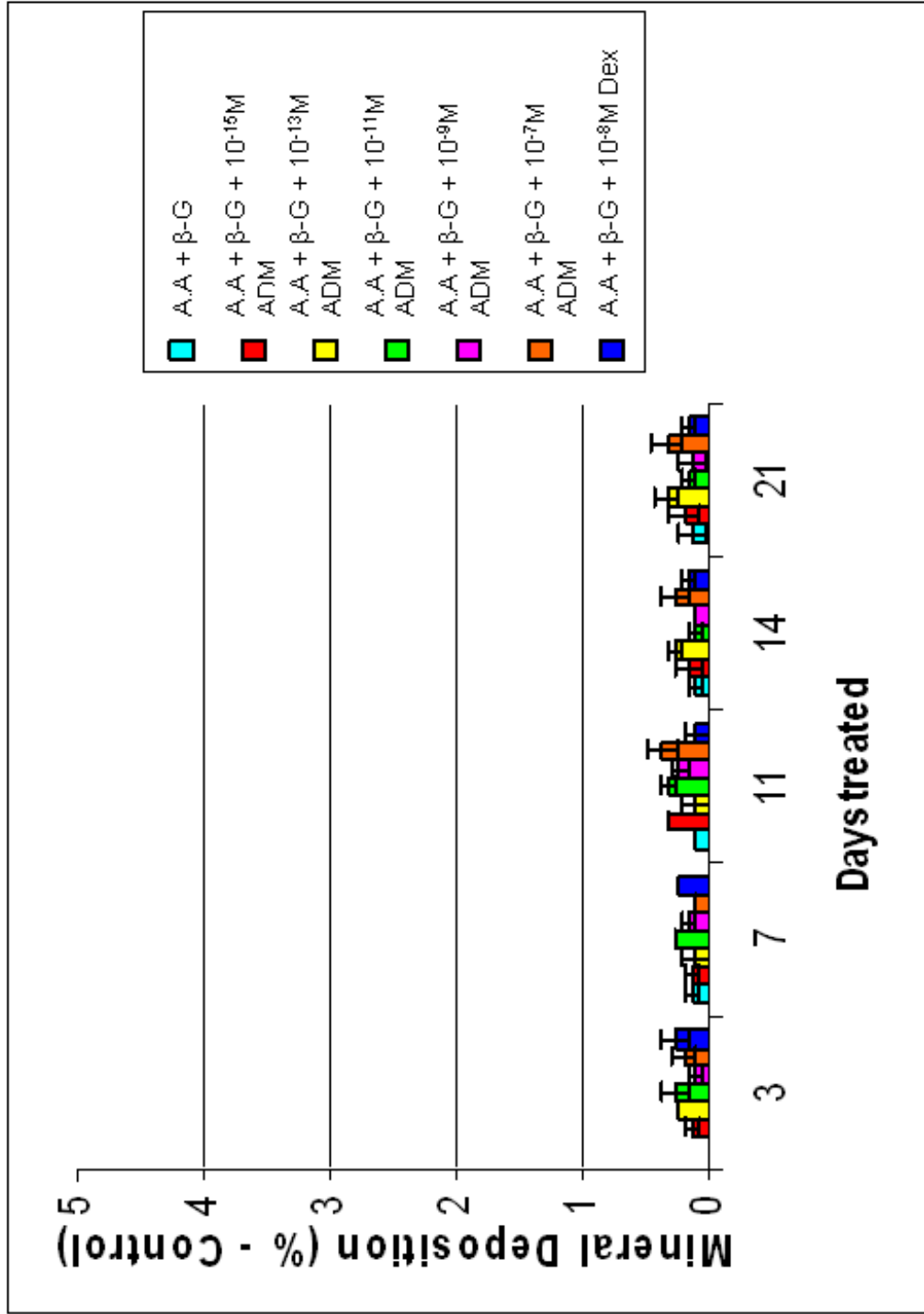
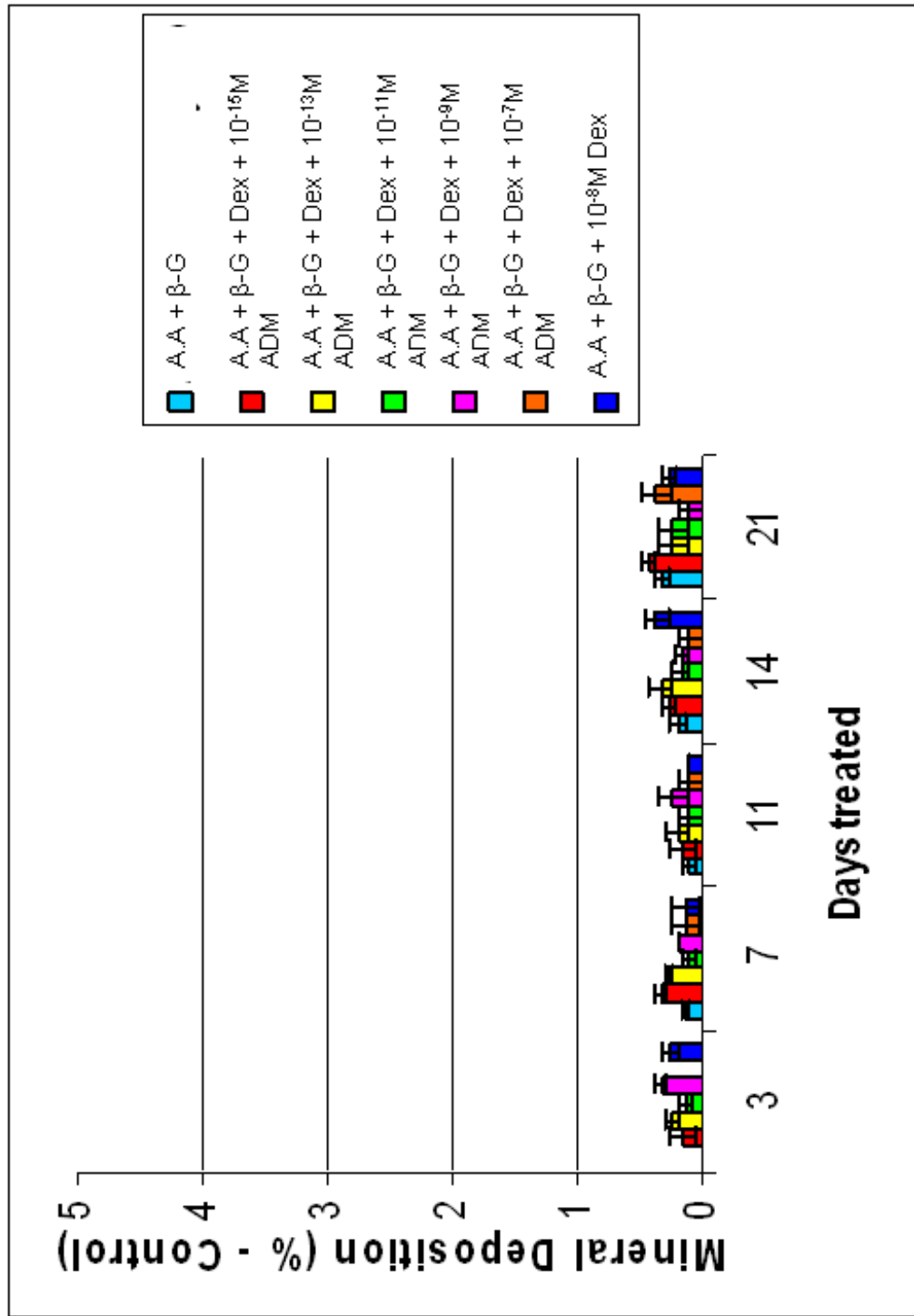


Figure 5.14: Changes in mineral deposition in samples of 3T3 cells treated with A: either 50µg/ml ascorbic acid (AA) and 10mM β-glycerophosphate (β-G), AA, β-G and a range of concentrations of ADM (10^{-15} M, 10^{-13} M, 10^{-11} M, 10^{-9} M and 10^{-7} M) or AA, β-G and 10^{-8} M Dex and B: either AA and β-G, AA, β-G and 10^{-8} M Dex or AA, β-G, 10^{-8} M Dex and a range of concentrations of ADM (10^{-15} M, 10^{-13} M, 10^{-11} M, 10^{-9} M and 10^{-7} M) for 3, 7, 11, 14 and 21 days.

*** = statistically significant difference compared to AA and β-G treated samples. * = statistically significant difference compared to AA, β-G and 10^{-8} M Dex. This experiment was carried out three times.**

B:



6.0 Results Chapter 4

6.1 Systemic administration of ADM to adult male Swiss mice

Previous results indicate that ADM i) is present in the cells responsible for tooth mineralisation (**Chapter 3**), ii) increases developmentally derived dental cell number *in vitro* (**Chapter 4**) and, iii) can promote mineralisation *in vitro* in these dental cell lines (**Chapter 5**). *In vivo*, ADM administration has been demonstrated to increase murine tibia bone length and to increase bone strength (Cornish *et al*, 2001). The following work was therefore performed with the aim of determining whether ADM affects dental and cranio-facial mineralised tissue biology *in vivo*.

To study the *in vivo* effects of ADM on dental and cranio-facial tissues, mice were kindly donated by Professor Cornish from the Bone Research Group at the University of Auckland, New Zealand. Animals had been systemically exposed to ADM with 20 injections of either ADM or saline (sham-treated, controls) over a 4-week experimental period (Cornish *et al*, 1997). Data obtained from these animals had previously demonstrated that ADM increase tibia bone length and strength (Cornish *et al*, 2001). To determine whether ADM affected the hard tissue volume of the teeth and study any changes in cranio-facial bone growth, tooth hard tissue volume was determined using micro-computed Tomography (μ CT) analysis (**Section 2.6**) and key mandibular measurements were determined using digital image analysis (**Section 2.7**), respectively. Briefly, 600 X-ray images were generated from sample murine skulls (see **Figure 6.1A - E** for example images) at 0.6° intervals, to provide full 360° coverage of the region of interest. Images were then converted into 2D bitmap images using CT Reconstruction (CTRecon) computer software (Skyscan, Belgium) (**Figure 6.1F - J**), provided with the μ CT equipment (Skyscan, Belgium). From the 2D bitmap

images, the teeth hard tissue volume was determined by segmented isolation of the tooth hard tissue area on each cross sectional image (**Figures 6.2A - D**), approximately 120 per molar and 215 per incisor. Subsequently, CT analysis (CTan) software (Skyscan, Belgium) was used to calculate the overall tooth volume. Mandible hard tissue volume was measured in a similar manner to tooth hard tissue volume described above, with mandible hard tissue outline isolated in each cross sectional image (**Figures 6.2E & F**), approximately 750 per mandible, and CTan software (Skyscan, Belgium) used to calculate overall mandibular volume. It is also possible to create 3D reconstructions of the mandible using CTRecon (Skyscan, Belgium) (**Figure 6.1K – O**). This is useful for determining morphological changes that may occur as a result of treatment, but lacks accuracy when precise measurements are required.

Measurements of cranio-facial bone length were also determined from macroscopically derived digital images using ImageJ software (downloaded from <http://rsbweb.nih.gov/ij>) analysis for key mandibular parameters, as proposed by Atchley *et al*, (1984), in control and test specimens (see **Sections 2.5 and 2.7** for detailed procedure). The approach used here was comparable to that applied by Cornish *et al*, (1997; 2001) which demonstrated ADM administration enhanced murine tibia bone growth parameters.

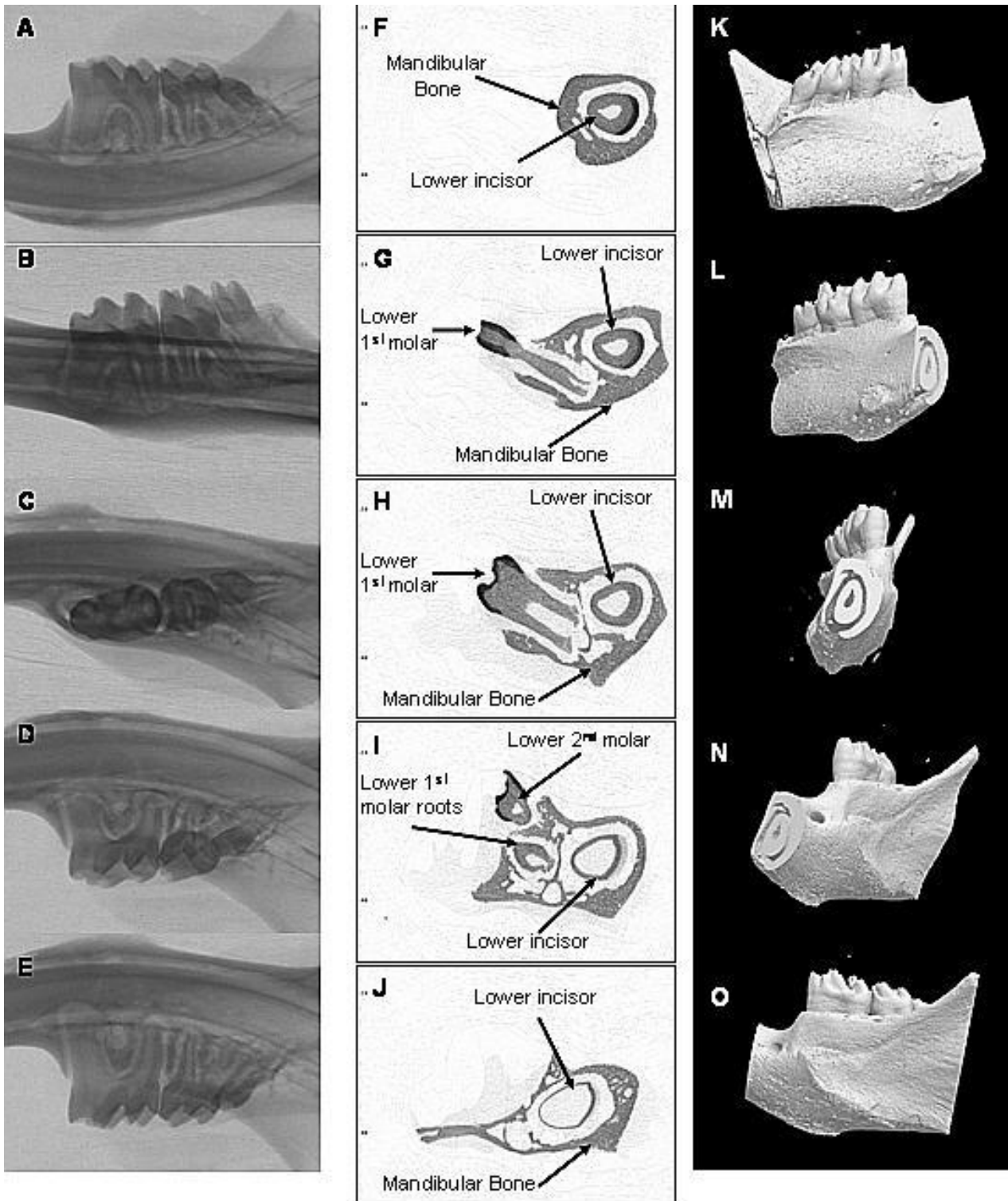


Figure 6.1: A – E: Example x-ray images of mouse mandible obtained on Skyscan 1172 (Skyscan, Belgium). F – J: Progressive 2D cross sectional images of mouse mandible reconstructed using CTrecon software (Skyscan, Belgium) showing the lower incisor, 1st and 2nd molars and the mandible through the axial plane. L – O: 3D reconstruction of mouse mandible obtained using CTrecon software (Skyscan, Belgium).

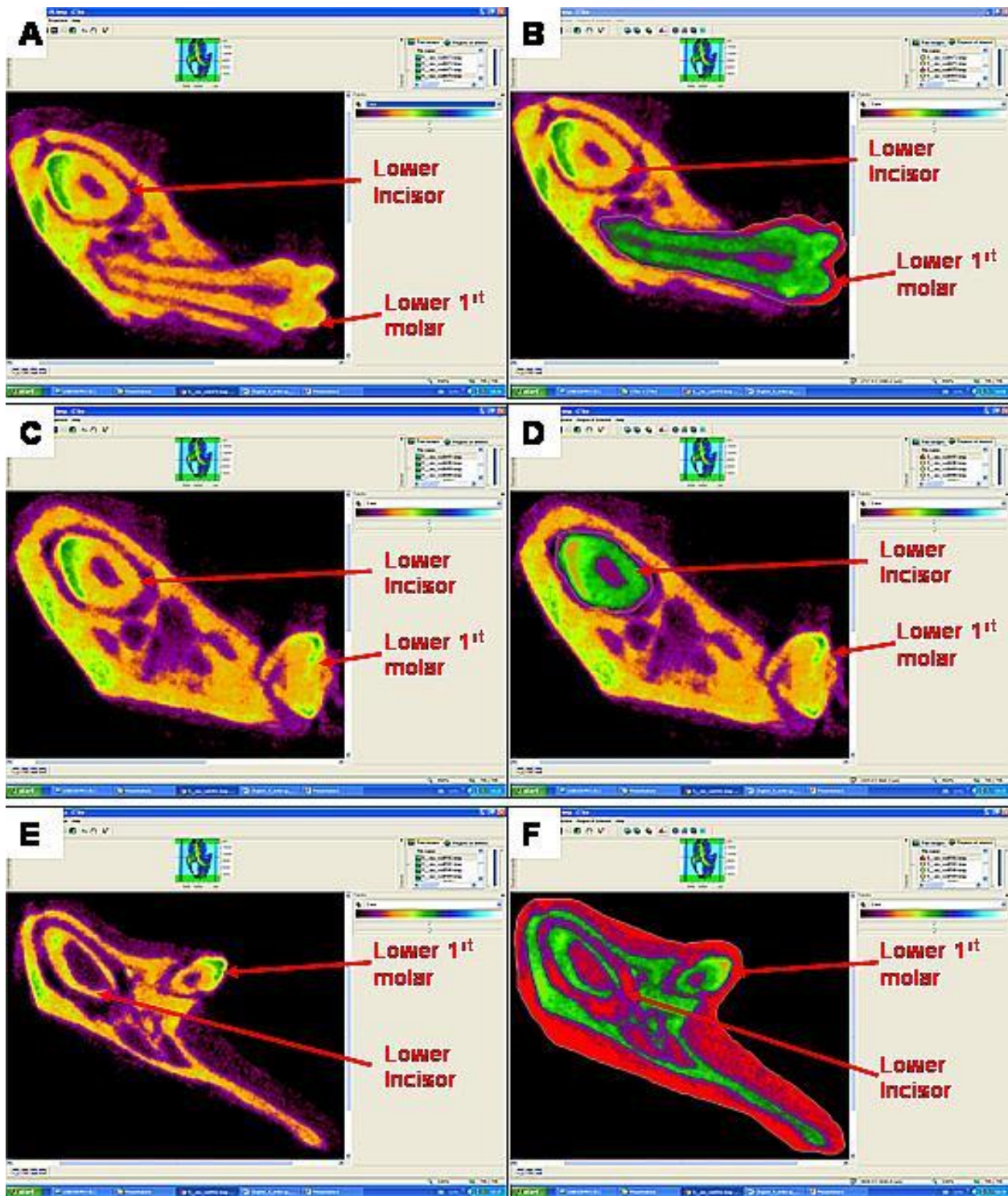


Figure 6.2: Sample pages from CTan software (Skyscan, Belgium) demonstrating the isolation of **A & B:** Mouse 1st Molar. **C & D:** Mouse Lower Incisor. **E & F:** Mouse Mandible hard tissue, for subsequent volumetric measurements. Tissue highlighted in green denotes regions of hard tissue that have been isolated for volumetric measurements.

6.2 Effect of systemic ADM administration on murine molar and lower incisor tooth hard tissue volume

The effect of ADM on tooth hard tissue volume was assessed by determining the volumes of hard tissue in the upper and lower molars and lower incisors of treated and untreated mice, n = 8. Mandible volume was also assessed to study the effect of ADM on cranio-facial bone volume, n = 3.

6.2.1 Effect of systemic ADM administration on murine molar hard tissue volume

Mice exposed to ADM exhibited marginally more hard tissue in their 1st molars than those of mice injected with saline solution (**Figure 6.3A**). The average volume of the ADM treated 1st molars was $13.6\mu\text{m}^3$ whereas the average of the control 1st molars was $12.55\mu\text{m}^3$. This difference, however, was not found to be statistically significant ($P < 0.05$).

Analysis of the 2nd molars of ADM treated and control mice indicated there was little difference in hard tissue volumes of these teeth. The sham treated and ADM exposed animals exhibited no significant ($P < 0.05$) difference in their hard tissue volume with averages of $6.92\mu\text{m}^3$ and $6.9\mu\text{m}^3$, respectively (**Figure 6.3B**). There was a negligible difference in the hard tissue volume of 3rd molars in ADM treated mice compared with those injected with saline solution (**Figure 6.3C**). ADM exposed mice had an average 3rd molar hard tissue volume of $2.39\mu\text{m}^3$ with control mice having a comparable average volume of $2.38\mu\text{m}^3$.

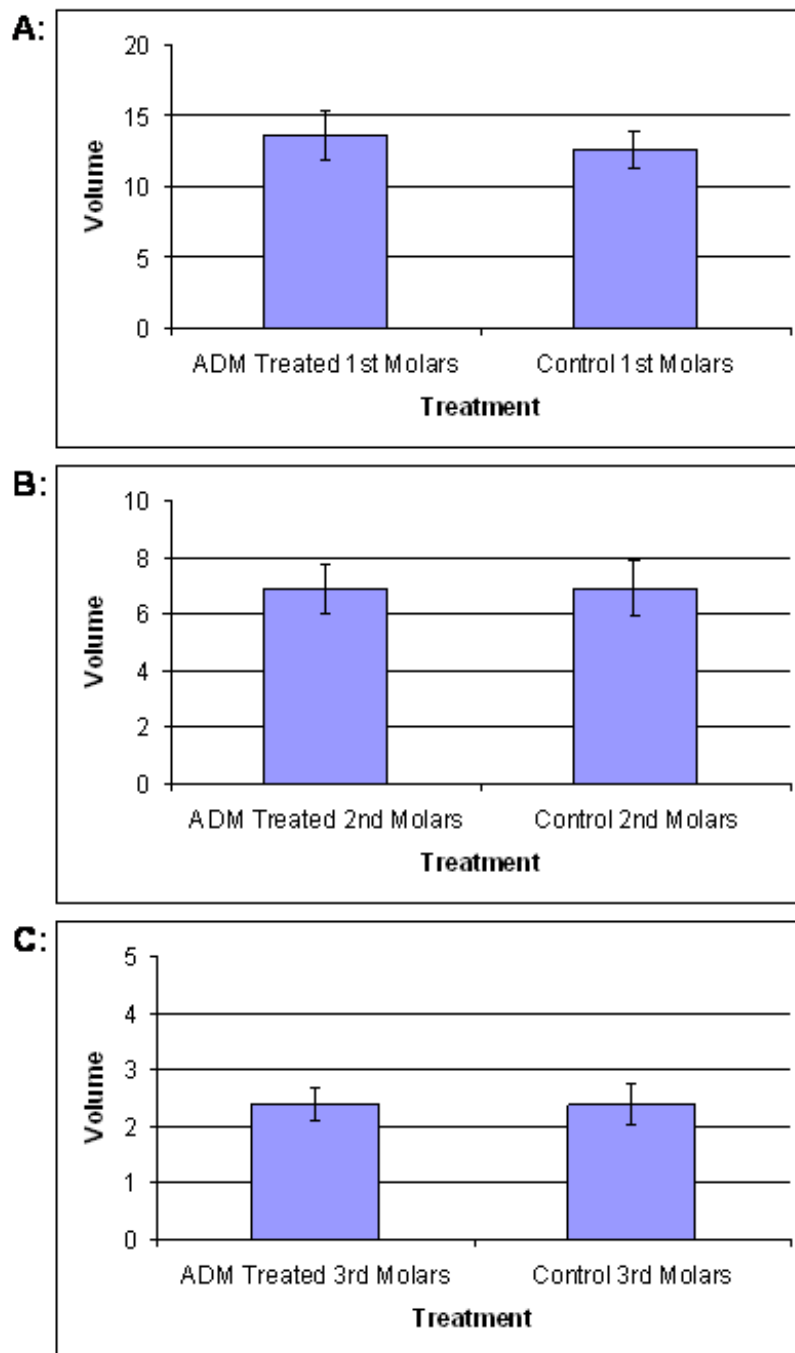


Figure 6.3: Graphical representation of the hard tissue volume (μm^3) measured in both control and ADM treated mice teeth ($n = 8$). ADM treated mice received 20 systemic injections of ADM over a period of 4 weeks, whilst control mice received 20 systemic injections of saline over a period of 4 weeks (See **Section 2.5**). **A:** Comparison of 1st molar hard tissue volume. **B:** Comparison of 2nd molar hard tissue volume. **C:** Comparison of 3rd molar hard tissue volume.

* = statistically significant difference compared to the control samples ($P < 0.05$)

6.2.2 Effect of systemic administration of ADM on murine lower incisor hard tissue volume

No significant differences were observed between the incisor hard tissue volumes of mice that had been exposed to saline solution compared to those exposed to ADM (**Figure 6.4A**). ADM exposed mice had a slightly lower mean incisor hard tissue volume of $46.2\mu\text{m}^3$, whilst the mean lower incisor hard tissue volume of the saline treated mice was $46.3\mu\text{m}^3$. This difference, however, was not found to be statistically significant ($P<0.05$).

6.2.3 Effect of systemic administration of ADM on total dentition hard tissue volume in mice

The mean hard tissue volume of all the teeth in the mice exposed to ADM was slightly higher than in the mice exposed to saline solution (**Figure 6.4B**). The ADM treated dentition hard tissue volume mean was $7.63\mu\text{m}^3$ compared to $7.29\mu\text{m}^3$ in the sham treated samples. This difference was also not found to be statistically significant ($P<0.05$).

6.3 Effect of systemic administration of ADM on murine mandible hard tissue volume

The mean mandible hard tissue volume of mice exposed to ADM was lower than that of sham control mice (**Figure 6.4C**). ADM treated mandibles exhibited a hard tissue volume of $219.27\mu\text{m}^3$ compared to sham treated mandibles measuring $221.1\mu\text{m}^3$. This difference was not found to be significant ($P<0.05$).

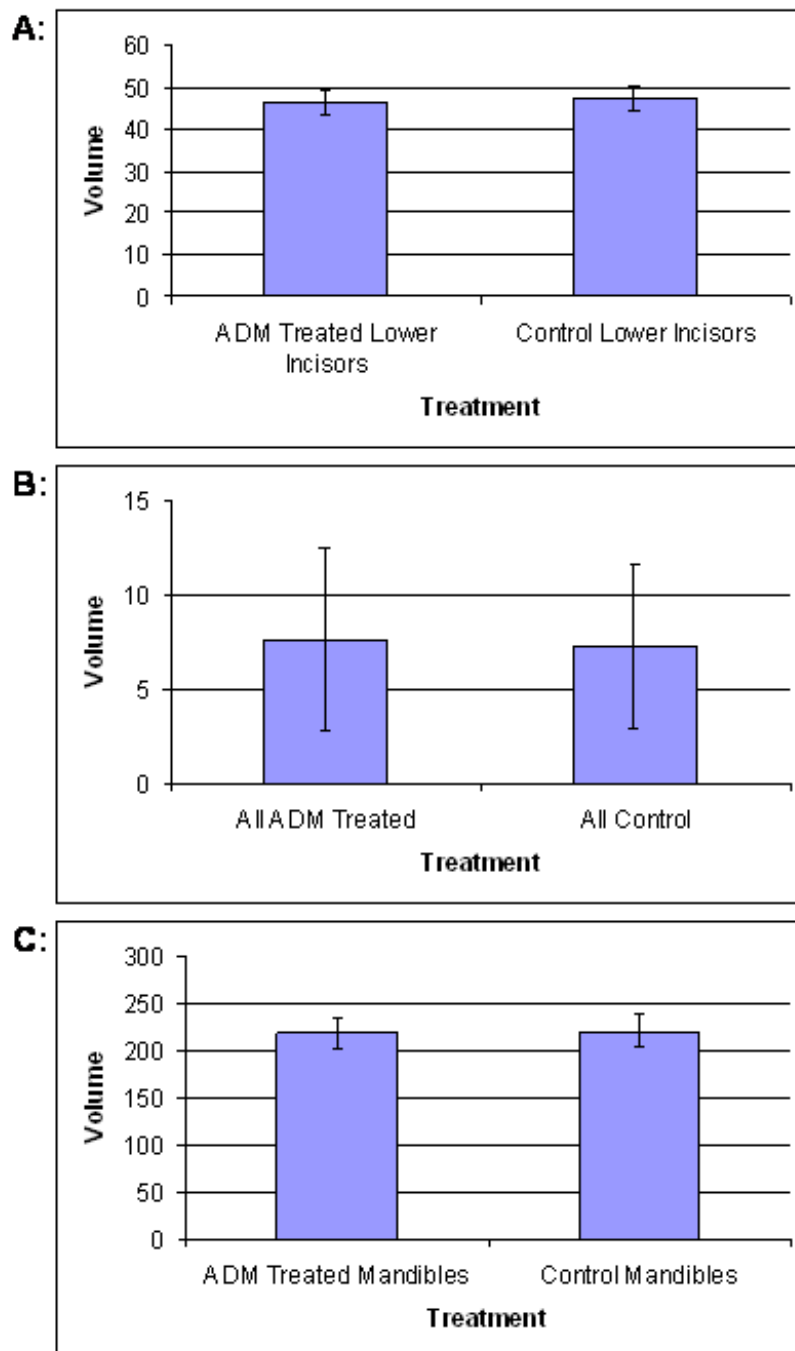


Figure 6.4: Graphical representation of the hard tissue volume (μm^3) measured in both control and ADM treated mice teeth ($n = 8$) and mandibles ($n = 3$). ADM treated mice received 20 systemic injections of ADM over a period of 4 weeks, whilst control mice received 20 systemic injections of saline over a period of 4 weeks (See section 2.5). **A:** Comparison of lower incisor hard tissue volume. **B:** Comparison of all dentition hard tissue volume. **C:** Comparison of mandible hard tissue volume.

* = statistically significant difference compared to the control samples ($P < 0.05$)

6.4 Effect of systemic administration of ADM on key murine mandibular measurements

The effect of systemic administration of ADM on murine mandible growth was assessed as previously described (see **Sections 2.5, 2.6 and 6.1**). Examples of digital images used for analysis are shown in **Figures 6.5A and 6.6A**.

6.4.1 Effect of systemic administration of ADM on mandibular corpus measurements

For measurement 1 (denoted by arrow 1 in **Figure 6.5A**) ADM treated mice did not show statistically significant differences ($P < 0.05$) in length compared to those of the sham control mice, averaging 1.25cm and 1.26cm, respectively (**Figure 6.5C**).

The length of measurement 2 (denoted by arrow 2 in **Figure 6.5A**) was marginally lower following systemic treatment with ADM compared to the control samples (**Figure 6.5D**). This measurement in ADM exposed mice averaged 0.96cm compared to the control mice averaging 0.97cm. The difference was also not found to be statistically significant ($P < 0.05$).

6.4.2 Effect of systemic administration of ADM on mandibular ramus and alveolar process measurements

Mice that were systemically treated with ADM had an average alveolar process length (denoted by arrow 3 in **Figure 6.5A**) of 325mm, which was not statistically significantly different ($P < 0.05$) from that found in sham treated samples which had an average alveolar process length of 323mm (**Figure 6.5E**).

The average length of measurement 4 (as denoted by arrow 4 in **Figure 6.5A**) from the samples systemically treated with ADM was marginally higher than the

average length of those treated with a saline solution, averaging 0.9 and 0.88cm, respectively (**Figure 6.5F**). This difference was also not statistically significant ($P < 0.05$).

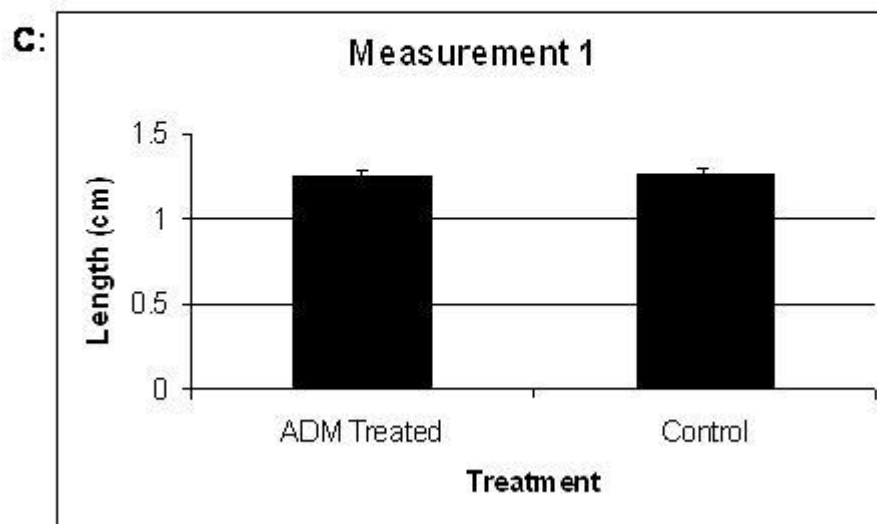
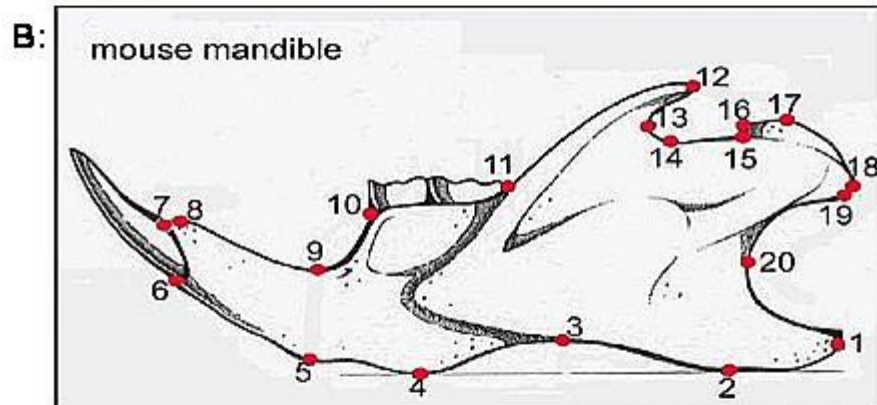
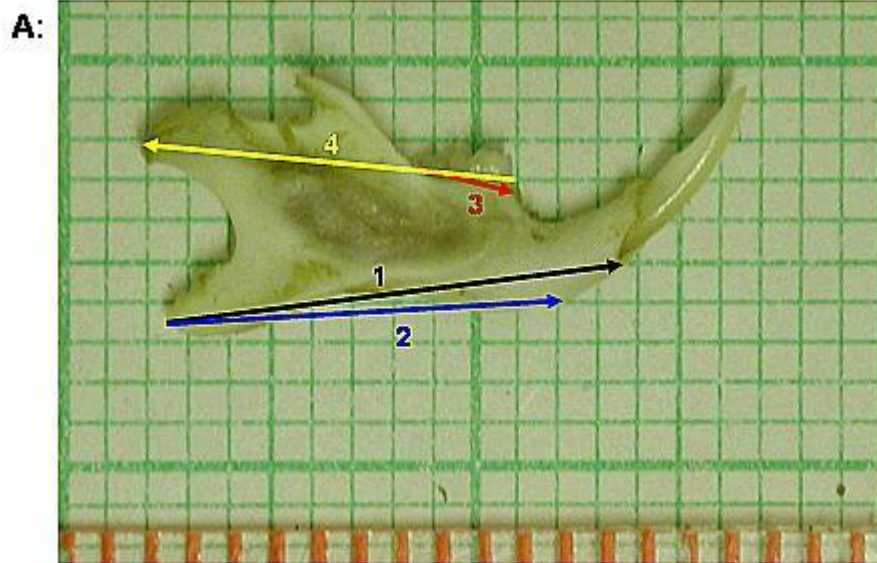
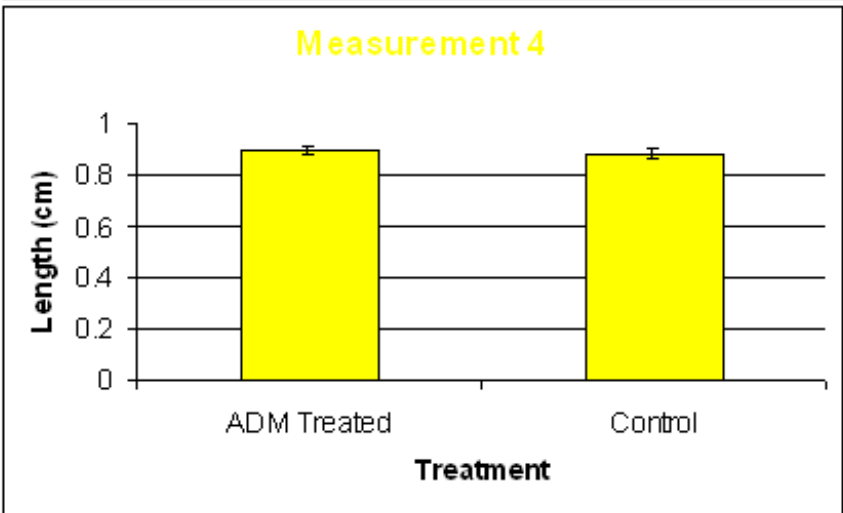
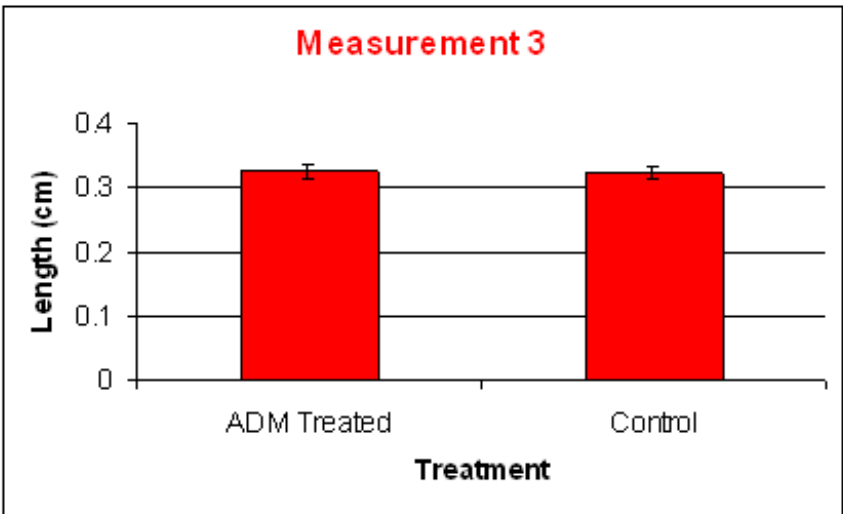
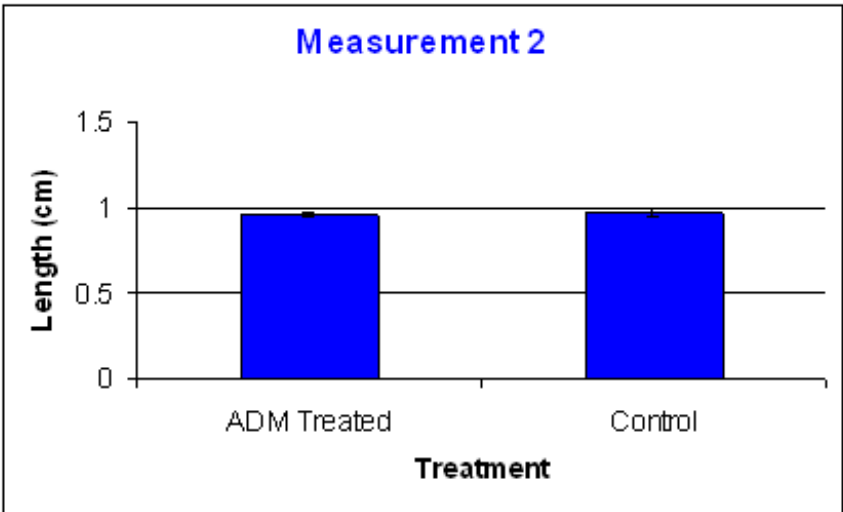


Figure 6.5: **A:** Image indicating the key mandibular lengths measured. **B:** Adaption of the key points from which measurements were taken (Atchley *et al*, 1984). **C-F:** Graphical representation of comparison between key mandibular measurements in mice systemically treated with ADM and mice systemically treated with saline solution over a period of four weeks. **C:** Comparison of measurement 1 highlighted in **A**. **D:** Comparison of measurement 2 highlighted in **A**. **E:** Comparison of measurement 3 highlighted in **A**. **F:** Comparison of measurement 4 highlighted in **A**. N = 10.

* = statistically significant difference ($P < 0.05$)



6.4.3 Effect of systemic administration of ADM on mandibular ramus and condylar measurements

Mice that had been systemically treated with ADM for four weeks had an mean ramus length (as denoted by arrow 1 in **Figure 6.6A**) of 0.58cm. This value was not statistically significantly different ($P<0.05$) from the mean length determined for the sham mice (**Figure 6.6C**).

The differences in measurement 2 (as denoted by arrow 2 in **Figure 6.6A**) between mice systemically treated with ADM and those treated with a saline solution, was found to be negligible. Values for ADM treated mice were not statistically significantly different ($P<0.05$) from those for control mice with this measurement, averaging 270mm compared to 260mm in sham treated animals (**Figure 6.6D**).

The average length of measurement 3 (as denoted by arrow 3 in **Figure 6.6A**) for mice systemically treated with ADM was statistically significantly higher than for those treated with saline solution ($P<0.05$). Values for ADM treated mice measured 432.5mm compared to 400mm measured in saline treated samples (**Figure 6.6E**).

Mice that were systemically exposed to ADM had a marginally higher average for measurement 4 (as denoted by arrow 4 in **Figure 6.6A**) than sham mice (**Figure 6.6F**). The mean length for this measurement in ADM exposed animals was 580mm compared to 550mm in the sham control group. This was not a statistically significant difference ($P<0.05$).

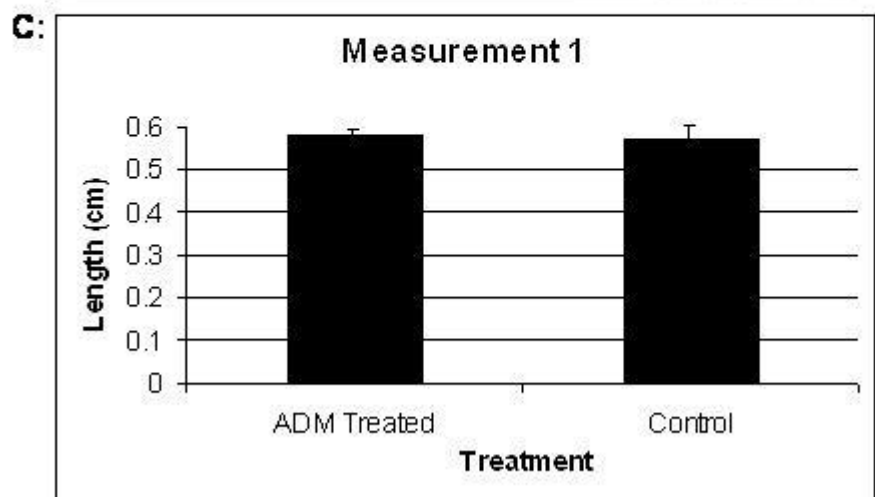
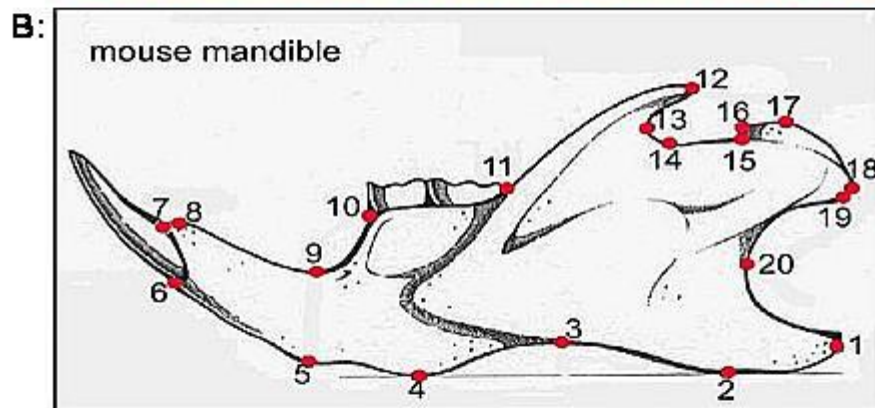
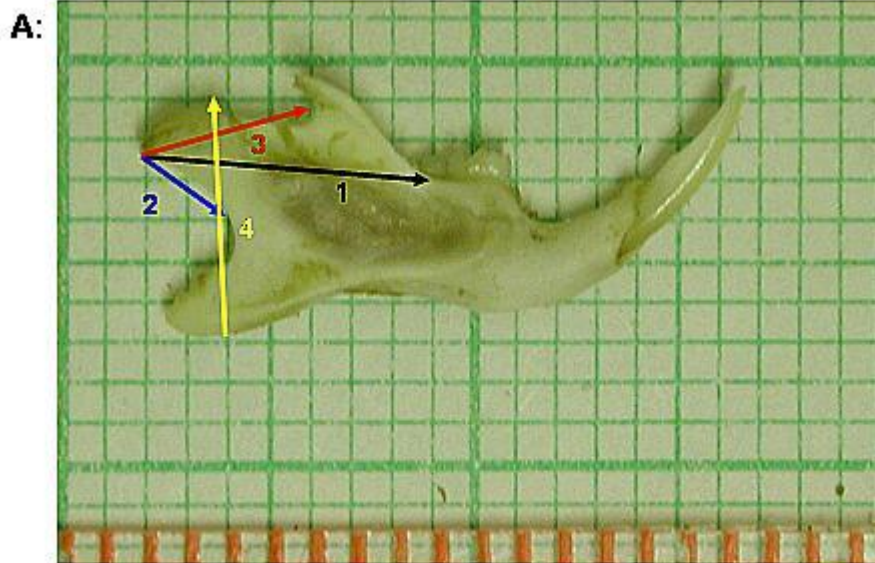
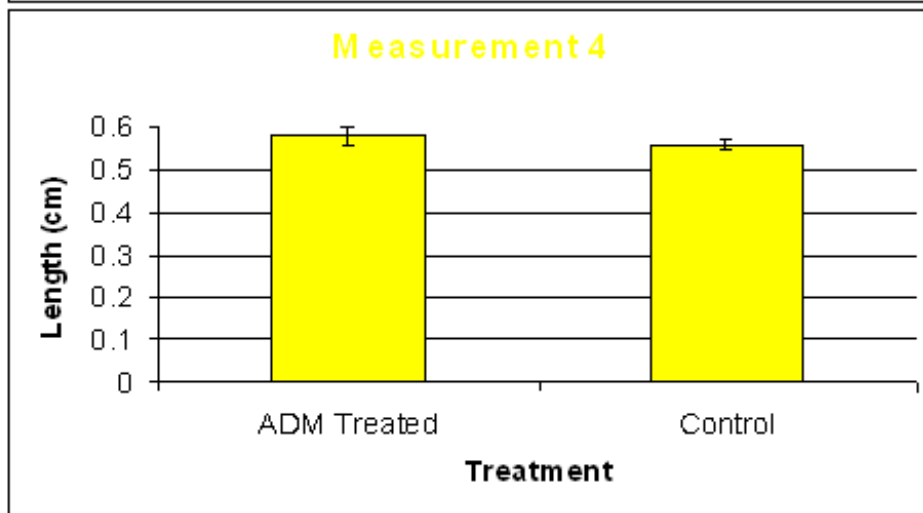
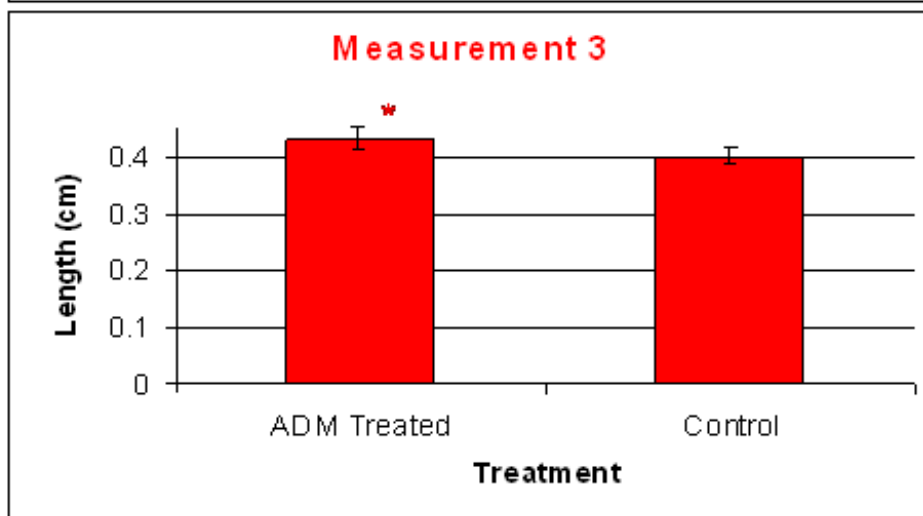
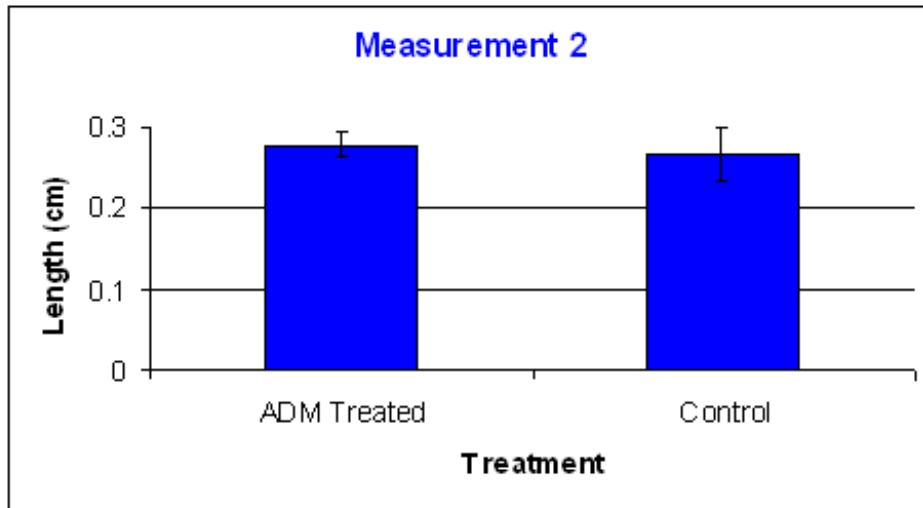


Figure 6.6: **A:** Image indicating the key mandibular lengths measured. **B:** Adaption of the key points from which measurements were taken (Atchley *et al*, 1984). **C-F:** Graphical representation of comparison between key mandibular measurements in mice systemically treated with ADM and mice systemically treated with saline solution over a period of four weeks. **C:** Comparison of measurement 1 highlighted in **A**. **D:** Comparison of measurement 2 highlighted in **A**. **E:** Comparison of measurement 3 highlighted in **A**. **F:** Comparison of measurement 4 highlighted in **A**. N = 10.

* = statistically significant difference (P<0.05)



7. Discussion

Recently, preliminary data has indicated the presence of ADM in the odontoblasts of a mouse developing tooth bud at E13 (Monuenga *et al*, 1997) and an immunohistochemical study has demonstrated similar temporo-spatial patterns of expression between ADM and TGF- β 1, a growth factor known to play a key role in tooth development, in the heart, lungs, kidney, skeletal forming tissues and neural system during mouse embryogenesis (Montuenga *et al*, 1998). Furthermore, in osteoblasts, cells which share many structural and functional similarities to odontoblasts, data demonstrates that ADM increases proliferation *in vitro* (Cornish *et al*, 1997; Cornish *et al*, 2001) and can promote mineralised bone volume and strength *in vivo* (Cornish *et al*, 1997; Cornish *et al*, 2001). This has lead to the hypothesis that ADM may play a key role in tooth development.

In this study, immunohistochemical analysis created novel data highlighting the expression of ADM in the developing tooth bud of rats over three developmental ages (E16, E18 and E20), during which key stages of tooth development occur. Particularly interesting was the expression of ADM in the cells responsible for signalling odontoblast differentiation and subsequently in secretory odontoblasts. This novel data goes some way to explaining the presence of ADM in dentine matrix proteins as it is expressed by secretory odontoblasts and subsequently it is likely to be deposited into the dentine matrix during dentinogenesis. Furthermore, this study demonstrated that TGF- β 1 was expressed in the odontoblasts of developing rat teeth at the E20 embryonic stage of development, the same temporo-spatial expression as ADM.

In vitro analysis demonstrated the expression of calcitonin receptor-like receptor (CRLR) and receptor activity modifying protein-2 (RAMP-2), which as a dimer forms an ADM receptor, in the developmentally derived dental cell lines, MDPC-23 and OD-21. In these cells ADM stimulated a biphasic response in dental cell growth with peak stimulation at 10^{-11} M, with a similar biphasic response in dental cell growth observed following exposure to DMPs and dexamethasone. Furthermore, ADM demonstrated an ability to promote mineral deposition that is indicative of mineralisation in dental cells at levels comparable to that of the known mineralising agent dexamethasone. However, analysis of tooth hard tissue volume and key mandibular measurements in Swiss mice systemically treated with ADM using techniques including micro-Computer Tomography did not identify significant differences in craniofacial mineralised tissue structures compared to sham treated controls.

Histological analysis of ADM and TGF- β 1 in developing rat dentition

Initially, a histological study was undertaken to determine the key stages of tooth development present in the Wistar rats used in the study. Given the difficulty distinguishing between these stages, which are present as a continuum, due to the often overlapping histological features, all developmental stages stated in this study were used as a guide.

The results from the histological observations and the measurement studies undertaken (**Section 3.2**) indicate that the Wistar rats developing 1st molars used in this study were approximately at the bud stage at age E16 (**Figure 3.1A & B**), cap stage by age E18 (**Figures 3.2D – I**) and subsequently demonstrated histological features of both cap and bell stages by age E20 (**Figure 3.3D – F**). In contrast the

developing incisors of the Wistar rats used in this study were at the cap stage at age E16 (**Figure 3.1C**), appeared to be in transition from cap to bell stages at E18 (**Figure 3.2A – C**) and almost entirely at the bell stage by E20 (**Figure 3.3A – C**). These data correspond with histological evidence previously published (Thesleff *et al*, 2003; Tucker and Sharpe, 2004) and suggest that key stages of tooth development, i.e. pre- and post-odontoblast differentiation, have been successfully identified for the immunohistochemical studies undertaken to more specifically describe the tempo-spatial expression of ADM during rat dentition development.

The positive control staining observed for ADM in rat heart tissue demonstrated that the ADM antibody utilised in this study was binding the correct epitope and therefore would provide reliable data in the rodent dentition analysis (**Figure 3.4A**) (Jougasaki *et al*, 1995). The reduction in positive staining observed following the pre-incubation of an ADM peptide with the ADM antibody (ADM blocking control) and a TGF- β 1 peptide with the TGF- β 1 antibody (TGF- β 1 blocking control) (**Figure 3.4B, 3.6C 3.7B & 3.7D**) also supported that fact that the positive staining observed was due to specific antigen binding. The absence of apparent immunoreactivity following incubation with the pre-bleed rabbit serum and in the absence of antibodies (negative sections) further supports the validity of the data obtained, as no significant background staining was observed.

Analysis of the developing rat dentition indicated immunoreactivity for ADM was initially isolated to the epithelial cells of the developing incisor in Wistar rats, which is perhaps unsurprising given that ADM expression has been demonstrated in a number of epithelial tissues, including bronchioles, skin and oral epithelium (Huttner and Bevins, 1999; Kapas *et al*, 2001; Kapas *et al*, 2001). ADM's prominent expression in epithelial cells is thought to be related to ADM's inflammatory

regulation properties (Elsasser and Kahl, 2002). Notably, immunoreactivity was observed in the internal dental epithelial cells during cap and early bell stage (ages E16 & E18) (**Figures 3.5 & 3.6**) and the cells of the external dental epithelium and oral epithelium were also positively stained for the presence of ADM during the cap stage of development (E16) (**Figure 3.5**). At the developmentally later bell stage of development (E20) the cells responsible for hard tissue formation (secretory odontoblasts and ameloblasts) were clearly visible and both exhibited positive staining for ADM (**Figure 3.7**). Notably these cells were also immunopositive to the TGF- β 1 antibody (**Figure 3.7C**), data which is consistent with that previously published (Vaahtokari *et al*, 1991; Begue-Kirn *et al*, 1994). This result demonstrates the presence of TGF- β 1 in the same developmental regions of the tooth as ADM at this key developmental stage when dentine and enamel is deposited. Furthermore, *in vitro* studies have demonstrated that TGF- β 1 and ADM can act to suppress each others expression (Huang *et al*, 2006), while *in vivo* studies in TGF- β 1 null mutant mice demonstrated a reduction in embryonic ADM expression in a number of developing tissues, including heart, lung, liver, kidney and chondrocytes (Bodegas *et al*, 2004). This previously published data indicates the existence of an inter-relationship between the two molecules and the possibility that there may be functional redundancy in the roles that these growth factors play. The novel data presented in this study showing the co-expression of ADM and TGF- β 1 in secretory odontoblasts explains their subsequent presence in dentine matrix proteins (Tomson *et al*, 2007; Graham, 2007).

The potential to initiate development of the tooth bud resides in the cells of the first arch epithelium prior to E12-13 in mice (Koller and Fisher, 1980; Mina and Koller, 1987; Lumsden, 1988), after which point the potential is assumed by the

ectomesenchyme (Koller and Fisher, 1980; Mina and Koller, 1987; Lumsden, 1988). ADM expression appears limited to epithelial cells post-E16 in Wistar rats (**Section 3.3**). As potential to initiate tooth development would likely reside in the mesenchymal cells at this time point (Koller and Fisher, 1980; Mina and Koller, 1987; Lumsden, 1988) this suggests that ADM may not be involved in the initiation of tooth development. However, a further immunohistochemical study into the expression of ADM in the developing rat jaw from E10 – E15 would be required to determine whether ADM likely plays a role in the initiation of tooth development. While an immunohistochemical study of both ADM and TGF- β 1 in developing teeth over a greater range of embryonic ages would better characterise ADM's potential inter-relationship with TGF- β 1.

Initiation of odontoblast differentiation is controlled by the inner dental epithelium and occurs in a well-defined temporo-spatial pattern (Lesot *et al*, 1994; Ruch *et al*, 1995; Smith and Lesot, 2001). ADM is demonstrably present in these cells during the approximate time of odontoblast differentiation (transition from cap to bell stage) (**Figure 3.6**) and in mature odontoblasts secreting dentine (**Figure 3.7**). This study has to some degree provided further supporting data indicating that TGF- β 1 shares the same spatial expression pattern as ADM at age E20 in the developing rat dentition (**Figure 3.7C**) as previous studies have also demonstrated TGF- β 1 is present in the inner dental epithelium at the onset of odontoblast differentiation (Vaahtokari *et al*, 1991; Heikinheimo *et al*, 1993; Begue-Kirn *et al*, 1994) the same time-point at which ADM is also expressed. Given that ADM has well characterized pleiotropic properties, demonstrating both pro- and anti-inflammatory properties (Elsasser and Kahl, 2002), being both antiapoptotic and proapoptotic depending on cell type (Filippatos *et al*, 2001), has demonstrated an ability to dose dependently enhance

astrocyte migration (Xia *et al*, 2004), is upregulated in carious teeth (McLachlan *et al*, 2002), can induce osteoblastic activity (Cornish *et al*, 1997) and appears to share potentially similar temporo-spatial patterns of expression to TGF- β 1, which is able to stimulate odontoblast differentiation and secretion of dentine extracellular matrix (Begue-Kirn *et al*, 1992; Ruch *et al*, 1995), it is reasonable to propose that ADM could be involved in signalling similar dentinogenic events both developmentally and potentially post-natally. There are a several lines of possible study that could be applied to aid elucidation of ADM's role(s) in development of the dentition and craniofacial structures. *In vivo* experimentation could be carried using genetically modified ADM mutant mice. While ADM^{-/-} mice are embryonically lethal, ADM^{+/-} mice are fertile and viable (Ando and Fujita, 2003). A simple histological examination comparing the developing dentition in ADM^{+/-} mice and the developing dentition of control mice would highlight whether a deficiency of ADM resulted in developmental deformities. Similar approaches have been utilised to study members of the TGF- β family (D'Souza and Litz, 1995; Letterio and Roberts, 1996; Atti *et al*, 2002), BMPs (Bandyopadhyay *et al*, 2006; Retting *et al*, 2009) and FGFs (Naganawa *et al*, 2008), and may provide information as to whether ADM is involved in key stages of tooth development. Furthermore, immunohistochemical analysis or *in situ* hybridisation comparing the developing dentition of ADM^{+/-} mice and control mice could also be performed to determine whether a deficiency of ADM affects the presence and expression levels of other key growth and transcription factors known to play a role in tooth development. Such data would increase our knowledge of the interactions ADM may be involved in during this process.

Other *in vivo* studies that would aid further elucidation of ADM's role in the development of the tooth could include the preparation of type V cavities in rodent

teeth (as discussed in **Section 1.10.1**) followed by localised administration of ADM. Similar studies have been performed using bone sialoprotein and BMP-7 which have shown their regenerative potential (Goldberg *et al*, 2001).

The ability of ADM to stimulate extracellular secretion could also be determined using an *ex vivo* organ culture model examining tooth slices. A similar approach to that previously utilised to demonstrate the ability of TGF- β 1 and -3 isoforms and BMP-7 to induce predentine extracellular secretion in rat incisors could conceivably be applied (Sloan and Smith, 1999; Sloan *et al*, 2000). *In vitro* analyses to study ADMs role in dental tissue development could involve the use of primary dental pulp cells or even dental pulp stem cells. A significant number of studies have utilised such approaches to study the ability of growth factors and dentine matrix extract administration on the ability of these cells to differentiate into odontoblasts and produce mineralised ECM (Iohara *et al*, 2004; Huojia *et al*, 2005; Liu *et al*, 2005; Almushayt *et al*, 2006; He *et al*, 2008), this indicates the potential utility of similar experimental approaches to characterize ADM activity.

Whilst these approaches are primarily methods for characterizing the post-natal effects of growth factors, such knowledge using these models would be extremely valuable as they may signify the likelihood of ADM's role in development, as the process of stem cell recruitment, odontoblast differentiation and the induction of dentine secretion from the new generation odontoblasts are thought to closely mimic those of tooth development (Smith and Lesot, 2001).

ADM related transcript expression in dental cell lines

To begin to understand ADMs mechanisms of action in dental tissues it was important to determine which cells were expressing it and/or may be exposed to it during development. For *in vitro* analysis it was also important to determine whether cells were likely able to respond to ADM via expression of relevant receptor complexes. ADM is part of the calcitonin superfamily of regulatory peptides (Kitamura *et al*, 1993) and exerts its effect upon cells via interactions with CRLR/RAMP-2 (AM-1) and CRLR/RAMP-3 (AM-2) receptor complexes (McLatchie *et al*, 1998). In the developmentally derived murine odontoblast-like and dental pulp-like cells, MDPC-23 and OD-21 cells, respectively, both CRLR and RAMP-2 transcripts were present (**Figures 4.1A & C**) indicating the potential of these cells to respond to ADM. Furthermore, their expression appeared to be potentially regulated following exposure to ADM (**Figures 4.1B & D**) possibly indicating a negative feedback response mechanism. However, as this experiment was only performed in duplicate, further repetitions of this experiment would be required to determine whether these findings were statistically significant and confirm this observation. The 3T3 skin fibroblast cells were used as control in these experiments due to a significant volume of data already analysing the effects of ADM on these cells (Withers *et al*, 1996; Isumi *et al*, 1998). Notably these cells were also found to express both CRLR and RAMP-2 (**Figure 4.1E**) as has been previously described (Withers *et al*, 1996; McLatchie *et al*, 1998). These data provided here therefore validated the experimental approach used, provided novel data on the receptor complexes present in these cells and initially supported the likelihood of the foetal derived dental cell lines, MDPC-23 and OD-21, ability to respond to ADM.

The expression of PCNA, a characterized surrogate marker for cell proliferation due to its increased expression in the nuclei of cells during DNA synthesis (Leonardi *et al*, 1992), appeared to increase following exposure of the cell lines to ADM. In MDPC-23 and OD-21 cells the peak increase in PCNA expression occurred following exposure to 10^{-11} M ADM (**Figures 4.1B & D**). These data therefore initially suggested that ADM may promote cell proliferation in these cell lines. In 3T3 cells there appeared a dose-dependent increase in PCNA expression following exposure to ADM (**Figure 4.1F**), which is in keeping with previously published data which demonstrated a dose-dependant increase in cell number following exposure of 3T3 cells to ADM (Isumi *et al*, 1998). However, further repetitions of this work are required to determine if the increases observed in the expression of PCNA in these cell lines was robust and represented statistically significant changes.

Effects of ADM on dental cell cultures

ADM reportedly stimulates proliferation in several cells types, including osteoblasts (Cornish *et al*, 2002), which share many structural and functional similarities to odontoblasts, with both responsible for the production and deposition of highly mineralised compounds. The increase in PCNA expression seen in the odontoblast- and pulp-like MDPC-23 and OD-21 cultures following exposure to ADM (**Figure 4.1A - D**), respectively, also suggested that ADM may induce a proliferative effect on these cell lines. Therefore, the effect of ADM on MDPC-23 and OD-21 cell number was determined and the 3T3 cell line was used as control due to it previously having been shown to increase in proliferation following ADM exposure (Isumi *et al*, 1998). A biphasic response in terms of cell number was observed in MDPC-23 and OD-21

cells following exposure to a range of concentrations of ADM (**Figure 4.2A & B**), with 10^{-11} M ADM producing the greatest increase in cell number in both cell lines. These biphasic responses may indicate varying, concentration dependent actions induced by ADM, for example ADM stimulates an increase in cell numbers at 10^{-11} M, but at higher concentrations, i.e. 10^{-7} M, ADM does not significantly affect cell number in culture. Whilst these results in dental cells are novel, they are comparable to those observed in osteoblasts (Cornish *et al*, 2002) and in agreement with the increases in PCNA transcript levels observed (**Section 4.2**). In 3T3 cells there was a dose-dependant increase in cell number following exposure to ADM, in agreement with both previously published data (Isumi *et al*, 1998) and the PCNA results observed (**Section 4.2**). The difference observed between cell numbers of MDPC-23, OD-21 and 3T3 cells exposed to ADM is perhaps not unsurprising given the cells are derived from diverse tissues, with MDPC-23 cells being odontoblast-like in nature, OD-21 cells being mesenchymal pulp-like cells in nature and 3T3 cells being derived from skin fibroblasts (Todaro and Green, 1963; Hanks *et al*, 1998) and the data presented here may indicate that *in vivo* dental cells, as compared to skin fibroblasts, may be more sensitive to local or systemic ADM levels.

Combined with the IHC data reported here, results suggest that *in vivo* ADM may increase specific dental cell proliferation during tooth development. The similar proliferative effects observed in odontoblast-like cells and osteoblasts following exposure of to ADM also suggests this molecule may promote mineralisation in dental cells and tissues *in vivo* comparable to that observed during bone development (Cornish *et al*, 1998; 2001). A relative simple *in vitro* approach which could be used to determine this would be to expose odontoblast-like cells to ADM and subsequent detection of mineral deposition, indicative of mineralisation, as has been performed in

this study (**Chapter 5**, subsequently discussed later in this chapter). However, to fully characterise ADMs ability to promote mineral deposition, further *in vivo* and *ex vivo* studies would be required which involve the use of the cavity preparation and organ-culture models previously described.

Similar biphasic patterns in cell number were observed following exposure of MDPC-23 and OD-21 cells to ADM and DMP concentrations (**Figure 4.5A & B**). DMP preparations are known to contain ADM, which, along with other key growth factors, are released following dentine dissolution via plaque bacterial acids or dental cavity etchants (Graham, thesis; Graham *et al*, 2006; Tomson *et al*, 2007). However, both the lower three of E-DMPs and ADM alone increased cell numbers, however the increases seen following exposure to the lower three concentrations of E-DMPs were higher than those seen with the lower three concentrations of ADM alone. While the two higher concentrations of E-DMPs significantly lowered cell number compared to the control. These findings suggest that there are other factors influencing cell number following E-DMP exposure to MDPC-23 and OD-21 cells, other than any ADM sequestered. Indeed, without including an ADM antagonist it is difficult to state ADM's role in these results. However, this data is the first to compare results and provides interesting avenues for future study such as analysing the effects on cell numbers of ADM in co-ordination with other growth factors and the inclusion of an ADM antagonist with E-DMP stimulation of cell number. *In vivo*, histological analysis and dentine-bridge measurements of cavities introduced to ferret teeth, subsequently exposed to DMPs etchants, have demonstrated their ability of to increase tertiary dentinogenesis and this is thought to be due to the release of the cocktail of growth factors sequestered within (Smith *et al*, 1990; Smith *et al*, 1994). As ADM constitutes one of these growth factors it is reasonable to suggest that once it

is released, ADM may be important in regulating tertiary dentine secretion either on its own or in synergy with other molecules present. Given ADMs pleiotropic actions it is also likely that it could be important in regulating several cellular aspects in response to dental trauma, such as caries. Notably, ADM displays antibacterial properties (Allaker and Kapas, 2003; Gröschl *et al*, 2009) and regulates inflammatory responses (Elsasser and Kahl, 2002), both of which would be important factors in the tooth's response during dental caries. In addition ADM may also act as a chemotactic agent for cells involved in the immune and regenerative response (Zudaire *et al*, 2006) and/or may also be important in signalling angiogenesis to facilitate repair (Ribatti *et al*, 2007). Clearly several of these processes may also be activated by ADM during tooth development. Potential studies which may elucidate ADM's ability to stimulate tertiary dentinogenesis could utilize the *in vivo* local administration of ADM to exposed pulp following cavity preparations, as previously discussed, or use of an *ex vivo* organ-culture model, whereby incisor tooth slices are exposed to agarose beads soaked in ADM (see Sloan *et al*, 1998; Sloan and Smith, 1999). *In vitro* exposure of cells to DMPs in the presence of an ADM antagonist, such as ADM₂₂₋₅₂, would increase our knowledge of ADMs role within the cocktail of growth factors. Induction of tertiary dentine formation may subsequently also support ADMs role in tooth development due to the overlap between the molecules and processes involved.

ADM₂₂₋₅₂ is a well characterized competitive antagonist of ADM activity *in vitro* (Eguchi *et al*, 1994; Hay *et al*, 2004). The data presented here demonstrate that at higher concentrations, ADM₂₂₋₅₂ debilitated ADMs capacity to increase cell number in MDPC-23 and OD-21 cells (**Figures 4.4A & B**) in a similar manner to that observed in other experiments (Hay *et al*, 2004). These results indicated that the

increases in cell numbers previously described were due to specific ADM interactions with the receptor components previously discussed.

A biphasic response in cell number, similar to that observed following exposure to ADM, was also detected in MDPC-23 and OD-21 cultures following dexamethasone exposure (**Figure 4.6A & B**). Significantly dexamethasone is well characterized *in vitro* with regards to its mineralising induction action (Cheng *et al*, 1996; Hildebrandt *et al*, 2009). In addition, *in vitro* dexamethasone is also known to induce the differentiation of bone marrow stromal cells into osteoblasts (Cheng *et al*, 1994) and has been reported to be able to regulate expression of ADM and/or its receptors (Nishimori *et al*, 1997; Hattori *et al*, 1999; Udono-Fujimori *et al*, 2004 and Uzan *et al*, 2004). Notably, a glucocorticoid receptor element has recently been identified in the regulatory sequences of ADM and the ADM receptor component, calcitonin receptor like receptor (CRLR) (Nikitenko *et al*, 2003; Zudaire *et al*, 2005). Suggesting the potential for ADM to regulate mineralisation in a similar manner to dexamethasone and/or even substitute for it in *in vitro* in cellular and biochemical assays. It is also conceivable that due to potential activity redundancy and regulatory control ADM may function downstream of dexamethasone signalling in these processes. These observations were also further supported by data indicating that dexamethasone was able to dose dependently reduce ADM expression in MDPC-23 and OD-21 cells (**Figure 4.7B & F**), indicating a potential negative feedback regulatory relationship. There was no significant response in 3T3 cells following exposure to the mineralising agent dexamethasone, data which is unsurprising given that these cells are derived from a non-mineralising organ, i.e. skin, and therefore are not predicted to respond in a similar manner as cells derived from mineralised tissues.

Effects of ADM on mineral deposition *in vitro*

Following the observation of comparable effects of ADM on cell growth in odontoblasts and osteoblasts, combined with the similar effects observed for ADM and the known mineralisation agent dexamethasone on dental cells, the ability of ADM to stimulate mineral deposition was analysed. In odontoblast-like MDPC-23 cultures, ADM appeared capable of acting as a substitute for dexamethasone in standard mineralising medium (**Section 5.2**). During the earlier stages of analysis (after 7 and 11 days exposure), when ADM was used in conjunction with dexamethasone, ADM appeared to increase mineral deposition compared to dexamethasone alone (**Section 5.2**). However, by the end of the study period (21 days exposure) there were negligible differences in the areas of mineral deposition detected following exposure to all concentrations of ADM or dexamethasone. This result could be explicable due to dexamethasone's ability to dose-dependently reduce ADM expression in MDPC-23 cells (**Figure 4.7B**), thereby inducing a negative feedback mechanism. It is reasonable to suggest that as ADM can increase cell numbers in MDPC-23 cultures, the increase in mineral deposition observed here was due to an increase in cells present in culture after this time period. However, increased mineral deposition was observed following exposure to all concentrations of ADM, while only 10^{-13}M and 10^{-11}M ADM produced significant increases in cell number (**Figure 4.2**). These data suggest that the increased areas of mineral deposits were not likely linked to increasing cell number. Overall, it seems reasonable to conclude that ADM can stimulate increases in mineral deposition that is indicative of mineralisation in odontoblast-like cells at comparable levels to the known mineralising agent dexamethasone, especially during the earlier stages of mineralisation.

In dental pulp-like OD-21 cells, the areas of mineral deposition detected were decreased compared to those determined in odontoblast-like MDPC-23 cells. These data are perhaps not unsurprising given that these cells are not characterized for their ability to secrete mineralised deposits, although they are reportedly capable of differentiating into odontoblast progenitor cells (Goldberg *et al*, 2008). When these cells were exposed to concentrations of ADM in the absence of dexamethasone they produced areas of mineral deposition that were significantly greater than those obtained following ascorbic acid and β -glycerophosphate exposure alone, whilst being significantly less than cells exposed to the standard mineralisation media containing dexamethasone. When concentrations of ADM were used in conjunction with dexamethasone there was minimal variation in the areas of mineral deposition detected. The fact that ADM increased mineral deposition compared to ascorbic acid and β -glycerophosphate exposure alone suggests that ADM is capable of inducing mineral deposition in pulp-like cells. Notably, however, dexamethasone significantly increased detectable mineral deposition in OD-21 cells compared to all concentrations of ADM after 21 days exposure (**Figure 5.12A**). These data indicate that dexamethasone is still the most potent inducer of mineral deposition in OD-21 cells. No discernable mineralised deposits were detected in 3T3 cells following exposure to any of the treatments. This result was therefore as predicted due to the skin fibroblast origin of 3T3 cells (Todaro and Green, 1963).

Effect of systemic ADM administration on dental and craniofacial mineralised tissue

As ADM had demonstrable ability to promote mineralisation in dental cells *in vitro* (**Chapter 5**) and *in vivo* can increase mouse long bone length and strength (Cornish *et al.*, 1998) it was reasonable to hypothesize that systemic ADM administration may also positively affect dental and craniofacial mineralised tissues. Such an opportunity to study this potential effect was provided via collaboration with Professor Cornish (Bone Research Group, University of Auckland, New Zealand).

Micro-computed tomography (μ CT) analysis of adult Swiss mice systemically treated with either ADM or saline solution over a period of four weeks revealed that there was no significant difference in the hard tissue volume in either sample group (**Section 6.2 & 6.3**). Furthermore, little variation in the key mandibular measurements obtained from digital images in either treatment group was observed (**Section 6.4**). The exception to this was that the condylar measurements, where the group systemically treated with ADM exhibited a significantly increased mean length compared to the saline control group (**Figure 6.4E**).

The lack of variation in dental hard tissue volume following systemic administration of ADM could be explicable due to several reasons. Firstly, the Swiss mice analysed were adults at the onset of the experiment; therefore, the entire dentition would be fully developed, no ameloblasts would be present and the odontoblasts would be fully mature, resulting in the odontoblasts having undergone a series of morphological changes that are associated with a pronounced down-regulation in dentine production. In this state the odontoblasts produce relatively low amounts of dentine whilst staying viable throughout the tooth's life (Begue-Kirn *et al.*, 1994; Linde & Goldberg, 1993; Ten Cate, 1998). Secondly, the mice were injected at

the base of the tail. Under normal physiological conditions ADM is bound to an accessory binding protein in blood which can modulate its physiological role and potentially increase its blood borne stability (Pio *et al*, 2001). Following external, systemic administration of unbound ADM it is unclear as to neither its stability nor, therefore, the concentration subsequently localized to the dentine-pulp complex. To potentially overcome the problems described a better experimental design could be applied, whereby mice were subjected to localised injections directly into the craniofacial tissues preferably at an age where the teeth are still undergoing hard tissue formation, i.e immediately post-natally. Another possible study modification could involve the use of cavity preparation in rodent teeth (as has been previously discussed in **Section 1.10.2**). These studies could provide further information into the *in vivo* effects of ADM on dental tissue biology.

Similarly in craniofacial tissue measurements minimal variation was observed between the different treatment groups. This could also be due to the localisation of the injections and the resulting concentration of ADM subsequently present in the mandibular region. A further consideration is the fact that the long bones studied by Cornish *et al*, 2001 and the bones of the cranio-facial region, such as the mandible studied here, are formed from developmentally different processes (Netter, 1987). Long bones are formed by a process known as endochondral ossification. Endochondral formed bone begins as cartilage, however, as it begins to develop a layer of osteoblasts form around the cartilage and deposit a thin layer of bone, ultimately resulting in the cell death of the cartilage forming chondrocytes. Subsequently, the cartilage begins to calcify and further bone is deposited, eventually forming the trabeculae of the long bones (Netter, 1987). Intramembranous ossification is responsible for the formation of so-called flat bones generally associated with the

craniofacial regions (Netter, 1987). In this model of bone development mesenchymal progenitor cells differentiate into osteoblast cells. These osteoblasts subsequently deposit non-mineralised osteoid, which mineralises to form the trabeculae of spongy bone (Netter, 1987). Potentially, such differences in developmental processes may account for why minimal changes were observed in ADM treated mandibles compared to sham treated animals. This data suggests that ADM could play a role in endochondral bone growth, but not intramembranous bone growth, however as ADM has demonstrably increased the indexes of bone formation and mineralized bone area of mouse calvaria *in vivo* (Cornish *et al*, 1997), an area that is formed by intramembranous ossification, this is unlikely. The significant increase observed in the key condylar measurement (**Figure 6.4E**) could be related to the fact that this region of the mandible is a major site of on-going growth (Enlow and Hans, 1996). To better determine whether ADM administration *in vivo* has potential for mandibular regeneration, a similar experimental design as that proposed above for the dental tissues could be applied, whereby localised or topical delivery mechanisms could be utilised, as in the study of mouse calvaria mineralization following local ADM delivery (Cornish *et al*, 1997).

Conclusion

Novel data presented here has demonstrated the expression of ADM in key temporo-spatial patterns in the developing tooth bud, specifically in the cells responsible for inducing odontoblast differentiation and in secretory odontoblasts. The presence of ADM in secretory odontoblasts is identical to the expression of a key growth factor in odontoblast differentiation and dentine secretion, TGF- β 1. This expression pattern could denote a key role for ADM in tooth development, potentially in odontoblast differentiation and dentine secretion.

In vitro, novel data was produced demonstrating that ADM increases dental tissue cell numbers and can promote mineral deposition that is indicative of mineralisation, whilst *in vivo*, it's effects on murine adult dental and craniofacial mineralised tissue biology appear minimal but require further characterisation.

Data presented here suggests it is plausible that ADM may play an important role in tooth development, a hypothesis supported by ADM's temporo-spatial expression pattern in developing teeth and the fact ADM can regulate mechanisms such as increasing cell number and extracellular matrix secretion in several cell types derived from developing foetal dentition. This study therefore provides a number novel discoveries indicating that further study of ADM in dental tissue biological processes is required, as its better understanding may aid development of novel biomimetic dental tissue regenerative procedures.

References

- About, I., Bottero, M.J., De Denato, P., Camps, J., Franquin, J.C. and Mitsiadis, T.A.** (2000). Human dentin production *in vitro*. *Exp Cell Res.* 258:33-41.
- Aiyar, N., Disa, J., Pullen, M. and Nambi, P.** (2001). Receptor activity modifying proteins interaction with human and porcine calcitonin receptor-like receptor (CRLR) in HEK-293 cells. *Mol Cell Biochem.* 224:123-133.
- Allaker, R.P. and Kapas, S.** (2003). Adrenomedullin and mucosal defence: interaction between host and microorganism. *Regul Pept.* 112:147-152.
- Amano, M., Agematsu, H., Usami, A., Matsunaga, S., Suto, K. and Ide, Y.** (2006). Three-dimensional analysis of pulp chambers in maxillary second deciduous molars. *Journ Dent.* 34:503-508.
- Ando, K. and Fujita, T.** (2003). Lessons from the adrenomedullin knockout mouse. *Regulat Pept.* 112:185-188.
- Andreoni, G., Angeretii, N., Lucca, E. and Forloni, G.** (1997). Densitometric quantification of neuronal viability by computerised image analysis. *Expl Neurol.* 148:281-287.
- Assoian, R.K., Komoriya, A., Meyers, C.A., Miller, D.M. and Sporn, M.B.** (1983). Transforming growth factor-beta in human platelets. Identification of a major storage site, purification and characterization. *J Biol Chem.* 258:7155-7160.
- Atchley, W.R., Herring, S.W., Riska, B. and Plummer, A.A.** (1984). Effects of the muscular dysgenesis gene on developmental stability in the mouse mandible. *J Craniofac Genet Dev Biol.* 4:179-189.
- Atti, E., Gomez, S., Wahl, S.M. Mendelsohn, R., Paschalis, E. and Boskey, A.L.** (2002). Effect of transforming growth factor-beta deficiency on bone development: A Fourier transform infrared imaging analysis. *Bone.* 31:675-684.

- Bandyopadhyay, A., Tsuji, K., Cox, K., Harfe, B.D., Rosen, V and Tabin, C.J.** (2006). Genetic analysis of the roles of BMP2, BMP4 and BMP7 in limb patterning and skeletogenesis. *PLoS Genet.* 2:EPub.
- Barthel, C.R., Rosenkranz, B., Leuenberg, A. and Roulet, J.F.** (2000). Pulp capping of carious exposures: treatment outcome after 5 and 10 years: a retrospective study. *Journ Endo.* 26:525-528.
- Basch, M.L., Garcia-Castro, M.I. and Bronner-Fraser, M.** (2004). Molecular mechanisms of neural crest induction. *Birth Defects Res C Embryo Today.* 72:109-123.
- Basdra, E.L. and Komposch, G.** (1997). Osteoblast-like properties of human periodontal ligament cells: an *in vitro* analysis. *Eur J Orthod.* 19:615-621.
- Batouli, S., Miura, M., Brahim, J., Tsutsui, T.W., Fisher, L.W., Gronthos, S., Robey, P.G. and Shi, S.** (2003). Comparison of stem-cell-mediated osteogenesis and dentinogenesis. *J Dent Res.* 82:976-981.
- van de Beek, D., de Gans, J., McIntyre, P. and Prasad, K.** (2007). Corticosteroids for acute bacterial meningitis. *Cochrane Database Syst Rev.* 1:CD004405.
- Bedell, M.A., Jenkins, N.A. and Copeland, N.G.** (1997). Mouse models of human disease. Part I: techniques and resources for genetic analysis in mice. *Genes Dev.* 11:1-10.
- Bègue-Kirn, C., Smith, A.J., Ruch, J.V., Wozney, J.M., Purchio, A., Hartmann, D. and Lesot, H.** (1992). Effects of dentin proteins, transforming growth factor beta 1 (TGF beta 1) and bone morphogenetic protein 2 (BMP2) on the differentiation of odontoblast *in vitro*. *Int J Dev Biol.* 36:491-503.
- Bègue-Kirn, C., Smith, A.J., Lorient, M., Kupferle, C., Ruch, J.V. and Lesot, H.** (1994). Comparative analysis of TGF betas, BMPs, IGF1, msxs, fibronectin, osteonectin and bone sialoprotein gene expression during normal and *in vitro* induced odontoblast differentiation. *Int Journ Dev Biol.* 38:405-420.
- Belloni, A.S., Trejter, M., Melendowicz, L.K. and Nussdorfer, G.G.** (2003). Adrenomedullin stimulates proliferation and inhibits apoptosis of immature rat thymocytes cultured *in vitro*. *Peptides.* 24:295-300.

Bergeron, E., Marquis, M.E., Chrétien, I. and Faucheux, N. (2007). Differentiation of preosteoblasts using a delivery system with BMPs and bioactive glass microspheres. *J Mater Sci Mater Med.* 18:255-263.

Bergmans, L., Van Cleynenbruegel, J., Wevers, M. and Lambrechts, P. (2001). A methodology for quantitative evaluation of root canal instrumentation using microcomputed tomography. *Int Endodontic Journal.* 34:390-398.

Bilezikian, J.P., Raisz, L.D. and Rodan, G.A. (1996). Principle of bone biology. 1st Edition. *Academic Press.*

Bloom, S.L., Sheffield, J.S., McIntire, D.D. and Leveno, J.K. (2001). Antenatal dexamethasone and decreased birth weight. *Obstet Gynecol.* 97:485-490.

Bodegas, E., Martinez, A., Ozbun, L.L., Garayoa, M., Letterio, J.J., Montuenga, L.M. and Jokowlew, S.B. (2004). *Int J Dev Biol.* 48:67-70.

Bonewald, L.F., Harris, S.E., Rosser, J., Dallas, M.R., Dallas, S.L., Camacho, N.P., Boyan, B. and Boskey, A. (2003). von Kossa staining alone is not sufficient to confirm that mineralization in vitro represents bone formation. *Calcif Tissue Int.* 72:537-542.

Bonewald, E. (1994). Osteocyte biology: its implications for osteoporosis. *J Musculoskeletal Neuronal Interact.* 4:101-104.

Botero, T.M., Mantellini, M.G., Song, W., Hanks, C.T. and Nor, J.E. (2003). Effect of lipopolysaccharides on vascular endothelial growth factor expression in mouse pulp cells and macrophages. *Eur J Oral Sci.* 111:228-234.

Brandes, M.E., Allen, J.B., Ogawa, Y. and Wahl, S.M. (1991). Transforming growth factor beta 1 suppresses acute and chronic arthritis in experimental animals. *J Clin Invest.* 87:1108-1113.

Bunton, D.C., Petrie, M.C., Hillier, C., Johnston, F. and McMurray, J.J. (2004). The clinical relevance of adrenomedullin: a promising profile? *Pharmacol Ther.* 103:170-201

Buhlmann, N., Leuthauser, K., Muff, R., Fischer, J.A. and Born, W. (1999). A receptor activity modifying protein (RAMP)2-dependent adrenomedullin receptor is a calcitonin gene-related peptide receptor when coexpressed with human RAMP1. *Endocrinology*. 140:2883-2890.

Butler, W.T. (1998). Dentin matrix proteins. *Eur J Oral Sci*. 106:204-210.

Cadigan, K.M. and Nusse, R. (1997). Wnt signaling: a common theme in animal development. *Genes Dev*. 11:3286-3305.

Cam, Y., Neumann, M.R., Oliver, L., Raulais, D., Janet, T. and Ruch, J.V. (1992). Immunolocalization of acidic and basic fibroblast growth factors during mouse odontogenesis. *Int J Dev Biol*. 36:381-389.

Cameron, V.A. and Fleming, A.M. (1998). Novel sites of adrenomedullin gene expression in mouse and rat tissues. *Endocrinology*. 139:2253-2264

Canalis, E. (2005) Mechanisms of glucocorticoid action in bone. *Curr Osteoporos Report*. 3:98-102

Cassidy, N., Fahey, M., Prime, S.S. and Smith, A.J. (1997). Comparative analysis of transforming growth factor-beta isoforms 1-3 in human and rabbit dentine matrices. *Arch Oral Biol*. 42:219-223.

Cerny, R., Lwigale, P., Ericsson, R., Muelemans, D., Epperlein, H.H. and Bronner Fraser, M. (2004). Developmental origins and evolution of jaws: new interpretation of "maxillary" and "mandibular". *Dev Biol*. 276:225-236

Chai, Y., Mah, A., Crohin, C., Groff, S., Bringas, P. Jr., Le, T., Santos, V. and Slavkin, H.C. (1994). Specific transforming growth factor-beta subtypes regulate embryonic mouse Meckel's cartilage and tooth development. *Dev Biol*. 162:85-103.

Chai, Y., Sasano, Y., Bringas, P. Jr., Mayo, M., Kaartinen, V., Heisterkamp, N., Groffen, J., Slavkin, H. and Shuler, C. (1997). Characterization of the fate of midline epithelial cells during the fusion of mandibular prominences in vivo. *Dev Dyn*. 208:526-535

- Chai, Y. and Maxson, R.E. Jr.** (2006). Recent advances in craniofacial morphogenesis. *Dev Dyn.* 235:2353-2375.
- Chang, C.P., Pearse II, R.V., O'Connell, S. and Rosenfeld, M.G.** (1993) Identification of a seven transmembrane helix receptor for corticotropin-releasing factor and sauvagine in mammalian brain. *Neuron* 11:1187–1195.
- Chen, T.L. and Bates, R.L.** (2000). Recombinant human transforming growth factor beta 1 modulates bone remodeling in a mineralizing bone organ culture. *J Bone Miner Res.* 8:423-34.
- Cheng, S.L., Wang, J.W., Rifas, L., Zhang, F.S and Avioli LV.** (1994). Differentiation of human bone marrow stromal cells *In Vitro*: Induction of osteoblast phenotype by dexamethasone. *Endocrinology.* 134: 277-286.
- Cheng, S.L., Zhang, S.F and Avioli LV.** (1996). Expression of Bone Matrix Proteins during dexamethasone-induced mineralization of bone marrow stromal cells. *J Cell Biochem.* 61:182-193.
- Chiang, C., Litingtung, Y., Lee, E., Young, K.E., Corden, J.L., Westphal, H. and Beachy, P.A.** (1996). Cyclopia and defective axial patterning in mice lacking Sonic hedgehog gene function. *Nature.* 383:407-413.
- Chini, E.N., Choi, E., Grande, J.P., Burnett, J.C. and Dousa, T.P.** (1995). Adrenomedullin suppresses mitogenesis in rat mesangial cells via cAMP pathway. *Biochem Biophys Res Commun* 215:868-873.
- Cnudde, V., Masschaele, B., Dierick, M., Vlassenbroeck, J., Van Hoorebeke, L. and Jacobs, P.** (2006) Recent progress in X-ray CT as a geosciences tool. *Applied Geochem.* 21:826-832.
- Cobourne, M.T., Hardcastle, Z. and Sharpe, P.T.** (2001). Sonic hedgehog regulates epithelial proliferation and cell survival in the developing tooth germ. *J Dent Res.* 80:1974-1979.
- Cobourne, M.T. and Sharpe, P.T.** (2002). Expression and regulation of hedgehog-interacting protein during early tooth development. *Connect Tissue Res.* 43:143-147.

Coppock, H.A., Owji, A.A., Austin, C., Upton, P.D., Jackson, M.L., Gardiner, J.V., Ghatei, M.A., Bloom, S.R. and Smith, D.M. (1999). Rat-2 fibroblasts express specific adrenomedullin receptors, but not calcitonin-gene-related-peptide receptors, which mediate increased intracellular cAMP and inhibit mitogen-activated protein kinase activity. *Biochem J.* 338:15-22.

Cornish, J., Callon, K.E., Coy, D.H., Jiang, N.Y., Xiao, L., Cooper, G.J. and Reid, I.R. (1997). Adrenomedullin is a potent stimulator of osteoblastic activity in vitro and in vivo. *Am J Physiol.* 273:1113-1120.

Cornish, J., Callon, K.E., Bava, U., Coy, D.H., Mulvey, T.B., Murray, M.A., Cooper, G.J. and Reid, I.R. (2001). Systemic administration of adrenomedullin(27-52) increases bone volume and strength in male mice. *J Endocrinol.* 170:251-257.

Cornish, J. and Reid, I.R. (2001). Effects of amylin and adrenomedullin on the skeleton. *J Musculoskelet Neuronal Interact.* 2:15-24.

Cornish, J. and Naot, D. (2002). Amylin and adrenomedullin: novel regulators of bone growth. *Curr Pharm Des.* 8:2009-2021.

Couly, G.F., Cotley, P.M. and Le Douarin, N.M. (1992). The developmental fate of the cephalic mesoderm in quail-chick chimeras. *Devel.* 14:1-15.

Cuttitta, F., Pio, R., Garayoa, M., Zudaire, E., Julian, M., Elsasser, T.H., Montuenga, L.M. and Martinez, A. (2002). Adrenomedullin functions as an important tumor survival factor in human carcinogenesis. *Microsc Res Tech.* 57:110-119.

Van Dalen, G., Blonk, H., van Aalst, H. and Hendriks, C.L. (2003). 3-D imaging of foods using X-ray microtomography. *Imag and Microsp.* 3:18-21.

Dassule, H.R. and McMahon, A.P. (1998). Analysis of epithelial-mesenchymal interactions in the initial morphogenesis of the mammalian tooth. *Dev Biol.* 202:215-227.

Davideau, J.L., Demri, P., Gu, T.T., Simmons, D., Nessman, C., Forest, N., MacDougall, M. and Berdal, A. (1999). Expression of DLX-5 during human embryonic craniofacial development. *Mech Dev.* 81183-81186.

- Davideau, J.L., Demri, P., Hotton, D., Gu, T.T., MacDougall, M., Sharpe, P., Forest, N. and Berdal, A.** (1999). Comparative study of MSX-2, DLX-5 and DLX-7 gene expression during early human tooth development. *Pediatr Res.* 46:650-656
- Davidson, D.** (1995). The function and evolution of Msx genes: pointers and paradoxes. *Trends Genet.* 11:405-411.
- Dickson, M.C., Martin, J.S., Cousins, F.M., Kulkarni, A.B., Karlsson, S. and Akhurst, R.J.** (1995). Defective haematopoiesis and vasculogenesis in transforming growth factor- beta 1 knock-out mice. *Devel.* 121:1845-1854.
- Dierick, M., Cnudde, V., Masschaele, B., Vlassenbroeck, J., Van Hoorebeke, L. and Jacobs, P.** (2007). Micro-CT of fossils preserved in amber. *Nucl Instru Meth Phys Res Sect A: Acc Spectro, Detect Assoc Equip.* 580:641-643.
- D'Souza, R.N., Bachman, T., Baumgardner, K.R., Butler, W.T. and Litz, M.** (1995). Characterization of cellular responses involved in reparative dentinogenesis in rat molars. *J Dent Res.* 74:702-709.
- D'Souza, R.N. and Litz, M.** (1995). Analysis of tooth development in mice bearing a TGF-beta 1 null mutation. *Connect Tiss Res.* 32:41-46.
- D'Souza, R.N., Cavander, A., Dickinson, D., Roberts, A. and Letterio, J.** (1998). TGF-beta 1 is essential for the homeostasis of the dental-pulp complex. *Eur J Oral Sci.* 106:185-191.
- Eames, B.F., Sharpe, P.T. and Helms, J.A.** (2004). Hierarchy revealed in the specification of three skeletal fates by Sox9 and Runx2. *Dev Biol.* 274:188-200.
- Echeverry, S., Shi, X.Q., Haw, A., Liu, H., Zhang, Z.W. and Zhang, J.** (2009). Transforming growth factor-beta 1 impairs neuropathic pain through pleiotropic effects. *Mol Pain.* 5:16
- Eguchi, S., Hirata, Y., Iwasaki, H., Sato, K., Watanabe, T.X., Inui, T., Nakajima, K., Sakakibara, S. and Marumo, F.** (1994). Structure-activity relationship of adrenomedullin, a novel vasodilatory peptide, in cultured rat vascular smooth muscle cells. *Endocrinol.* 135:2454-2458.

Eichner, A., Brock, J., Heldin, C.H. and Souchelnytskyi, S. (2002). Bone morphogenic protein-7 (OP1) and transforming growth factor-beta1 modulate 1,25(OH)₂-vitamin D₃-induced differentiation of human osteoblasts. *Exp Cell Res.* 275:132-142.

Elsasser, T.H. and Kahl, S. (2002). Adrenomedullin has multiple roles in disease states: development and remission of the inflammatory response. *Microsc Res Tech.* 57:120-129

Enlow, D.H. and Hans, M.G. (1996) Essentials of facial growth. *W. B. Saunders Co.*

Filippatos, G.S., Gangopadhyay, N., Lalude, O., Parameswaran, N., Said, S.I., Spielman, W. and Uhal, B.D. (2001). Regulation of apoptosis by vasoactive peptides. *Am J Physiol Lung Cell Mol Physiol.* 28149-28161.

Finkelman, R.D., Mohan, S., Jennings, J.C., Taylor, A.K., Jepsen, S. and Baylink, D.J. (1990). Quantitation of growth factors IGF-I, SGF/IGF-II, and TGF-beta in human dentin. *J Bone Miner Res.* 5:717-723.

Frayon, S., Cuille, C., Gnidehou, S., de Vernejoul, M.C. and Garel, J.M. (2000). Dexamethasone increases RAMP1 and CRLR mRNA expressions in human vascular smooth muscle cells. *Biochem Biophys Res Commun.* 270:1063-1067.

Garayoa, M., Bodegas, E., Cuttitta, F. and Montuenga, L.M. (2002). Adrenomedullin in mammalian embryogenesis. *Microsc Res Tech.* 57:40-54.

Goldberg, M., Six, N., Decup, F., Buch, D., Soheili Majd, E., Lastfargues, J.J., Salih, E. and Stanislawski, L. (2001). Application of bioactive molecules in pulp-capping situations. *Adv Dent Res.* 15:91-95.

Goldberg, M. and Smith, A.J. (2004). Cells and extracellular matrices of dentin and pulp: a biological basis for repair and tissue engineering. *Crit Rev Oral Biol Med.* 15:13-27.

Goldberg, M., Farges, J.C., Lacerda-Pinheiro, S., Six, N., Jegat, N., Decup, F., Septier, D., Carrouel, F., Durand, S., Chaussain-Miller, C., Denbesten, P., Veis, A. and Poliard, A. (2008). Inflammatory and immunological aspects of dental pulp repair. *Pharmacol Res.* 58:137-147.

Graham, L. (2007) PhD thesis.

Graham, L., Cooper, P.R., Cassidy, N., Nor, J.E., Sloan, A.J. and Smith, A.J. (2006). The effect of calcium hydroxide on solubilisation of bio-active dentine matrix components. *Biomater.* 27:2865-2873.

Gregory, C.A., Gunn, W.G., Peister, A. and Prockop, D.J. (2004). An alizarin red-based assay of mineralization by adherent cells in culture: comparison with cetylpyridinium chloride extraction. *Anal Biochem.* 329:77-84.

Grigoriou, M., Tucker, A.S., Sharpe, P.T. and Pachnis, V. (1998). Expression and regulation of Lhx6 and Lhx7, a novel subfamily of LIM homeodomain encoding genes, suggests a role in mammalian head development. *Development.* 125:2063-2074.

Gronthos, S., Mankani, M., Brahim, J., Gehron Robey, P. and Shi, S. (2000). Postnatal human dental pulp stem cells (DPSCs) *in vitro* and *in vivo*. *PNAS.* 25:13625-13630.

Gronthos, S., Brahim, J., Li, W., Fisher, L.W., Cherman, N., Boyde, A., DenBesten, P., Gehron Robey, P. and Shi, S. (2002). Stem cell properties of human dental pulp stem cells. *J Dent Res.* 81:531-535.

Gröschl, M., Wendler, O., Topf, H.G., Bohlender, J. and Kohler, H. (2009). Significance of salivary adrenomedullin in the maintenance of oral health: Stimulation of oral cell proliferation and antibacterial properties. *Regul Pept.* 154:16-22.

Grossi, S.G. and Genco, R.J. (1998) Periodontal disease and diabetes mellitus: a two-way relationship. *Ann Periodontol.* 3:51-61.

Grzesik, W.J., and Narayanan, A.S. (2002). Cementum and periodontal wound healing and regeneration. *Crit Rev Oral Biol Med.* 13:474-484.

- Hakki, S.S., Bozkurt, S.B., Hakki, E.E. and Belli, S.** (2009). Effects of mineral trioxide aggregate on cell survival, gene expression associated with mineralized tissues, and biomineralization of cementoblasts. *J Endod.* 35:513-519.
- Hall, B.K. and Coffin-Collins, P.A.** (1990). Reciprocal interactions between epithelium, mesenchyme, and epidermal growth factor (EGF) in the regulation of mandibular mitotic activity in the embryonic chick. *J Craniofac Genet Dev Biol.* 10:241-261.
- Hall, B.K. and Miyake, T.** (2000). Craniofacial development of avian and rodent embryos. *Methods Mol Biol.* 135:127-137.
- Hamada, H., Kitamura, K., Chosa, E., Eto, T. and Tajima, N.** (2007). Adrenomedullin stimulates the growth of cultured normal human osteoblasts as an autocrine/paracrine regulator. *Peptides.* 23:2163-2168.
- Hammerman, M.R.** (1995). Growth factors in renal development. *Semin Nephrol.* 15:291-299.
- Hanks, C.T., Sun, Z.L., Fang, D.N., Edwards, C.A., Wataha, J.C., Ritchie, H.H. and Butler, W.T.** (1998). Cloned 3T6 cell line from CD-1 mouse fetal molar dental papillae. *Connect Tissue Res.* 37:233-249.
- Hardcastle, Z., Mo, R., Hui, C.C. and Sharpe, P.T.** (1998). The Shh signalling pathway in tooth development: defects in Gli2 and Gli3 mutants. *Development.* 125:2803-2811.
- Hardouin, S.M. and Nagy, A.** (2000). Mouse models for human disease. *Clin Genet.* 57:237-244.
- Harris, S.A., Enger, R.J., Riggs, B.L. and Spelsberg, T.C.** (1995). Development and characterization of a conditionally immortalized human fetal osteoblastic cell line. *J Bone Miner Res.* 10:178-186.
- Hattori, Y., Mimura, A., Akimoto, K. and Kasai, K.** (1999). Transcriptional regulation of adrenomedullin in rat vascular smooth muscle cells. *Mol Cell Endocrinol.* 147:143-147.

Hay, D.L., Howitt, S.G., Conner, A.C., Schindler, M., Smith, D.M. and Poyner, D.R. (2003). CL/RAMP2 and CL/RAMP3 produce pharmacologically distinct adrenomedullin receptors: a comparison of effects of adrenomedullin22-52, CGRP8-37 and BIBN409BS. *Br J Pharmacol.* 140:477-486.

Hay, D.L., Conner, A.C., Howitt, S.G., Takhshid, M.A., Simms, J., Mahmoud, K. and Poyner, D.R. (2004). The pharmacology of CGRP-responsive receptors in cultured and transfected cells. *Peptides.* 25:2019-2026

He, W.X., Cao, T., Smith, D.A., Myers, T.E. and Wang, X.J. (2001). Smads mediate signaling of the TGFbeta superfamily in normal keratinocytes but are lost during skin chemical carcinogenesis. *Oncogene.* 20:471-483.

He, W.X., Niu, Z.Y., Zhao, S.L., Jin, W.L., Gao, J. and Smith, A.J. (2004). TGF-beta activated Smad signalling leads to a Smad3-mediated down-regulation of DSPP in an odontoblast cell line. *Arch Oral Biol.* 49:911-918.

He, W.X., Niu, Z.Y., Zhao, S.L., Smith, A.J. (2005). Smad protein mediated transforming growth factor beta1 induction of apoptosis in the MDPC-23 odontoblast-like cell line. *Arch Oral Biol.* 50:929-936.

Heywood, B.R. and Appleton, J. (1984). The ultrastructure of the rat incisor odontoblast in organ culture. *Arch Oral Biol.* 29:327-329.

Heikinheimo, K., Happonen, R.P, Miettinen, P.J. and Rivtos, O. (1993). Transforming growth factor beta 2 in epithelial differentiation of developing teeth and odontogenic tumours. *Journ Clin Invest.* 91:1019-1027.

Helder, M.N., Karg, H., Bervoets, T.J., Vukicevic, S., Burger, E.H., D'Souza, R.N., Woltgens, J.H., Karsenty, G. and Bronckers, A.L. (1998). Bone morphogenetic protein-7 (osteogenic protein-1, OP-1) and tooth development. *J Dent Res.* 77:545-554.

Helms, J.A. and Schneider, R.A. (2003). Cranial skeletal biology. *Nature.* 423:326-331.

Hildebrandt, C., Büth, H. and Thielecke, H. (2008). Influence of cell culture media conditions on the osteogenic differentiation of cord blood-derived mesenchymal stem cells. *Ann Anat.* 191:23-32.

Hinson, J.P., Kapas, S. and Smith, D.M. (2000). Adrenomedullin, a multifunctional regulatory peptide. *Endocr Rev.* 21:138-167.

Holdsworth, D.W. and Thornton, M.M. (2002). MicroCT in small animal and specimen imaging. *Trends in Biotechnology.* 20:34-39.

Horsted, P., Sondergaard, B., Thylstrup, A., El Ataar, K. and Fejerskov, O. (1985). A retrospective study of direct pulp capping with calcium hydroxide compounds. *Endodontics and Dental Traumatology.* 1:29-34.

Huang, H., Ma, C., Yang, M., Tang, C. and Wang, H. (2005) Adrenomedullin impairs the profibrotic effects of transforming growth factor-beta1 through recruiting Smad6 protein in human renal tubular cells. *Cell Physiol Biochem.* 15:117-124.

Huang, W., Wang, L., Yuan, M., Ma, J and Hui, Y. (2004). Adrenomedullin affects two signal transduction pathways and the migration in retinal pigment epithelial cells. *Invest Ophthalmol Vis Sci.* 45:1507-1513.

Hung, H.C., Willett, W., Merchant, A., Rosner, B.A., Ascherio, A. and Joshipura, K.J. (2003). Oral health and peripheral arterial disease. *Circulation.* 107:1152-1157.

Ioannidis, J.P., Hesketh, P.J. and Lau, J. (2000). Contribution of dexamethasone to control of chemotherapy-induced nausea and vomiting: a meta-analysis of randomized evidence. *J Clin Oncol.* 18:3409-3422.

Isumi, Y., Minamino, N., Katafuchi, T., Yoshioka, M., Tsuji, T., Kangawa, K. and Matsuo, H. (1998). Adrenomedullin production in fibroblasts: its possible function as a growth regulator of Swiss 3T3 cells. *Endocrinology.* 139:2552-2563.

Ito, Y., Bringas, P. Jr., Mogharei, A., Zhao, J., Deng, C. and Chai, Y. (2002). Receptor-regulated and inhibitory Smads are critical in regulating transforming growth factor beta-mediated Meckel's cartilage development. *Dev Dyn.* 224:69-78.

Jernvall, J., Keranen, S.V. and Thesleff, I. (2000). Evolutionary modification of development in mammalian teeth: quantifying gene expression patterns and topography. *Proc Natl Acad Sci U S A.* 97:14444-14448.

Jiang, W., Yang, J.H., Wang, S.H., Pan, C.S., Qi, Y.F., Zhao, J. and Tang, C.S. (2004). Effects of adrenomedullin on aldosterone-induced cell proliferation in rat cardiac fibroblasts. *Biochim Biophys Acta.* 1690:265-275.

Johnson, R.L. and Tabin, C. (1995). The long and short of hedgehog signaling. *Cell.* 81:313-316.

Johnson, R.L. and Tabin, C.J. (1997). Molecular models for vertebrate limb *Development.* *Cell.* 90:979-990.

Jontell, M., Okiji, T., Dahlgren, U. and Bergenholtz, G. (1998). Immune defense mechanisms of the dental pulp. *Crit Rev Oral Biol Med.* 9:179-200.

Jougasaki, M., Wei, C.M., Heublein, D.M., Sandberg, S.M. and Burnett, J.C. Jr. (1995). Immunohistochemical localization of adrenomedullin in canine heart and aorta. *Peptides.* 16:773-775.

Kaartinen, V., Voncken, J.W., Shuler, C., Warburton, D., Bu, D., Heisterkamp, N. and Groffen, J. (1995). Abnormal lung development and cleft palate in mice lacking TGF-beta 3 indicates defects of epithelial-mesenchymal interaction. *Nat Genet.* 11:415-421

Kaneko, Y., Saito, M., Mori, A., Sakamoto, K., Nakahara, T. and Ishii, K. (2006). Vasodilator effects of adrenomedullin on retinal arterioles in streptozotocin-induced diabetic rats. *J Ocul Pharmacol Ther.* 22:317-322.

Kapas, S., Brown, D.W., Farthing, P.M. and Hagi-Pavli, E. (1997). Adrenomedullin has mitogenic effects on human oral keratinocytes: involvement of cyclic AMP. *FEBS Lett.* 418:287-290.

Kassem, M., Okazaki, R., Harris, S.A., Spelsberg, T.C., Conover, C.A. and Riggs, B.L. (1998). Estrogen effects on insulin-like growth factor gene expression in a human osteoblastic cell line with high levels of estrogen receptor. *Calcif Tissue Int.* 62:60-66.

Kato, K., Kitamura, K., Kuwasako, K., Tanaka, M., Ishiyama, Y., Shimokubo, T., Ichiki, Y., Nakamura, S., Kangawa, K. and Eto, T. (1995). Plasma adrenomedullin in patients with primary aldosteronism. *Am J Hypertens.* 10:997-1000.

Keeting, P.E., Scott, R.E., Colvard, D.S., Anderson, M.A., Oursler, M.J., Spelsberg, T.C. and Riggs, B.L. (1992) Development and characterization of a rapidly proliferating, well-differentiated cell line derived from normal adult human osteoblast-like cells transfected with SV40 large T antigen. *J Bone Miner Res.* 7:127-136

Kikuchi, H., Sawada, T. and Yanagisawa, T. (2004) Effects of a functional agar surface on in vitro dentinogenesis induced in proteolytically isolated, agar-coated dental papillae in rat mandibular incisors. *Arch Oral Biol.* 41:871-883.

Killough, S.A., Lundy, F.T. and Irwin, C.R. (2009) Substance P expression by human dental pulp fibroblasts: a potential role in neurogenic inflammation. *J Endod.* 35:73-77.

Kinney, J.H., Balooch, M., Marshall, G.W. and Marshall, S.J. (1999) A micromechanics model of the elastic properties of human dentine. *Arch Oral Biol.* 44:813-822

Kitamura, K., Kangawa, K., Kawamoto, M., Ichiki, Y., Nakamura, S., Matsuo, H. and Eto, T. (1993) Adrenomedullin: a novel hypotensive peptide isolated from human pheochromocytoma. *Biochem Biophys Res Commun.* 192:553-560.

Klopcic, B., Maass, T., Meyer, E., Lehr, H.A., Metzger, D., Chambon, P., Mann, A and Blessing, M. (2007). TGF-beta superfamily signalling is essential for tooth and hair morphogenesis and differentiation. *Eur J Cell Biol.* 86:781-799.

Kodama, H.A., Amagai, Y., Koyama, H. and Kasai, S. (1982) A new preadipose cell line derived from newborn mouse calvaria can promote the proliferation of pluripotent hemopoietic stem cells in vitro. *J Cell Physiol.* 112:89-95.

Koller, E.J. and Fisher, C. (1980). Tooth induction in chick epithelium: expression of quiescent genes for enamel synthesis. *Science.* 207:993.

Kondo, S., Tamura, Y., Bawden, J.W. and Tanase S. (2001). The immunohistochemical localization of Bax and Bcl-2 and their relation to apoptosis during amelogenesis in developing rat molars, *Arch Oral Biol,* 46:557-568.

- Kontges, G. and Lumsden, A.** (1996) Rhombencephalic neural crest segmentation is preserved throughout craniofacial ontogeny. *Development*. 122:3229-3242.
- Kosmacheva, S.M., Volk, M.V., Yeustratenka, T.A., Severin, I.N. and Potapnev, M.P.** (2008) In vitro growth of human umbilical blood mesenchymal stem cells and their differentiation into chondrocytes and osteoblasts. *Bull Exp Biol Med*. 145:141-145.
- Kraus, P. and Lufkin, T.** (1999) Mammalian Dlx homeobox gene control of craniofacial and inner ear morphogenesis. *J Cell Biochem*. 33:133-140
- Kumegawa, M., Ikeda, E., Tanaka, S., Haneji, T., Yora, T., Sakagishi, Y., Minami, N. and Hiramatsu, M.** (1994) The effects of prostaglandin E2, parathyroid hormone, 1,25 dihydroxycholecalciferol, and cyclic nucleotide analogs on alkaline phosphatase activity in osteoblastic cells. *Calcif Tissue Int*. 36:72-76.
- Lee, J.H., Kim, M.J., Choi, W.S., Yoon, P.Y., Ahn, K.M., Myung, H., Hwang, S.J., Seo, B.M., Choi, J.Y., Choung, P.H. and Kim, S.M.** (2004) Concomitant reconstruction of mandibular basal and alveolar bone with a free fibular flap. *Int J Oral Maxillofac Surg*. 33:150-156
- Leis, H.J., Hulla, W., Gruber, R., Huber, E., Zach, D., Gleispach, H. and Windischhofer, W.** (1997) Phenotypic heterogeneity of osteoblast-like MC3T3-E1 cells: changes of bradykinin-induced prostaglandin E2 production during osteoblast maturation. *J Bone Miner Res*. 12:541-551.
- Leonardi E, Girlando S, Serio G, Mauri FA, Perrone G, Scampini S, Dalla Palma P, Barbareschi M.** (1992). PCNA and Ki67 expression in breast carcinoma: correlations with clinical and biological variables. *J. Clin. Pathol*. 45:416–419
- Lesot, H., Smith, A.J., Tziafas, D., Begue-Kirn, C., Cassidy, A. and Ruch, J.V.** (1994). Biologically active molecules and dental tissue repair: a comparative review of reactionary and reparative dentinogenesis with induction of odontoblast differentiation *in vitro*. *Cell Materials*. 4:199-218.

Letterio, J.J. and Roberts, A.B. (1996) Transforming growth factor-beta1-deficient mice: identification of isoform-specific activities in vivo. *J Leukoc Biol.* 59:769-774.

Lin, H.Y. and Lodish, H.F. (1993) Receptors for the TGF-beta superfamily: multiple polypeptides and serine/threonine kinases. *Trends Cell Biol.* 3:14-19.

Lin, C.R., Kioussi, C., O'Connell, S., Briata, P., Szeto, D., Liu, F., Izpisúa-Belmonte, J.C. and Rosenfeld, M.G. (1999) Pitx2 regulates lung asymmetry, cardiac positioning and pituitary and tooth morphogenesis. *Nature.* 401:279-282.

Linde, A. and Goldberg, M. (1993) Dentinogenesis. *Crit Rev Oral Biol Med.* 4:679-728.

Liu, H., Li, W., Shi, S., Habelitz, S., Gao, C. and Denbesten, P. (2005) MEPE is downregulated as dental pulp stem cells differentiate. *Arch Oral Biol.* 50:923-928.

Liu, J., Jin, T., Chang, S., Ritchie, H.H., Smith, A.J. and Clarkson, B.H. (2007) Matrix and TGF-beta-related gene expression during human dental pulp stem cell (DPSC) mineralization. *In Vitro Cell Dev Biol Anim.* 43:120-128.

López-Casillas F, Wrana JL, Massagué J. (1993) Betaglycan presents ligand to the TGF beta signaling receptor. *Cell.* 73:1435-1444.

Lumsden, A.G. (1988). Spatial organization of the epithelium and the role of neural crest cells in the initiation of the mammalian tooth germ. *Development.* 103:155-169.

Maas, R. and Bei, M. (1997) The genetic control of early tooth development. *Crit Rev Oral Biol Med.* 8:4-39.

Magne, P. (2006). Efficient 3D finite element analysis of dental restorative procedures using micro-CT data. *Dental Materials.* 958:1-10.

Mantellini, M.G., Botero, T., Yaman, P., Dennison, J.B., Hanks, C.T. and Nor, J.E. (2005). Adhesive resin and the hydrophilic monomer HEMA induce VEGF expression on dental pulp cells and macrophages. *Dent Mater.* Epub

Marks, S.C. Jr., Cahill, D.R., and Wise, G.E. (1983). The cytology of the dental follicle and adjacent alveolar bone during tooth eruption in the dog. *Am J Anat.* 168:277-289.

Martínez, A., Elsasser, T.H., Muro-Cacho, C., Moody, T.W., Miller, M.J., Macri, C.J. and Cuttitta, F. (1997) Expression of adrenomedullin and its receptor in normal and malignant human skin: a potential pluripotent role in the integument. *Endocrinol.* 138:5597-5604.

Massagué, J. (1990). The transforming growth factor-beta family. *Annu Rev Cell Biol.* 6:597-641.

Massagué, J. (1992). Receptors for the TGF-beta family. *Cell.* 69:1067-1070.

Massagué, J. (1996) TGFbeta signaling: receptors, transducers, and Mad proteins. *Cell.* 85:947-950.

Massagué, J. (1998). TGF-beta signal transduction. *Annu Rev Biochem.* 67:753-791.

Massagué, J., Blain, S.W. and Lo, R.S. (2000). TGFbeta signaling in growth control, cancer, and heritable disorders. *Cell.* 103:295-309.

McCabe, K.L., Manzo, A., Gammill, L.S. and Bronner-Fraser, M. (2004). Discovery of genes implicated in placode formation. *Dev Biol.* 274:462-477

McGonnell, I.M., Clarke, J.D. and Tickle, C. (1998). Fate map of the developing chick face: analysis of expansion of facial primordia and establishment of the primary palate. *Dev Dyn.* 212:102-118.

McLachlan, J.L., Smith, A.J., Bujalska, I.J. and Cooper, P.R. (2002) Gene expression profiling of pulpal tissue reveals the molecular complexity of dental caries. *Biochim Biophys Acta.* 1741:271-281.

McLatchie, L.M., Fraser, N.J., Main, M.J., Wise, A., Brown, J., Thompson, N., Solari, R., Lee, M.G. and Foord, S.M. (1998). RAMPs regulate the transport and ligand specificity of the calcitonin-receptor-like receptor. *Nature.* 393:333-339.

- Meijlink, F., Beverdam, A., Brouwer, A., Oosterveen, T.C. and Berge, D.T.** (1999). Vertebrate aristaless-related genes. *Int J Dev Biol.* 43:651-663.
- Melton, D.W.** (1994). Gene targeting in the mouse. *Bioessays.* 16:633-638.
- Mina, M. and Kollar, E.J.** (1987). The induction of odontogenesis in non-dental mesenchyme combined with early murine mandibular arch epithelium. *Arch Oral Biol.* 32:123-127.
- Mina, M., Upholt, W.B. and Kollar, E.J.** (1994). Enhancement of avian mandibular chondrogenesis in vitro in the absence of epithelium. *Arch Oral Biol.* 39:551-562.
- Mina, M.** (2001). Regulation of mandibular growth and morphogenesis. *Crit Rev Oral Biol Med.* 12:276-300.
- Mina, M.** (2001). Morphogenesis of the medial region of the developing mandible is regulated by multiple signaling pathways. *Cells Tissues Organs.* 169:295-301.
- Mitsiadis, T.A. and Rahiotis, C.** (2004). Parallels between Tooth Development and Repair: Conserved Molecular Mechanisms following Carious and Dental Injury. *J Dent Res* 83:896-902.
- Mitra, S and Bourreau, J.P.** (2006) Gi and Gs coupling of adrenomedullin in adult rat ventricular myocytes. *Am J Physiol Heart Circ Physiol.* 290: 1842-1947.
- Mohammed, A., Saravanan, R., Zammit, J. and King, R.** (2008). Intramedullary tibial nailing in distal third tibial fractures: distal locking screws and fracture non-union. *Int Orthop.* 32:547-549.
- Montuenga, L.M., Martínez, A., Miller, M.J., Unsworth, E.J. and Cuttitta, F.** (1997). Expression of adrenomedullin and its receptor during embryogenesis suggests autocrine or paracrine modes of action. *Endocrinology.* 138:440-451.
- Montuenga LM, Mariano JM, Prentice MA, Cuttitta F, Jakowlew SB.** (1998). Coordinate expression of transforming growth factor-beta1 and adrenomedullin in rodent embryogenesis. *Endocrinology.* 139:3946-3957.

Morszeck, C., Moehl, C., Götz, W., Heredia, A., Schäffer, T.E., Eckstein, N., Sippel, C. and Hoffmann, K.H. (2005) In vitro differentiation of human dental follicle cells with dexamethasone and insulin. *Cell Biol Int.* 29:567-575.

Mount, G.J. and Hume, W.R. (1998). Preservation and restoration of tooth structure. *Mosby.*

Moustakas, A., Pardali, K., Gaal, A. and Heldin, C.H. (2002). Mechanisms of TGF-beta signaling in regulation of cell growth and differentiation. *Immunol Lett.* 82:85-91.

Muff, R., Born, W. and Fischer, J.A. (2001). Adrenomedullin and related peptides: receptors and accessory proteins. *Peptides.* 22:1765-1772.

Mueller, R.J. and Richards, R.G. (2004). Immunohistological identification of receptor activator of NF-kappaB ligand (RANKL) in human, ovine and bovine bone tissues. *J Mater Sci Mater Med.* 15:367-72.

Mulder, L., Van Groningen, L.B., Potgieser, Y.A., Koolstra, J.H. and Van Eijden, T.M.G.J. (2006). Regional differences in architecture and mineralisation of developing mandibular bone. *The Anatomical Record* 288A:954-961.

Murray, P.E. and Garcia-Godoy, F. (2004) Stem cell responses in tooth regeneration. *Stem Cells Dev.* 13:255-262.

Nakashima, M. (2005). Bone morphogenetic proteins in dentin regeneration for potential use in endodontic therapy. *Cytokine and Growth Factor Reviews.* 16:369-376.

Naganawa, T., Xiao, L., Coffin, J.D., Doetschman, T., Sabbieti, M.G., Agas, D. and Hurley, M.M. (2008). Reduced expression and function of bone morphogenetic protein-2 in bones of Fgf2 null mice. *J Cell Biochem.* 103:1975-1988.

Netter, F.H. (1987). Musculoskeletal system: anatomy, physiology, and metabolic disorders. *Summit, New Jersey*

Nikitenko, L.L., Smith, D.M., Bicknell, R and Rees, M.C.P. (2003). Transcriptional regulation of the CRLR gene in human microvascular endothelial cells by hypoxia. *FASEB Journal*.

Nishimori, T., Tsujino, M., Sato, K., Imai, T., Marumo, F. and Hirata, Y. (1997). Dexamethasone-induced up-regulation of adrenomedullin and atrial natriuretic peptide genes in cultured rat ventricular myocytes. *J Mol Cell Cardiol*. 29:2125-2130.

Noden, D.M. (1988). Interactions and fates of avian craniofacial mesenchyme. *Development*. 103:121-140.

Nomura, M. and Li, E. (1998). Smad2 role in mesoderm formation, left-right patterning and craniofacial development. *Nature*. 393:786-790.

Oi, T., Saka, H. and Ide, Y. (2004). Three-dimensional observation of pulp cavities in the maxillary first premolar tooth using micro-CT. *International Endodontic Journal*. 37:46-51.

Oka, S., Oka, K., Xu, X., Sasaki, T., Bringas Jr, P and Chai, Y. (2007). Cell autonomous requirement for TGF-beta signalling during odontoblast differentiation and dentin matrix formation. *Mech Dev*. 124:409-415.

Oliver, K.R., Kane, S.A., Salvatore, C.A., Mallee, J.J., Kinsey, A.M., Koblan, K.S., Keyvan-Fouladi, N., Heavens, R.P., Wainwright, A., Jacobson, M., Dickerson, I.M. and Hill, R.G. (2001). Cloning, characterization and central nervous system distribution of receptor activity modifying proteins in the rat. *Eur J Neurosci*. 14:618-628.

Osumi-Yamashita, N., Ninomiya, Y. and Eto, K. (1997). Mammalian craniofacial embryology in vitro. *Int J Dev Biol*. 41:187-194.

Park, B.W., Hah, Y.S., Choi, M.J., Ryu, Y.M., Lee, S.G., Kim, D.R., Kim, J.R. and Byun, J.H. (2009). In vitro osteogenic differentiation of cultured human dental papilla-derived cells. *J Oral Maxillofac Surg*. 67:507-514.

Peters, H., Neubuser, A., Kratochwil, K. and Balling, R. (1998). Pax9-deficient mice lack pharyngeal pouch derivatives and teeth and exhibit craniofacial and limb abnormalities. *Genes Dev*. 12:2735-2747.

Petersen, P.E. (2003). The World Health Organisation Report: Continuous improvement of oral health in the 21st century – the approach of the WHO Global Oral Health Program. [Online] http://www.who.int/oral_health/publications/report03/en/

Pio, R., Martinez, A., Unsworth, E.J., Kowalak, J.A., Bengoechea, J.A., Zipfel, P.F., Elsasser, T.H. and Cuttitta, F. (2001). Complement factor H is a serum-binding protein for adrenomedullin, and the resulting complex modulates the bioactivities of both partners. *J Biol Chem.* 276:12292-122300.

Proetzel G, Pawlowski SA, Wiles MV, Yin M, Boivin GP, Howles PN, Ding J, Ferguson MW, Doetschman T. (1995). Transforming growth factor-beta 3 is required for secondary palate fusion. *Nat Genet.* 11:409-414.

Puchtler, H., Meloan, S.N. and Terry, M.S. (1969). On the history and mechanism of alizarin and alizarin red S stains for calcium. *J Histochem Cytochem.* 17:110-124

Puchtler, H. and Meloan, S.N. (1978). Demonstration of phosphates in calcium deposits: a modification of von Kossa's reaction. *Histochem.* 56:177-185.

Retting, N., Song, B., Yoon, B.S. and Lyons, K.M. (2009). BMP canonical Smad signaling through Smad1 and Smad5 is required for endochondral bone formation. *Development.* 136:1093-1104.

Ribatti, D., Conconi, M.T. and Nussdorfer, G.G. (2007). Nonclassic endogenous novel [corrected] regulators of angiogenesis. *Pharmacol Rev.* 59:185-205.

Richman, J.M. and Tickle, C. (1989). Epithelia are interchangeable between facial primordia of chick embryos and morphogenesis is controlled by the mesenchyme. *Dev Biol.* 136:201-210.

Roberts-Clark, D.J. and Smith, A.J. (2000). Angiogenic growth factors in human dentine matrix. *Arch Oral Biol.* 45:1013-1016.

Roberts, A.B. and Sporn, M.B. (1993). Physiological actions and clinical applications of transforming growth factor-beta (TGF-beta). *Growth Factors.* 8:1-9.

Rocchi, P., Boudouresque, F., Zamora, A.J., Muracciole, X., Lechevallier, E., Martin, P.M. and Ouafik, L. (2001). Expression of adrenomedullin and peptide amidation activity in human prostate cancer and in human prostate cancer cell lines. *Cancer Res.* 61:1196-1206.

Rohr Inglehart, M. and Bagramian, R.A. (2002). Oral health-related quality of life. *Chicago:Quintessence.*

Ruch, J.V., Lesot, H. and Begue-Kirn, C. (1995). Odontoblast differentiation. *Int Journ Dev Biol.* 39:51-68.

Ruch, J.V. (1998). Odontoblast commitment and differentiation. *Biochem Cell Biol.* 76:923-938.

Russo, L.G., Maharajan, P. and Maharajan, V. (1998). Basic fibroblast growth factor (FGF-2) in mouse tooth morphogenesis. *Growth Factors.* 15:125-133.

Saygin, N.E., Giannobile, W.V. and Somerman, M.J. (2000). Molecular and cell biology of cementum. *Periodontol* 24:73-98.

Saha, P.K. and Wehrli, F.W. (2004). Measurement of trabecular bone thickness in the limited resolution of *in vivo* MRI by fuzzy distance transform. *IEEE Trans Med Imaging* 23:53-62.

Sanford, L.P., Ormsby, I., Gittenberger-de Groot, A.C., Sariola, H., Friedman, R., Boivin, G.P., Cardell, E.L. and Doetschman, T. (1997). TGFbeta2 knockout mice have multiple developmental defects that are non-overlapping with other TGFbeta knockout phenotypes. *Development.* 124:2659-2670.

Sarkar, L., Cobourne, M., Naylor, S., Smalley, M., Dale, T. and Sharpe P.T. (2000). Wnt/Shh interactions regulate ectodermal boundary formation during mammalian tooth development. *Proc Natl Acad Sci U S A.* 97:4520-4524.

Sartoris, D.J. (1996). Osteoporosis: Diagnosis and Treatment. *Marcel Dekker Inc.* NY.

Sassa Benedete, A.P., Sobral, A.P., Lima, D.M., Kamibeppu, L., Soares, F.A and Lourenco, S.V. (2008). Expression of transforming growth factor –beta1, -beta2 and -beta3 in human developing teeth: immunolocalization according to odontogenesis phases. *Pediatr Dev Pathol.* 11:206-212.

Sasagawa, I and Ishiyama, M. (2005) Fine structural and cytochemical observations on the dental epithelial cells during cap enameloid formation stages in *Polypterus senegalus*, a bony fish (Actinopterygii). *Connect Tissue Res.* 46:33-52.

Satokata, I., Ma, L., Ohshima, H., Bei, M., Woo, I., Nishizawa, K., Maeda, T., Takano, Y., Uchiyama, M., Heaney, S., Peters, H., Tang, Z., Maxson, R. and Maas R. (2000). *Msx2* deficiency in mice causes pleiotropic defects in bone growth and ectodermal organ formation. *Nat Genet.* 24:391-395.

Schröder, U. (1985). Effects of calciumhydroxide containing agent on pulp cell migration, proliferation and differentiation. *J Dent Res.* 64:541-548

Shen, H., Nutt, S. and Hull, D. (2004). Direct observation and measurement of fiber architecture in short fiber-polymer composite foam through micro-CT imaging. *Comp Sci and Tech.* 64: 2113-2120.

Shimekake, Y., Nagata, K., Ohta, S., Kambayashi, Y., Teraoka, H., Kitamura, K., Eto, T., Kangawa, K. and Matsuo, H. (1995) Adrenomedullin stimulates two signal transduction pathways, cAMP accumulation and Ca²⁺ mobilization, in bovine aortic endothelial cells. *J Biol Chem* 270:4412–4417.

Shuler, C.F. (1995). Programmed cell death and cell transformation in craniofacial development. *Crit Rev Oral Biol Med.* 6:202-217.

Silver, N., Best, S., Jiang, J. and Thein, S.L. (2006). Selection of housekeeping genes for gene expression studies in human reticulocytes using real-time PCR. *BMC Molecular Biology.* 7:

Simon, S., Cooper, P., Smith, A. J., Picard, B., Ifi, C.N. and Berdal, A. (2008). Evaluation of a new laboratory model for pulp healing: preliminary study. *Int Endod J.* 41:781-90

Six, N., Lasfargues, J.J. and Goldberg, M. (2000). In vivo study of the pulp reaction to Fuji IX, a glass ionomer cement. *J Dent.* 28:413-422.

Skaleric, U., Kramar, B., Petelin, M., Pavlica, Z. and Wahl, S.M. (1997). Changes in TGF-beta 1 levels in gingiva, crevicular fluid and serum associated with periodontal inflammation in humans and dogs. *Eur J Oral Sci.* 105:136-1342.

Sloan, A.J., Shelton, R.M., Hann, A.C., Moxham, B.J. and Smith, A.J. (1998). An in vitro approach for the study of dentinogenesis by organ culture of the dentine-pulp complex from rat incisor teeth. *Arch Oral Biol.* 43:421-430.

Sloan, A.J. and Smith, A.J. (1999). Stimulation of dentin-pulp complex of rat incisor teeth by transforming growth factor-beta isoforms 1-3 *in vitro*. *Arch Oral Biol.* 44:149-156.

Sloan, A.J., Rutherford, R.B. and Smith, A.J. (2000). Stimulation of the rat dentine-pulp complex by bone morphogenetic protein-7 *in vitro*. *Arch Oral Biol.* 45:173-177.

Smith, A.J., Tobias, R.S., Plant, C.J., Browne, R.M., Lesot, H. and Ruch, J.V. (1990). *In vivo* morphogenetic activity of dentine matrix proteins. *Journ Biol Buccale.* 18:123-129.

Smith, A.J., Tobias, R.S., Cassidy, N., Plant, C.J., Browne, R.M., Bègure-Kirn, C., J.V. and Lesot, H (1994). Odontoblast stimulation in ferrets by dentine matrix components. *Arch Oral Biol.* 39:13-22.

Smith, A.J, Cassidy, N., Perry, H., Begue-Kirn, C., Ruch, JV and Lesot, H. (1995). Reactionary dentinogenesis. *Int J Dev Biol.* 39:273-280.

Smith, A.J. and Lesot, H. (2001). Induction and regulation of crown dentinogenesis: embryonic events as a template for dental tissue repair? *Crit Rev Oral Biol Med.* 12:425-437.

Smith, A.J. (2003). Vitality of the dentin-pulp complex in health and disease: growth factors as key mediators. *J Dent Educ.* 67:678-689.

St Amand, T.R., Zhang, Y., Semina, E.V., Zhao, X., Hu, Y., Nguyen, L., Murray, J.C. and Chen, Y. (2000). Antagonistic signals between BMP4 and FGF8 define the expression of Pitx1 and Pitx2 in mouse tooth-forming anlage. *Dev Biol.* 217:323-332.

Sun, Z.L., Fang, D.N., Wu, X.Y., Ritchie, H.H., Begue-Kirn, C., Wataha, J.C., Hanks, C.T. and Butler, W.T. (1998). Expression of dentin sialoprotein (DSP) and other molecular determinants by a new cell line from dental papillae, MDPC-23. *Connect Tissue Res.* 37:251-261.

Sun H, Dai K, Tang T, Zhang X. (2008). Regulation of osteoblast differentiation by slit2 in osteoblastic cells. *Cells Tissues Organs.* 190:69-80.

Ten Cate, A.R. (1998). Oral Histology: Development, Structure and Function. 5th Edition. Mosby.

Thesleff, I., Vaahtokari, A., Kettunen, P. and Aberg, T. (1995). Epithelial-mesenchymal signaling during tooth development. *Connect Tissue Res.* 32:9-15.

Thesleff, I., Vaahtokari, A. and Partanen, A.M. (2002). Regulation of organogenesis. Common molecular mechanisms regulating the development of teeth and other organs. *Int J Dev Biol.* 39:35-50.

Tjaderhane, L., Salo, T., Larjava, H., Larmas, M. and Overall, C.M. (1998). A novel organ culture method to study the function of human odontoblasts in vitro: gelatinase expression by odontoblasts is differentially regulated by TGF-beta1. *J Dent Res.* 77:1486-1496.

Todaro, G.J. and Green, H. (1963). Quantitative studies of the growth of mouse embryo cells in culture and their development into established lines. *J Cell Biol.* 17:299-313.

Tomson, P.L., Grover, L.M., Lumley, P.J., Sloan, A.J., Smith, A.J. and Cooper, P.R. (2007). Dissolution of bio-active dentine matrix components by mineral trioxide aggregate. *J Dent.* 35:636-642.

Trumpp, A., Depew, M.J., Rubenstein, J.L., Bishop, J.M. and Martin, G.R. (1999). Cre-mediated gene inactivation demonstrates that FGF8 is required for cell survival and patterning of the first branchial arch. *Genes Dev.* 13:3136-3148.

Tsakamoto, Y., Fukutani, S., Shin-Ike, T., Kubota, T., Sato, S., Suzuki, Y. and Mori, M. (1992). Mineralized nodule formation by cultures of human dental pulp-derived fibroblasts. *Arch Oral Biol.* 37:1045-1055.

- Tsuruda, T., Kato, J., Kitamura, K., Kawamoto, M., Kuwasako, K., Imamura, T., Koiwaya, Y., Tsuji, T., Kangawa, K. and Eto, T.** (1999). An autocrine or a paracrine role of adrenomedullin in modulating cardiac fibroblast growth. *Cardiovasc Res.* 43:958-967.
- Tucker, A.S., Matthews, K.L. and Sharpe, P.T.** (1998). Transformation of tooth type induced by inhibition of BMP signaling. *Science.* 282:1136-1138.
- Tucker, A.S. and Sharpe, P.T.** (2004). The cutting edge of mammalian development; how the embryo makes teeth. *Nature reviews: Genetics.* 5:499-509
- Tureckova, J., Sahlberg, C., Aberg, T., Ruch, J.V., Thesleff, I. and Peterkova, R.** (1995). Comparison of expression of the *msx-1*, *msx-2*, *BMP-2* and *BMP-4* genes in the mouse upper diastemal and molar tooth primordia. *Int J Dev Biol.* 39:459-468.
- Tyler, M.S. and Hall, B.K.** (1977). Epithelial influences on skeletogenesis in the mandible of the embryonic chick. *Anat Rec.* 188:229-239.
- Tziafas, D., Alvanou, A., Papadimitriou, S., Gasic, J. and Komnenou, A.** (1998). Effects of recombinant basic fibroblast growth factor, insulin-like growth factor-II and transforming growth factor-beta 1 on dog dental pulp cells in vivo. *Arch Oral Biol.* 43:431-444.
- Tziafas, D., Smith, A.J. and Lesot, H.** (2000). Designing new treatment strategies in vital pulp therapy. *J Dent.* 28:77-92.
- Udono-Fujimori, R., Totsune, K., Murakami, O., Arihara, Z., Kikuchi, K., Tamai, M., Shibahara, S. and Takahashi, K.** (2004). Suppression of cytokine-induced expression of endothelin-1 by dexamethasone in human retinal pigment epithelial cells. *J Cardiovasc Pharmacol.* 44:471-473.
- Unda, F.J., Martin, A., Hernandez, C., Perez-Nanclares, G., Hilario, G and Arechaga, J.** (2001). FGFs -1 and -2 and TGF β 1 as inductive signals modulating *in vitro* odontoblast differentiation. *Adv Dent Res.* 15:34-38.
- Unsworth, J., Kaneez, S., Harris, S., Ridgway, J., Fenwick, S., Chenery, D. and Harrison, A.** (2007). Pulsed low intensity ultrasound enhances mineralisation in preosteoblast cells. *Ultrasound Med Biol.* 33:1468-1474

Uzan, B., de Vernejoul, M.C. and Cressent, M. (2004). RAMPs and CRLR expressions in osteoblastic cells after dexamethasone treatment. *Biochem Biophys Res Commun.* 321:802-808.

Vaahokari, A., Vainio, S. and Thesleff, I. (1991). Associations between transforming growth factor beta 1 RNA expression and epithelial-mesenchymal interactions during tooth morphogenesis. *Development.* 113:985-994.

Vainio, S., Karavanova, I., Jowett, A. and Thesleff, I. (1993). Identification of BMP-4 as a signal mediating secondary induction between epithelial and mesenchymal tissues during early tooth development. *Cell.* 75:45-58.

Yee, R. and Sheiham, A. (2002). The burden of restorative dental treatment for children in third world countries. *International Dental Journal.* 52:1-9.

Wahl, S.M., Costa, G.L., Mizel, D.E., Allen, J.B., Skaleric, U. and Mangan, D.F. (1993). Role of transforming growth factor beta in the pathophysiology of chronic inflammation. *J Periodontol.* 64:450-455.

Wang, D., Christensen, K., Chawla, K., Xiao, G., Krebsbach, P.H. and Franceschi, R.T. (1999). Isolation and characterization of MC3T3-E1 preosteoblast subclones with distinct in vitro and in vivo differentiation/mineralization potential. *J Bone Miner Res.* 14:893-903.

Wang, Y., Zhang, J.S., Huang, G.C., Cheng, Q. and Zhao, Z.H. (2005). Effects of adrenomedullin gene overexpression on biological behavior of hepatic stellate cells. *World J Gastroenterol.* 11:3549-3553.

Wang, Y., Zhang, J.S., Qian, J., Huang, G.C. and Chen, Q. (2006) Adrenomedullin regulates expressions of transforming growth factor-beta1 and beta1-induced matrix metalloproteinase-2 in hepatic stellate cells. *Int J Exp Pathol.* 3:177-184.

Wedden, S.E (1987). Epithelial-mesenchymal interactions in the development of chick facial primordia and the target of retinoid action. *Development.* 99:341-351.

Wessells N: Tissue interactions and development. Menlo Park, CA: Benjamin Cummins, 1977.

Winnier, G., Blessing, M., Labosky, P.A. and Hogan, B.L. (1995). Bone morphogenetic protein-4 is required for mesoderm formation and patterning in the mouse. *Genes Dev.* 9:2105-2116.

Wise, G.E., Marks, S.C. Jr. and Cahill, D.R. (1985). Ultrastructural features of the dental follicle associated with formation of the tooth eruption pathway in the dog. *J Oral Pathol.* 14:15-26.

Withers, D.J., Coppock, H.A., Seufferlein, T., Smith, D.M., Bloom, S.R. and Rozengurt, E. (1996). Adrenomedullin stimulates DNA synthesis and cell proliferation via elevation of cAMP in Swiss 3T3 cells. *FEBS Lett.* 378:83-87.

Wong, L.Y., Cheung, B.M., Li, Y.Y. and Tang, F. (2005). Adrenomedullin is both proinflammatory and antiinflammatory: its effects on gene expression and secretion of cytokines and macrophage migration inhibitory factor in NR8383 macrophage cell line. *Endocrinology.* 146:1321-1327.

Xia, C.F., Yin, H., Borlongan, C.V., Chao, J. and Chao, L. (2004). Adrenomedullin gene delivery protects against cerebral ischemic injury by promoting astrocyte migration and survival. *Hum Gene Ther.* 15:1243-1254.

Xu, Y. and Krukoff, T.L. (2005). Adrenomedullin stimulates nitric oxide release from SK-N-SH human neuroblastoma cells by modulating intracellular calcium mobilization. *Endocrinology.* 146:2295-2305.

Xu, X., Jeong, L., Han, J., Ito, Y., Bringas JR, P and Chai, Y. (2003) Developmental expression of SMAD 1-7 suggests critical function of TGF β /BMP signalling in regulating epithelial-mesenchymal interaction during tooth morphogenesis. *Int J Dev Biol.* 47:31-39.

Zhang, H., Ahmad, M. and Gronowicz, G. (2003). Effects of transforming growth factor-beta 1 (TGF-beta1) on in vitro mineralization of human osteoblasts on implant materials. *Biomaterials.* 24:2013-2020.

Zhang, Q., van 't Hof, M.A., Truin, G.J., Bronkhorst, E.M. and van Palenstein Helderma, W.H. (2006). Caries-inhibiting effect of chlorhexidine varnish in pits and fissures. *J Dent Res.* 85:469-472.

Zudaire E, Martínez A, Ozbun LL, Cuttitta F. (2004). Characterization of adrenomedullin in non-human primates. *Biochem Biophys Res Commun.* 321:859-869.

Zudaire, E., Portal-Núñez, S. and Cuttitta, F. (2006). The central role of adrenomedullin in host defense. *J Leukoc Biol.* 80:237-244.